THÈSE

En vue de l'obtention du

DOCTORAT DE L'UNIVERSITÉ DE TOULOUSE

Délivré par :

Institut National Polytechnique de Toulouse (Toulouse INP)

Discipline ou spécialité :

Ecologie Fonctionnelle

Présentée et soutenue par :

M. TY SOK

le vendredi 24 septembre 2021

Titre :

Dynamique des transports sédimentaires et nutritifs au sein du bassin versant du Mékong et rôle du lac Tonlé Sap: couplage des données d'observations et des approches de modélisation

---

Ecole doctorale :

Sciences de l'Univers de l'Environnement et de l'Espace (SDU2E)

Unité de recherche :

Laboratoire Ecologie Fonctionnelle et Environnement (ECOLAB)

Directeur(s) de Thèse :

M. JOSE-MIGUEL SANCHEZ-PEREZ

M. CHANTHA OEURNG

Rapporteurs :

M. DIDIER ORANGE, CENTRE REGIONAL IRD

MME THI PHUONG QUYNH LE, VIETNAM ACADEMY OF SCIENCE & TECHNOLOGY

Membre(s) du jury :

M. SYLVAIN OUILLON, OBS MIDI-PYRENEES TOULOUSE, Président

M. CHANTHA OEURNG, INSTITUT DE TECHNOLOGIE DU CAMBODGE, Membre

. JOSE MARIA BODOQUE DEL POZO, UNIVERSITE CASTILLA LA MANCHA ALBACETE, Membre

M. JOSE-MIGUEL SANCHEZ-PEREZ, UNIVERSITE TOULOUSE 3, Membre

MME SABINE SAUVAGE, UNIVERSITE TOULOUSE 3, Invité(e)

ACKNOWLEDGEMENT

First and foremost, I am extremely grateful to my supervisors, **Dr. José Miguel Sánchez-Pérez and Dr. Chantha Oeurng.** Also, to **Sabine Sauvage** for her guidance. Their immense knowledge and plentiful experience have encouraged me in all the time of my academic research in PhD study and daily life. Their continuous support, patience, motivation and enthusiasm, valuable advice, comments, and guidance were very helpful in accomplishing this study and in further study.

I gratefully acknowledge Les Bourses du Gouvernement Français (BGF) and the Institute of Technology of Cambodia to provide financial support during my PhD. Special thanks to Laboratoire Ecologie Fonctionnelle et Environnement for hosting during the Ph.D. study.

Besides my supervisors, I would like to thank the team: **Ilan Ich, Kaing Vinhteang, Huot Menghour, Say Vuthy, Kimleang Chhum, Song Layheang and Mong Marith and others that I cannot count them all in Cambodia and Toulouse**. Without such a team behind me.

In my daily life, there are also many lovely people around. I am particularly grateful to my father, **Mr. KHUT Sok** and my mother, **Mrs. YEM Vanna**. I also wish to express my wholehearted thanks to my brothers and my sister for everything they have done to support me during these times and from the beginning of my life.

Finally, I would like to thank all my teachers from the beginning of my study since kid, to friends and related persons to support me spiritually throughout this program period.

My mission of PhD study in Toulouse and ITC might be over and accomplished, but my career journey is about to begin. I will take and consider what I have learned during these periods, both in science, academic life and life lesson, to continue improving and prove myself, to continue learning, to continue devoting to research, science and development wherever I live and to be.

One of many advice which inspires me and worth to include and past to the other:

"A big success in life comes from small prices of success combing together while the future of yours depends upon the quality of your thoughts." Oeurng Chantha

Toulouse, July 2021

SOK Ty

CONTENTS

LIST OF FIGURES

LIST OF TABLES

LIST OF ABBREVIATIONS

3S Basin	Se Kong, Se San, and Sre Pok
AMLE	Adjusted Maximum Likelihood Estimation
BGF	Les Bourses du Gouvernement Français
CN2	Curve number at moisture condition II
DEM	Digital elevation model
DIN	Dissolved inorganic nitrogen
FAO	The Food and Agriculture Organization of the United Nations
GPCC	Global Precipitation Climatology Centre
HRUs	Hydrologic response units
LAD	Least Absolute Deviation
LMB	Lower Mekong basin
LOADEST	LOAD ESTimator
MERIT DEM	Multi-Error-Removed Improved-Terrain DEM
MK	Mann-Kendall
MLE	Maximum Likelihood Estimation
MOWRAM	Ministry of Water Resources and Meteorology of Cambodia
MRB	Mekong River Basin
MRC	Mekong River Commission
MUSLE	Modified universal soil loss
N	Nitrogen
NEX	NASA Earth Exchange
NNB	Nitrate Net Balance
NNBR	Nitrate Net Balance Rate
NO_3^-	Nitrate
NP	Nitrate Production
NR	Nitrate Removal

INTRODUCTION GENERALE

Le flux total de sédiments allant vers les océans a été évalué entre 12,6 et 18,5 Gt an-1, l'Asie étant le continent exportant le plus de sédiments (~4,8 Gt an-1) (Gordeev, 2006 ; Syvitski et al., 2011 ; Syvitski et al., 2005b). D'importantes charges sédimentaires sont une caractéristique commune à de nombreux bassins asiatiques en raison de la topographie prononcée de la région, en particulier les bassins provenant du plateau himalayen-tibétain, tels que le Mékong, le fleuve Rouge, le Yangtze et les fleuves Jaunes (Evans et al., 2012 ; Ludwig et Probst, 1998 ; Milliman et Syvitski, 1992). Cependant, l'étude à l'échelle mondiale et l'évaluation actuelle des exportations en sédiments présente certaines contraintes et incertitudes en raison du manque de données à travers le monde (Cohen et al., 2013 ; Walling et al., 2003). Pas seulement les flux de sédiment total à l'échelle mondiale, mais également les exports mondiaux en nutriments des grands fleuves vers les océans ont été triplés au cours de la seconde moitié du siècle. La charge en éléments nutritifs est particulièrement préoccupante dans les régions tropicales soumis à un développement accéléré, parmi ces fleuves, le bassin du Mékong est l'une des préoccupations principales.

Les lacs et les plaines inondables sont des systèmes hydrologiquement dynamiques caractérisés par une hydrologie de surface très complexe soumise à des épisodes d'inondations ou de mise à sec à grande échelle sur des périodes saisonnières (Bonnet et al., 2008 ; Li et al., 2019a ; Li et al., 2020 ; Thomas et al. , 2015). On estime qu'il y a entre 0,8 million et 2,2 millions de km^2 de rivières et de plaines inondables liées aux lacs dans le monde (Entwistle et al., 2019). Les lacs et les plaines inondables sont des points d'intérêt de la biodiversité et des services écosystémiques qui sont naturellement productifs et précieux (Dudgeon et al., 2006), fournissant une gamme de fonctions hydrologiques et écologiques, telles que la régulation des inondations, l'épuration de l'eau, la rétention des nutriments, la diversité des habitats fauniques essentiels ainsi que l'agriculture et l'élevage (Funk et al., 2019 ; Robinson et al., 2015 ; van der Most et Hudson, 2018). À notre connaissance, un grand nombre de études en hydrologie et en bilan hydrique des lacs se sont principalement concentrées sur les lacs fermés, les lacs terminaux et certains lacs du Plateau dans différentes zones climatiques (Li et al., 2020). Compte tenu de l'importance hydrologique et écologique des lacs, ils n'ont reçu que peu d'attention jusqu'ici et n'ont pas été suffisamment étudié au niveau de leurs processus hydrologiques et de leur bilan hydrique en lien avec les flux liés à qualité de l'eau.

L'un des plus grands fleuves transfrontaliers d'Asie, le Mékong, prend sa source dans la région tibétaine de la Chine et couvre 795 000 km^2. La variation saisonnière en eau, en sédiments et en nutriments du bassin du Mékong (MRB) contraint la productivité agricole, écologique et halieutique du Bas Mékong, notamment du bassin du lac Tonlé Sap et de sa plaine inondable ainsi que du delta du Mékong (Arias et al., 2014, Kummu et al., 2008a, Lamberts, 2006). Le fait que le bassin du Mékong s'étende sur six pays a rendu complexe l'étude du système. Une grande importance est accordée à la modélisation en termes de développement d'une gestion durable des ressources en eau à l'échelle du bassin hydrographique, qui peut à la fois, aider à évaluer les ressources en eau actuelles, identifier les sources de pollution et améliorer le développement durable (Bouraoui et al., 2005). Certaines études à grande échelle sur les nutriments dans le bassin du Mékong ont été menées jusqu'ici. Cependant, une étude plus détaillée sur les flux de nitrates et les sources de nutriments au sein du bassin du Mékong est nécessaire afin d'améliorer les connaissances scientifiques régionales et la gestion du bassin. Les données de surveillance spatiale sur le long terme des bassins versants sont rares en raison du coût des dépenses nécessaires; cependant, les modèles de qualité de l'eau permettent de mettre en place des simulations sur le long terme.

En tant qu'élément indispensable du système fluvial du Mékong, le lac Tonlé Sap au centre du Cambodge est la plus grande masse d'eau douce permanente d'Asie du Sud-Est et est le réservoir naturel essentiel dont bénéficie le fleuve Mékong (Kummu et al., 2008b). En outre, le lac Tonlé Sap et ses plaines inondables connectés au cours d'eau principal du Mékong via la rivière Tonlé Sap dépendent également des régimes sédimentaires du Mékong, car la principale source d'approvisionnement en sédiments du lac Tonlé Sap est le transport de sédiments du fleuve Mékong (Kummu et al., 2008b ; Lu et al., 2014). Dans même, le Tonlé Sap contribue de manière significative aux sédiments et aux éléments nutritifs du fleuve Mékong pendant la période d'étiage.

Comprendre et modéliser la dynamique du flux de nutriments et la source de ces nutriments dans le fleuve Mékong sont essentiels pour résoudre le problème et combler les lacunes susmentionnées. Les sédiments et les éléments nutritifs du Mékong sont importants pour maintenir la géomorphologie des plaines inondables et en particulier du lac Tonlé Sap. De même, le lac Tonlé Sap contribue aux sédiments et aux nutriments du delta du Mékong. Par conséquent, l'évaluation des sédiments et des nutriments dans le Mékong et de la connexion entre le cours d'eau du Mékong et le lac Tonlé Sap est nécessaire pour mieux comprendre les apports en sédiments et en nutriments

du Mékong. Cette évaluation est également cruciale pour estimer les fonctions écosystémiques du Tonlé Sap et pour mieux comprendre le rôle du système du lac Tonlé Sap pour le fleuve Mékong et son delta.

L'objectif principal de cette thèse est d'évaluer le transport dynamique des sédiments et des nutriments dans le bassin du Mékong et d'évaluer le rôle du Tonlé Sap vers le Mékong à travers une approche couplant données et modélisations. Les objectifs spécifiques sont les suivants : (1) analyser de manière exhaustive et présenter une quantification du transport des sédiments et des nutriments aux échelles annuelles, saisonnières et mensuelles entre le lac Tonlé Sap et le cours d'eau principal du Mékong à travers le système d'inversion hydrologique ; (2) évaluer l'hydrologie du bassin en se concentrant sur les composantes du bilan hydrologique, comprendre la contribution des différents compartiments du bassin à l'apport en eau, et quantifier la charge sédimentaire et l'apport en sédiment spatialisé dans le bassin du Mékong ; (3) modéliser le flux des nitrates et déterminer la variabilité spatiale des rendements en nitrates dans le bassin du Mékong ; et (4) Définir le rôle du lac Tonlé Sap dans la connexion des éléments nutritifs avec le fleuve Mékong

EXTENDED ABSTRACT

Global sediment flux to the oceans was estimated from 12.6 to 18.5 Gt yr^{-1}, and Asia exported the most sediments (~4.8 Gt yr^{-1}) among continents (Gordeev, 2006; Syvitski et al., 2011; Syvitski et al., 2005b). High sediment loads are a common feature in many Asian basins due to the pronounced topography of the region, especially the basins originating from the Himalayan-Tibetan Plateau, such as the Mekong, the Red, the Yangtze and the Yellow Rivers (Evans et al., 2012; Ludwig and Probst, 1998; Milliman and Syvitski, 1992). However, Investigating global value and the current trend in sediment exports has some constraints and uncertainties due to the data scarcity across the globe and the data series (Cohen et al., 2013; Walling et al., 2003). Not only global sediment but the global nutrient inputs from major rivers into the oceans have also tripled during the second half of the last century. Nutrient loading is a particular concern in tropical regions undergoing rapid development, and the Mekong basin is one of the major rivers of concern.

Lake and floodplains are hydrologically dynamic systems characterized by highly complex surface hydrodynamics subjected to wide-ranging wetting and drying over seasonal timeframes (Bonnet et al., 2008; Li et al., 2019a; Li et al., 2020; Thomas et al., 2015). It is estimated that there are between 0.8 million and 2.2 million km^2 of rivers and lake-related floodplains worldwide (Entwistle et al., 2019). Lake and floodplains are hotspots of biodiversity and ecosystem services that are naturally productive and valuable (Dudgeon et al., 2006), providing a range of hydrological and ecological functions, including flood regulation, water purification, nutrient retention, critical wildlife habitats, and agriculture and livestock products (Funk et al., 2019; Robinson et al., 2015; van der Most and Hudson, 2018). To the best of our knowledge, a large number of previous investigations of lake hydrological and water balance analysis mainly focused on closed lakes, terminal lakes, and some Plateau lakes in different climatic zones (Li et al., 2020). Given the hydrological and ecological importance of lakes, they still have received little attention and not been adequately characterized concerning their hydrological processes and water balance with the link to water quality circulations.

One of the largest transboundary rivers in Asia, the Mekong River, originates in China's Tibetan region and covers 795,000 km^2. The seasonal delivery of water, sediments, and nutrients of the Mekong River basin (MRB) are responsible for the agricultural, ecological, and fish productivity of the Lower Mekong, notably the Tonle Sap Lake basin and its floodplain and Mekong Delta

(Arias et al., 2014; Kummu et al., 2008a; Lamberts, 2006). The fact that the Mekong River basin spreads across six countries has made studying the system a complex task. Much importance is given to modelling in terms of developing sustainable management of water resources at the river basin scale, which can help evaluate current water resources, identify pollution sources, and improve sustainable development (Bouraoui et al., 2005). Some large-scale studies on nutrients in the Mekong Basin have been conducted. However, a more detailed study on nitrate flux and spatial nutrient sources for the Mekong Basin is still limited and deserves regional scientific knowledge and basin management. Long-term and spatial watershed monitoring data are rare due to the expense involved; however, long-term simulations are possible using water quality models. As a requisite part of the Mekong River system, the Tonle Sap Lake in central Cambodia is Southeast Asia's largest permanent freshwater body and the essential natural reservoir from which the Mekong River benefits (Kummu et al., 2008b). Further, the Tonle Sap Lake and its floodplains connecting with the Mekong mainstream through the Tonle Sap River rely as well upon the Mekong sediment regimes since the primary source of sediment supply to the Tonle Sap Lake is sediment transport from the Mekong (Kummu et al., 2008b; Lu et al., 2014). At the same time, Tonle Sap contributes significantly to sediment and nutrient to the Mekong during the low flow period.

Understanding and modelling the nutrient flux dynamic and its source in the Mekong River are crucially for addressing the problem mentioned above and the aforementioned gaps. Sediment and nutrient in the Mekong River are important to sustain the geomorphology of the floodplains and particularly the Tonle Sap Lake. At the same time, Tonle Sap Lake are contributing the sediment and nutrient for the Mekong delta. Therefore, the sediment and nutrient assessment in the Mekong River and linkage between the Mekong mainstream and the Tonle Sap Lake would be necessary to better understand as the sediment and nutrient input from the Mekong is crucial for the Tonle Sap's ecosystem functions and better understand the role of Tonle Sap Lake system to the Mekong River and its delta.

The main objective is to assess the dynamic transport of the sediment and nutrient in the Mekong River Basin and evaluate the role of the Tonle Sap to the Mekong River through the coupling data and modelling approaches. The specific objectives are: (1) To comprehensively analyses and present a quantification of annual, seasonal and monthly nitrate the sediment and nutrient transport exchange between Tonle Sap Lake and the mainstem Mekong River through the hydrological

reversal system; (2) To assess basin hydrology, focusing on the water balance components and contribution of the different compartments of the basin to water yield and quantifying the sediment load and spatial sediment yield in the Mekong River Basin; (3) To model the nutrient flux of nitrate transport and determine the spatial variability of nitrate yields in the Mekong River Basin; and (4) To define the role of Tonle Sap Lake in Nutrient connection with Mekong River through the assessment coupling data and modelling approaches.

A physical-based hydro-ago-environmental model, the Soil and Water Assessment Tool (SWAT) model, was used in this study for 80% of the Mekong River basin to simulate the water regime and suspended sediment and nutrient flux of the Mekong River. The SWAT model was calibrated based on observed discharge at eight gauge stations, suspended sediment load at six stations and nutrient data at five stations from 1995 to 2016 (the outlets of the main tributaries and the continent basin) at a monthly time step. To understand the role of Tonle Sap Lake in sediment and nutrient exchange with Mekong River, the study included the balanced of the monthly, seasonal and annual of Tonle Sap reverse system from 1995-2018. The exchange of sediment and nutrient flux between the Mekong-Tonle Sap system included the balanced of the monthly, seasonal and annual of Tonle Sap reverse system from 1995-2018.

Mekong River from 1985-2016, the mean annual rainfall was 1540 mm; 67% (1032 mm) of the average annual rainfall was removed by evapotranspiration and 33% (508 mm) for the streamflow. A water yield of 508 mm has come from surface runoff (proportion of 34%), lateral flow (proportion of 21%), and groundwater (proportion of 45%). The overall proportion of streamflow in the Mekong River in the study modelled by SWAT was 34% from surface runoff, 21% from lateral flow, 45%from the contribution of groundwater.

Sediment loads in various stations along the main river align with some previous studies that suggest sediment discharge to the South China Sea varies from 40 to 160 Mt/year. At Kratie, before entering the confluence of the Mekong and Tonle Sap Lake and delta, the sediment load is found 72±26 Mt/year from 1995-2016 with a decreasing trend. Sediment yields by major area, the highest sediment yield (1295 t/km^2/year) can be found in Chiang Saen to Luang Prabang in the northern part of Laos. In the upper Mekong part of China (where the river is called Lancang River), despite high topography and steep slope, the sediment load is lower than Chiang Saen to Luang Prabang due to covered by the various forest type. It is noticed that in the Mekong Basin in Thailand

(Mukdahan to Pakse section), despite the high agricultural activity, the sediment yield is low (78 t/km^2/year) since most of the area covers by gentle slope. In between Pakse and Kratie (including 3S, the largest tributary of Mekong), the average sediment yield was found 138 t/km2/year; however, we found high yields at the upstream part of the 3S basin (>500 t/km^2/year). The annual sediment yield of the upper 80% Mekong River basin (310 t/km^2/year) is comparable with sediment yields reported for other major rivers in Asia, which is lower than the Yellow and Red river but higher than Peal, Yenisei Rivers.

From 1995 to 2000, the Tonle Sap contributed more sediment load to the Mekong River than was deposited in the lake, on an average of 0.65 Mt annually. However, the rate decreased, and then since 2001, an average net 1.35±0.7 Mt of sediment has been deposited in the lake annually. An assessment of water discharge and sediment loads variability of the Mekong River and Tonle Sap system presented in this study helps clarify the exchange annual discharge and sediment load toward the Mekong delta. Tonle Sap Lake provided sediment load to the Mekong system and delta annually 0.65±0.6 Mt from 1995 to 2000. However, since 2001 Tonle Sap Lake has become a sediment sink for about 1.35±0.7 Mt annually, thereby reducing the annual sediment transport to the Mekong delta. This reduction in sediment supply compounds the threat to the delta from accelerated subsidence and sea-level rise. The sudden change appears to be due to increased TSS concentrations from the Mekong to Tonle Sap Lake. The concentration of TSS in Kratie appears to have been largely unchanged.

Exchanging nutrient flux between Tonle Sap Lake and Mekong River, the amount of annual nitrate and TP flux from Tonle Sap Lake to the Mekong on average was approximately 34±13.8 kt/yr and 6.6±1.4 kt/yr. Furthermore, the amount of inflow nutrients to the lake from the Mekong amounted to 35.8±12.5 kt/yr of nitrate and 8.7±3.3 kt/yr of total phosphorus, respectively. The study also pointed out that Tonle Sap Lake was the nitrate sinks during 2000-2012 and 2007-2015 for total phosphorus. The study has emphasized the interaction role of Tonle Sap Lake and Mekong in nutrient supply. This study provided the first findings regarding nutrient exchanges between Mekong River and Tonle Sap Lake, set up the baseline result for the long-term nutrient dynamics, and load in Tonle Sap River.

The Tonle Sap is an example of a lake-channel system, a lake (usually on a floodplain) that connects with the main river (via defined channels as well as overbank flow) and that absorbs flood

peaks and releases waters gradually back into the main river as flood stage recedes. With its channel sized reverse flow pattern, combined with broad, shallow lateral inundation of floodplains during the wet season, the Tonle-Sap-Mekong exchange represents a uniquely developed and important channel-floodplain exchange of sediment and nutrient flux.

CHAPTER I

Scientific Context and Objectives

This chapter addresses the general context of the research, research problematic and questions, the objectives of the thesis and follows by chapter descriptions containing in the thesis.

1. Chapter I. Scientific Context and Objectives

1.1. Global Major Rivers and Its Discharge

The hydrological regime of rivers is of great importance for social and economic development, such as in references (Syvitski et al., 2009; Vörösmarty et al., 2003; Walling, 2006). River discharge, which represents the accumulation of surface water flowing into rivers and ultimately into the ocean or other water bodies, is one of the most important components in the global water cycle and can be essential to water availability and consequently human lives (Vörösmarty et al., 2003; Walling et al., 2003), such as in water resources management (Carriquiry and Sánchez, 1999; Fanos, 1995; Khafagy et al., 1993), hydropower generation (Walling, 2006), flood control (Syvitski et al., 2009), and fisheries (Mikhailova, 2003). For many of the major rivers around the world, river discharge recorded at gauging stations is regarded as an integrated signal of hydrological processes in the upstream of the corresponding gauging stations, which can provide reliable hydrological information with high accuracy (Moran et al., 2018; Walling et al., 2003; Wang et al., 2007; Yang et al., 2006). However, the global knowledge of river discharge is still poor (Galipeau et al., 2013; Kondolf et al., 2018b; Peng et al., 2010). On the one hand, the distributed networks of gauging stations are sparse, especially in less developed countries; on the other hand, river discharge measurements are usually proprietary in many countries and cannot be shared to the public (Galipeau et al., 2013). Until recently, satellite observations, which can provide spatially dense coverage and characterize river discharge variation similar to that performed at gauging stations, have been applied for mapping global river discharge; see (Adamson et al., 2009; Galipeau et al., 2013; Rex et al., 2014; Walling et al., 2003).

Water resources and their availability attract global attention for ecosystem and food security reason. Through the report from the Food and Agriculture Organization of the United Nations (FAO, 2003), it estimated that the total water resources in the world were about 43,750 $km^3\ yr^{-1}$; at the continental level, America has the largest share of the world's total freshwater resources, account for 45%, followed by Asia (28%), Europe (15.5%) and Africa (9%) (FAO, 2003). In terms of resources per inhabitant in each continent, America has 24,000 $m^3\ yr^{-1}$, Europe 9,300 $m^3\ yr^{-1}$, Africa 5,000 $m^3\ yr^{-1}$, and Asia 3,400 $m^3\ yr^{-1}$ (FAO, 2003). The discharge of river water to the coastline reflects the global distribution of precipitation, drainage basin area and relief, the loss of moisture back to the atmosphere through various mechanisms of evaporation and sublimation, and the time-dependent release of stored water to drainage channels (Figure 1-1). Discharge to the

coastal zone reflects this global variability. Many large Asian rivers are among the largest in the world in terms of river length, area of the drainage basin, and mean annual runoff (**Figure 1-2**). The headwaters of six of Asia's major rivers begin on the Tibetan Plateau. China, which requires water to meet the needs of 20 per cent of the world's population.

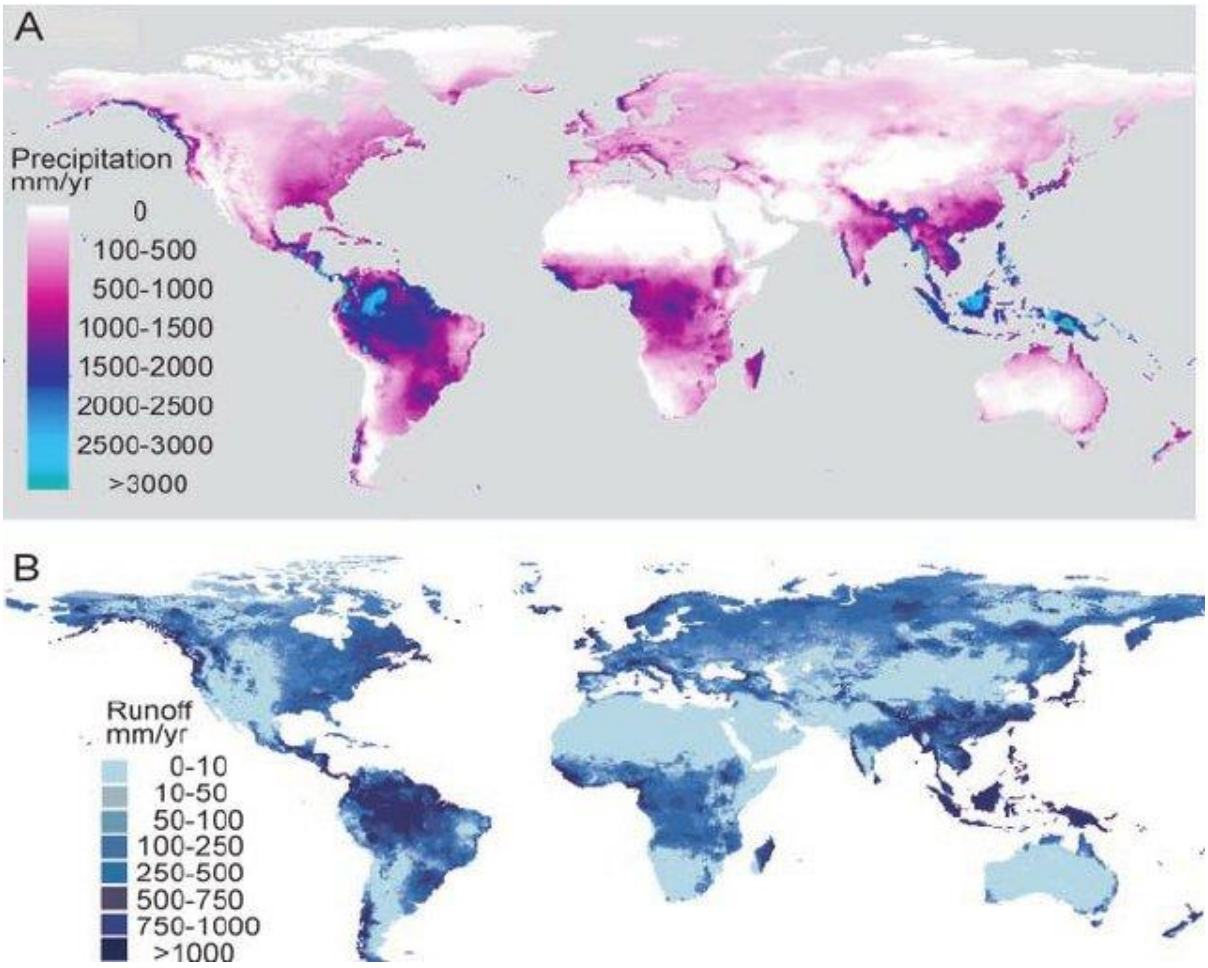

Figure 1-1: *Water flux around the globe (Li et al., 2018). (a) Global precipitation (mm yr^{-1}) (Syvitski et al.2003). (b) Hydrological runoff (mm. yr^{-1}) after accounting for all forms of evapotranspiration and human-induced consumption (Syvitski et al., 2005a). The hydrological runoff divided by the drainage area equals the water discharge ($km^3.yr^{-1}$).*

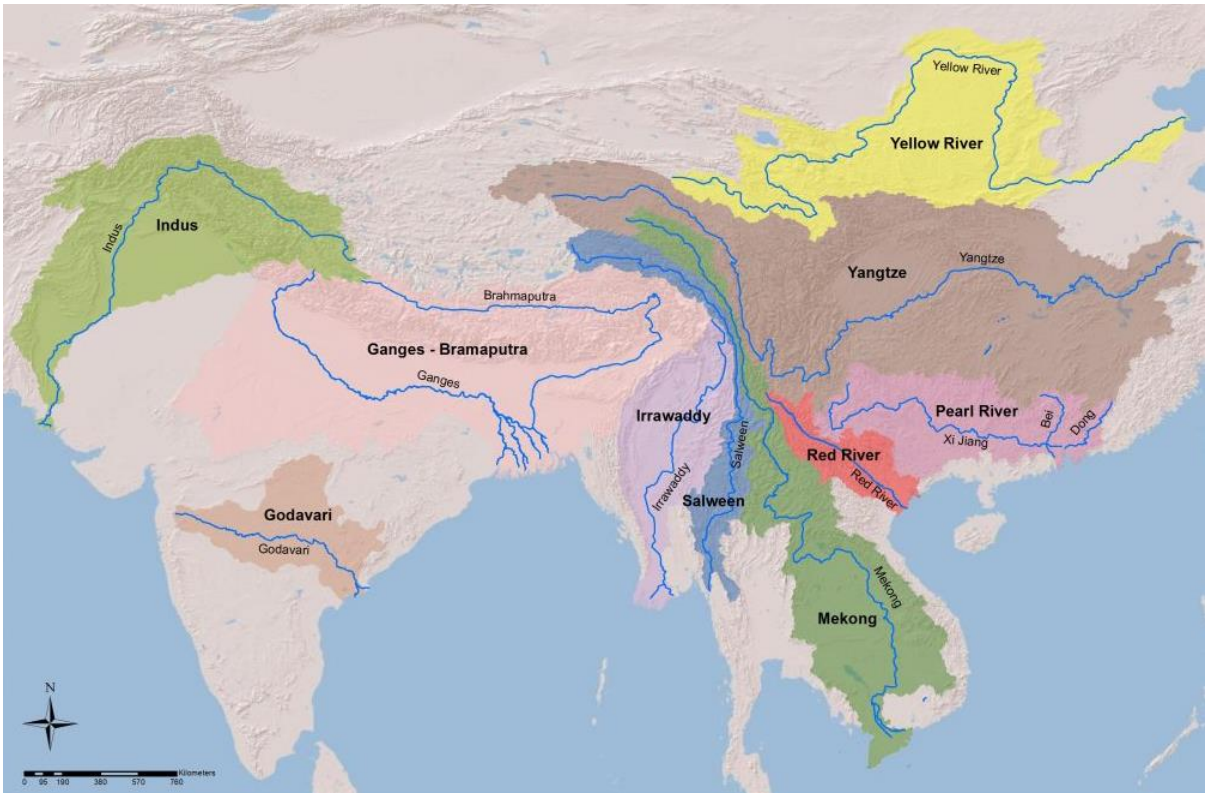

(Source : https://editions.lib.umn.edu/openrivers/)

Figure 1-2: *Major watersheds and Rivers Southern and Eastern Asia. Tibet is considered the sources area of the continent and headwaters location for six of the largest rivers on the Asian continent and provides the water needs to around 20 per cent of the world's population.*

1.2. Global and Regional Sediment Transports

Global sediment flux to the oceans was estimated from 12.6 to 18.5 Gt yr^{-1}, and Asia exported the most sediments (~4.8 Gt yr^{-1}) among continents (Gordeev, 2006; Syvitski et al., 2011; Syvitski et al., 2005b) (**Figure 1-3**). High sediment loads are a common feature in many Asian basins due to the pronounced topography of the region, especially the basins originating from the Himalayan-Tibetan Plateau, such as the Mekong, the Red, the Yangtze and the Yellow Rivers (Evans et al., 2012; Ludwig and Probst, 1998; Milliman and Syvitski, 1992).

Investigating global value and the current trend in sediment exports has some constraints and uncertainties due to the data scarcity across the globe and the data series (Cohen et al., 2013; Walling et al., 2003). Firstly, the lack of sediment data in many rivers, especially in the rivers in developing and underdeveloped countries, can cause an underestimation of the global sediment exports. Even the sediment flux data is available, but the measurement only considers suspended

sediment flux, not the bed load transport. Secondly, analysis of annual sediment flux temporal trends requires records of enough length data. Long-term sediment monitoring programs, however, are rare in many areas of the world.

However, Africa and Asia showed the largest reduction in sediment flux to the coast in rivers (such as the Nile, Orange, Niger, and the Zambezi in Africa and the Yangtze, Indus, and Yellow in Asia), and 31% of the total sediment load retained in reservoirs were indicated in Asia and 25% in Africa (Syvitski et al., 2005b). Asian rivers were estimated to export 4.8 Gt yr^{-1} sediment to the oceans (Syvitski et al., 2011). Asian rivers export high sediment fluxes to the oceans, especially the Himalayan-Tibetan Plateau originating rivers (Evans et al., 2012; Ludwig and Probst, 1998; Milliman and Syvitski, 1992) (**Figure 1-4**). Most estimations of sediment flux were calculated based on a monthly or an annual scale.

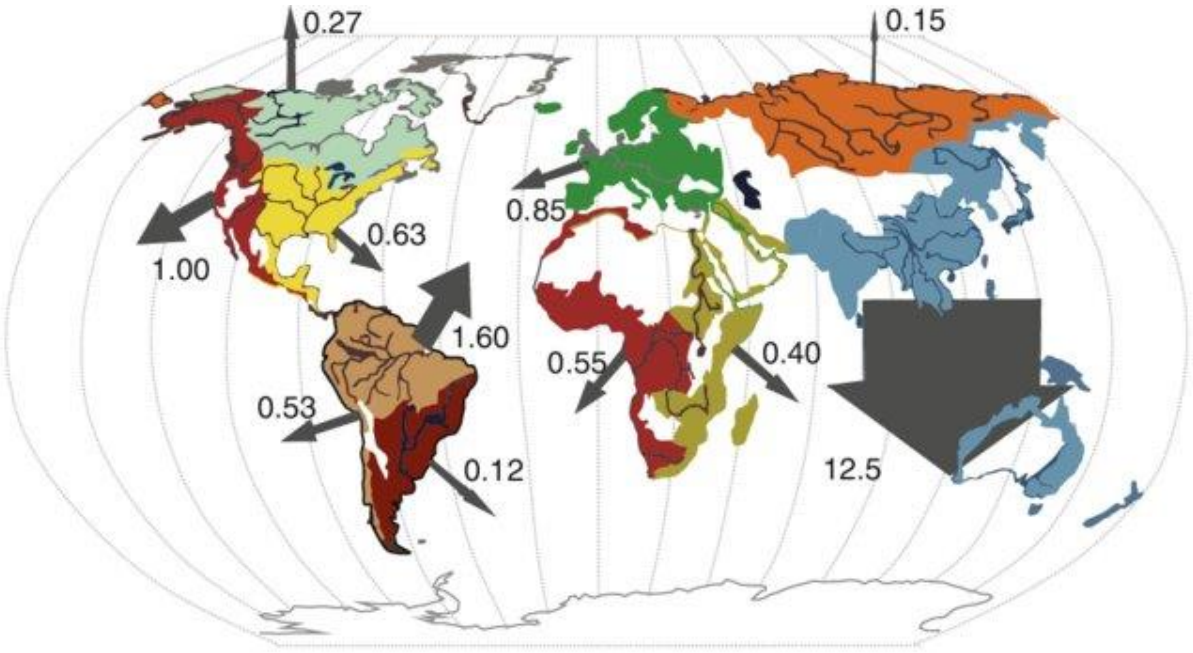

Figure 1-3: *Annual discharge of TSS to the global coastal ocean. Fluxes in Gt.y $^{-1}$. The total sediment mass is approximately 19 Gt.y $^{-1}$ (Depetris et al., 2014; Milliman and Farnsworth, 2011).*

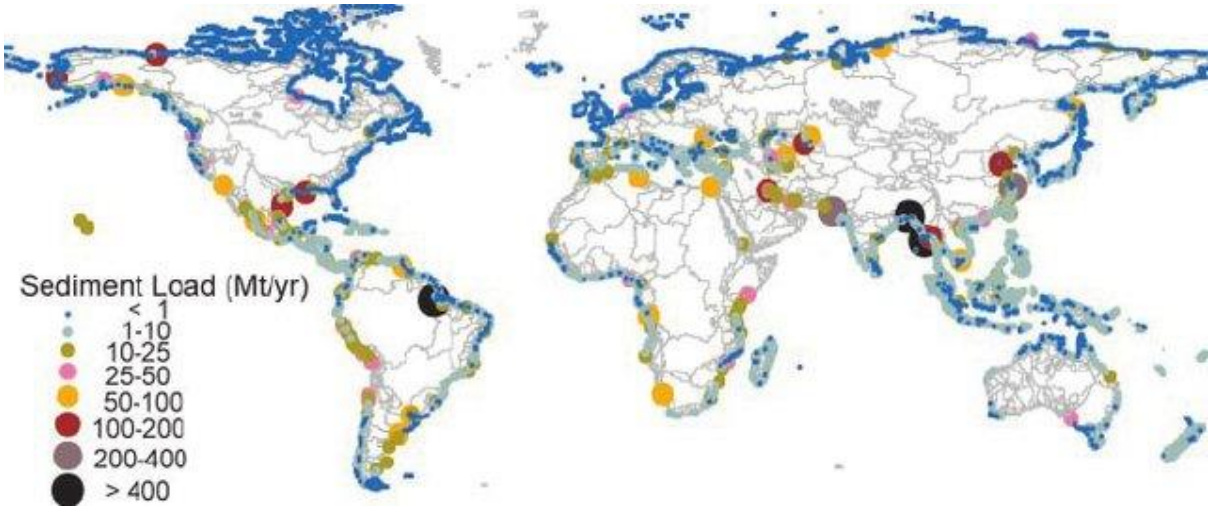

Figure 1-4: *Sediment flux. Predictions of the sediment load of rivers with basins larger than 25,000 km^2 (Arthurton et al.). Much of the world sediment is shed from the rivers that drain the Himalayas and the Tibetan Plateau.*

1.3. Global and Regional Riverine Nutrient Transports

Global nutrient inputs from major rivers into the oceans have tripled during the second half of the last century (Jennerjahn et al., 2004). Looking to the past five decades through anthropogenic activities such as increasing fertilizer use and cultivation of leguminous crops, the rate at which biologically available nitrogen enters the terrestrial biosphere has more than doubled (Galloway et al., 2004). These changes in global nutrient cycles have had both positive and negative effects (Li and Bush, 2015b). On the one hand, nitrogen and phosphorus are the most limiting elements for primary production and most responsible for eutrophication (Conley et al., 2009; Li et al., 2011; Stevens et al., 2004; Wassen et al., 2005). Changes in nutrient are a particular concern in tropical regions undergoing rapid development, and the Mekong basin is one of the major rivers to be concerned (Galloway et al., 2004). These global spatial patterns are reflected in variation in the relative contribution of different watershed sources and human drivers to river export between 2000 and 2030 (Seitzinger et al., 2010a) (**Figure 1-5**).

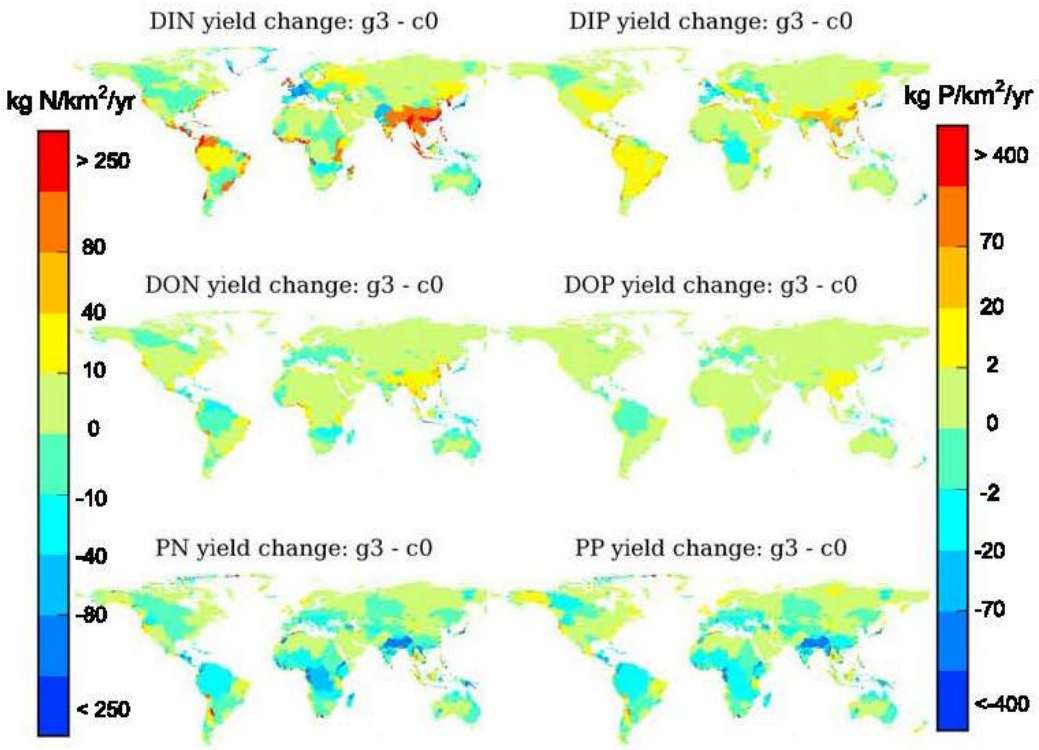

Figure 1-5: *Change in yields ($kg.km^{-2}.yr^{-1}$) between 2000 and 2030 from the 5761 basins for DIN, DON, and PN and DIP, DOP, and PP under the Global Orchestration scenario (Seitzinger et al., 2010b)*

Some studies have connected riverine supplement exports with anthropogenic driven changes on freshwater, coastal and marine biological systems at regional watershed scales (Meybeck, 1982; Seitzinger et al., 2005a; Seitzinger et al., 2010b; Turner and Rabalais, 1994), as well as at the river basin scale such as Yangtze (Duan et al., 2008; Duan et al., 2007; Liu et al., 2003; Müller et al., 2012), Mississippi (Lane et al., 2004; Raymond et al., 2008; Turner et al., 2003; Turner and Rabalais, 1994) and European rivers (Ludwig et al., 2010; Ludwig et al., 2009). The contribution of anthropogenic sources widely affects riverine fluxes of nitrate and phosphate, which have demonstrated sharp increases in some river systems (Li and Bush, 2015b).

The global anthropogenic P load to freshwater systems from both diffuse and point sources is estimated at 1.5 Mt/yr. In the period 2002–2010, the total global P input was 24 Mt of P per year (Mekonnen and Hoekstra, 2018a). Mineral fertilizer contributed most to the input of P in croplands, accounting for 71% of the global P input. Manure and irrigation water contributed another 24% and 5% of the total input, respectively. More than half of this total load was in Asia, followed by Europe (19%) and Latin America and the Caribbean (13%). The domestic sector

contributed 54% to the total, agriculture 38%, and industry 8%. In agriculture, cereals production had the largest contribution to the P load (31%), followed by fruits, vegetables, and oil crops, each contributing 15% (Mekonnen and Hoekstra, 2018b). China contributed most to the total global anthropogenic P load, about 30%, followed by India (8%), the USA (7%), and Spain and Brazil (6% each) (Mekonnen and Hoekstra, 2018a). The spatial variation in the intensity of anthropogenic loads of P is shown in **Figure 1-6**.

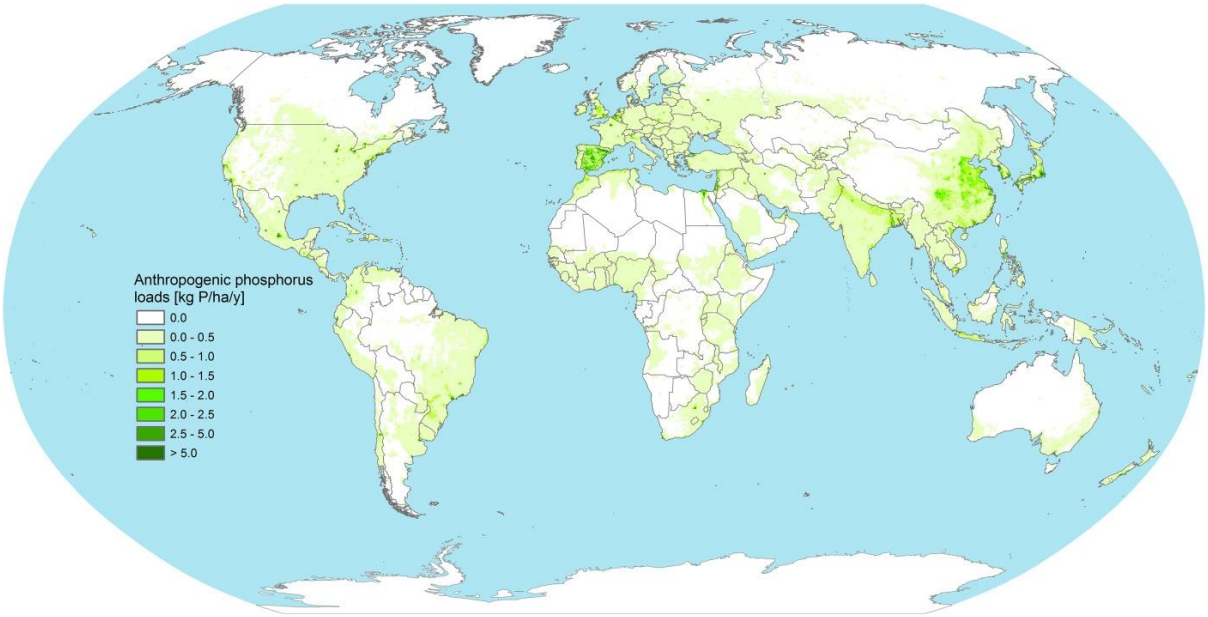

Figure 1-6: *Global spread of anthropogenic phosphorus loads to freshwater from agriculture, industrial, and domestic sectors from 2002 to 2010 (Mekonnen and Hoekstra, 2018a).*

1.4. Nutrient Transport Associated with Water Erosion

Along with the major water erosion process, large amounts of soil nutrient can be transported to water bodies that may degrade the erosion sites and result in water pollution problems in the nutrient-receiving water bodies. Because of the far-reaching ecological and environmental impacts of the nutrient transport processes during water erosion, much research has been done on this topic.

Rainfall and runoff are, respectively, the trigger and carrier for nutrient transport during water erosion. Nutrient losses tend to correlate positively with rainfall intensity and runoff volume (Kleinman et al., 2006). Raindrop impacts are essential in transferring nutrient solutes, as demonstrated by experiments showing that total dissolved nutrient losses with simulated rainfall were higher than the losses in simulations with only surface runoff (Fierer and Gabet, 2002). Linear relations can be established between nutrient losses and rainfall-runoff erosivity (Fen-Li, 2005).

Spatiotemporal variability of surface runoff generation triggers source area dynamics of sediments and sediment-associated nutrient transport (Ollesch et al., 2006; Wainwright et al., 2002). Nutrients can be transported in dissolved and particulate forms. P and N, the two nutrients of major concern, behave differently in soils and during the water erosion process.

Soil structure has important implications for nutrient transport in the erosion process, which is recognized as selective in physical and chemical properties. Nutrient loss is also significantly influenced by climate and topography. For example, nitrate's loss in runoff is affected by climate, with a sharp decrease in loss during the drought caused by the decreased runoff volume. Conversely, a significant increase of nitrate mass loss will be leachate during the drought (Grigg et al., 2004). Land use and land cover can regulate nutrient losses effectively. Vegetative cover influences the infiltration coefficient of rainwater and thus the runoff flow velocity (Li et al., 2006); soil erosion and nutrient loss are reduced accordingly.

1.5. Role of Lake Channel and floodplain in the Major Rivers

Floodplains are hydrologically dynamic systems characterized by highly complex surface hydrodynamics subjected to wide-ranging wetting and drying over seasonal timeframes (Bonnet et al., 2008; Li et al., 2019a; Li et al., 2020; Thomas et al., 2015). It is estimated that there are between 0.8 million and 2.2 million km^2 of rivers and lake-related floodplains worldwide (Entwistle et al., 2019).

Floodplains are hotspots of biodiversity and ecosystem services that are naturally productive and valuable (Dudgeon et al., 2006), providing a range of hydrological and ecological functions, including flood regulation, water purification, nutrient retention, critical wildlife habitats, and agriculture and livestock products (Funk et al., 2019; Robinson et al., 2015; van der Most and Hudson, 2018). However, floodplain areas have long been recognized as globally threatened ecosystems that are presently highly sensitive to anthropogenic interventions and climate change (Entwistle et al., 2019; Karim et al., 2015; Li et al., 2019b; van der Most and Hudson, 2018).

Several attempts have been conducted to analyze the water balance and hydrological regime of the Amazon River-floodplain (Rudorff et al., 2014), the Tonle Sap Lake-floodplain (Kummu et al., 2014), the Tana Lake-floodplain (Chebud and Melesse, 2009; Dessie et al., 2015), a North German river-floodplain (Krause et al., 2007), and the Bug River-floodplain systems (Dawidek et al., 2014). To the best of our knowledge, a large number of previous investigations of lake

hydrological and water balance analysis mainly focused on closed lakes, terminal lakes, and some Plateau lakes in different climatic zones (Li et al., 2020). Given the hydrological and ecological importance of floodplain lakes, they still have received little attention and not been adequately characterized concerning their hydrological processes and water balance with the link to water quality circulations. The large extent and remoteness of the majority of lake-floodplains worldwide have limited the establishment of a dense network of field-based monitoring, making sufficient investigations of their hydrological behaviours technically tricky and time-consuming (Khaki and Awange, 2019; Ovando et al., 2018). Given this background, improving understanding of data-limited floodplains can substantially aid in the assessment of their floodplain environment for scientists and managers (Li et al., 2020).

An inventory of large lakes of the world (Herdendorf, 1982), defined as those lakes with a surface area greater than 500 km, has identified 253 large natural lakes which span the globe from 80 ° N to 60 ° S (**Figure 1-7**). One hundred eighty-nine contain fresh water and are the reservoirs for over 68% of the fresh liquid surface water on earth (Reid and Beeton, 1992). However, despite their importance, large lakes and their role of Lake Channel and floodplain in the major river remain relatively unstudied by the scientific community.

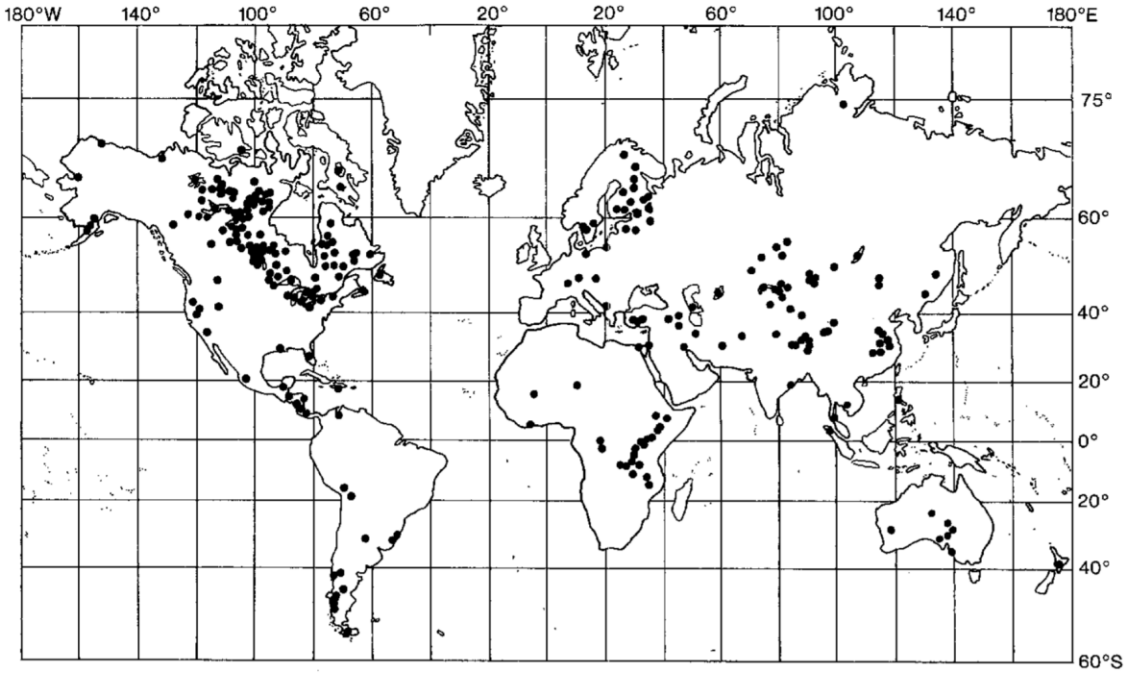

Figure 1-7: *Map showing the locations of the 253 identified large lakes of the world (Herdendorf, 1982; Reid and Beeton, 1992)*

1.6. Model Choice

Necessity and constraint of models: It is difficult to describe the rate of soil erosion in the watershed over spatial and time scales due to limitations in the field measurements for each part of the watershed. Long-term measurements are also needed in order to investigate the response of erosion rates to alterations in climate and land use or the efficiency of erosion control measures. Computer-based physical models can be used to counter these difficulties for erosion prediction over a wide range of conditions. The model result can be compared with field measurements to ensure and validate the model result. A desirable model should satisfy the requirements of universal acceptability, reliability, robustness in nature, and ease in use with a minimum of data, and the ability to take account of changes in land use, climate and conservation practices.

Benefits of physically-based models: Physically-based spatially distributed models can be used to identify critical areas by providing the output at any desired location within the watershed with increased accuracy of simulation compared to empirical or conceptual models. Erosion and sediment yield models represent a powerful tool to predict the effect of man-induced as well as natural environmental changes and impacts on the sediment dynamics. However, the potential of most of these models to be applied to evaluate scenarios of changing land use management or climate is not too high (De Vente et al., 2013). The main contributions of physically-based models to understand and simulate soil erosion processes in comparison with empirical/conceptual approaches are, i) more accurate extrapolation to different land use; ii) correct representation of erosion/deposition processes; iii) application to more complex conditions including spatially varying soil properties and surface characteristics; iv) more accurate estimation of erosion/deposition and sediment yield on a single storm event basis (Lane et al., 2001).

An exhaustive review of worldwide applications of the reviewed models revealed SWAT, WEPP, AGNPS, ANSWERS and SHETRAN models to be the most promising ones for simulation of erosion and sediment transport processes (Pandey et al., 2016).

SWAT model: SWAT (Soil Water Assessment Tool) is a hydro-agro-climatological model developed by USDA Agricultural Research Service (USDA-ARS; Temple, TX, USA) and Texas A&M AgriLife Research (College Station, TX, USA; Arnold et al., 1998). SWAT is firstly designed to predict impacts of human activities management on water, sediment, and agricultural chemical yields in ungauged catchments and can provide continuous simulations for dissolved and particulate elements (Arnold et al., 1998) (**Figure 1-8**). Its performance has already been tested at

multiple catchment scales in various climatic and soil conditions on hydrology but also water chemistry, especially TSS and nitrogen exports (Douglas-Mankin et al., 2010; Faramarzi et al., 2013; Krysanova and White, 2015; Kuzin et al., 2010; Schuol et al., 2008). Importantly, both the SWAT model and the ArcSWAT interface are open source and free, allowing reproducibility of the results once the input data are well documented (Olivera et al., 2006). Theory and details of hydrological processes integration of SWAT model are available online in the SWAT documentation (http://swatmodel.tamu.edu/).

Although SWAT has been applied to many Asian basins and subtropical or/and tropical areas, most of them were at a scale of 77 to 105,000 km^2 (Bannwarth et al., 2015; Graham and Butts, 2005; Lweendo et al., 2017; Shrestha et al., 2018; Tan et al., 2019). The SWAT model has already been tested in Southeast Asia systems (Tan et al., 2019), and It has proved its applicability on a global scale, too, for it has been tested in various countries.

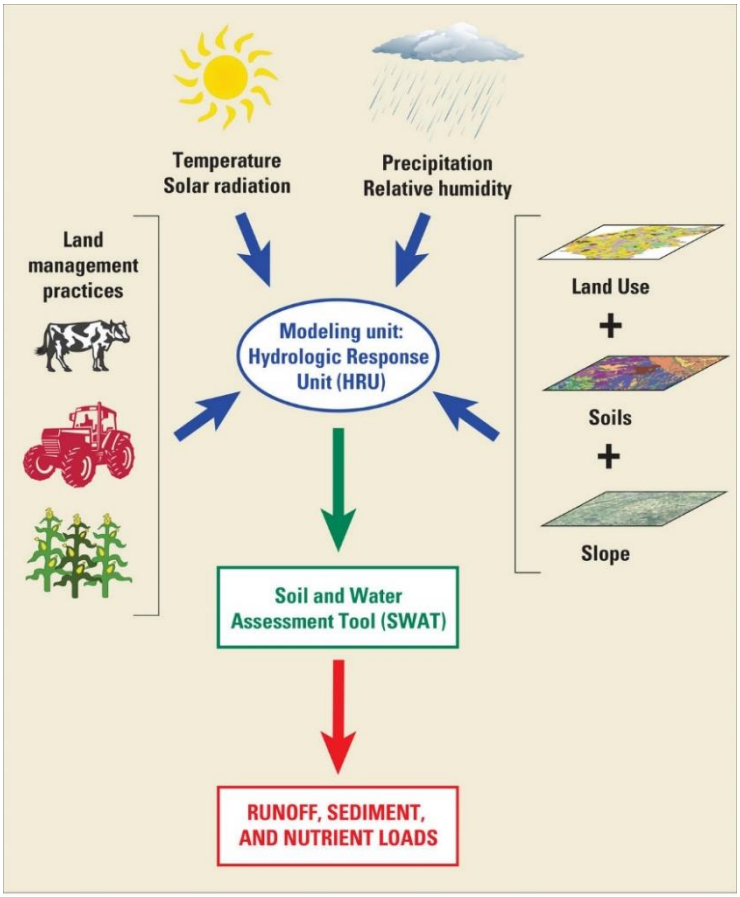

(https://www.usgs.gov/media/images/glri-edge-field-swat-modeling-inputs-and-outputs)

Figure 1-8: *Input and output products of the Soil Water Assessment Tool (SWAT) used for edge-of-field modelling*

1.1. Context and problematic

The processes of erosion, sediment delivery and sediment transport are key components and measures of the functioning of the earth system. The sediment load of a river provides an important measure of its morpho-dynamics, the hydrology of its drainage basin, and the erosion and sediment delivery processes operating within that basin. The magnitudes of the sediment loads transported by rivers have important implications for the functioning of the system; for example, through their influence on material fluxes, geochemical cycling, water quality, channel morphology, delta development, and the aquatic ecosystems and habitats supported by the river.

Similarly, the sediment loads of rivers can exert an important control on the use of a river for water supply, transport and related purposes. Changes in land-ocean sediment transfer will result in global biogeochemical cycles, particularly in the carbon cycle, since sediment plays an important role in the flux of many key elements and nutrients, including organic carbon. At the regional and local levels, changes in erosion rates can have important implications for agricultural production and food security sustainability.

Sediment in the Mekong River is important to sustain the geomorphology of the floodplains and particularly the Tonle Sap Lake and provide essential nutrients for the lake's productive ecosystem (Kummu et al., 2008b). As a requisite part of the Mekong River system, the Tonle Sap Lake in central Cambodia is Southeast Asia's largest permanent freshwater body and the essential natural reservoir from which the Mekong River benefits (Kummu et al., 2008b). Further, the Tonle Sap Lake and its floodplains connecting with the Mekong mainstream through the Tonle Sap River rely as well upon the Mekong sediment regimes since the primary source of sediment supply to the Tonle Sap Lake is sediment transport from the Mekong (Kummu et al., 2008b; Lu et al., 2014). The Mekong River is responsible for the majority (more than 70%) of the sediment delivered to Tonle Sap Lake (Kummu et al., 2008b; Ty et al., 2020). The fact that the Mekong River basin spreads across six countries has made studying the system a complex task. Much importance is given to modelling in terms of developing sustainable management of water resources at the river basin scale, which can help evaluate current water resources, identify pollution sources, and improve sustainable development (Bouraoui et al., 2005).

Compared to other rivers in Asia, such as the Ganges and the Yangtze, the annual nitrogen load in the Mekong was still low in the twenty-century (Seitzinger et al., 2005a). However, the Mekong is facing the disruption of its nutrient balance as large increases of nutrient inputs to surface water

are expected in the twenty-first century due to increases in agricultural production and infrastructure development (Commission, 2003; Galloway et al., 2004; Liljeström et al., 2012). Long-term and spatial watershed monitoring data are rare due to the expense involved (Santhi et al., 2001); however, long-term simulations are possible using water quality models (Wu and Chen, 2009).

Therefore, the sediment and nutrient assessment in the Mekong River and linkage between the Mekong mainstream and the Tonle Sap Lake would be necessary to better understand as the sediment and nutrient input from the Mekong is crucial for the Tonle Sap's ecosystem functions and better understand the role of Tonle Sap Lake system to the Mekong River and its delta.

1.7. Objective of Research

The specific objectives are:

(1) To comprehensively analyses and present a quantification of annual, seasonal and monthly nitrate the sediment and nutrient transport exchange between Tonle Sap Lake and the mainstem Mekong River through the hydrological reversal system.
(2) To assess basin hydrology, focusing on the water balance components and contribution of the different compartments of the basin to water yield and quantifying the sediment load and spatial sediment yield in the Mekong River Basin.
(3) To model the nutrient flux of nitrate transport and determine the spatial variability of nitrate yields in the Mekong River Basin.
(4) To define the role of Tonle Sap Lake in Nutrient connection with Mekong River through the assessment coupling data and modelling approaches.

1.8. Thesis Structure

The thesis consists of four publications (two accepted, one under review, and one to be submitted).

- **Chapter I** addressed the general context of the research, research problems and questions, the thesis's objectives, and chapter descriptions are containing the thesis**.**
- **Chapter II** started with describes the materials and methods used to accomplish the objectives. The materials concern with the description of the study area (localization, soil, land use and hydro-climatic regime), water quality database used in the study. The model selection and description were also attributed.

- **Chapter III** involved the temporal variability of sediment loads in Tonle Sap and Lower Mekong Rivers in Cambodia, assessing the sediment linkage between the Tonle Sap Lake and the Mekong mainstream, which is connected by a seasonally reverse flow through the Tonle Sap River. This chapter presented an accepted paper in the Journal of Catena.
- **Chapter IV** provided the first attempt to estimate inter-annual and intra-annual variability of nutrients fluxes of the Lower Mekong River and Tonle Sap River in Cambodia and assessed the nutrients flux linkage between Mekong River and Tonle Sap Lake. This chapter was written in the form of publication and under review in Ecological Engineering.
- **Chapter V** deals with hydrology and sediment transport of the Mekong River Basin to assess long-term basin hydrology, quantify the part of erosion and sediment yield, and identify contributing erosive zones in the Mekong River Basin. This chapter was written in the form of publication accepted in Water.
- **Chapter VI** examined the spatial and temporal differences in nitrate loads together with nitrate net balance, including nitrate removal and nitrate production of the Mekong River basin. This chapter will be submitted to the journal of Ecohydrology.
- **Chapter VII** provides a general discussion of the whole results on sediment and nutrient issue related to the Mekong river basin.
- **Chapter VIII** summarized the main findings of the thesis and their applications, followed by some perspectives for future research.

CHAPTER II

Materials and Methods

This chapter describes the overall and specific materials and methods used to accomplish the objectives. The materials covered the description of the study area (climate, soil, land-use and hydrology regime), sediment load calculation, and trend detection method. The model selection and description of the model concepts were also described.

2. Chapter II. Materials and Methods

2.1. Global Theme of the Materials and Method

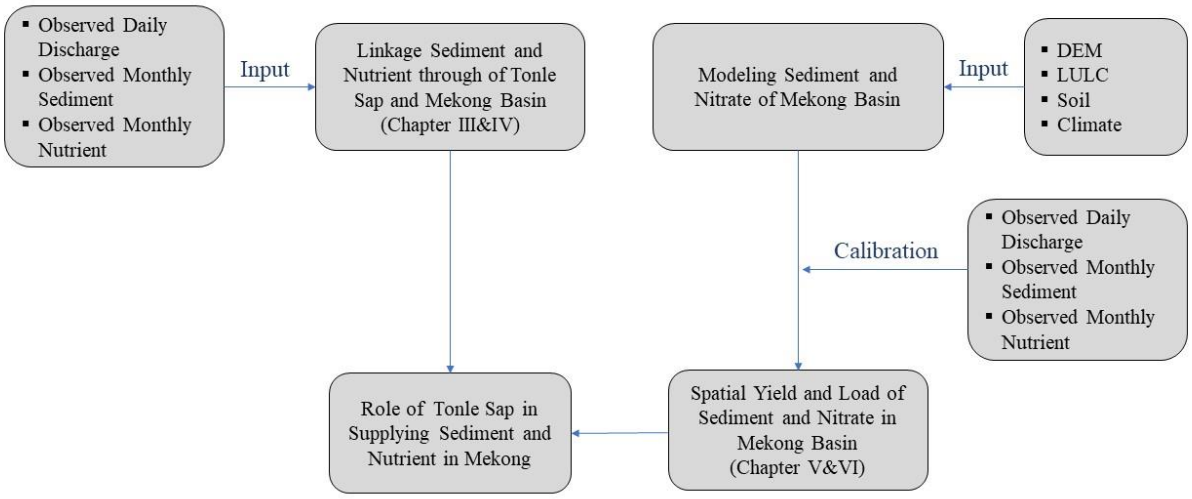

Figure 2-1: *Theme of materials and methods for this study.*

2.2. Study Area

2.2.1. General Information

The Mekong River in Southeast Asia is the 12th longest river in the world (4,800 km) has the 21st largest river basin area at 795,000 km^2, and the 8th largest average annual runoff, 470 km^3. The Mekong River basin is conventionally divided into two basins: The Upper Mekong basin (UMB), with 24% of the total basin area (21% in China, 3% in Myanmar), and the Lower Mekong basin (LMB), with 76% of the total basin area (Laos 25%, Thailand 23%, Cambodia 20% and Vietnam 8%) (**Figure 2-2**). In the Upper Mekong River Basin in China's Yunnan Province, the tributaries are small. As the river widens in the Northern Highlands, large tributaries – including the Nam Ta, Nam Ou, Nam Soung and Nam Khan – enter the Mekong River's left Nam Mae Kok and Nam Mae Ing enter on the right bank. Further downstream in the Khorat Plateau, the mainstream is joined by the gently sloping Songkhram and Mun Rivers on the right bank and the steep Nam Ca

Dinh, Se Bang Fai and Se Bang Hiang Rivers on the left bank. The Se Kong, Se San, and Sre Pok (3S Basin) are the main tributaries entering on the left bank of the Mekong.

The Tonle Sap River drains the Great Lake (or Tonle Sap Lake) into the Mekong River during the dry season and reverses its flow during the rainy season. Near the Cambodian capital Phnom Penh, the Bassac River, the Mekong's largest distributary, branches off. This is where the Mekong Delta begins as the Mekong and Bassac Rivers enter a large fertile plain in southern Viet Nam. In this area, known as the 'Nine Dragons', a series of smaller distributaries split off Mekong and Bassac's mainstream.

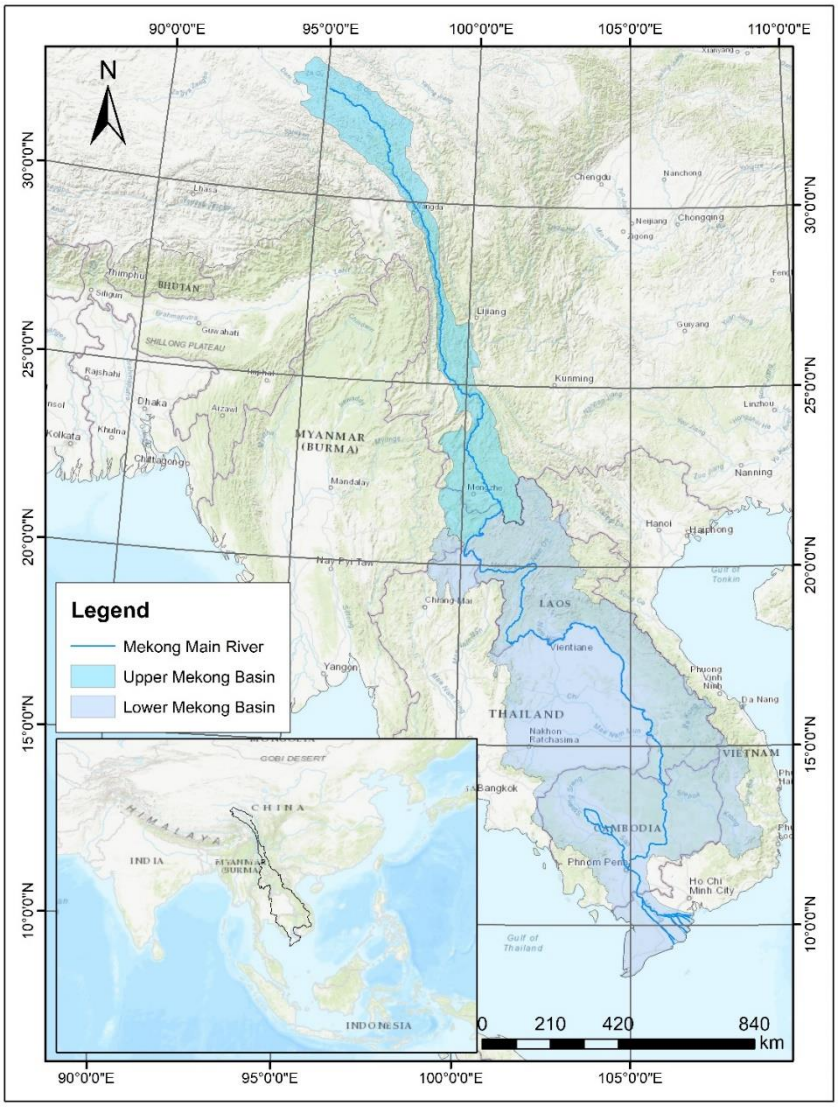

Figure 2-2: *Mekong River basin is conventionally divided into two basins: The Upper Mekong basin (UMB), with*

24% of the total basin area, and the Lower Mekong Basin (LMB), with 76% of the total basin area

The Mekong Basin climate is the Southwest Monsoon divided into two distinct seasons: wet and dry seasons of more or less equal length. The monsoon season commonly lasts from May until late September (or early October). Annual average rainfalls over the Cambodian floodplain and the Vietnamese delta are less than 1,500 mm. The highest rainfalls occur in the Central Highlands and within the mainstream valley in central Laos. At altitudes above 500 masl, dry season temperatures are lower, though not by much. In the warmest months of March and April, the average temperature ranges from 30°C to 38°C. Rainy season means temperatures decrease significantly from south to north, from 26°C to 27°C in Phnom Penh to 21°C to 23°C in Thailand northern part. The discharge of the Mekong river reaching the sea is averagely 15 000 m^3/s (Adamson et al., 2009; Gupta and Liew, 2007).

In Cambodia, the Mekong River connects with Tonle Sap Lake (the most extensive permanent freshwater body in Southeast Asia) via the Tonle Sap River at the Chaktomuk confluence at Phnom Penh (**Figure 2-2**). Tonle Sap Lake (TSL) has a unique hydrological system governed by a flood pulse from the Mekong River. The lake is approximately 120 km long and 35 km wide and covers 2,500 km^2 in the dry season, but it expands up to 250 km long and 100 km wide and covers 17,500 km^2 in the wet season because high stages in the mainstem Mekong River drive flow upstream through the Tonle Sap River (Campbell et al., 2009). From October to April, flow in the mainstem Mekong recedes, and water flows back from Tonle Sap Lake to the Mekong River via the Tonle Sap River (Fujii et al., 2003; Masumoto, 2000). The majority of water in the Lake in the wet season is from the Mekong mainstem (Kummu et al., 2014). This water's delayed release provides important freshwater to the Mekong Delta in Cambodia and Vietnam during the low flow period (dry season), protecting the fertile agricultural lands from saltwater intrusion from the sea (Hai et al., 2008).

2.2.2. Topography

The UMB is characterized by high mountains, steep slopes, deep gorges, and narrow catchment areas. The Mekong cascade down more than 4000m over a distance of 2000 km from its headwater in China to Chiang Saen in northern Thailand, with an average slope of 2 m/km (Lauri et al., 2012). The LMB of Laos, Thailand, Cambodia and Vietnam (76% of total Basin area) includes the Northern Highlands, Korat Plateau, Tonle Sap Basin, and Mekong Delta physiographic regions

(MRC, 2010). From Chiang Saen in China to Kratie in central Cambodia, the Mekong has a moderately steep slope, falling about 500 m over 2000 km, with an average slope of 0.25 m/km (Laurie et al.). Further downstream, the river is nearly flat, losing only 15 m in elevation over the final 500 km of the Mekong Delta region to the South China Sea (MRC, 2005).

Figure 2-3 presents the elevation maps, which were developed by removing multiple error components (absolute bias, stripe noise, speckle noise, and tree height bias) from the existing space-borne DEMs (SRTM3 v2.1 and AW3D-30m-v1). The elevation distribution varies from -23 m to 6720 m as representing the topographic condition for the Mekong River Basin.

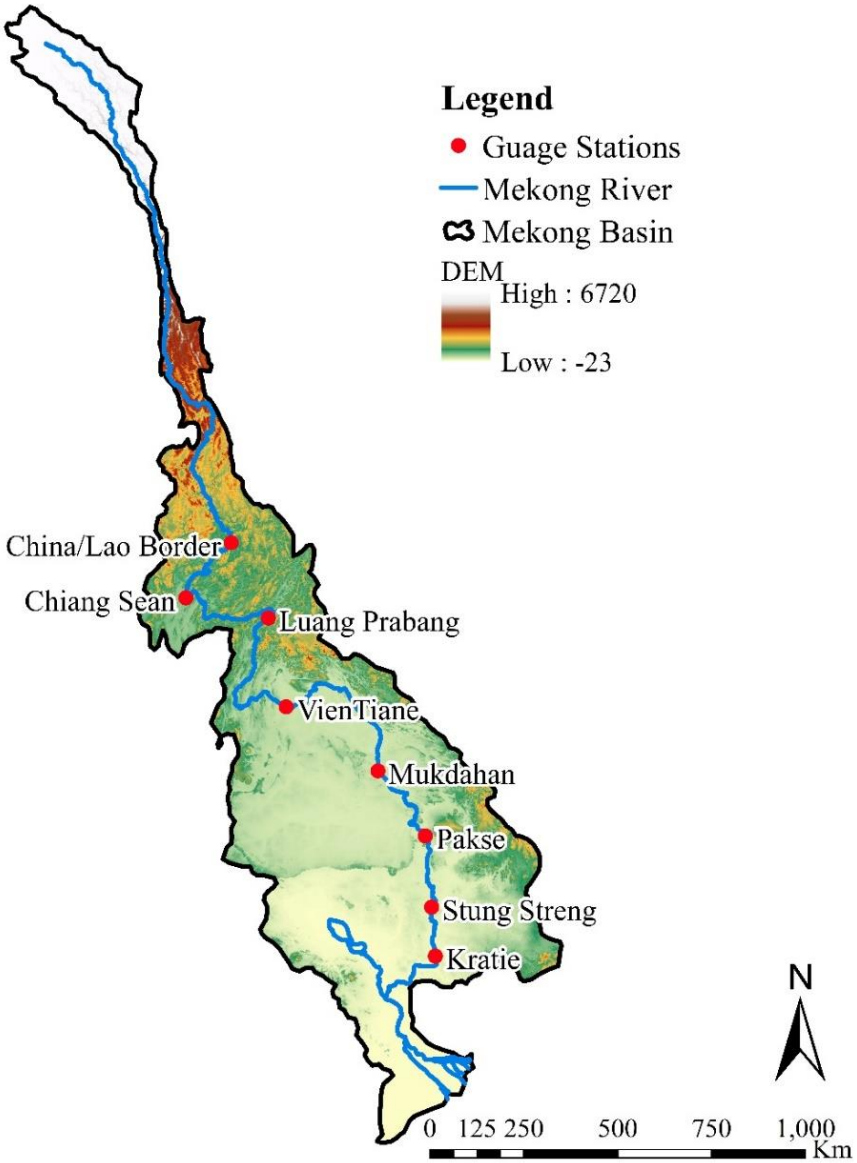

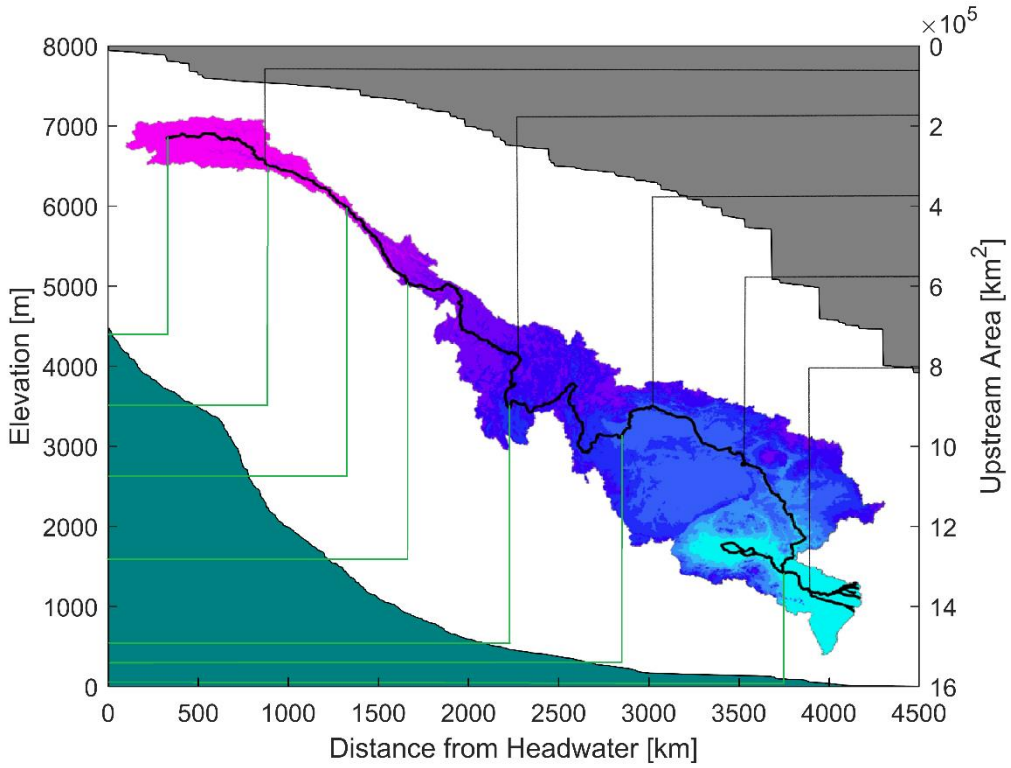

Figure 2-3: *Elevation of Mekong River Basin and longitudinal profile of the Mekong River*

2.2.3. Climate Characteristic

The climate of the Mekong Basin is dominated by the Southwest Monsoon, which generates wet and dry seasons of more or less equal length (**Table 2-1**). The monsoon season usually lasts from May until late September or early October. There is usually heavy rainfall (> 5 mm) on one day in two over most of the region. Later in the rainy season, tropical cyclones occur over much of the area, so August and September, and even October (in the delta) are the wettest months of the year.

Table 2-1: *Generalized climate seasons in the Mekong River basin*

Cool/Cold			Hot/Dry		Wet						Cool/Cold
Jan	Feb	Mar	Apr	May	Jun	Jul	Aug	Sep	Oct	Nov	Dec
NE Monsoon			Transition		SW Monsoon						NE Monsoon

The Northeast Monsoon, which sets in towards late October, brings lower temperatures. During the months of the NE Monsoon, rainfall is generally confined to Viet Nam since the rest of the Lower Mekong region lies in the lee of the Annamite Mountains or the Central Highlands. In the Upper Basin, Yunnan province of China has a similar monsoon climate, although there is considerable variation with local topography. The climate varies from tropical and subtropical monsoons in the south of Yunnan to temperate monsoons in the north. The land rises from a mean elevation of 2,500 meters above sea level (masl) to 4,000 masl on Tibet's Plateau.

Temperature and Evaporation

The seasonal range of mean temperatures in the lowlands and river valleys of the Lower Basin is not large. There are, however, significant changes, both season to season and from day to night at increasing altitudes and in the more temperate climates to the north. The mean monthly temperature data for both the Upper and Lower Mekong are in **Table 2-2**.

Table 2-2: *Mekong basin monthly temperature data (ºC) at selected sites (Data from MRC)*

Site	Altitude masl	Jan	Feb	Mar	Apr	May	Jun	Jul	Aug	Sep	Oct	Nov	Dec
Deqen (China)	4,000	-4	-2	2	5	10	13	13	13	11	11	6	-3
Chiang Rai	382	21	22	26	30	29	27	28	27	27	27	23	21
Luang Prabang	305	22	23	26	28	28	28	28	28	27	27	24	21
Vietiane	170	24	25	28	29	29	29	28	28	28	28	25	23
Khon Kaen	166	24	25	28	29	28	28	27	27	26	26	25	23
Pakse	102	26	27	30	30	29	29	28	28	28	28	26	25
Phnom Penh	10	27	28	30	31	30	29	28	28	28	28	27	26

Annual evapotranspiration rates range between 1 and 2 meters, with little variability from year to year—the high relative humidity results in relatively constant annual values. The Korat Plateau in Northeast Thailand, mainly the Mun and Chi Basins, is one of the driest areas in Southeast Asia. In many climate classification systems, this region is defined as semi-arid. For example, at Khon Kaen, the mean annual rainfall is 1,200 mm, compared to a mean annual evaporation rate of 1,900 mm. Lack of soil moisture in the area becomes critical during the late dry season from February to April.

Further south in the Cambodian and Vietnamese parts of the Basin, annual evaporation rates are somewhat lower at 1,500 to 1,700 mm. To the north at Chiang Rai, the rate is around 1,400 mm. Within the Lower Basin, anywhere below an altitude of 500 masl, annual evapotranspiration rates generally do not fall below 1,000 mm. In the Upper Basin, evaporation rates are more complex due to rapid altitude and slope orientation changes. Data for many climate variables are only useful within local areas.

The Rainfall

The distribution of mean annual rainfall over the Lower Basin is mapped in **Figure 2-4**. This figure shows a range from less than 1,500 mm in most Thai sub-basins to over twice in the Central Highlands of Lao PDR. The map clearly shows that the left bank tributaries of Lao PDR generate most of the flows to the mainstream.

The Lower Basin is divided into six sub-regions to compare annual and monthly rainfall and changes in space and time. **Table 2-3** compares long-term averages. Annual average rainfalls over the Cambodian floodplain and the Vietnamese delta are equally low and less than 1,500 mm. elsewhere. The highest rainfalls are in the Central Highlands and within the mainstream valley at Pakse. Rainfall is lower in the more temperate northern regions around Chiang Rai. July, August and September are generally the months of highest rainfall. However, there is evidence of a shift to later in Cambodia and the delta, where more rain falls in September and October.

Table 2-3: *Mekong Basin annual and seasonal average rainfall (mm) for representative sub-regions (Data from MRC)*

Month	Northern Region	Central Region	Korat Plateau	Central Highlands	Cambodian Floodplain	Vietnam Delta
	Chiang Rai	Pakse	Khon Kaen	Pleiku	Phnom Penh	Chau Doc
Jan	13	2	5	6	8	8
Feb	10	7	15	6	3	3
Mar	20	20	35	25	15	15
Apr	85	70	60	85	65	75
May	190	220	170	225	115	165
Jun	210	380	180	350	125	110
Jul	310	390	160	360	160	140
Aug	390	500	185	460	160	170

Sep	280	320	260	360	265	160
Oct	140	100	120	220	255	250
Nov	60	20	10	75	130	160
Dec	20	3	3	20	20	40
Annual	1,730	2,050	1,210	2,200	1,320	1,300

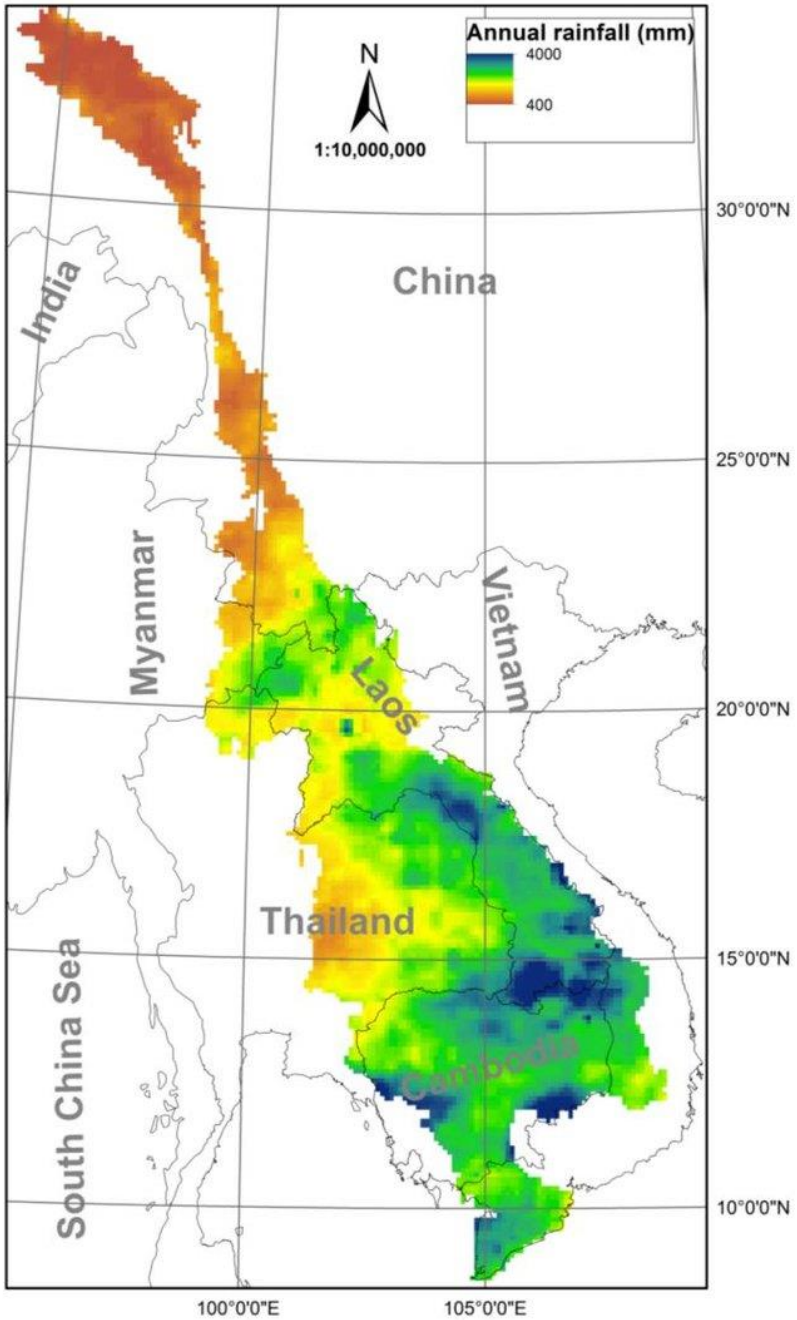

Figure 2-4: *Annual rainfall patterns in the Mekong. Data from MRC*

2.2.4. Hydrology Characteristic

Flows in the Mainstream and Major Tributaries

The mean annual discharge of the Mekong is approximately 475 cubic kilometres (km^3). Of this amount, about 16 per cent comes from China and only 2 per cent from Myanmar. Most of the remainder comes from Lao PDR and the major left bank tributaries, notably the tributaries that enter downstream of Vientiane (***Figure 2-5***).

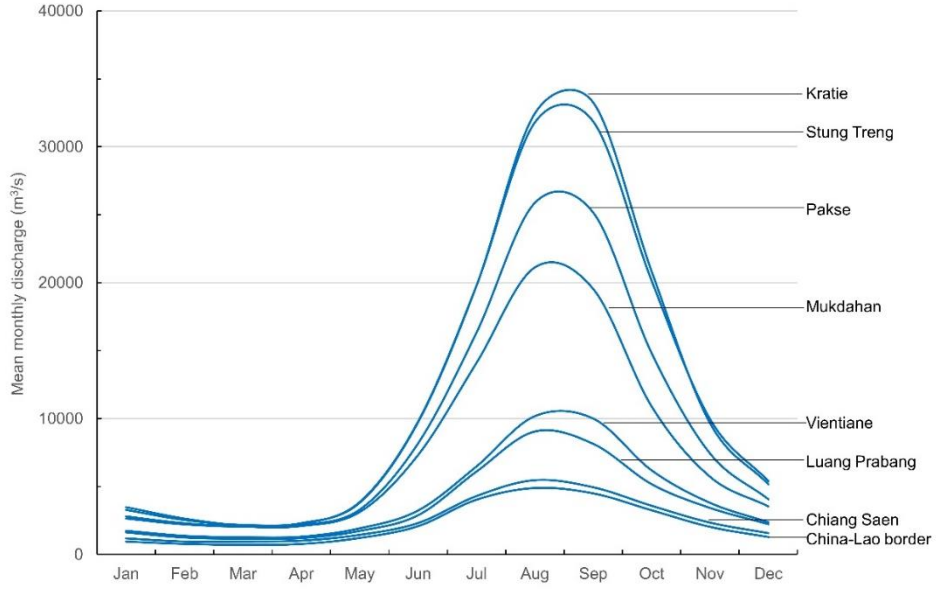

Figure 2-5: *Mean monthly discharge at various sites on the mainstream (Data from MRC)*

Table 2-4 Summarizes the mean annual flows along the mainstream. The mean annual flow entering the lower Mekong from China is equivalent to a relatively modest 450 mm depth of runoff. This increases to over 600 mm as the principal left bank tributaries to enter the mainstream downstream of Vientiane. The flow level falls again, even with the right bank from Thailand. Runoff in the mainstream increases again with the entry from the left bank of the Se Kong from southern Lao PDR and Se San and Sre Pok from Viet Nam and Cambodia. Flows at Chiang Saen entering the Lower Basin from Yunnan make up about 15 per cent of the wet season flow at Kratie. This rises to 40 per cent during the dry season, even this far downstream.

Table 2-4: *Mekong Mainstream mean annual flow (1960 to 2004) at selected sites (MRC)*

Mainstream Site	Catchment area km^2	Mean annual flow as			as % total Mekong
		Discharge (m^3/s)	Volume km^3	Runoff mm	
Chiang Saen	189,000	2,700	85	450	24
Luang Prabang	268,000	3,900	132	460	34
Vientiane	299,000	4,400	139	460	38
Mukdahan	391,000	7,600	240	610	49
Pakse	545,000	9,700	306	560	69
Stung Treng	635,000	13,100	413	650	80
Kratie	646,000	13,200	416	640	81

Kratie is generally regarded as the point in the Mekong system where the hydrology and hydrodynamics of the river change significantly (MRC, 2005). Upstream from this point, the river generally flows within a clearly identifiable mainstream channel. In all but the extreme flood years, this channel contains the full discharge with only local over-bank natural storage. Interestingly, Kratie is located at about 600 km from the point of discharges of Mekong River at the South China Sea. Downstream from Kratie, seasonal floodplain storage dominates the annual regime, and there is significant movement of water between channels over flooded areas, the seasonal refilling of the Great Lake and the flow reversal in the Tonle Sap. There is extreme hydrodynamic complexity in both time and space, and it sometimes becomes impossible to measure channel discharge. Water levels, not flow rates and volumes, determine the movement of water across the landscape.

2.2.5. Land use/Land Cover and Soil Characteristic

Base on the land use distribution in the Mekong River Basin, which was obtained from the Global Land Cover Database (www.usgs.gov) at a 1 km resolution, the land use and their distribution of the watershed were divided into 18 categories, which was separated by five major types of land-use can be found in the Mekong River Basin (**Figure 2-6**). The largest land-use area is forest, followed by agriculture, grass and shrub, urban, and water resources. The forest area includes deciduous, grass cover, evergreen, shrub cover, tree cover, flooded and coniferous forests covering

an area of 648,438 km^2, accounting for 72.54% of the whole basin. The agricultural land comprises cultivated area, cropland, artificial surface, and broadleaved cover of 230,641 km^2, which accounts for 25.8% of the Mekong River Basin. The others area includes urban and water covering 14,848 km^2, accounting for 1.66% of the total watershed.

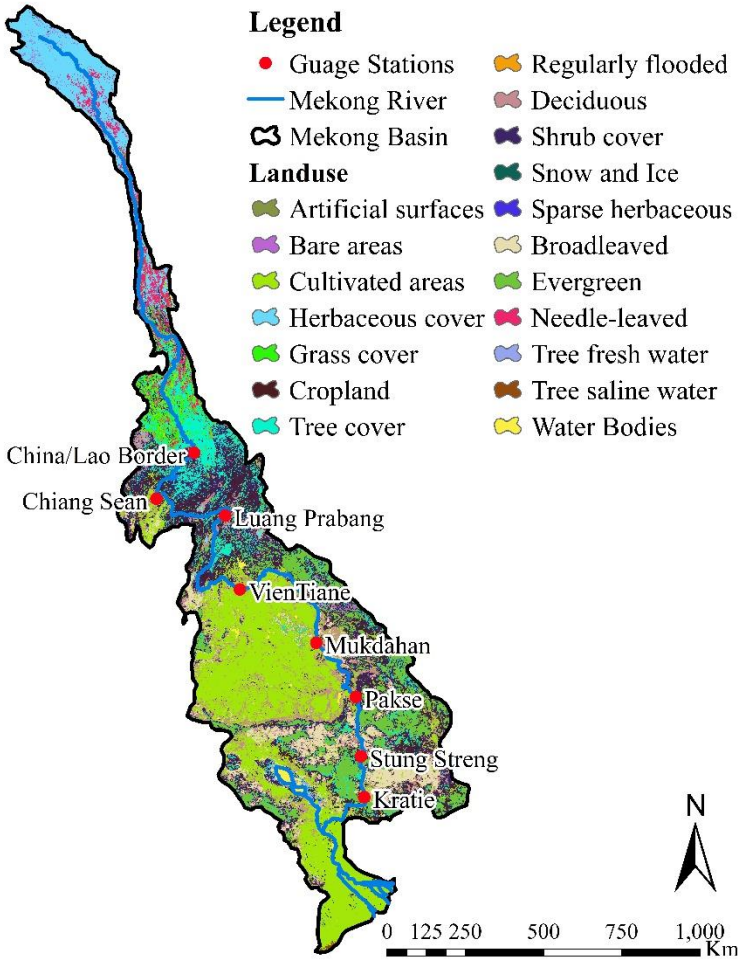

Figure 2-6: *Land use/Land cover classification and distribution of the Mekong River Basin*

Base on the land use distribution in the Mekong River Basin, which was obtained from Global Soil data by FAO (www.fao.org/) (**Figure 2-7**). Seven major types of soil, namely Acrisols, Leptosols, Gleysols, Nitisols, Luvisols, Cambisols and Ferralsols, can be found in the Mekong River Basin. Such soils can stand alone or be mixed to create 22 soil types of the whole basin. The dominant soil type is Acrisols covering 620,617 km^2, accounting for 69.5% of the whole basin. Leptosols is covering an area of 66,803 km^2, accounting for 7.5% of the whole basin. Gleysols are covering an area of 60,897 km^2, accounting for 6.8% of the whole basin. Nitisols, Luvisols, Cambisols and Ferralsols are coverage an area of 25,470 km^2, 22,376 km^2, 19,571 km^2, and 19,243 km^2,

accounting for 2.85%, 2.5%, 2.19%, and 2.15% of the whole basin, respectively. For others area covering an area of 58,952 km^2, accounting for 6.6% of the total watershed.

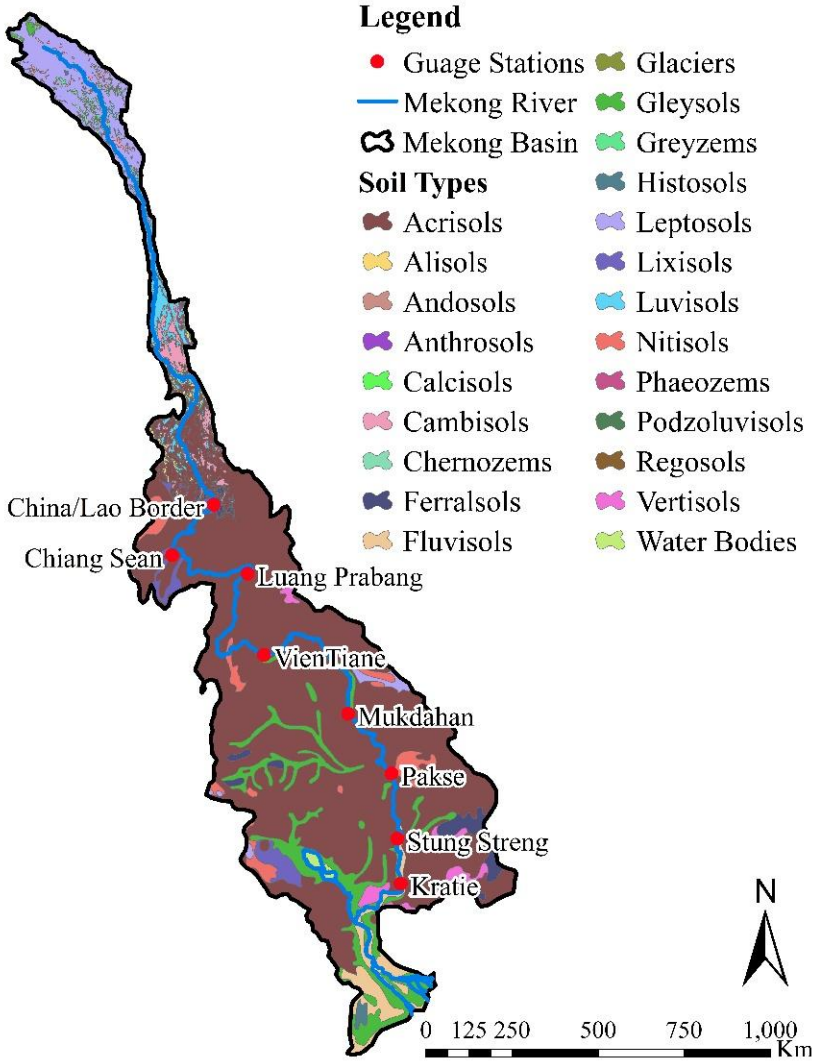

Figure 2-7: *Soil characteristic classification and distribution of the Mekong River Basin (Global Soil data by FAO)*

2.2.6. Tonle Sap Lake, Floodplain and Basin

The Cambodian Floodplain and the Tonle Sap Lake Basin

The Tonle Sap River and Great Lake System represent one of the world's most productive ecosystems. This river-lake system supports the world's largest freshwater fishery and directly or indirectly provides a livelihood for most of Cambodia's population. This high biological productivity depends on the transfer of floodwater from the Mekong during the wet season when

increased water levels in the mainstream at the confluence with the Tonle Sap River cause the water in the river to flow upstream and back into the Great Lake:

- The lake area increases from a dry season average of 2,500 km^2 to a typical flood season area of 15,000 km^2.
- Typically mean depth increases from 1 m to 6-9 m.
- During the wet season, the lake volume rises to between 60 and 70 km^3 from a dry season figure of less than 1.5 km^3.

The lake functions as a natural storage reservoir for Mekong floodwater. When the water in the lake is slowly released from October onwards, it becomes a crucial source of water supply to the delta during the dry season.

The Tonle Sap Lake Basin consists of the Tonle Sap Lake and 11 major tributaries, with a total catchment area of 86,000 km^2 (**Figure 2-8**). The majority of the basin consists of lowlands less than 100 m above the mean sea level and with gentle slopes.

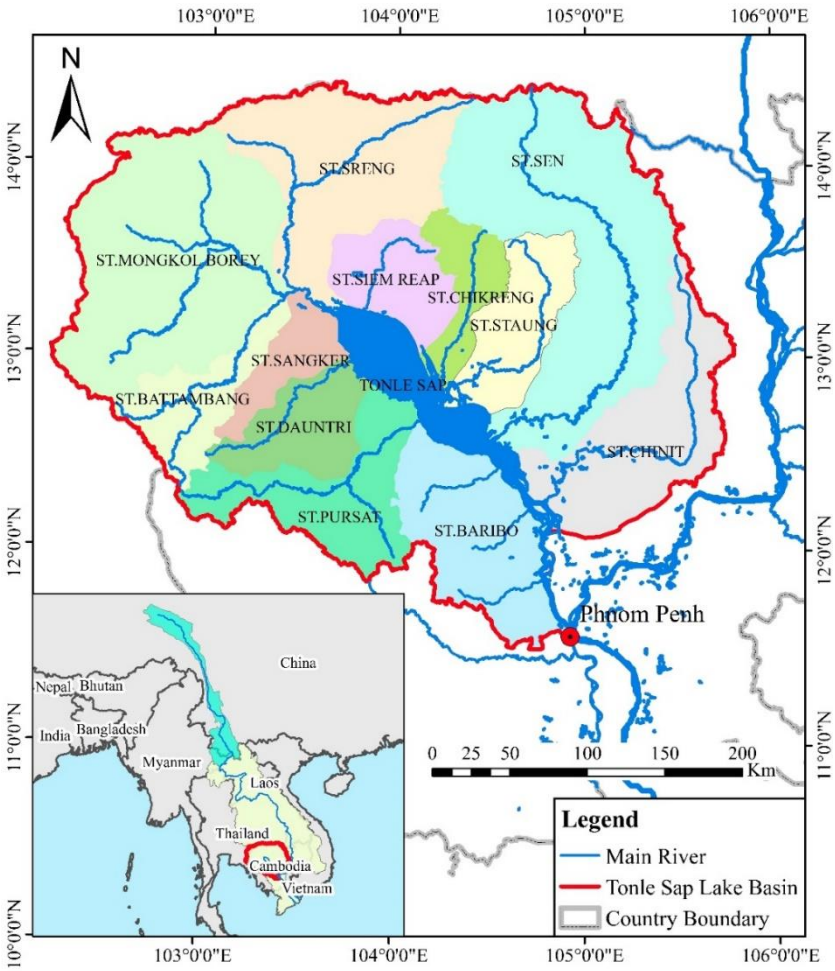

Figure 2-8: *Tonle Sap Lake Basin consists of the Tonle Sap Lake and 11 major tributaries*

The mean annual reverse flow volume in the Tonle Sap is 30 km^3 or about half of the maximum lake volume. A further 10 per cent is estimated to enter the system by overland flow from the Mekong. The lake's natural catchment drains most of western and northwestern Cambodia, in all amounting to about 25 per cent of the country's total area. Typically, this drainage would supply between 40 and 50 per cent of the lake's flood volume. Therefore, interventions upstream of the lake could impact the system and its ecological productivity equal to any in the wider Mekong system. In all, the Tonle Sap System covers 85,000 km^2 and contributes about 6 per cent of the Mekong Basin's mean annual flow.

Tonle Sap and Other Lake-Channel Systems

The Tonle Sap is an example of a lake-channel system, a lake (usually on a floodplain) that connects with the main river (via defined channels and overbank flow), and that absorbs flood peaks and releases waters gradually back into the main river as flood stage recedes. Retaining floodwaters in the lake for extended periods can substantially deposit sediment from suspension, potentially impacting the riverine sediment budget. Thus, we can ask how the Tonle Sap system compares with other major lake-channel systems, such as Dongting Lake on the Yangtze River floodplain, the second-largest freshwater lake in China, and the channel-floodplain systems of the Amazon River.

The Dongting Lake- Yangtze River system is similar to the floodplain lake-channel exchanges of TSL and Mekong River. Dongting Lake plays a vital role in regulating the flood stage and is an important sink of sediments. In flood season, water pours into Dongting Lake through three natural distributary channels from the Yangtze (just downstream of its exit from Three Gorges onto the broad alluvial plain) to Dongting Lake. Unlike the Tonle Sap system, when Dongting Lake drains, it does not flow back through the same channel to the river but drains through different channels back to the river when the river stage declines. Thus, the lake and its connecting channels function as a flood bypass and backwater. The Lago Grand de Curuaı´ floodplain of Amazon is a complex system of more than 30 interconnected lakes, linked to the Amazon River by several channels, two of which (both with the permanent flow) carry return flow from the floodplain into the mainstream (Bourgoin et al., 2007). However, unlike the Amazon, most of the Mekong's course follows a narrow bedrock-controlled path, so there is a minimal exchange of sediment between channel and

floodplain until the reach downstream of Kratie, where the floodplains of the Cambodian lowlands and the Mekong delta are inundated, allowing significant fluxes of material and energy between the floodplain and mainstem river channel (Gupta and Liew, 2007).

With its channel sized reverse flow pattern, combined with broad, shallow lateral inundation of floodplains during the wet season, the Tonle-Sap-Mekong exchange represents a uniquely developed and important channel-floodplain exchange (**Figure 2-9**). In fact, the Mekong-Tonle-Sap exchange is arguably among the best developed such river-floodplain-lake exchange systems in the world, and it supports a fishery that is globally exceptional in many respects (Campbell et al., 2009).

The unique flow reversal is possible because of the low, flat landscape throughout Central Cambodia. The seasonal timing and discharge rates associated with water movement into and out of the Tonle Sap system are indicated in **Figure 2-10**. Inflow generally starts in late May, with maximum rates of flow of around 10,000 m^3/s by late August. This is over 25 per cent of the average mainstream discharge at that time of the year. Outflow starts typically in late September and reaches the same discharge volumes in the opposite direction in only a few weeks.

Around 34% of Tonle Sap Lake's waters originate from the Tonle Sap drainage basin, while about 53.5% of the lake's waters originate from the Mekong River, and 12.5% is derived from precipitation (Kummu et al., 2014). This distribution, however, is highly seasonal, as the Tonle Sap system is fed exclusively by its 11 tributaries for approximately six months (November through May) every annual hydrological cycle.

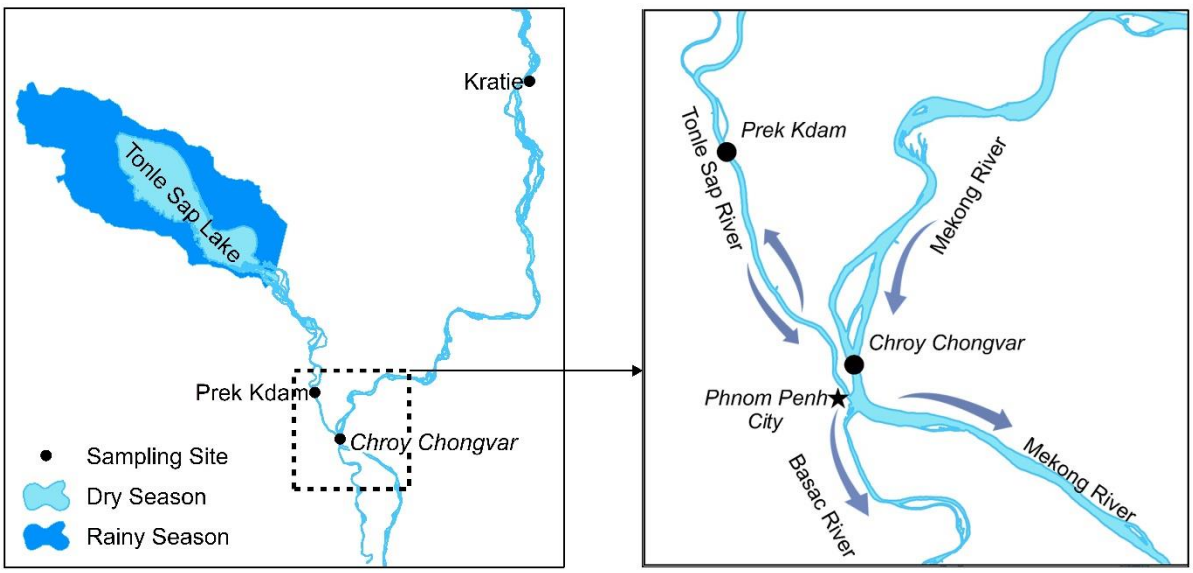

Figure 2-9: *Mekong River is connecting with the Tonle Sap Lake through the Tonle Sap River. (a): The Mekong River Basin, (b): The connecting of Tonle Sap Lake and Mekong River at the Chatumuk confluence (c). The Chatumuk confluence and the flow directions during the rising (rainy season) and receding stage (dry season) of the Mekong River.*

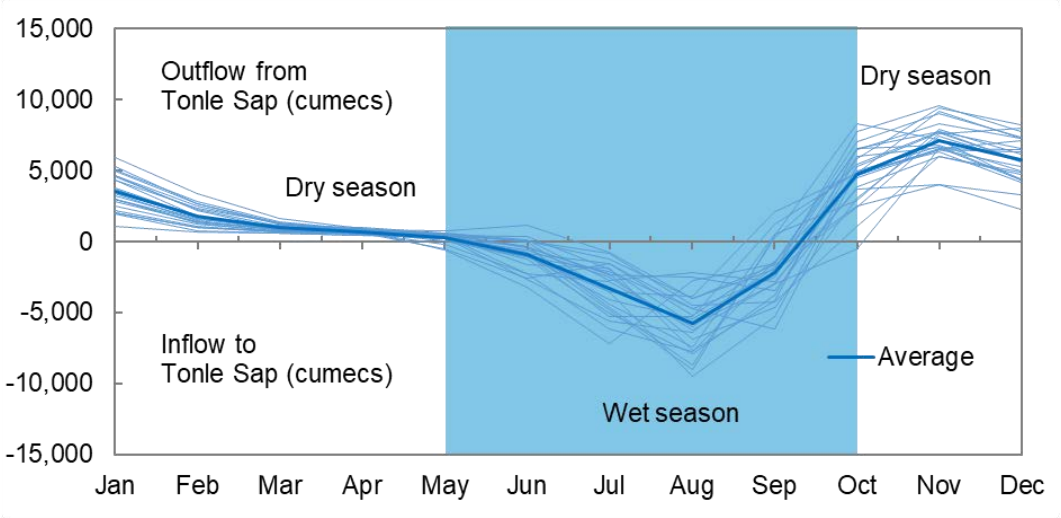

Figure 2-10: *Average monthly inflow and outflow hydrograph to and from the Tonle Sap Lake base on the observed data at Prek Kdam from July 1980-2018*

2.3. Hydrological and water quality dataset

Daily water discharges were generated at the three sites using rating curves and water level data provided by the Cambodian Ministry of Water Resources and Meteorology (MOWRAM) from 1993 to 2018. We obtained sediment data from MOWRAM under the Mekong River Commission framework: Water Quality Monitoring Network (WQMN). The Total suspended sediment (TSS) concentration from the WQMN dataset also have been used sediment load estimation in previous studies such as Kummu and Varis (2007), Kummu et al. (2008) and Wang et al. (2011b) for sediment load estimation in the Lower Mekong River. Total suspended sediment (TSS) concentration was obtained from the water quality sampling conducted on a monthly basis by MOWRAM from 1995 to 2018 at Kratie station and 1993 to 2017 at Chroy Changvar station. For Tonle Sap River, the monthly basis water sampling (once every month) also carried out from 1995 to 2018. **Table 2-5** summarizes the data (TSS and water discharge) coverage period and the number of sampling used in this study. In the WQMN database, the TSS samples were collected at 0.3 m below the water surface in the middle of the mainstem cross-section at each station. The

samples were at the designated laboratories by MRC and recommended analytical method for TSS analysis (2540-D-TSS-SM) (Kongmeng and Larsen, 2016).

The reader should bear in mind that these were not depth-integrated samples but single, near-surface samples from the approximate mid-point of the river. To the extent that the suspended sediments in the river are well-mixed, the samples may represent true loads. However, suppose concentrations are heterogeneous in the vertical columns or across the channel. In that case, the measured TSS may not represent the average sediment concentration channel-wide and may under-represent suspended sand especially, as sand concentrations would tend to greater near the bed. Note that since we analyzed flow and sediment records based on the hydrological year, our period of record analyzed (by hydrological year) is one year shorter than the period of available data expressed in calendar years (i.e. if the calendar year is 1995-2018; thus the study expressed as the hydrological year 1995-2017).

Table 2-5: *Recorded streamflow, sediment and water quality data used in this study (Data from MRC)*

Name of station	Basin Coverage		Streamflow record used	Sediment record used	Nitrate record used
	(km^2)	(%) of total basin			
China-Lao border	164,226	18%	1985-2007		
Chiang Saen	199,008	21%	1985-2016	1995-2011	
Luang Prabang	288,380	31%	1985-2016	1995-2011	1995-2011
Vientiane	323,027	34%	1985-2016	1995-2011	1995-2011
Mukdahan	429,210	46%	1985-2016	2001-2011	2001-2011
Pakse	621,404	66%	1985-2016	1995-2011	1995-2011
Stung Treng	728,828	78%	1985-2016		
Kratie	747,958	80%	1985-2016	1995-2016	1995-2016

2.4. Load Estimation and Trend detection Approach

Nutrient fluxes were estimated using the LOAD ESTimator (LOADEST) model (Runkel et al., 2004). LOADEST incorporates daily discharge, seasonality, and measured constituent data to parameterize a multiple-regression model that allows a continuous time series to be estimated from discrete measurements (Bouraoui and Grizzetti, 2011b; Hanley et al., 2013). LOADEST calculates fluxes by applying the adjusted maximum likelihood estimation method while eliminating

collinearity by centring discharge and concentration data. The regression model is automatically selected from one of 11 predefined regression models to fit the data based on the Akaike Information Criterion (Johnston et al., 2018). There are 11 equations used in the LOADEST model for loads estimation. To estimate the loads in the LOADEST model, the concentration data and flow have to be collected. During the calculation, LOADEST can create the 11 equation of regression model. In this study, LOADEST is determined to select the best regression model automatically to calibrate the loads and concentration:

(l) $\ln L = a_0 + a_1 \ln Q$

(2) $\ln L = a_0 + a_1 \ln Q + a_2 \ln Q^2$

(3) $\ln L = a_0 + a_1 \ln Q + a_2 \text{dtime}$

(4) $\ln L = a_0 + a_1 \ln Q + a_2 \text{Sin}(2\pi.\text{dtime}) + a_3 \text{Cos}(2\pi.\text{dtime})$

(5) $\ln L = a_0 + a_1 \ln Q + a_2 \ln Q^2 + a_3 \text{dtime}$

(6) $\ln L = a_0 + a_1 \ln Q + a_2 \ln Q^2 + a_3 \text{Sin}(2\pi.\text{dtime}) + a_4 \text{Cos}(2\pi.\text{dtime})$

(7) $\ln L = a_0 + a_1 \ln Q + a_2 \text{Sin}(2\pi.\text{dtime}) + a_3 \text{Cos}(2\pi.\text{dtime}) + a_4 \text{dtime}$

(8) $\ln L = a_0 + a_1 \ln Q + a_2 \ln Q^2 + a_3 \text{Sin}(2\pi.\text{dtime}) + a_4 \text{Cos}(2\pi.\text{dtime}) + a_5 \text{dtime} + a_6.\text{dtime}^2$

(9) $\ln L = a_0 + a_1 \ln Q + a_2 \ln Q^2 + a_3 \text{Sin}(2\pi.\text{dtime}) + a_4 \text{Cos}(2\pi.\text{dtime}) + a_5 \text{dtime}^2$

(10) $\ln L = a_0 + a_1 \text{per} + a_2 \ln Q + a_3 \ln Q_{per} + a_4 \ln Q^2 + a_5 \ln Q_{per}^2$

(11) $\ln L = a_0 + a_1 \text{per} + a_2 \ln Q + a_3 \ln Q_{per} + a_4 \ln Q^2 + a_5 \ln Q_{per}^2$

Where: Load = constituent load (kg/d), *Ln Q = Ln(Q)* - center of *Ln(Q),* dtime = decimal time - center of decimal time and a_i = Model coefficient

Flux estimation considers datasets of at least 120 observations (Hirsch, 2014); thus, our dataset is validated. The use of LOADEST to estimate the flux in the major river such as the Mekong can be found at Sun et al. (2013) in Yangtze River using monthly Nitrogen and TP concentration data, as well as daily streamflow, Hanley et al. (2013) in temperate rivers of North America using monthly measurement of water quality, Bouraoui and Grizzetti (2011a) used for rivers discharging in European seas using monthly nutrient data collection. In our study, LOADEST was used to extrapolate the monthly nitrate concentration measurements to daily nutrient load as follow regression models:

2.5. Trend detection Approach

To detect if trends can be identified in annual or seasonal series, we applied the *Mann-Kendall*, a non-parametric test originally proposed by Mann (1945) and updated later by Kendall (1975). The test has 3 alternative hypotheses in the series evolution: negative (i.e., decreasing trend), null (no trends in the series), and positive (increasing trend) (Howden and Burt, 2009). Pre-whitening (PW) is used to eliminate serial correlation (Yue and Wang, 2002).

The Mann-Kendall (MK) test is a non-parametric test to determine if trends can be identified in a temporal series including a seasonal component. This nonparametric trends test is the result of an improved test initially studied by Mann and followed by Kendall, being finally optimized by test (Howden and Burt, 2009). The test is based on the null hypothesis H_0 meaning that there are no trends in the series. The test has three alternative hypotheses in the series evolution: negative, null and positive. The Mann- Kendall Test- statistic *S* is given as:

The Mann- Kendall Test- statistic S is given as:

$$S = \sum_{k=1}^{n-1} \sum_{j=k+1}^{n} \operatorname{sgn}(x_j - x_k)$$

where

$$\begin{aligned} S = \operatorname{sgn}(x_j - x_k) &= 1 \quad \text{if } x_j - x_k > 0 \\ &= 0 \quad \text{if } x_j - x_k = 0 \\ &= -1 \quad \text{if } x_j - x_k < 0 \end{aligned}$$

The variance of *S* denoted by σ_S^2 is computed as:

$$\sigma_S^2 = \frac{n(n-1)(2n+5) - \sum_{j=1}^{q} t_j (t_j - 1)(2t_j + 5)}{18}$$

where *n* is the number of data points, *q* is the number of tied groups in the data set, and t_j is the number of data points in the j^{th} tied group.

Then S and σ_S^2 were used to compute the test statistic Z_s as:

$$Z_s = \frac{S-1}{\sigma} \quad \text{if } S > 0$$
$$= 0 \quad \text{if } S = 0$$
$$= \frac{S+1}{\sigma} \quad \text{if } S < 0$$

A positive value of S indicates that there is an increasing trend and a negative value indicates a decreasing trend. The null hypothesis H_0 that there is no trend in the data is either accepted or rejected depending if the computed Z_S statistics is less than or more than the critical value of Z-statistics obtained from the normal distribution table at 5% significance level.

2.6. Modelling Approaches

The Soil and Water Assessment Tool (SWAT) watershed-scale ecohydrological model (Arnold et al. 1998; Arnold and Fohrer 2005; Gassman et al. 2007) is currently one of the most widely used ecohydrological models, and it has been extensively tested for a wide variety of watershed scales and environmental conditions worldwide (Gassman et al. 2007, 2014; Douglas-Mankin et al. 2010; Tuppad et al. 2011; Krysanova and White 2015; Bressiani et al. 2015). Applications of SWAT typically involve delineating a watershed into sub-watersheds/subbasins that are then further subdivided into hydrologic response units (HRUs). HRUs are homogeneous areas of aggregated landuse, soil, and slope and are the smallest modeling units used in the model. The incorporation of HRUs in SWAT has provided flexibility for simulating a broad spectrum of conditions and supports adaptation of the model for watershed scales ranging from small field plots to entire river basins (Gassman et al. 2007).

The SWAT model also requires many input parameters related to landuse, soil, weather, topography, water quantity and quality, which may need to be calibrated and validated prior to using the model for specific analyses. Calibration and validation of a SWAT model for a watershed are essential for reducing uncertainties and increasing user confidence for effective and efficient analysis (White and Chaubey 2005; Jha 2011). SWAT can be calibrated and validated at the daily, monthly or annual time scales depending on the purpose of the specific modelling exercise. The most commonly calibrated SWAT output is streamflow, especially at annual and monthly time steps, although an increasing number of SWAT studies are reporting testing of daily streamflow results (Arnold et al. 2012; Gassman et al. 2007, 2014; Douglas-Mankin et al. 2010; Tuppad et al. 2011; Bressiani et al. 2015). Streamflow is calibrated more often than water quality in part because it is essential for the other water quality components of the model (Gikas et al. 2005) and

also because observed flow data are relatively abundant. On the other hand, sediment and nutrient parameters are not calibrated and validated as often, especially at the daily time scale (Arnold et al. 2012; Gassman et al. 2007, 2014; Douglas-Mankin et al. 2010; Tuppad et al. 2011; Bressiani et al. 2015). Calibration and validation of water quality parameters (sediment and nutrients) of SWAT at coarser time scales are mainly attributed to the scarcity of observed water quality data at finer time scales (Wu and Chen 2009).

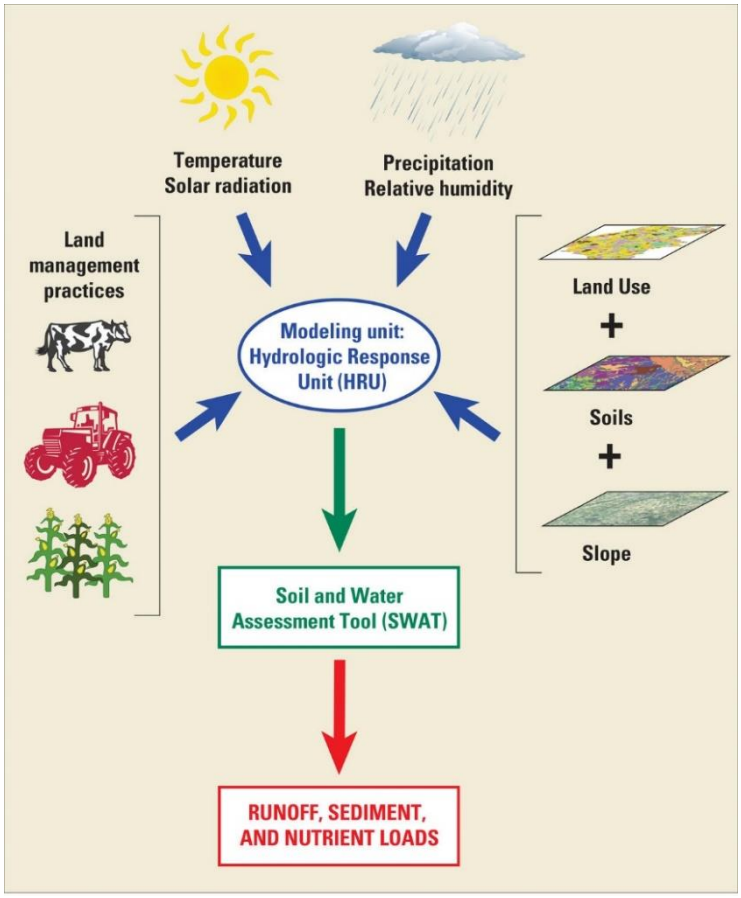

(Source: https://www.usgs.gov/media/images/glri-edge-field-swat-modeling-inputs-and-outputs)

Figure 2-11: *Input and output products of the Soil Water Assessment Tool (SWAT) used for edge-of-field modelling*

For water quantity and quality analysis in SWAT, there are three groups of parameters: Flow, Sediment, and Nutrients, which could be calibrated either separately (e.g., Muleta and Nicklow 2005; Gikas et al. 2005; Jha et al. 2007; Chahinian et al. 2011, etc…) or simultaneously (Kaur et al. 2004; Tolson and Shoemaker 2008; Wu and Chen 2009, etc...). Though challenging, the latter procedure seems to be preferable for improved calibration and validation results (Chahinian et al. 2011) since specific parameters, such as the curve number at moisture condition

II (CN2), affect all flow, sediment, and nutrient concentrations. The proliferation of computers with high processing capacity is likely to lead to greater use of simultaneous calibration.

The prediction streamflow of the SWAT model is based on the water balance equation:

$$SW_t = SWL_0 + \sum_{i=0}^{t} (R_{day} - Q_{surf} - E_a - W_{seep} - Q_{gw})$$

SW_t is the final soil water content (mm H_2O)
t is the time (day)
SWL_0 is the initial water content on day $i\,(mm)$
R_{day} is the amount of precipitation on day i (mm H_2O)
Q_{surf} is the amount of surface runoff on day i (mm H_2O)
E_a is the amount of evaporanspiration on day i (mm H_2O)
W_{seep} is the amount of water entring the vadose zone from the soil profile on i (mm H_2O)
Q_{gw} is the amount of return flow on day i (mm H_2O)

Water balance is the driving force in SWAT regardless of what kind of problems users want to deal with. Two major divisions are considered in simulating the hydrology of a watershed: the hydrological cycle over the lands (Figure 2-12). The land phase of the hydrologic cycle controls the amount of water, sediment, nutrient and pesticide loadings to the main channel in each sub-basin. The instream routing phase of the hydrologic cycle is the movement of water, sediments, etc…, through the channel network of the basin to the outlet.

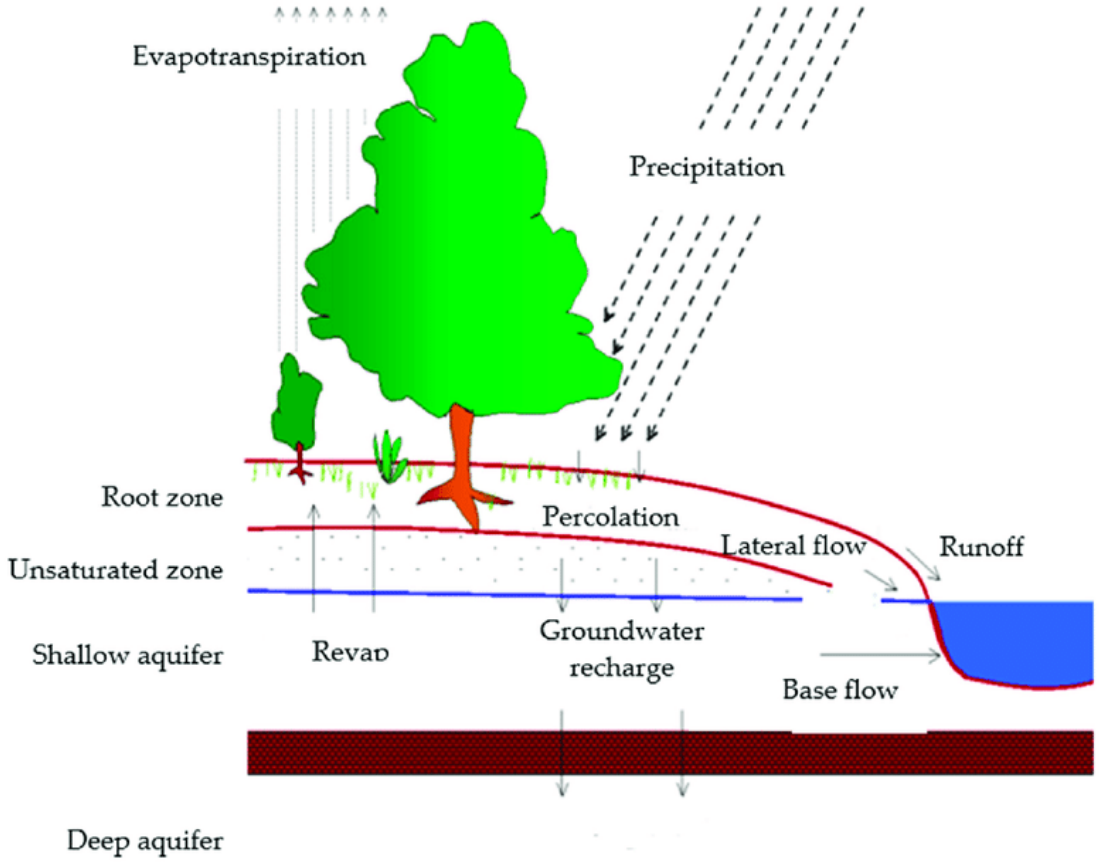

Figure 2-12: *The land phase of the hydrologic cycle in SWAT (Neitsch et al., 2009)*

SWAT considers sediment transport both over the landscape component and in the channel component (**Figure 2-13**). In the landscape component, sediment comes from erosion, geologic erosion and accelerated erosion (induced by human activities). SWAT model tracks particle size distribution of eroded sediments and routes them through ponds, channels, and surface water bodies. The sediment routing in the channel is a function of two processes: deposition and degradation, operating simultaneously in the reach. SWAT will compute deposition and degradation using the same channel dimensions for the entire simulation. Each subbasin has the main routing reach where sediment from upland sub-basins is routed and then added to downstream reaches.

The prediction of the sediment of the SWAT model is based on the modified universal soil loss (MUSLE) equation where rainfall and runoff are the main reason for soil loss.

$$sed=11.8\ (Q_{surf}\times q_{peak}\times area_{hru})^{0.56}\times(K_{USLE}\times C_{USLE}\times P_{USLE}\times LS_{USLE}\times CFRG)$$

sed is the sediment yield on a given day (metric tons)
Q_{surf} is the surface runoff volume (mm H_2O / ha)
q_{peak} is the peak runoff rate (m^3/s)
$area_{hru}$ is the area of the HRU (ha)
K_{USLE} is the USLE soil erodibility factor (0.13 metric ton m^2 hr/(m^3 metric ton cm))
C_{USLE} is the USLE cover and management factor
P_{USLE} is the USLE support practice factor
LS_{USLE} is the USLE topographic factor
$CFRG$ is the coarse fragment factor

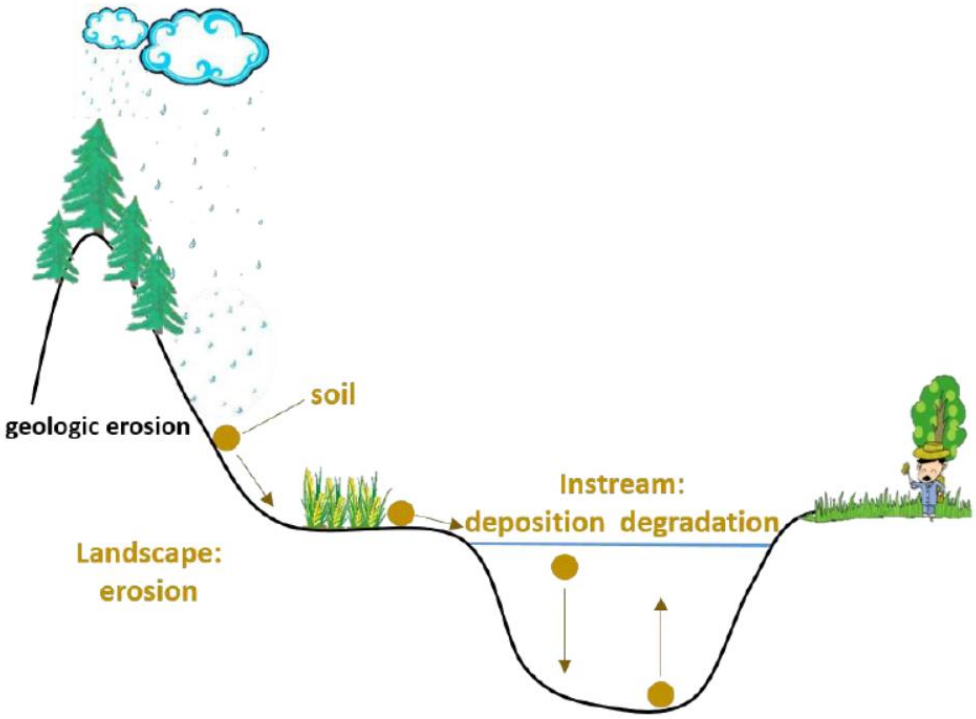

Figure 2-13: *Sediment transport in landscape and channel components.*

The current SWAT version uses the simplified stream power concept that the maximum amount of sediment that can be transported from a reach segment is a function of the peak channel velocity, that is:

$$\text{max sediment transported} = \text{peak channel velocity } \left(v_{ch,pk}\right)$$

The peak channel velocity, $V_{ch,pk}$, is calculated from:

$$v_{ch,pk} = \frac{q_{ch,pk}}{A_{ch}}$$

Where $q_{ch,pk}$ is the peak flow rate

A_{ch} is the flow cross-sectional area

The maximum concentration of sediment calculated:

$$sed_{dep} = \left(conc_{sed,ch,i} - conc_{sed,ch,mx}\right) V_{ch} = \text{sediment deposition}$$

Where $conc_{sed,ch,I}$ is the sediment concentration at beginning time step

V_{ch} is the water volume in the river reach

If $conc_{sed,ch,i} < conc_{sed,ch,mx}$ degradation is the dominant process in the reach segment

The SWAT-CUP software (Abbaspour, 2008) was used to calibrate the SWAT model automatically. The user interaction or manual component of the SWAT-CUP calibration forces the user to understand better the overall hydrologic processes (e.g., baseflow ratios, evapotranspiration, sediment sources, etc... sinks, crop yields, and nutrient balances) and of parameter sensitivity (Arnold et al., 2012). The Sequential Uncertainty Fitting (SUFI-2) algorithm (Abbaspour et al., 2004; Abbaspour et al., 2007) was used for the parameter optimization. SUFI-2 enables sensitivity analysis, calibration, validation, and uncertainty analysis of SWAT models. This algorithm is known to produce comparable results with widely used other auto-calibration methods (Yang et al., 2008). To run the automatic calibration in SUFI-2, the parameters to be calibrated (most sensitive ones) and their initial ranges were specified based on a literature review (Neitsch et al., 2011; Shrestha et al., 2013). In SUFI-2, there are two ways to change parameter values during calibration: directly changing the absolute value of a parameter and changing the absolute value relative to the initial value specified for the parameter. Readers are referred to Abbaspour et al. (2007) for details of the SUFI-2 approach.

The calibrated models were evaluated by comparing the simulated with the observed constituents using the Nash-Sutcliffe efficiency (NS), Coefficient of Determination (R^2) and per cent bias (PBIAS). NS and R^2 are the most widely applied and well-recommended performance measures (Masih et al., 2011).

2.7. Modelling Setup for Hydrology, Sediment and Nutrient

SWAT Model Set-Up and Data Inputs for the Mekong River Basin

The SWAT model has been set up to cover the total area of about 748 00 km^2 from the most upstream (80%) of the total Mekong River basin. The SWAT application of this study in the

Mekong Basin can be divided into eight zones, as availability of recorded streamflow and sediment used in this study for SWAT setup. The setup model was subjected to be studied as major sub-basin as follow: (1) from Most Upstream to Chinese Border, (2) Chinese Border to Chiang Saen, (3) Chiang Saen to Luang Prabang, (4) Luang Prabang to Vientiane, (5) Vientiane to Mukdahan, (6) Mukdahan to Pakse, (7) Pakse to Stung Treng and (8) Stung Treng to Kratie. Kratie station is selected as the most downstream for model set up since this location is not affected by the tidal influence (Ogston et al., 2017) and the buffering of the flood wave in the Tonle Sap lake system (Hung et al., 2012).

Each data input is obtained from different sources, which is summarized in **Table 2-6**. The precipitation used in this study obtained from the Global Precipitation Climatology Centre (GPCC) (www.gcmd.nasa.gov), and daily temperature were downloaded from NASA Earth Exchange (NEX) (www.nasa.gov/nex). The study used the Multi-Error-Removed Improved-Terrain DEM (MERIT DEM) (www.hydro.iis.u-tokyo.ac.jp/~yamadai/). The MERIT DEM was developed by removing multiple error components (absolute bias, stripe noise, speckle noise, and tree height bias) from the existing space-borne DEMs (SRTM3 v2.1 and AW3D-30m v1) (Yamazaki et al., 2017). The elevation distribution varies from 8 m to 6612 m as representing the topographic condition of the SWAT Model Set-up for the Mekong River Basin. Land use distribution in the Mekong River Basin for this study was obtained from the Global Land Cover 2000 Database (www.usgs.gov) at a 1 km resolution. Soil type distribution was downloaded from Global Soil data by FAO (www.fao.org/). The watershed had been discretized into small 345 sub-basins, which is equal to 345 HRUs from 14 land uses class, 20 soils and five slopes classes (0-1%, 1%-2%, 2%-5%, 5%-20%, and >20%). The SWAT model has included six major dams in the Upper Mekong Basin, the Manwan Dam operating in 1993, Dachaoshan in 2001, Jinghong in 2008, Xiaowan in 2009, Gongguoqiao in 2011, and Nuozhadu in 2012, which total reservoirs have an accumulated total and active reservoir storage capacity of approximately 400×10^8 m^3 and 230×10^8 m^3, respectively (Lu et al., 2014b).

Each data is obtained from different sources and present in **Table 2-6**. The daily precipitation and temperature obtained from the Global Precipitation Climatology Centre (GPCC) (www.gcmd.nasa.gov) and from NEX: NASA Earth Exchange (www.nasa.gov/nex), respectively. The study based on the Multi-Error-Removed Improved-Terrain DEM (www.hydro.iis.u-

tokyo.ac.jp/~yamadai/) (Yamazaki et al., 2017). Land use distribution in the Mekong River Basin was obtained from the Global Land Cover 2000 Database (www.usgs.gov) at a 1 km resolution. Land use distribution was downloaded from Global Soil data by FAO (www.fao.org/).

Table 2-6: *Data input and sources in the SWAT model in the study*

Data type	Description	Spatial resolution	Temporal resolution	Data sources
Topography map	DEM	90m		MERIT DEM: Multi-Error-Removed Improved-Terrain DEM http://hydro.iis.u-tokyo.ac.jp/~yamadai/MERIT_DEM/
Land use map	Land use classification	250m × 250m	2002	Global Land Cover Characterization (GLCC): https://www.usgs.gov/
Soil Map	Soil types	250m × 250m	2002	Global Soil data: http://www.fao.org/
Meteorological data	Gridded daily rainfall	1°	Daily, 1982-2016	Global Precipitation Climatology Centre: https://gcmd.nasa.gov/
Meteorological data	Temperature	0.25°	Daily, 1982-2016	NASA Earth Exchange (NEX) https://www.nasa.gov/nex
Hydrological data	Observed streamflow	8 stations	Daily, 1980-2016*	MoWRAM and MRC
Sediment data	Observed TSS	6 stations	Monthly, 1980-2016*	MoWRAM and MRC

* Data used depending on data available to this study for each station.

2.8. Calibration Process

The SWAT simulates the overall hydrologic balance for each HRU (hydrologic response units), and model output is available in daily, monthly, and annual time steps. The SWAT version used in this study is SWAT2012 rev. 664 (http://swat.tamu.edu/ software/arcswat/) (Arnold et al., 2012; Arnold et al., 1998). The streamflow calibration had been done manually and expertise by comparison to observed data and literature review information for water and sediment. The Penman-Monteith method was selected to calculate potential evapotranspiration. The parameters were calibrated/validated for each sub-basin (based on the gauge stations). The calibration results showed the importance of parameters, such as Soil_AWC, Soil_K, and ALPHA_BF (groundwater parameter) in the studied flow of the analyzed Mekong Basin (Table 3). The parameter CN2 is related to the quantity of runoff and is based on soil use. Soil_K and Soil_AWC are related to the quantity of soil-water relationships in various soil types of the region. For sediment load,

calibration was also calibrated manually. The parameter PRF_BSN has been calibrated to reduce the impact of streamflow peaks on erosion rate and sediment load at reaches, while the USLE_K parameter has been calibrated depending on the permafrost type to slow down erosion comparing to literature reviews. The nutrient model parameters were fitted through a semi-auto calibration procedure for the six-location using SWAT-CUP using a sequential uncertainty fitting algorithm (SUFI-2) (Abbaspour, 2013). **Table 2-7** shows the fitted values of parameters used to calibrate streamflow, sediment load and nitrate load calibration.

The model performance was subjected to evaluation by comparing the simulated with the observed constituents using Nash-Sutcliffe efficiency (NSE) (Nash and Sutcliffe, 1970) and Coefficient of determination (R^2). NSE was used to indicate how well the plot of observed versus simulated data fits the 1:1 line. A calibrated model could be judged satisfactory if NSE and R^2 are higher than 0.6 for mean behaviour (Benaman et al., 2005; Gupta et al., 2009; Moriasi et al., 2007; Moriasi et al., 2015)

Table 2-7: *Calibrated values of SWAT parameters*

Parameter	Name	Input File	Literature range	Calibrated value
Hydrology:				
ALPHA_BF	Baseflow alpha factor (days)	.gw	0-1	0.005
CANMX	Maximum canopy storage (mm H2O)	.hru	0-100	100
CN2	Curve number	.mgt	35-98	35-70
ESCO	Soil evaporation compensation factor	.bsn	0-1	0.35
GW_DELAY	Groundwater delay (days)	.gw	0-500	31
GW_REVAP	Groundwater "revap" coefficient	.gw	0.02-0.2	0.05
REVAPMN	Threshold depth of water in the shallow aquifer for "revap" to occur (mm)	.gw	0-500	150
SOL_AWC	Available water capacity of the soil layer (mm H_2O/mm soil)	.sol	0-1	0.2-0.4
SOL_K	Depth soil surface to bottom of layer (mm/hr)	.sol	0-2000	50; 90; 100
SOL_Z	Saturated hydraulic conductivity (mm/hr)	.sol	0-3500	495
Sediment:				
PRF_BSN	Peak rate adjustment factor for sediment routing	.bsn	0-1	0.8
USLE_K	USLE equation soil erodibility factor	.sol	0-0.65	0.2-0.6
SPCON	Linear factor for channel sediment routing	.bsn	0.0001-0.01	0.0025
SPX	Exponential factor for channel sediment routing	.bsn	1-2	1.15
Nutrient:				
ERORGN	Organic N enrichment ratio	.hru	1-5	3.9
RSDCO	Residue decomposition coefficient	.bsn	0.03-0.06	0.058
SOL_NO_3	Initial NO3 concentration in the soil layer [mg/kg]	.chm	0-100	23.1
CMN	Rate factor for humus mineralization of active organic nitrogen	.bsn	0.0001-0.002	0.0018

SHALLST_N	Concentration of nitrate in groundwater contribution to streamflow from subbasin (mg N/l)	.gw	0-500	454.5
AI1	Fraction of algal biomass that is nigrogen	.wwq	-0.5-0.5	-0.317
BC2_BSN	Rate constant for biological oxidation NO2 to NO3 (1/dayy)	.bsn	0.3-1.5	0.618
CH_ONCO	Organic nitrogen concentration in the channel (ppm)	.rte	0-30	25.83
SOL_ORGN	Initial organic N concentration in the soil layer [mg/kg]	.chm	10-30	28.78
NPERCO	Nitrogen percolation coefficient	.bsn	-0.5-0.5	-0.467
LAT_ORGN	Organic N in the baseflow (mg/l)	.gw	0-50	1.95

2.9. Model performance and evaluation

Model Calibration and Validation

The SWAT model was calibrated and validated for streamflow. The parameters for the flow simulations were fitted through an auto-calibration procedure, using SWAT-CUP for the study. The daily flow calibration from 2000 to 2006 was also carried out using a sequential uncertainty fitting algorithm (SUFI-2) with SWAT-CUP (Abbaspour, 2011). The initial parameter ranges for optimization were based on the likely maximum range recommended for each parameter, by the SWAT model efficiency factor (NSE) was used as the objective function.

Model Performance

Daniel N Moriasi et al. (2007) recommended quantitative statistics be used in the model performance evaluation in watershed simulations: the Nash-Sutcliffe efficiency (NSE), the coefficient of determination (R^2).

$$NSE = 1 - \left[\frac{\sum_{i=1}^{n} (Q_i^{obs} - Q_i^{sim})^2}{\sum_{i=1}^{n} (Q_i^{obs} - \overline{Q}_i^{obs})^2} \right]$$

$$R^2 = \frac{\sum_{i=1}^{n} \left(Q_i^{obs} - \overline{Q}_i^{obs} \right) \left(Q_i^{sim} - \overline{Q}_i^{sim} \right)}{\sqrt{\left(\sum_{i}^{n} \left(Q_i^{obs} - \overline{Q}_i^{obs} \right)^2 \right) \times \left(\sum_{i}^{n} \left(Q_i^{sim} - \overline{Q}_i^{sim} \right)^2 \right)}}$$

Where Q_i^{obs} and Q_i^{sim} are the observed and simulated values, n is the total number of paired value, $\overline{Q}_i^{obs}$ is the mean observed value and $\overline{Q}_i^{sim}$ is the mean simulated value. NSE is a normalized statistic that compares the residual variance with the observed data variance (Nash and Sutcliffe, 1970).

A calibrated and validated model could be deemed satisfactory if NSE and R^2 are higher than 0.60 for mean behaviour.

Table 2-8: *Streamflow, sediment load and nutrient calibration and validation at monthly scale of SWAT model in the Mekong River basin*

Stations		Discharge			Sediment			Nitrate		
		Period	NSE	R^2	Period	NSE	R^2	Period	NSE	R^2
China/Lao border	Cal	1985-1994	0.64	0.66						
	Val	1995-2007	0.65	0.75						
Chiang Saen	Cal	1985-1999	0.63	0.65	1995-2004	0.30	0.60			
	Val	2000-2016	0.67	0.72	2005-2011	0.69	0.74			
Luang Prabang	Cal	1985-1999	0.80	0.83	1995-2004	0.46	0.74	1995-2004	0.72	0.77
	Val	2000-2016	0.80	0.85	2005-2011	0.57	0.70	2005-2011	0.31	0.57
Vientiane	Cal	1985-1999	0.79	0.84	1995-2004	0.55	0.79	1995-2004	0.71	0.73
	Val	2000-2016	0.80	0.85	2005-2011	0.71	0.78	2005-2011	0.60	0.71
Mukdahan	Cal	1985-1999	0.89	0.91	2001-2006	0.82	0.89	2001-2006	0.59	0.66
	Val	2000-2016	0.87	0.92	2007-2011	0.66	0.82	2007-2011	0.54	0.69
Pakse	Cal	1985-1999	0.88	0.89	1995-2005	0.72	0.80	1995-2005	0.20	0.58
	Val	2000-2016	0.90	0.92	2006-2011	0.58	0.77	2006-2011	0.20	0.56
Stung Treng	Cal	1985-1999	0.88	0.89						
	Val	2000-2016	0.90	0.92						
Kratie	Cal	1985-1999	0.88	0.89	1995-2005	0.77	0.80	1995-2005	0.66	0.71
	Val	2000-2016	0.90	0.92	2006-2016	0.30	0.86	2006-2016	0.52	0.67

CHAPTER III

Sediment Load Variabilities Mekong-Tonle Sap

This chapter was published in the Catena Journal. The work of this chapter is the base of the following works in the following chapters. This chapter aims to estimate the temporal variability of sediment loads in Tonle Sap River and Lower Mekong River in Cambodia and assess the sediment linkage between Tonle Sap Lake and Mekong River. This chapter is the base work for the following steps to estimate the sediment load and its trend in Tonle Sap River and Mekong River

Sok, T., Oeurng, C., Kaing, V., Sauvage, S., Kondolf, G.M. and Sánchez-Pérez, J.M., 2021. Assessment of suspended sediment load variability in the Tonle Sap and Lower Mekong Rivers, Cambodia. CATENA, 202, p.105291. https://doi.org/10.1016/j.catena.2021.105291

3. Chapter III. Sediment Load Variabilities Mekong-Tonle Sap

3.1. Scientific Context and Objectives

Tonle Sap Lake, connected to the Mekong River via Tonle Sap River, has a unique hydrological environment that plays an important role in the active exchange between Tonle Sap Lake and the Mekong River through the reversal flow (Siev et al., 2016). A better understanding of the sediment exchanging between the Tonle Sap Lake system and Mekong mainstem is needed because sediment load provided by the Mekong River is pivotal for the productivity of Tonle Sap (Arias et al., 2014). The sediment exchange between Tonle Sap Lake and Mekong River was previously estimated by (Kummu et al., 2008) over 1997–2003 and by Lu et al. (2014a) during 2008–2010. Lu et al. (2014a) sediment load delivered from the lake was higher than that to the lake. However, Kummu et al. (2008) sediment inflow was higher. However, a complete study of the sediment and nutrient transport linkage between the Mekong mainstem and Tonle Sap River has been needed to understand better the highly productive Tonle Sap Lake system's functioning and estimate sediment load delivery to the Mekong delta. This article aims to clarify and fill the gaps between the already known and contradictory sediment exchange in Tonle Sap Lake-Mekong River linkage for 25 consecutive hydrological years from 1993-2018. Therefore, the study objectives are to estimate the temporal variability of sediment loads in Tonle Sap River and Lower Mekong River in Cambodia and assess the sediment linkage between Tonle Sap Lake and Mekong River.

3.2. Materials and Methods

The study objectives are to estimate the temporal variability of sediment loads in Tonle Sap River and Lower Mekong River in Cambodia and assess the sediment linkage between Tonle Sap Lake and Mekong River. Total suspended sediment (TSS) concentration was obtained from water quality sampling conducted on a monthly basis by MOWRAM from 1995 to 2018 at Kratie station and 1993 to 2017 at Chroy Changvar station. For Tonle Sap River, the monthly basis water sampling (once every month) also carried out from 1995 to 2018. Sediment Loads were estimated at Kratie, Chroy Changvar, and Prek Kdam Station using the LOAD ESTimator (LOADEST) (Runkel et al., 2004). Trend analysis of annual sediment load was investigated using the Mann-Kendall (Kendall, 1975; Mann, 1945), a non-parametric test to detect if trends can be identified in annual or seasonal series.

3.3. Results and Discussions

The reversal began in late May to early June, with water flowing from Mekong River upstream into TSL for 70 to 157 days per year (average of 118 days), whereas flow downstream from TSL to the Mekong River occurred for 209 to 295 days (average 247 days). The peak reverse flow in Prek Kdam generally occurred in July and August, before the peak discharge of Mekong River (August and September). Peak outflow from the lake to Mekong River mainly took place a few months later, during the outflows from October to December. During the observed periods, the maximum water discharge of the lake was 10,679 m^3/s for inflow and 10,104 m^3/s for outflow. The seasonal outflow of TSL averaged 68,000 Mm^3, which equalled 18% of the annual discharge of Mekong River at Chroy Changvar. The seasonal reverse flow into the lake from the Mekong River averaged 36,000 Mm^3, about 10% of the annual discharge of Lower Mekong River at Chroy Changvar.

Between June and October, water in the Mekong River was opaque, with TSS concentrations from 90 to 200 mg/l as it carried sediments derived from erosion across the land surface. On the falling limb beginning in December, the TSS concentration dropped to less than 20 mg/l on average. Using sediment data, we estimated the sediment load in the mainstem Mekong River averaged 72± 38 Mt at Kratie (1993-2017) and averaged 78±22 Mt at Chroy Changvar (1995-2018). Net annual sediment loads averaged 3.7 Mt in reverse flows into Tonle Sap Lake, equivalent to 4.8% of the annual average sediment load at Chroy Changvar of the Mekong mainstem.

The sediment load from the lake to Mekong River was 2.9 Mt/yr, which is equal to 3.7% of the average annual sediment load in Chroy Changvar. Thus, we can estimate that Tonle Sap Lake gained an average of 0.8 Mt of sediment annually from the Mekong River. However, as this term is calculated as a residual, it must be treated with curation (as such residual terms incorporate and hide errors in other terms). However, the net sediment pattern transfers changed over the observation period. From the hydrological year 1995 to 2000, Tonle Sap River contributed more sediment load to Mekong River than it received via reverse flows. However, from the hydrological year 2001-2017, the Lake received more sediment from the Mekong River than it contributed, averaging 1.35±0.7 Mt per year.

3.4. Conclusion and Perspectives

We estimated sediment load in the main Mekong River averaged 72± 38 Mt at Kratie and 78±22 Mt at Chroy Changvar from 1993-2018, lower than previous studies for the period before the 2000s, i.e., prior to dam construction on the Mekong mainstem and tributaries. Over the study period, the Lower Mekong River showed a significant decrease in sediment load, consistent with trends documented in other major rivers in the region and globally. The seasonal and annual sediment load linkage between the Mekong mainstem and Tonle Sap Lake are controlled principally by suspended sediment concentrations and water discharge, in both the reverse flows into the lake and outflows from the lake, both via the Tonle Sap River. The annual water inflow to the lake via reverse flow was 36 km^3, while outflow to the Mekong was 68 km^3. The great water outflow can be attributed to runoff from the Tonle Sap Lake basin and also flows across the floodplain lying to the west of the Mekong River. TSS concentrations of the reverse flow to TSL from Mekong River were nearly twice the concentrations of the outflow from TSL, resulting in a net transfer of sediment into the Lake. The net sediment loads averaged 3.7 Mt in reverse flows into Tonle Sap Lake, 2.9 Mt/yr inflows from the lake to Mekong River. We found Tonle Sap Lake provided 0.65±0.6 Mt of net sediment to the Mekong annually from 1995 to 2000 but was a sediment sink for an average of 1.35±0.7 Mt annually from 2001 onwards. The changing pattern of sediment load linkage can be attributed to a trend of increased TSS concentrations from the Mekong to Tonle Sap Lake

Further beyond this part of the work, the study on nutrient flux in the Mekong Tonle Sap system needs to be investigated and the modelling required.

3.5. Full paper: Sok, T., Oeurng, C., Kaing, V., Sauvage, S., Kondolf, G.M. and Sánchez-Pérez, J.M., 2021. Assessment of suspended sediment load variability in the Tonle Sap and Lower Mekong Rivers, Cambodia. CATENA, 202, p.105291.

Assessment of Suspended Sediment Load Variability in the Tonle Sap and Lower Mekong Rivers, Cambodia

Ty SOK[1,2*], Chantha OEURNG[1], Vinhteang KAING[1], Sabine SAUVAGE[2], Mathias G. KONDOLF[3], José Miguel SANCHEZ PEREZ[2]

[1]Faculty of Hydrology and Water Resources Engineering, Institute of Technology of Cambodia, Russian Federation Blvd., P.O.BOX 86, Phnom Penh Cambodia.
[2]Laboratoire Ecologie Fonctionnelle et Environnement UMR 5245 CNRS/UPS/INPT ENSAT, Avenue de l'Agrobiopole, BP 32607, Auzeville Tolosane, 31326 CASTANET TOLOSAN, France
[3] Department of Landscape Architecture and Environmental Planning, University of California, Berkeley, CA 94720, USA

Abstract: The Mekong River in Southeast Asia, one of the world's great rivers, has been facing disruption of its sediment balance and resultant impacts on nutrient fluxes, aquatic ecology, floodplains and the delta. Using monitoring data from 1993-2018, we estimated the temporal variability of sediment loads in Tonle Sap and Lower Mekong Rivers in Cambodia, assessing the sediment linkage between the Tonle Sap Lake and the Mekong mainstem, which are connected by a seasonally reversing flow through the Tonle Sap River. We estimated the annual sediment in the Mekong mainstem of 72±38 Mt/year at Kratie (upstream) and 78±22 Mt/year at Chroy Changvar from 1993-2018 (just upstream of the Tonle Sap confluence). Our sediment load estimation of the Mekong River is consistent with other recent estimates of sediment load on the Lower Mekong. However, the result is lower than reported in some older studies (prior to the 2000s), which is consistent with sediment trapping by dams on Upper Mekong mainstem and major tributaries. Our analysis indicates that Tonle Sap Lake provided 0.65±0.6 Mt/year of sediment annually to the Lower Mekong River from 1995 to 2000. However, since 2001, Tonle Sap Lake has become a sink for sediment, accumulating an average of 1.35±0.7 Mt annually. Net storage of sediment in Tonle Sap Lake reduces the annual sediment transport to the delta, further compounding the effects of reduced sediment delivery to the delta resulting from upstream dam development and instream sand mining.

Keywords: Temporal variability, Sediment load; Mekong River; Tonle Sap Lake

[*] Corresponding Author: Ty SOK (sokty@itc.edu.kh)

1. Introduction

In many river basins, changes in sediment supply have affected the geomorphology of river channels, floodplains, and deltas (Peng et al., 2010). Sediment transport has important influences on river morphology, water quality and persistence of geomorphic features such as deltas (Walling, 2009). In recent decades, river processes have been greatly influenced by anthropogenic activities such as hydropower dam development, which alters downstream river discharge and sediment load (Vörösmarty et al., 2003). Recent studies have shown substantial changes in water and sediment fluxes for rivers globally from prior decades (Li et al., 2020). The largest rivers of the North and East Asia in Russia and China, such as Amur, Yellow, Yangtze, Pearl, evinced sediment load changes due to human impacts (Chalov et al., 2018). Rivers with high relief and erodible lithologies like the Ganges, Danube and Amazon Rivers are likely to respond to higher than average precipitation with increased sediment yields (Cohen et al., 2014). An increasing trend is also visible in long-term records of water and sediment fluxes of the Blue Nile in Africa from 1980-2010 (Li et al., 2020). However, at global scale, the mean annual water and sediment fluxes to seas from the world's large rivers have decreased (Li et al., 2020; Walling et al., 2003; Walling, 2006). Within the same context, the estimated suspended sediment to the Arctic Ocean delivered from all Arctic rivers has declined (including Yenisei River) (Bobrovitskaya et al., 2003; Fabre et al., 2019) Suspended sediment discharge in the Mississippi River declined by at least 50% due to impoundments and other engineering alterations since the early 1950s (Meade and Moody, 2010). Declines in water discharge and suspended sediment flux of the Para Paraná River, one of the majors in South America, has been observed (Stevaux et al., 2009). The sediment flux of all the major river of Mainland China have declined below their long-term averages (Cheng et al., 2008), including about a 60-80% reduction from Qiantang and Yangtze the Pearl River Basin (Liu et al., 2007).

From its headwaters on the Tibet-Qinghai plateau in Asia and sharing the same water source Yangtze and Yellow River, the Mekong River flows 4,800 km with the average annual discharge of 470 km^3. The river's uppermost 2,000 km (195,000 km^2 basin area), flows through China (including small part in Myanmar) and is known as the Lancang. The total area of the lower Mekong Basin is approximately 600,000 km^2 including Thailand, Laos, Cambodia, and Vietnam. This important basin is facing extensive landuse/cover disturbance, water diversion and reservoir

construction, and mining of sediment from the river bed for construction aggregate (Lu and Siew, 2005).

Delivery of water and nutrients underpins a vibrant fishery and highly productive agriculture supporting over 60 M people, notably the highly productive Tonle Sap Lake, floodplains of Cambodia, and the Delta of Vietnam (Arias et al., 2014; Kummu et al., 2008). Changes in the Lancang-Mekong River's sediment load have attracted wide research interest because such changes can affect river channel form, nutrient fluxes, river ecology, and the sustainability of the delta. Hydropower development is altering sediment loads in the Mekong, first from dams in upper basin (Kummu and Varis, 2007). Analysis of sediment flux from Upper Mekong at Gaju to Khong Chiam at Lower Mekong at seven stations documented by Liu et al. (2013), at five stations in the Lower Mekong (from Chiang Saen to Khong Chiam located in Laos) from 1985-2000 by Wang et al. (2011), and nutrient loads for these stations from 1985–2011 by Li and Bush (2015) all show decreases. However, these studies covered the river only down to Pakse in Laos. Sediment loads in the lowermost reach of the Mekong, through Cambodia and into the delta, including 3S river system (Sekong, Sesan, and Srepok), the biggest sub-basins of the Mekong Basin, and the Tonle Sap Lake system have received more limited study. Tonle Sap Lake, connected to the Mekong River via Tonle Sap River, has a unique hydrological environment that plays an important role in the active exchange between Tonle Sap Lake and the Mekong River through the seasonal reversal in flow (Siev et al., 2016). A better understanding of the sediment exchanging between the Tonle Sap Lake system and Mekong mainstem is needed because sediment load provided by the Mekong River is pivotal for the productivity of Tonle Sap (Arias et al., 2014). Kummu et al. (2008) analysed sediment exchange between Tonle Sap Lake and Mekong River for the period 1997–2003 and found a net sediment inflow from the Mekong into the lake. In contrast, Lu et al. (2014a) studied the period 2008–2010 and concluded that the net sediment transfer was from the lake to the river. Given the critical role of the sediment and nutrient transport linkage between the Mekong mainstem and Tonle Sap River for the highly productive Tonle Sap Lake system and for sediment delivery to the Mekong delta, the objective of our study was to comprehensively analyse the sediment exchange between Tonle Sap Lake and the mainstem Mekong River over 25 consecutive hydrological years from 1993-2018.

2. Materials and Methods

Study area

Located in Southeast Asia, the Mekong River is the world's 12th longest river (4,800 km), has the 8th largest average annual runoff (470 km^3) and the 21st largest basin area (795,000 km^2). The basin of Mekong River is commonly subdivided into the Upper Mekong basin (or UMB) covering 24% of total basin (21% in China, 3% in Myanmar), and the Lower Mekong basin (or LMB), with 76% of the total basin area (Laos 25%, Thailand 23%, Cambodia 20% and Vietnam 8%).

The Mekong Basin is characterized by distinctly wet and dry seasons, driven by the Southwest Monsoon. The wet season commonly extends from May to late September (or early October). The average rainfall of Mekong floodplain of Cambodia and the delta of Vietnam annually are up to 1,500 mm, while the maximum intensity occurs in central Laos. At elevations above 500 m above mean sea-level, dry season temperatures are lower, though not by much. The average rainy season temperatures greatly decline through south to north, from 26-27°C at Phnom Penh Cambodia to 21-23°C at northern part of Thailand. The discharge of Mekong river reaching to the sea averages 15 000 m^3/s (Adamson et al., 2009; Gupta and Liew, 2007).

In Cambodia, the Mekong River connects with Tonle Sap Lake (TSL) (the largest permanent freshwater lake in the Southeast Asia) via Tonle Sap River at Chaktomuk confluence at Phnom Penh (**Figure 3-1**). Tonle Sap Lake was seasonally influenced by Mekong River flood pulse. The lake is approximately 120 km long and 35 km wide and covers 2,500 km^2 in the dry season, but it expands up to 250 km long and 100 km wide, and covers 17,500 km^2 in the wet season because high stages in mainstem Mekong drive flow into TSL through the Tonle Sap River (Campbell et al., 2009). From October to April, flow in the mainstem Mekong recedes, and flows reverse direction, draining from Tonle Sap Lake to the Mekong mainstream via Tonle Sap River (Fujii et al., 2003; Masumoto, 2000). The majority of water in the Lake in the wet-season is from the Mekong mainstem (Lu et al., 2014b), and the delayed release of this water provides important fresh water to the Mekong delta in Cambodia and Vietnam in low flow period (dry season) and prevents saltwater intrusion from the sea into fertile agricultural lands (Hai et al., 2008).

We selected three stations with continuous records of discharge and total suspended solids: The Mekong River at Kratie, the Mekong at Chroy Changvar (just upstream of the Tonle Sap

confluence) reflecting discharge and sediment load above interactions with the Tonle Sap, and the Prek Kdam station on the Tonle Sap River. Background information on these three stations of this study is detailed in Vinhteang et al. (2019). We analyzed flow and sediment by hydrological year from May 1 to April 30 following year (Kummu and Sarkkula, 2008; Lu et al., 2014b).

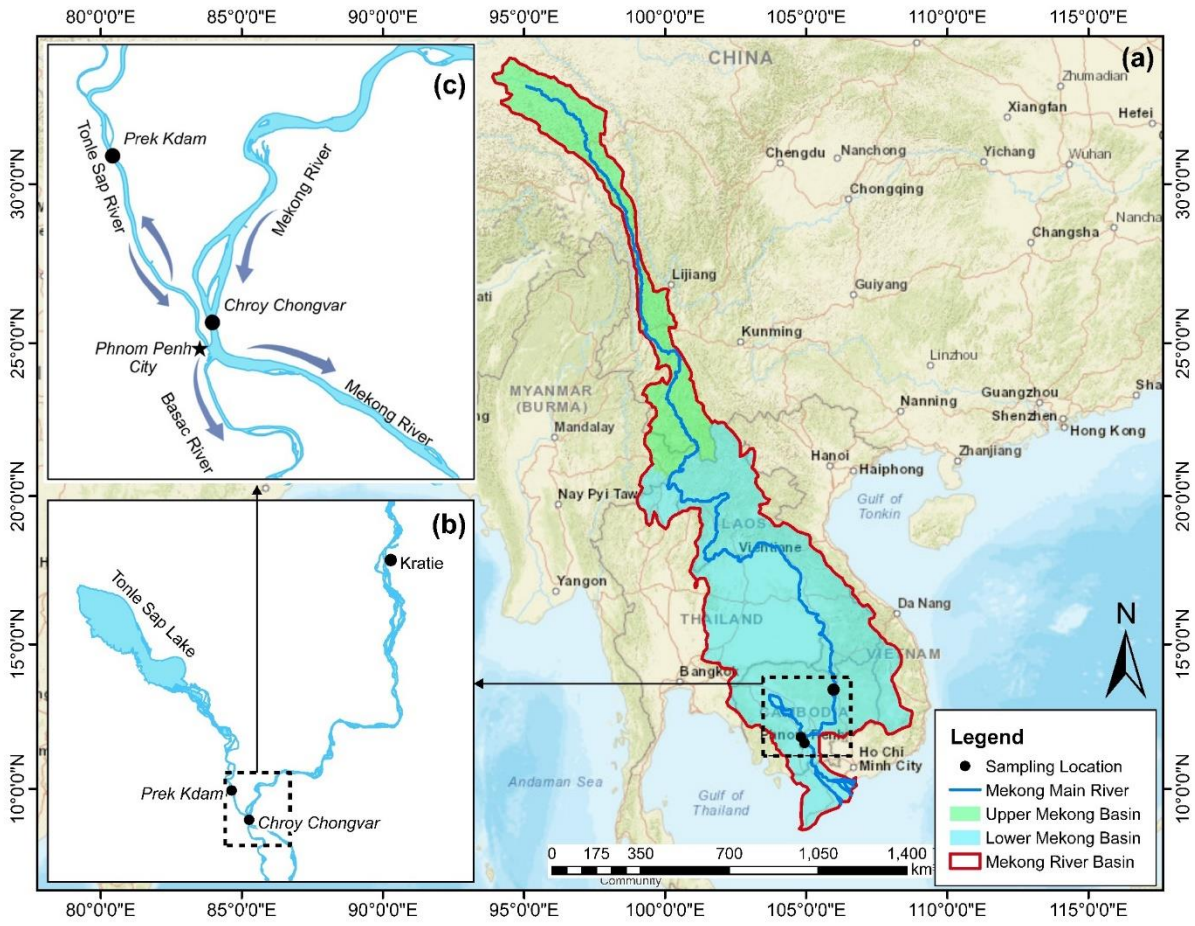

Figure 3-1: *Maps of the study area. (a): The Mekong river Baisin, (b): three sampling sites located at Kratie of the Mekong River, Chroy Changvar at Phnom Penh, and at Prek Kdam of Tonle Sap River. (c). the Chatumuk confluence located near Phnom Penh City.*

Water Discharge and Total Suspended Solids Data

Daily water discharges were generated at the three sites using rating curves and water level data provided by the Cambodian Ministry of Water Resources and Meteorology (MOWRAM) during period 1993 to 2018. Also, from MOWRAM, we obtained total suspended solids (TSS, hereafter referred as suspended sediment) concentration data collected under the Mekong River Commission framework: Water Quality Monitoring Network (WQMN). The WQMN dataset has been used to estimate suspended sediment loads in previous studies such as Kummu and Varis (2007), Kummu

et al. (2008) and Wang et al. (2011). TSS concentrations were obtained from water quality sampling conducted on a monthly basis by MOWRAM from 1995 to 2018 on the Mekong at Kratie, from 1993 to 2017 on the Mekong at Chroy Changvar, and from 1995 to 2018 on the Tonle Sap River at Prek Kdam. **Table 3-1** summarizes the data (TSS and water discharge) coverage period and number of samples used in this study. In the WQMN sampling program, individual samples were collected 0.3 m below the surface in the middle of the river cross-section. The samples were analyzed at laboratories designated by MRC, following recommended analytical methods for TSS analysis (2540-D-TSS-SM) (Kongmeng and Larsen, 2016). The reader should bear in mind that these were not depth-integrated samples but single, near-surface "grab" samples from the approximate mid-point of the river. To the extent that the suspended sediments in the river are well-mixed, the samples may be representative of true loads, but if concentrations are heterogeneous in the vertical columns or across the channel, the measured TSS may not be representative of the average sediment concentration channel-wide, and may under-represent suspended sand especially, as sand concentrations would tend to greater near the bed.

Moreover, total suspended solids (TSS) may not be directly comparable to suspended sediment concentration (SSC) determinations because TSS samples are collected from only a single point (0.3 m below the water surface mid-river) in the cross section, while SSC samples are collected from the full water column and at multiple points on the cross section. If the sediments are not well-mixed through the water column but stratified, the two methods can yield different suspended sediment concentrations. Moreover, there are differences in analytical methods that can yield different particle-size distributions (Gray, 2000; Murphy and Sciences, 2020). SSC is determined by measuring the dry weight of all sediment from a water sample of a known volume, normally large samples (1 L) which to represent the entire water column. Several techniques are used to determine TSS, and most techniques similarly measure the dry weight of all sediment from a water sample of a known volume. However, as defined by the TSS protocol (APHA, 1995) this technique weighs the sediment in only a 100-250 mL sub-sample from the original water sample. As described by Gray (2000), generally, only finer suspended particle sizes are captured by TSS, while SSC characterizes the entire suspended particle-size distribution of the water column. The bias of TSS compared to SSC is most important at sites with larger proportions of sand-sized sediment. In the Lower Mekong River, the suspended sediments are generally dominated by silt and clay (Walling, 2005). Koehnken (2012) found that from downsteam of Pakse, suspended

sediments are mainly composed of silt- and clay-size particles, and typically at Kratie all suspended sediments size are less than 63 µm. Generally, suspended particles smaller than 60 µm are uniformly vertically distributed in the water column (Partheniades, 1977). Given that the suspended sediments are well-mixed in the water column, the load estimation using TSS should be comparable to the load estimation using SSC in the Lower Mekong River.

Table 3-1: *Data coverage period and the number of total suspended solids sampling and water discharge*

	Kratie	Chroy Changvar	Prek Kdam		Time step
			TSL towards Mekong	Mekong towards TSL	
TSS (number of samples)	246	259	170	72	Monthly
TSS Data coverage period	1995-2018	1993-2017	1995-2018	1995-2018	-
Discharge data	1995-2018	1993-2017	1995-2018	1995-2018	Daily

Sediment Load Estimation and Trend analysis of annual sediment load

LOADEST: Sediment Loads were estimated at Kratie, Chroy Changvar, and Prek Kdam Station using the LOAD ESTimator (LOADEST) (Runkel et al., 2004). LOADEST provides three methods for load estimation, such as Maximum Likelihood Estimation (MLE), Adjusted Maximum Likelihood Estimation (AMLE), and Least Absolute Deviation (LAD) (**Table 3-2**) (Vinhteang et al., 2019).

Table 3-2: *Load estimation methods in LOADEST*

Loads Estimation method	Model residuals Assumption	Function
MLE	Normal distribution	$L = \exp(a_o + \sum_{j=1}^{M} a_i X_i).\mathrm{g}_m(m, s^2, V)$
AMLE	Normal distribution	$L = \exp(a_o + \sum_{j=1}^{M} a_i X_i).\mathrm{H}(m, \mathrm{b}, s^2, \alpha, \kappa)$
LAD	Non-normal distribution	$L = \exp(a_o + \sum_{j=1}^{M} a_i X_i).\frac{\sum_{k=1}^{n} \exp(e_k)}{n}$

Where

- m is the number of degree of freedom, s^2 is the residual variance, and V is a function of the explanatory variables.
- $[g_m(m,s^2,V)]$ is the bias correction factor
- of the maximum likelihood method.
- a and b are functions of the explanatory variables.
- α and κ are parameters of the gamma distribution.
- $[H(a,b,s^2,\alpha,\kappa)]$ is the bias correction factor.
- e is the residual error, and n is the number of uncensored observation in the calibration dataset.

Trend analysis of annual sediment load

To detect if trends can be identified in annual or seasonal series, we applied the *Mann-Kendall*, a non-parametric test originally proposed by Mann (1945) and updated later by Kendall (1975). The test has 3 alternative hypotheses in the series evolution: negative (i.e., decreasing trend), null (no trends in the series), and positive (increasing trend) (Howden and Burt, 2009). Pre-whitening (PW) is used to eliminate serial correlation (Yue and Wang, 2002).

3. Results

Water Discharge and Suspended Sediment Dynamics in the Lower Mekong River at Kratie and Chroy Changvar

Figure 3-2 shows the hydrographs of the daily water discharge and observed TSS at Kratie from 1995 to 2018 and Chroy Changvar from 1993 to 2017. The daily water discharge clearly reflects the annual dry and rainy seasons, with low flows in March and April (down to approximately 2,000 m^3/s), followed by onset of the rainy season and increased discharges in May, and high flows in August and September (up to approximately 30,000 m^3/s). At Kratie, the maximum discharge reached 58,205 m^3/s in the rainy season of 1996 while the minimum discharge was 1,073 m^3/s in the dry season of 1995. At Chroy Changvar station, maximum discharge reached 40,556 m^3/s in the rainy season of 2014, while minimum lowest discharge was 405 m^3/s in the dry season of 1995.

We calculated descriptive statistics such as minimum, maximum, mean, and standard deviation to illustrate the temporal distribution of important water quality parameters and to highlight specific characteristics. Additionally, we calculated skewness and kurtosis to determine if the data were skewed with positive or negative tails, and to determine the peakness of the distributions, respectively. The summary statistics of TSS concentrations from 1993-2017 at Kratie and Chroy

Changvar are summarized in **Table 3-3**. Between June and October, water in the Mekong River was opaque, with TSS concentrations from 90 to 200 mg/l as it carried sediments derived from erosion across the basin. On the falling limb beginning in December, the TSS concentration drop to less than 20 mg/l on average. **Figure 3-3** illustrates the rating curve of observing daily water discharge and TSS at Kratie and Chroy Changvar station (1993 to 2017). Discharge and TSS concentrations showed significant statistical relations, with R^2=0.53 for Kratie station and R^2=0.65 for Chroy Changvar.

The TSS and Q relations in rivers, especially for a large river like the Mekong, are typically governed by multiple and relatively complex processes, which can produce hysteresis loops. Higgins et al. (2016) outlined four factors affecting hysteresis loops: a sudden increase in rainfall, the availability of sedimentary material in riverbeds, the interaction of deep soil layers, and aggressive flooding that causes the damming of sediment in flood plains upstream. Williams (1989) identified five common types of hysteresis loops: a single-valued line, a clockwise loop, a counter-clockwise loop, a single-valued line plus a loop, and a figure-8 loop. However, our TSS data set consists of monthly samples, and hysteresis loops would be evident only in data collected on a shorter time step, such as daily. To identify possible hysteresis loops and their possible causes would require in-depth studies such those undertaken by Pietroń et al. (2015) and Chalov et al. (2017).

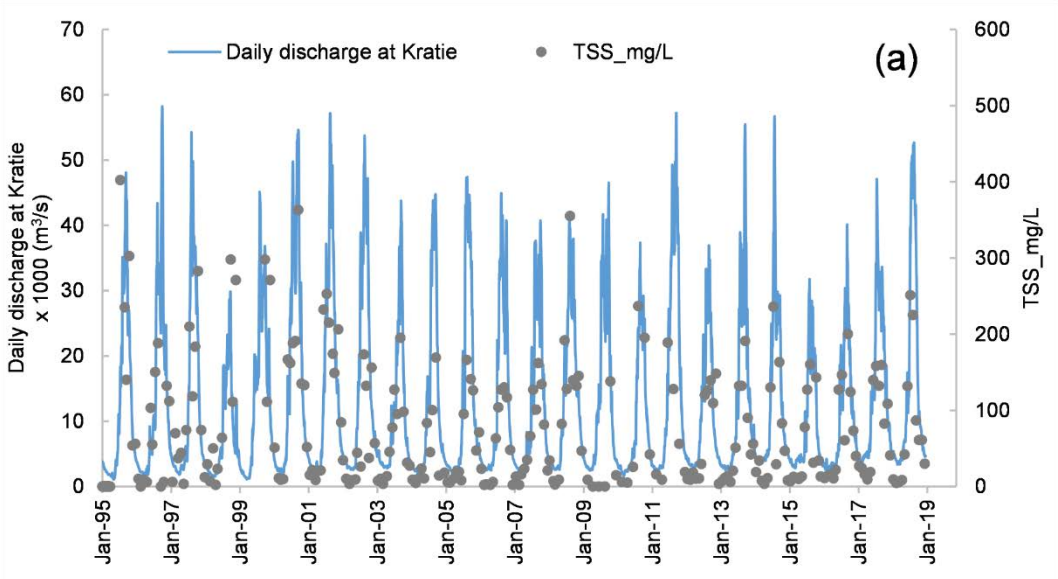

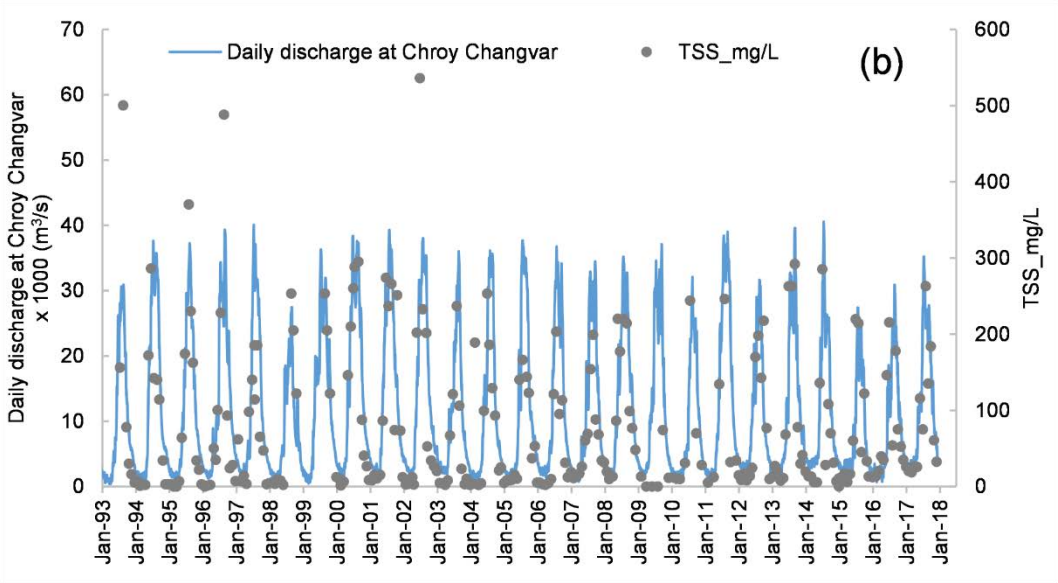

Figure 3-2: *Variation in the water discharge at the daily time step and total suspended solids concentration (monthly time step) at (a) Kratie (1995 to 2018) and (b) Chroy Changvar (1993 to 2017). Data from Cambodia MOWRAM.*

Table 3-3: *Descriptive statistics of sediment concentration at Kratie and Chroy Changvar*

	Month	May	Jun	Jul	Aug	Sep	Oct	Nov	Dec	Jan	Feb	Mar	Apr
Kratie	Min	3	8	26	29	31	6	31	2	6	2	3	2
	Max	167	232	402	355	363	303	271	112	51	70	50	44
	Mean	35	96	159	157	175	118	108	37	17	14	13	12
	SD	41	61	85	72	74	69	74	28	13	15	12	10
	Skewness	2.3	0.7	1.2	0.8	0.9	1.1	1.1	1.0	1.3	2.9	2.2	2.0
	Kurtosis	5.5	-0.3	2.7	1.7	1.7	2.1	0.4	0.9	1.3	10.0	5.0	5.3
Chroy Changvar	Min	2	2	69	28	45	23	3	3	2	3	1	2
	Max	146	220	536	370	500	218	251	73	31	62	189	39
	Mean	24	93	204	204	209	104	57	26	12	12	19	10
	SD	35	67	108	74	114	53	53	17	8	13	42	9
	Skewness	2.7	0.5	1.5	-0.5	1.4	0.9	2.7	0.9	0.9	3.1	4.2	2.1
	Kurtosis	7.8	-0.7	4.0	1.4	2.0	0.1	8.6	1.1	0.4	11.7	17.9	5.3

Note: Min, max, mean, and SD are concentrations in mg/l;
Skewness and Kurtosis are dimensionless.

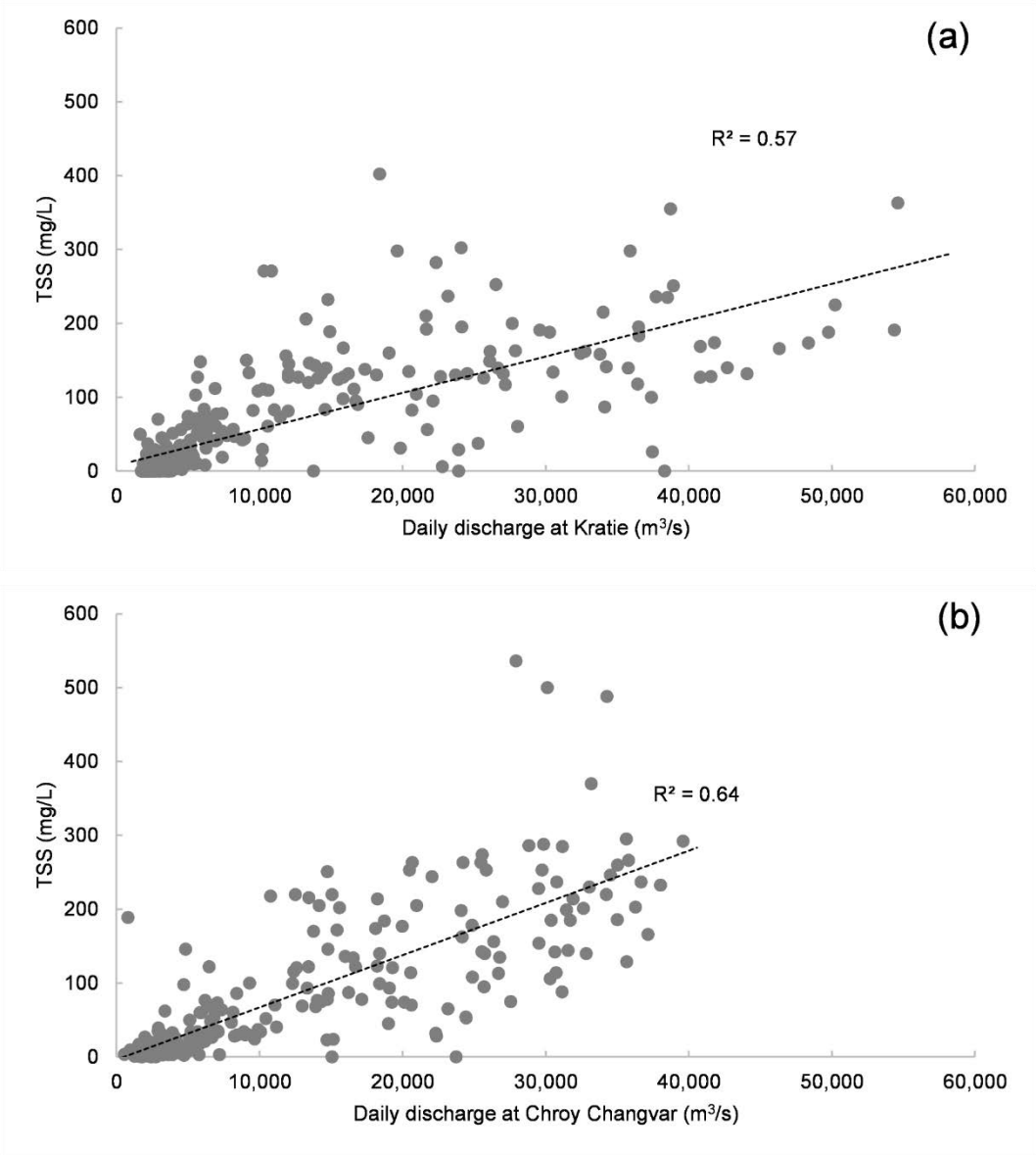

Figure 3-3: *Relationship of TSS concentration and daily water discharge in the Lower Mekong River at (a) Kratie (from 1995 to 2018) and (b) Chroy Changvar (1993 to 2017). Data from Cambodia MOWRAM*

Water Discharge and Suspended Sediment load in Tonle Sap River at Prek Kdam

Prek Kdam station records discharge and sediment of the Tonle Sap River, downstream from TSL to Mekong River during low water stage, and reverse, upstream flow during high stage of the Mekong River (**Figure 3-4**)**.** We plotted inflow from the Mekong River into TSL as negative

values of water discharge and sediment concentration, plotted outflow from TSL to the Mekong River as positive values.

The number of outflowing and inflowing days exchanging between TSL and Mekong River fluctuated from year to year. The reversal began in late May to early June, with water flowing from Mekong River upstream into TSL for 70 to 157 days per year (average of 118 days), whereas flow downstream from TSL to the Mekong River occurred for 209 to 295 days (average 247 days). 1995 and 2014 were years with the fewest days of reverse flow, 73 and 70 days, respectively. The peak reverse flow in Prek Kdam generally occurred in July and August, before the peak discharge of Mekong River (August and September) at Chroy Changvar station. Peak outflow from the lake to Mekong River mainly took place a few months later, during the outflows from October to December. During the observed periods, the maximum water discharge of the lake was 10,679 m^3/s for inflow, and 10,104 m^3/s for outflow.

Suspended sediment concentrations at Prek Kdam were governed by distinct flow directions (**Table 3-4**). TSS concentrations for outflow from lake to the Mekong (October to March) averaged 41 mg/l, while TSS concentrations during reverse flows from the Mekong River towards TSL (May to September) averaged 74 mg/l. Thus, TSS concentrations of the inflow were nearly twice the concentrations of the outflow from TSL, implying a net transfer of sediment into the Lake. The sediment rating curves at Prek Kdam show distinct relations when plotted separately for outflow and reverse-flow periods (**Figure 3-5**), with TSS concentrations lower in outflows from TSL to the Mekong (**Figure 3-5**.a) than in reverse flows to TSL (**Figure 3-5**.b), with all parameters having only a weak relationship in linearity with discharge ($R^2 < 0.1$) in both flow periods.

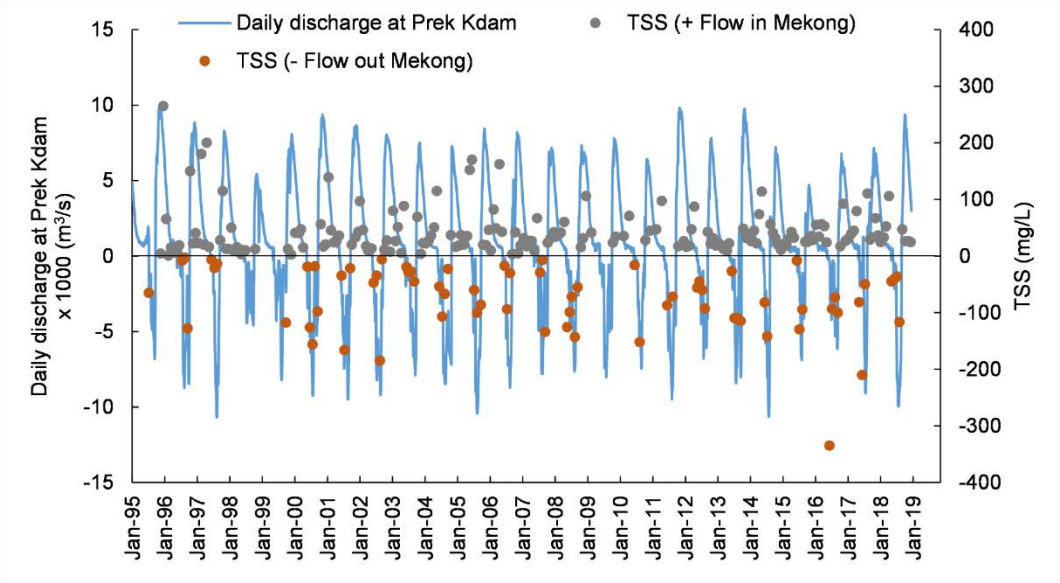

Figure 3-4: *Variation in the water discharge at the daily time step and total suspended solids (TSS) at Prek Kdam (monthly time step). The negative values of concentration and discharge are (reverse) inflow into the TSL from Mekong River, while positive values are the outflow from the lake towards Mekong River. Data from Cambodia MOWRAM.*

Table 3-4: *Descriptive statistics include minimum values (min), maximum values (max), mean values, standard deviation (SD), skewness coefficients and Kurtosis of sediment concentration at Kratie from 1995-2018.*

	From Tonle Sap Lake towards Mekong River	From Mekong River towards Tonle Sap Lake
Min	1.0	3.0
Max	265	335
Mean	41.7	74.0
SD	39.6	58.1
Skewness	2.55	1.54
Kurtosis	8.27	4.46

Note: Min, max, mean, and SD are concentrations in mg/l;
Skewness and Kurtosis are dimensionless.

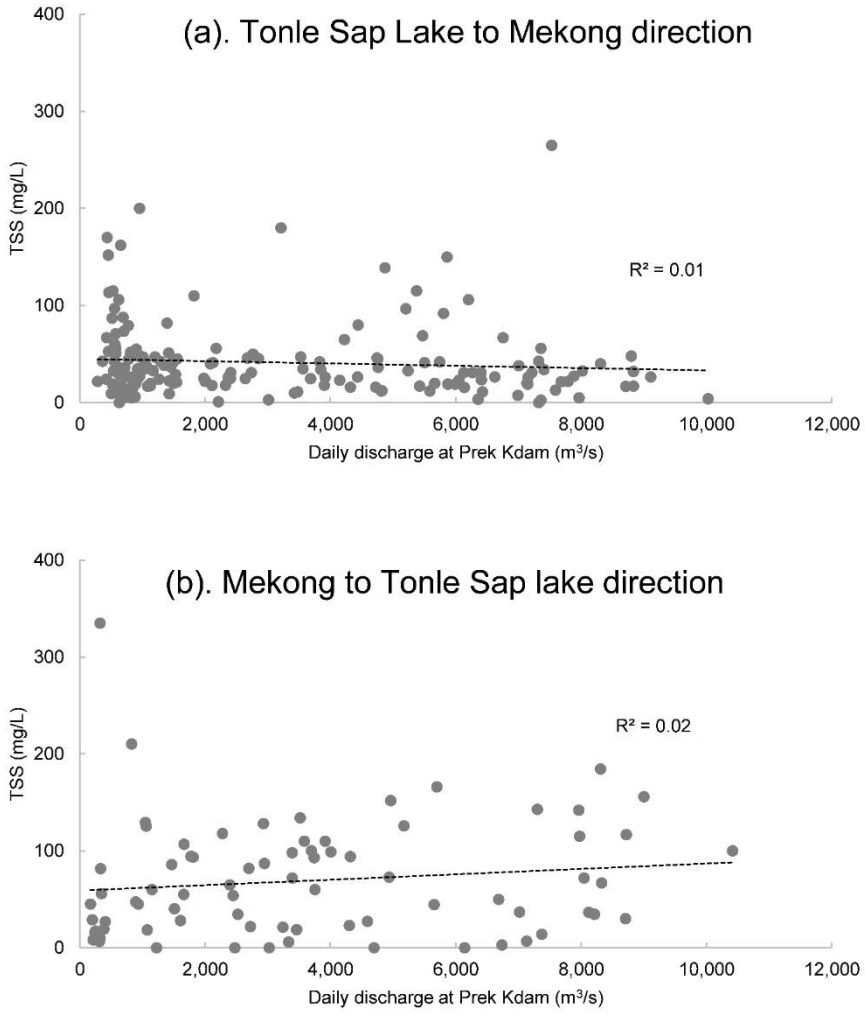

Figure 3-5: *Relationship of TSS concentration and daily discharge of Tonle Sap River at Prek Kdam for the period 1995-2018. (a) Outflow from TSL to Mekong River (in low water stage) and (b) Reverse flow direction from Mekong River to TSL (in high water stage). Data from Cambodia MOWRAM.*

Temporal Variability of Water Discharge and Sediment Load in the Mekong River at Kratie and Chroy Changvar

Annual water discharge and computed sediment loads on the mainstem show higher flows and sediment loads at Kratie than at Chroy Changvar (**Figure 3-6**). Annually, 80% of annual flow occurred during rainy season (from May to October), while 20% of the annual flow occurred during dry season (from November to April). On average, the annual water discharge in Kratie was 404,000 Million cubic meters (Mm^3/yr), 36,000 Mm^3/yr higher than the annual water discharge at Chroy Changvar (368,000 Mm^3/yr). This pattern is similar to the pattern of the flow

in Kratie and Stung Treng (Cambodia-Laos border, about 150 km upstream of Kratie). MRC (2019) reported in their observed flows for the Mekong mainstream stations over the period 2000-2017, Stung Treng discharge is found higher than the downstream at Kratie. After Kratie the Mekong enters extensive floodplains and then delta. Water flow in this reach is very complex (due to downstream backwater effects, overbank flows and temporary water storage on the floodplain) especially during the flood season when hydraulic conditions define the flow distribution between different river branches. The downstream reduction in gauged flow at Kratie and Chroy Changvar occurred mainly at higher flows and can be attributed to overbank flow from the Mekong River traversing the floodplain to TSL and by flow into major distributaries between Kratie and Chroy Changvar. During the flood season, water starts to spillover both banks of the Mekong River between upstream of Kompong Cham (150 km upstream of Chroy Changvar) and Chroy Changvar station. Part of the water spilling over the right bank reaches the Tonle Sap Lake as overland flow. This overland flow was reported to average 2,500 Mm^3/yr by Lu et al. (2014b). On the left bank of the main river at Kampong Cham, part of the Mekong flow is partly diverted into the Tonle Toch River, which then discharges back into the Mekong further downstream of Chroy Changvar in the Mekong delta. The bypass discharge by this river has not been previously reported in the literature. The trend analysis confirmed a decreasing trend in annual water discharge at Chroy Changvar (statistically significant ($p<0.05$)), but we found no significant trend at Kratie upstream

(Table 3-6).

The annual sediment load over the 24-year period averaged 72±26 Mt/yr at Kratie, 78±22 Mt/yr at Chroy Changar (**Figure 3-6**). A pronounced temporal trend was visible at Kratie, where annual sediment loads decreased from 123 Mt/yr in 1995 to 40 Mt/yr in recent years, with the MK test documenting a statistically significant ($p<0.05$) decreasing trend. At Chroy Changar, sediment loads fluctuated over the study period (from 32 Mt in the dry year 1998 to 128 Mt in 2011), but no temporal trend was detected (**Table 3-6**).

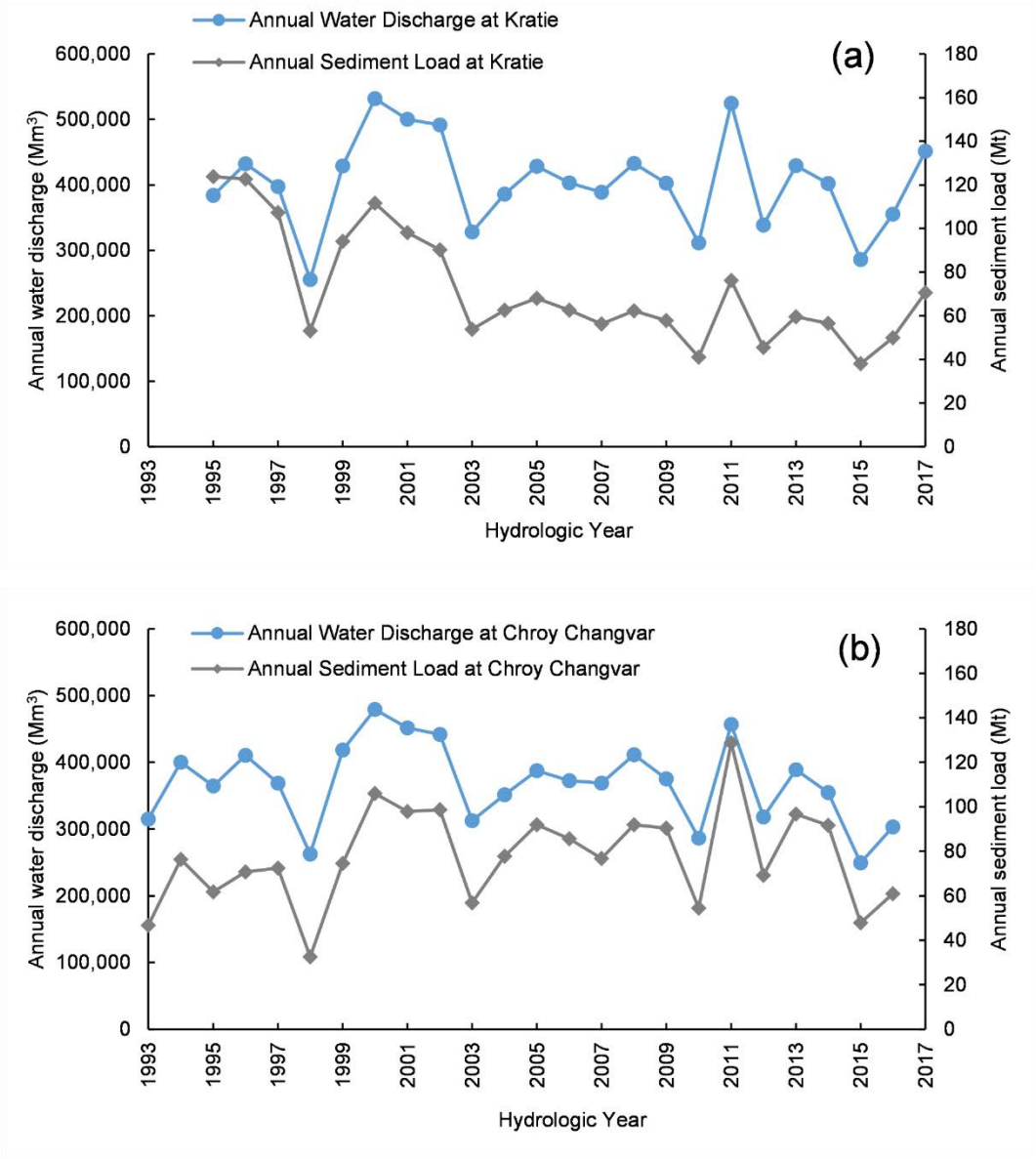

Figure 3-6: *Annual sediment load dynamics and water discharge in the Mekong river at (a) Kratie (hydrological year 1995-2017) and (b) Chroy Changvar stations (hydrological year 1993-2016).*

Table 3-5: *Summary of annual water Discharge and sediment load in the Mekong River at Kratie and Chroy Changvar*

Location	Average	Maximum	Minimum	Trend direction	Significant level
Water Discharge at Kratie (Mm^3)	404,000	532,000	256,000	No trend	
Water Discharge at Chroy Changvar (Mm^3)	368,000	480,000	250,000	Decrease	Significant at α= 0.05

Sediment Load at Kratie (Mt)	72	124	38	Decrease	Significant at α=0.05
Sediment Load at Chroy Changvar (Mt)	78	129	33	No trend	

The monthly discharge and sediment load distribution curves of the entire recorded periods (hydrological year 1995-2017 at Kratie, hydrological year 1993-2016 at Chroy Changvar) (**Figure 3-7**) show similar monthly patterns in high and low sediment load (i.e., equal or exceeding 5% and 95%). However, monthly highest discharge differed significantly. The flow distribution at Kratie and Chroy Changvar confirmed the downstream reduction in gaged flow at Chroy Changvar occurring at higher flows. The peaks of discharge and sediment loads were 133 km^3/month and 40 Mt/month at Kratie, 95 km^3/month and 33 Mt/month at Chroy Changvar.

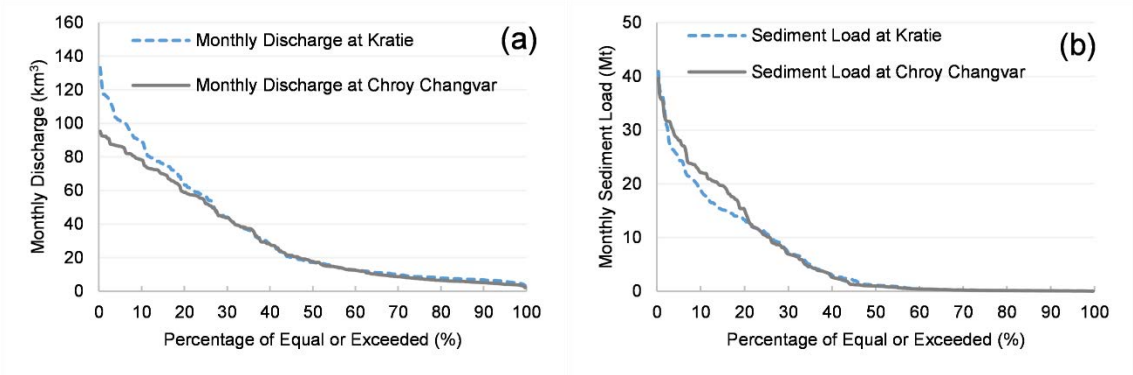

Figure 3-7: *Monthly water discharge and loads sediment load distribution curves at Kratie and Chroy Changvar station.*

Temporal Variability of Water Discharge and Sediment Load in the Tonle Sap River at Prek Kdam

Cumulative seasonal flow volumes are presented in **Figure 3-8**, with negative values indicating inflow from the Mekong to TSL, and positive values for outflow from TSL to the Mekong River. The seasonal outflow of TSL averaged 68,000 Mm^3, which was equivalent to 18% of annual discharge of Mekong River at Chroy Changvar. The seasonal reverse flow into the lake from the Mekong River averaged 36,000 Mm^3, about 10% of annual discharge of Lower Mekong River at Chroy Changvar. Thus, the outflow from the lake was almost twice the reverse flow from the Mekong River. Some of this difference can be attributed to runoff from the 760,000 km^2 drainage lake basin, some to overbank flow from the Mekong mainstem across floodplains into the lake. Mean annual overland runoff into the lake was estimated as 2,600 Mm^3, while runoff from the

drainage basin of the lake was nearly the same, about 2,700 Mm^3 (Lu et al., 2014b). Looking at temporal trends, the reverse flows to the lake showed decreases over the 24-year period, but these were not statistically significant (p, 0.05); outflows also showed decreases, which were significant (p<0.05) (**Table 3-6**).

Net annual sediment loads averaged 3.7 Mt in reverse flows into Tonle Sap Lake, equivalent to 4.8% of annual average sediment load at Chroy Changvar of the Mekong mainstem. (**Figure 3-9**). The sediment load from the lake to Mekong River was 2.9 Mt/yr, which is equal to 3.7% of average annual sediment load in Chroy Changvar. Thus, we can estimate that Tonle Sap Lake gained an average of 0.8 Mt of sediment annually from the Mekong River. However, as this term is calculated as a residual, it must be treated with caution, as such residual terms incorporate and hide errors in other terms (Kondolf and Matthews, 1991). Sediment loads in reverse flow increased over the observed period (statistically significant at $p<0.05$), while sediment load of the lake outflow evinced no trend.

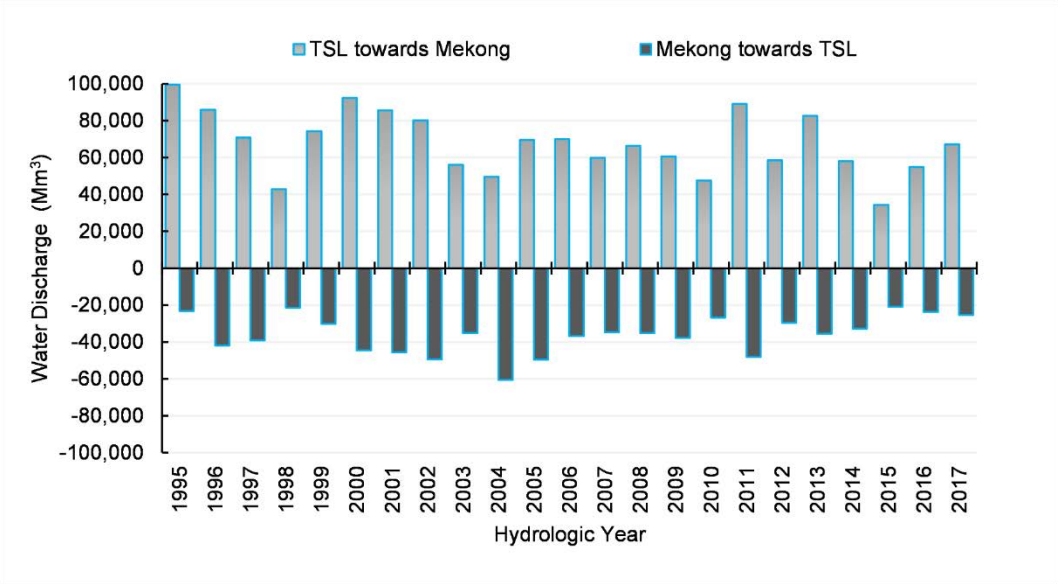

Figure 3-8: *Seasonal water discharge exchange between TSL and Mekong River at Prek Kdam station for the hydrological year 1995 to 2017. The negative values of discharge are (reverse) inflow into the Tonle Sap Lake from Mekong River, while positive values are the outflow from the lake towards Mekong River*

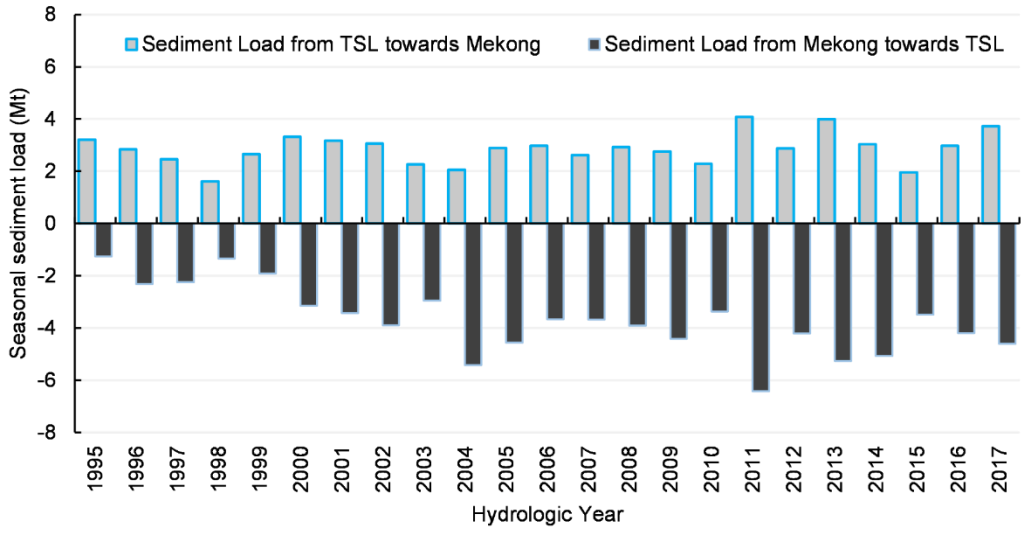

Figure 3-9: *Seasonal sediment load exchange between TSL and Mekong River through Tonle Sap River at Prek Kdam for the hydrological year 1995 to 2017. The negative values of sediment load are (reverse) inflow into the TSL from Mekong River, while positive values are the outflow from the lake towards Mekong River*

Table 3-6: *The percentage share of water discharge and sediment load between TSL and Mekong River at Chroy Changvar, averaged over hydrological year 1995-2017.*

Flow stations/Direction	Water discharge (Million m^3)	Percentage sharing with Mekong at Chroy Changvar (%)	Annual Trend	
			Trend direction	Significant level
TSL to Mekong River	67 600	18	Decrease	Significant at α= 0.05
Mekong River to TSL	3 600	10	No trend	
Mekong mainstem at Chroy Changvar	368 000			
Sediment stations/Direction	**Sediment Load (Mt)**	**Percentage sharing with Mekong at Chroy Changvar (%)**	**Annual Trend**	
			Trend direction	Significant level
TSL to Mekong River	2.9	3.7	No trend	
Mekong River to TSL	3.7	4.8	Increase	Significant at α= 0.05
Mekong mainstem at Chroy Changvar	78			

Sediment Load Linkage between Tonle Sap Lake and Mekong River and Towards the Mekong Delta

The overall balance of flow and sediment load between TSL and Mekong River over the observation hydrological year 1995-2017 shows a net contribution of water from Tonle Sap Basin, as would be expected from such a large drainage area (**Figure 3-10**.a). 2004 was an exception, when the Mekong River at Chroy Changvar reached its maximum discharge 60,000 Mm^3. The annual water balance indicates that TSL contributes an average of 33,000 Mm^3 during the low-flow period to the Mekong delta. However, the net sediment transfers changed over the observation period. From hydrological year 1995 to 2000, Tonle Sap River contributed more sediment load to Mekong River than it received via reverse flows, but from hydrological year 2001-2017 the lake received more sediment from the Mekong River than it contributed (**Figure 3-10**.b), averaging 1.35±0.7 Mt per year.

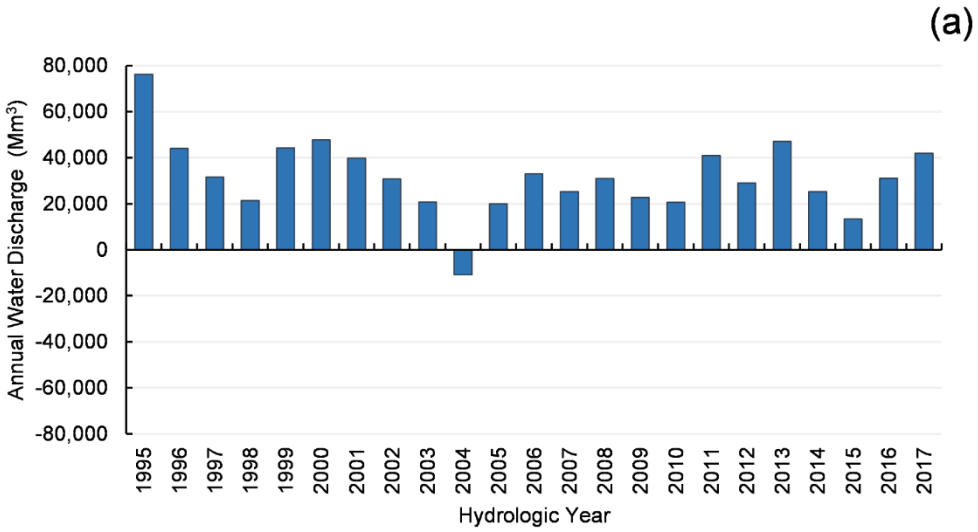

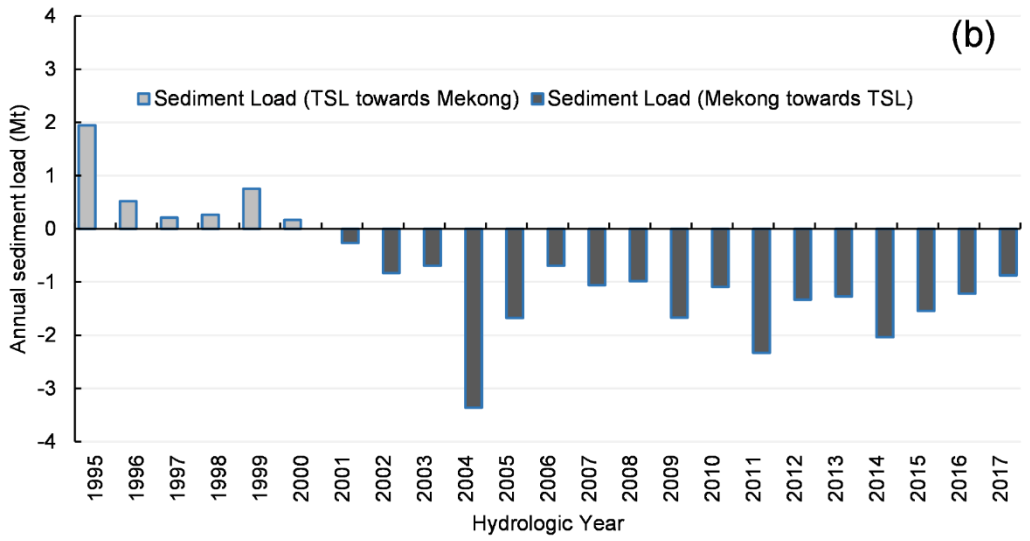

Figure 3-10: *Water discharge and sediment loads balance between TSL and Mekong River through Tonle Sap River at Prek Kdam station for hydrological years 1995 to 2017. (a) Net water discharge, (b) Net sediment load. Annual water discharge and sediment load obtained as residuals by subtracting seasonal water discharge and load in reserve flow from Mekong River and outflow from TSL. Negative values reflect net inflow to the TSL from Mekong River, while positive values are the net outflow from the lake to the Mekong River.*

4. Discussion

Sediment load in the Lower Mekong River

Estimation of the total flux of Mekong to the delta is complicated by interactions with the Tonle Sap system (Kummu and Varis, 2007) since large volumes of flood water enter the Tonle Sap floodplain, where a part of the sediment loads deposited. Our estimated loads at Kratie (72± 38 Mt from 1993-2017) and Chroy Changvar (78±22 Mt from 1995-2018) are similar to those proposed by prior authors, such as Dang et al. (2016), who reported suspended sediment flux of 87±28 Mt/year (1981–2005), Lu et al. (2014a), who reported 50-91 Mt/year of suspended sediment load from 2008 to 2010, and Manh et al. (2014), who estimated 106 Mt/year at Kratie (2010-2011). However, the more recent estimates cover relatively short periods after major dam construction in the upper Mekong mainstem. Looking over longer time scales reflected in stratigraphic analysis of Holocene sediment cores, Ta et al. (2002) proposed 144±34 Mt/year of long-term mean sediment load to the sea, which is consistent with pre-dam estimate of 145 Mt/year by Liu et al. (2013).

As noted above, our study used TSS data from single-depth, mid-channel samples collected as part of a larger water quality dataset (WQMN). It would be preferable to use depth-integrated samples, but these data are extremely limited in time and space (Koehnken, 2012). Prior studies also relied on TSS from single-depth mid-channel samples to estimate sediment load in the Lower Mekong River (Kummu and Varis, 2007), (Kummu et al., 2008) and (Wang et al., 2011). Wang et al. (2011) compared the sediment loads calculated at Chiang Saen in Laos (the most upstream of Lower Mekong) using both the TSS data from the WQMN database and the suspended sediment concentrations (SSC) derived from depth-integrated sampling from the HYMOS dataset (another MRC dataset). This comparison revealed no underestimation using the TSS data at Luang Prabang and Khong Chiam (Laos). For 2008-2010, Lu et al. (2014a) collected suspended sediment samples at 3 evenly-spaced points across the Mekong and Tonle Sap rivers, at 3 depths each (0.5m, 0.2 and 0.8 depth), and found "no major differences in suspended sediment concentrations within the profile."

The results of our trend analysis of sediment load are broadly consistent with patterns observed in major rivers in the region and the world. With the exception of the Amazon, whose suspended sediment discharge increased about 20% 1995-2007 (while water discharge held steady) (Martinez et al., 2009), most rivers have displayed decreases in sediment load. Vörösmarty et al. (2003) suggested that large reservoirs controlled over 40% of runoff of global rivers and trap more than half of the pre-dam sediment load. Walling and Fang (2003) assessed sediment load trends for 145 rivers globally and found that most showed decreasing sediment loads. Li et al. (2020) assessed water and sediment fluxes measured at 138 rivers and found that finding 50 rivers had stable water flows but decreasing sediment flux, while 41 rivers decreased in both water and sediment fluxes. Mean annual water and sediment fluxes to sea from the world's large rivers decreased by 58–98 km^3/yr (0.25%) and 2617–2715 Mt/yr (20.8%) respectively over the recent five to ten year timescale, mainly due to the reduction in water and sediment fluxes that occurred in Asia (by 1.6%–2.0% in water discharge, and by 13.1%–13.2% in sediment fluxes (Li et al., 2020). Displaying a different trend, the largest rivers of North and East Asia (Russia and China), such as Yenisei, Amur, Yellow, Yangtze, Pearl Rivers have experienced suspended sediment load reduction attributed to sediment trapping by dams (Chalov et al., 2018). An earlier study by Liu et al. (2007) found that major rivers in Southern China (e.g., Yangtze, Qiantang, and Pearl rivers) were transporting only about 60% to 80% of their pre-dam loads, while their annual runoff was

reported relatively stable. Gupta et al. (2012) estimated that the combined annual sediment flux of the large Chinese rivers decreased from 1800 Mt to about 370 Mt over the previous five decades.

On the Mekong itself, a number of authors have converged on significant impacts to the river's sediment load. The first mainstem dam was the Manwan Dam on the Upper Mekong (Lancang) in China in 1993, which reduced sediment loads by about 60% (Fu et al., 2008). Projecting effects of completing 8 large mainstem dams on the Lancang, Kummu et al. (2010) estimated a cumulative reduction by half of the river's annual load of 140 million tons. On the Lower Mekong, 11 mainstream dams are planned, of which three (Xayaburi, Pak Beng and DonSahong) are built or under construction (Fox and Sneddon, 2019). The future of the proposed Sambor dam in the Kratie Province of Cambodia is uncertain, but if built as originally proposed, it would likely trap 38Mt/y of an estimated 77Mt/y that would be delivered to the dam under a scenario of 38 dams built on the mainstem and tributaries (Wild and Loucks, 2015).

The concern stems not only from dam development on Mekong mainstem but also on its main tributaries. For example, the Sekong, Sesan, and Srepok basin (so-called '3S basin', the largest tributary of the Mekong) formerly contributed a large portion of the sediment load reaching TSL and the Delta (Wild and Loucks, 2014), but this has been mostly cut off by the recently completed Lower Sesan 2 dam, which blocks the Srepok and Sesan. Overall, construction of the approximately 140 dams planned for the Mekong and its tributaries would trap 96% of the sediment that was naturally delivered to the Mekong Delta (Kondolf et al., 2014). Reduced sediment supply threatens the long-term sustainability of the Mekong Delta (Campbell, 2007; Saito et al., 2007). Beside the dam development in Mekong River Basin, climate change and land-use change are also the crucial factors affecting sediment transport in the basin. Deforestation alters basin erosion, increases sediment delivery to reservoirs and can decrease productivity of hydropower (Kaura et al., 2019). Shrestha et al. (2013) point to uncertainties in the direction and magnitude of variability of flow and sediment yields due to climate change, and Darby et al. (2016) have documented reductions in sediment supply from the basin as runoff from tropical cyclones, delivering about 32% of the suspended sediment load reaching the delta, has been halved since 1981 as cyclone tracks shifted north.

Our study did not explicitly include bed-load due to a lack of data. Suspended sediment load data are more common globally because suspended sediment load is the dominant component of total load and is easier to measure (Milliman and Farnsworth, 2013; Walling, 2009). In the absence of direct measurements of bed load transport, it is frequently assumed that the bed load is up to 10% of the total load (Gregory and Walling, 1973; Milliman and Meade, 1983). For most larger rivers, the bed load much less, e.g. <2% for the Yukon River of North America (Brabets et al., 2000); < 5% for the lowermost Mississippi River (Nittrouer et al., 2008). On the Mekong River, (Koehnken, 2012) reported bed-load in Kratie measured in 2011 was only 1.6 Mt/year, approximately 1.4% of suspended sediment load.

The Mekong River and major regional rivers in term of sediment

Of the total natural global sediment flux to the oceans of about 12.6 to 18 Gt/year, Asia exported the most sediments (~4.8 Gt/year) among continents (Gordeev, 2006; Syvitski et al., 2011; Syvitski et al., 2005). High sediment loads are a common feature of many Asian rivers, especially those originating from the Himalayan-Tibetan Plateau, such as the Yellow Rivers, the Yangtze, the Red and the Mekong, and due to the pronounced topographic relief of the region (Evans et al., 2012; Ludwig and Probst, 1998; Milliman and Syvitski, 1992). However, Africa and Asia showed the largest reduction in sediment flux to the coast in rivers (such as the Nile, Orange, Niger, and Zambezi in Africa and the Yangtze, Indus, and Yellow in Asia), and 31% of the total sediment load retained in reservoirs were indicated in Asia and 25% in Africa (Syvitski et al., 2005). The world's largest river, the Amazon exports around ~550–1500 Mt/yr of sediment to the Atlantic (Dunne et al., 1998; Gaillardet et al., 1997; Guyot et al., 2005; Martinez et al., 2009; Meade et al., 1979). The Mekong's annual sediment load is comparable to loads reported for other major rivers in Asia and elsewhere (**Table 3-7**).

Table 3-7: *The annual mean of sediment is comparable with other major rivers in Asia and continents.*

River	Region	Basin area (10^6 km^2)	River length (km)	Water Discharge km^3/yr	Sediment yield t/km^2/yr	Sediment load (Mt/yr)	References
Yenisei	North Asia	2.5	4800	630	9.54	23.85	Fabre et al., (2019)
Yellow	East Asia	0.77	5464	49	1400	1080	Wang et al., (2011)
Yangtze	East Asia	1.94	6300	900	250	480	Wang et al., (2011)
Pearl	East Asia	0.44	2129	302	88.6	39	Chalov et al., (2018); Lai et al., (2016)
Red	East Asia	0.12	1139	123	780	107	Wei et al., (2021)
Mekong	Southeast Asia	0.79	4800	ND 404	202 102	160 78	Walling, (2008) (This study)
Irrawaddy	Southeast Asia	0.43	2210	410	846	364	Robinson et al., (2007)
Brahmaputra	South Asia	0.61	2900	625	819	500	Rahman et al., (2018)
Congo	Africa	3.7	4700	1300	9.4	33	Laraque et al., (2013)
Mississippi	North American	1.15	3778	530	120	400	Allison and Neill, (2002)
Orinoco	South America	1.0	2140	1000	88	74	Laraque et al., (2013)
Amazon	South America	6.1	6400	6600	100	610	Wittmann et al., (2011)

Sediment exchange between Tonle Sap River and Mekong mainstream

As reported above, our analysis shows that from 1995 to 2000, the Tonle Sap contributed more sediment load to Mekong River than was deposited in the lake, on the average 0.65 Mt annually, but the rate decreased, and then since 2001, an average net 1.35±0.7 Mt of sediment has been deposited in the lake annually. Our results are in the same range but differ from prior studies, which covered shorter time periods, such as Kummu et al. (2008) who estimated for the period 1997-2003 that the TSL received a net transfer of sediment from the Mekong of 3.7 Mt/y, from an average of 5.1 Mt/year to TSL from the Mekong by reverse flow, and an average of 1.4 Mt/year from TSL to the Mekong via outflow. For the period 2008-2010, Lu et al. (2014a) estimated

average sediment load inflow of 6.3 Mt/year into the lake from Mekong mainstem and 7 Mt/year in the outflow, for a net deposition within Tonle Sap Lake, inconsistent with our results. Our estimate of mean annual sediment load in reverse flow from the Mekong River mainstem to Tonle Sap Lake of 4.2 Mt/year is lower than the estimation of Kummu et al. (2008) (5.1 Mt) and Lu et al. (2014a) (6.3 Mt). The mean annual sediment outflow from the Tonle Sap Lake estimated in our study (3.1 Mt /year) is higher than mean value (1.4 Mt/year) estimated by Kummu et al. (2008) but lower than the mean value of 7 Mt/year calculated by Lu et al. (2014a).

By consider the same period (1997-2003) with Kummu et al. (2008), we found that Tonle Sap Lake obtained 2.7 Mt from Mekong mainstem and returned 2.65 Mt annually while Kummu et al. (2008) suggested Tonle Sap Lake obtained 5.1 Mt from Mekong mainstem and returned 1.4 Mt. Kummu et al. (2008) used single-point surface water sample measuring TSS at Prek Kdam with monthly basis from MRC, which is the same data source as our study. This should be the reason, we come up with consistency. Whereas, the different in value might be from the different of method as we applied load estimator, LOADEST base on Least Absolute Deviation (LAD) method, while Kummu et al. (2008) applied sediment transport module of 3D EIA model. With the same study period (2008-2010), we estimated the lake system received 3.9 Mt and shared 2.66 Mt of sediment annual from and to the Mekong mainstem. These values are lower than those suggested by Lu et al. (2014a) which was 6.3 Mt and 7 Mt. The inconsistency of the lake sink or source of sediment and the value between our study and Lu et al. (2014a) might come from various reasons. Firstly, the sampling points are different. We estimated the load from Prek Kdam stations in the Tonle Sap River, while Lu et al. (2014a) from Phom Penh port, which is only located few kilometers toward the Mekong mainstem. Secondly, the different in data source, we used water and sediment data collected by MOWRAM under the MRC water quality program. As noted above, these were not depth-integrated samples, so the accuracy of suspended load estimates from these depends on how well mixed are sediment concentrations vertically and horizontally.

Prior studies also relied on TSS from single-depth mid-channel samples to estimate sediment load in the Lower Mekong River e.g. Kummu and Varis (2007), Kummu et al. (2008) and Wang et al. (2011). While, sampling in 2008-2010 at multiple depths across the cross section of the Mekong at Chroy Changvar and the Tonle Sap River at Phnom Penh Port by Lu et al. (2014a) indicated that suspended sediment was well-mixed. However, within the MRC depth-integrated measurement campaign for year 2011, the inflow (6.4 t/yr) and outflow (1.5 Mt/yr) at Prek Kdam

(Koehnken, 2012) were in line with our finding and Kummu et al. (2008). Thirdly, we used different method for load estimation, Lu et al. (2014a) estimated sediment load base on the developed sediment rating curve and discharge at a given station. By using this, the estimated load can be represented a natural chrematistic flow and concentration with a specific time, however, it cannot be represented or cannot cover the range of characteristic of the water and sediment dynamic in the past and near future. While our estimation base on regression model that developed base on wide range of dataset that would be able to capture characteristic of the water and sediment dynamic for long period. Even there are some inconsistencies, our study can provide anther confirmation to the conflict of previous study and better understand the sediment dynamic between Mekong River and Tonle Sap Lake with longer study periods and extend the discuss within basin scale and reginal scale.

An assessment of water discharge and sediment loads variability of Mekong River and Tonle Sap system presented in this study helps clarify the exchange annual discharge and sediment load toward the Mekong delta. Tonle Sap Lake provided sediment load to the Mekong system and delta annually 0.65±0.6 Mt from 1995 to 2000, but since 2001 Tonle Sap Lake has become a sediment sink for about 1.35±0.7 Mt annually, thereby reducing the annual sediment transport to the Mekong delta. This reduction in sediment supply compounds the threat to the delta from accelerated subsidence and sea level rise (Pokhrel et al., 2018; Syvitski and Higgins, 2012). Decreased sediment loads to the delta and altered sediment transport processes will impact numerous livelihoods which depend on ecosystem services services (Kondolf et al., 2018). The sudden change appears to be due to increased TSS concentrations from the Mekong to Tonle Sap Lake. The concentration of TSS in Kratie appears to have been largely unchanged, but the river could have picked up sediment as it overflowed the wide floodplain, used for agriculture and thus exposed to erosion without the protection of native vegetation (Chea et al., 2016). The instream TSS levels in the lower part of the Mekong River are likely influenced by the interaction between land use/land cover, rainfall-runoff, and anthropogenic activities within the basin (Ly et al., 2020).

The Tonle Sap Compared with Other Lake-Channel Systems

The Tonle Sap is an example of a lake-channel system, a lake (usually on a floodplain) that connects with a main river (via defined channels as well as overbank flow), and that absorbs flood

peaks and releases waters gradually back into the main river as flood stage recedes. Retaining floodwaters in the lake for extended periods of time can result in substantial deposition of sediment from suspension, with potentially significant influences on the riverine sediment budget. Thus, we can ask how the Tonle Sap system compares with other major lake-channel systems, such as Dongting Lake on the Yangtze River floodplain, the second largest freshwater lake in China, and the channel-floodplain systems of the Amazon River.

The Dongting Lake- Yangtze River system is similar to the floodplain lake-channel exchanges of TSL and Mekong River, in that Dongting Lake plays an important role in regulating flood stage and is an important sink of sediments. In flood season water pours into Dongting Lake through three natural distributary channels from the Yangtze (just downstream of its exit from Three Gorges onto the broad alluvial plain) to Dongting Lake. Unlike the Tonle Sap system, when Dongting Lake drains, it does not flow back through the same channel to the river, but drains through different channels back to the river when river stage declines. (Thus, the lake and its connecting channels function as a flood bypass and backwater.) The Yangtze River and Dongting Lake are strongly influenced by operation of The Three Gorges Project upstream. In addition to an important flood-flow-regulating function, Datong Lake functions as sediment sink, receiving 110 Mt/yr from the Yangtze River, while losing only 39 Mt/yr via return flow back to the Yangtze (Dai et al., 2017). The area of Dongting Lake has been reduced over the centuries by construction of dykes to protect farmland encroaching onto the fertile lake bottom during dry years between big floods, a problem that was documented at least back to the Ming Dynasty and continued through the 20th century (Perdue, 1982).

The Amazon is characterized by strong exchanges of water, sediment, nutrients, and biota between channel and its extensive floodplains. The Lago Grand de Curuaı´ floodplain is a complex system of more than 30 interconnected lakes, linked to the Amazon River by several channels, two of which (both with permanent flow) carry return flow from the floodplain into the mainstream (Bourgoin et al., 2007). Lago Grand de Curuaı´ floodplain is a sediment sink, with more than 80% of the suspended solids entering the floodplains deposited (Mertes et al., 1996), but the water storage in the floodplain is more transient than that of the Tonle Sap Lake system, which contributes baseflow back to Mekong River and delta through most of the dry season, as demonstrated in our analysis. On the Amazon floodplain, sediment accumulation (simulated

deposition rate is of about 0.3 Mt km^{-1} yr^{-1}) occurs during the five months of the flood rise, and export of sediments to the mainstream occurs during the recession limb of the seasonal hydrograph (Bourgoin et al., 2007; Mangiarotti et al., 2013).

Thus, the channel-floodplain systems of the Amazon River can act as important sinks of sediments, not only via channelized flow to the Lago Grand de Curuaı´ complex, but also via diffuse overbank flow. However, unlike the Amazon, most of the Mekong's course follows a narrow bedrock-controlled path, so there is very limited exchange of sediment between channel and floodplain, until the reach downstream of Kratie, where the floodplains of the Cambodian lowlands and the Mekong delta are inundated, allowing important fluxes of material and energy between the floodplain and mainstem river channel (Gupta and Liew, 2007). With its channel sized reverse flow pattern, combined with broad, shallow lateral inundation of floodplains during the wet season, the Tonle-Sap-Mekong exchange represents a uniquely developed and important channel-floodplain exchange. In fact, the Mekong-Tonle-Sap exchange is arguably among the best developed such river-floodplain-lake exchange systems in the world, and it supports a fishery that is globally exceptional in many respects (Campbell et al., 2009).

5. Conclusion

The study assessed temporal variability of sediment loads in Lower Mekong River in Cambodia and the sediment linkage between Tonle Sap Lake and Mekong River from 1993 to 2017. Sediment load in the main Mekong River averaged 72± 38 Mt at Kratie and 78±22 Mt at Chroy Changvar from 1993-2018, showing a significant decrease in sediment load, consistent with trends documented in other major rivers in the region and globally. The seasonal and annual sediment load linkage between the Mekong mainstem and Tonle Sap Lake are controlled principally by suspended sediment concentrations and water discharge, in both the reverse flows into the lake and outflows from the lake, both via the Tonle Sap River. The annual water inflow to the lake via reverse flow was 36 km^3, while outflow to the Mekong was 68 km^3. The great water outflow can be attributed to runoff from the Tonle Sap Lake basin and also flows across the floodplain lying to the west of the Mekong River. TSS concentrations of the reverse flows to TSL from Mekong River were nearly twice the concentrations of the outflow from TSL, resulting in a net transfer of

sediment into the Lake. The net sediment loads averaged 3.7 Mt in reverse flows into Tonle Sap Lake, 2.9 Mt/yr in flows from the lake to Mekong River. We found Tonle Sap Lake provided 0.65±0.6 Mt of net sediment to the Mekong annually from 1995 to 2000, but was a sediment sink for an average of 1.35±0.7 Mt annually from 2001 onwards. The change pattern of sediment load linkage can be attributed to a trend of increased TSS concentrations from the Mekong to Tonle Sap Lake. This change in sediment concentration constitutes the most important variable in explaining sediment linkages between the Mekong River and Tonle Sap Lake. This study helps clarify the sediment exchange between Mekong River and Tonle Sap Lake and reveals an important change since 2001, with implications for the sustainability of the delta.

Acknowledgement:

Ty SOK would like to acknowledge Les Bourses du Gouvernement Français (BGF) and Laboratoire Ecologie Fonctionnelle et Environnement (UMR CNRS/Université de Toulouse) for hosting during his PhD study.

References:

Adamson, P.T., Rutherfurd, I.D., Peel, M.C., Conlan, I.A., 2009. The hydrology of the Mekong River, The Mekong. Elsevier, pp. 53-76.

Allison, M.A., Neill, C.F., 2002. Accumulation rates and stratigraphic character of the modern Atchafalaya River prodelta, Louisiana.

APHA, 1995. Standard Methods for the Examination of Water and Wastewater, 19th edition. American Public Health Association, Washington, D.C.

Arias, M.E. et al., 2014. Impacts of hydropower and climate change on drivers of ecological productivity of Southeast Asia's most important wetland. 272, 252-263.

Bobrovitskaya, N.N., Kokorev, A.V., Lemeshko, N.A.J.G., Change, P., 2003. Regional patterns in recent trends in sediment yields of Eurasian and Siberian rivers. 39, 127-146.

Bourgoin, L.M. et al., 2007. Temporal dynamics of water and sediment exchanges between the Curuaí floodplain and the Amazon River, Brazil. 335, 140-156.

Brabets, T.P., Wang, B., Meade, R.H.J.W.-R.I.R., 2000. Environmental and hydrologic overview of the Yukon River Basin, Alaska and Canada. 99, 4204.

Campbell, I.C., 2007. Perceptions, data, and river management: Lessons from the Mekong River. Water Resources Research, 43.

Campbell, I.C., Say, S., Beardall, J., 2009. Tonle Sap Lake, the heart of the lower Mekong, The Mekong. Elsevier, pp. 251-272.

Chalov, S. et al., 2017. A toolbox for sediment budget research in small catchments. 10, 43-68.

Chalov, S.R. et al., 2018. Environmental and human impacts on sediment transport of the largest Asian rivers of Russia and China. 77, 274.

Chea, R., Grenouillet, G., Lek, S.J.P.o., 2016. Evidence of water quality degradation in lower Mekong basin revealed by self-organizing map. 11, e0145527.

Cheng, L., Jueyi, S., Zhao-Yin, W.J.I.J.o.S.R., 2008. Sediment load reduction in Chinese rivers. 23, 44-55.

Cohen, S., Kettner, A.J., Syvitski, J.P.J.g., change, p., 2014. Global suspended sediment and water discharge dynamics between 1960 and 2010: Continental trends and intra-basin sensitivity. 115, 44-58.

Dai, M., Wang, J., Zhang, M., Chen, X.J.I.J.o.S.R., 2017. Impact of the Three Gorges Project operation on the water exchange between Dongting Lake and the Yangtze River. 32, 506-514.

Dang, T.D., Cochrane, T.A., Arias, M.E., Van, P.D.T., de Vries, T.T., 2016. Hydrological alterations from water infrastructure development in the Mekong floodplains. Hydrological processes, 30, 3824-3838.

Darby, S.E. et al., 2016. Fluvial sediment supply to a mega-delta reduced by shifting tropical-cyclone activity. 539, 276-279.

Dunne, T., Mertes, L.A., Meade, R.H., Richey, J.E., Forsberg, B.R.J.G.S.o.A.B., 1998. Exchanges of sediment between the flood plain and channel of the Amazon River in Brazil. 110, 450-467.

Evans, A.E., Hanjra, M.A., Jiang, Y., Qadir, M., Drechsel, P.J.I.J.o.W.R.D., 2012. Water quality: assessment of the current situation in Asia. 28, 195-216.

Fabre, C.m. et al., 2019. Assessment of sediment and organic carbon exports into the Arctic ocean: The case of the Yenisei River basin. 158, 118-135.

Fox, C.A., Sneddon, C.S., 2019. Political borders, epistemological boundaries, and contested knowledges: Constructing dams and narratives in the Mekong River basin. Water, 11, 413.

Fu, K., He, D.M., Lu, X.X.J.Q.I., 2008. Sedimentation in the Manwan reservoir in the Upper Mekong and its downstream impacts. 186, 91-99.

Fujii, H. et al., 2003. Hydrological roles of the Cambodian floodplain of the Mekong River. 1, 253-266.

Gaillardet, J., Dupre, B., Allegre, C.J., Négrel, P.J.C.g., 1997. Chemical and physical denudation in the Amazon River Basin. 142, 141-173.

Gordeev, V.J.G., 2006. Fluvial sediment flux to the Arctic Ocean. 80, 94-104.

Gray, J.R., 2000. Comparability of suspended-sediment concentration and total suspended solids data. US Department of the interior, US Geological Survey.

Gregory, K.J., Walling, D.E., 1973. Drainage basin form and process.

Gupta, A., Liew, S.C., 2007. The Mekong from satellite imagery: A quick look at a large river. Geomorphology, 85, 259-274.

Gupta, H., Kao, S.-J., Dai, M., 2012. The role of mega dams in reducing sediment fluxes: A case study of large Asian rivers. Journal of Hydrology, 464, 447-458.

Guyot, J.L., Filizola, N., Laraque, A., 2005. Régime et bilan du flux sédimentaire de l'Amazone à Óbidos (Pará, Brésil) de 1995 à 2003, Proceedings of Sediment Budget symposium held during the Seventh IAHS Scientific Assembly. IAHS Publication Foz do Iguaçu, pp. 347-354.

Hai, P.T., Masumoto, T., Shimizu, K., 2008. Development of a two-dimensional finite element model for inundation processes in the Tonle Sap and its environs. Hydrological Processes: An International Journal, 22, 1329-1336.

Higgins, A., Restrepo, J.C., Ortiz, J.C., Pierini, J., Otero, L.J.I.J.o.S.R., 2016. Suspended sediment transport in the Magdalena River (Colombia, South America): Hydrologic regime, rating parameters and effective discharge variability. 31, 25-35.

Howden, N., Burt, T., 2009. Statistical analysis of nitrate concentrations from the Rivers Frome and Piddle (Dorset, UK) for the period 1965–2007. Ecohydrology, 2, 55-65.

Kaura, M., Arias, M.E., Benjamin, J.A., Oeurng, C., Cochrane, T.A., 2019. Benefits of forest conservation on riverine sediment and hydropower in the Tonle Sap Basin, Cambodia. Ecosystem Services, 39, 101003.

Kendall, M., 1975. Rank correlation measures. Charles Griffin, London, 202, 15.

Koehnken, L.J.P.D.A.o.P.R., 2012. IKMP discharge and sediment monitoring program review, recommendations and data analysis.

Kondolf, G., Rubin, Z., Minear, J., 2014. Dams on the Mekong: Cumulative sediment starvation. Water Resources Research, 50, 5158-5169.

Kondolf, G.M., Matthews, W.G.J.W.R.R., 1991. Unmeasured residuals in sediment budgets: a cautionary note. 27, 2483-2486.

Kondolf, G.M. et al., 2018. Changing sediment budget of the Mekong: Cumulative threats and management strategies for a large river basin. Science of The Total Environment, 625, 114-134.

Kongmeng, L., Larsen, H., 2016. Lower Mekong Regional water quality monitoring report. Vientiane, Lao PDR: Mekong River Commission.

Kummu, M., Lu, X., Wang, J., Varis, O., 2010. Basin-wide sediment trapping efficiency of emerging reservoirs along the Mekong. Geomorphology, 119, 181-197.

Kummu, M., Penny, D., Sarkkula, J., Koponen, J.J.A.A.J.o.t.H.E., 2008. Sediment: curse or blessing for Tonle Sap Lake? , 37, 158-163.

Kummu, M., Sarkkula, J.J.A.A.J.o.t.H.E., 2008. Impact of the Mekong River flow alteration on the Tonle Sap flood pulse. 37, 185-192.

Kummu, M., Varis, O.J.G., 2007. Sediment-related impacts due to upstream reservoir trapping, the Lower Mekong River. 85, 275-293.

Lai, C. et al., 2016. Spatio-temporal variation in rainfall erosivity during 1960–2012 in the Pearl River Basin, China. 137, 382-391.

Laraque, A. et al., 2013. A comparison of the suspended and dissolved matter dynamics of two large inter-tropical rivers draining into the Atlantic Ocean: The Congo and the Orinoco. 27, 2153-2170.

Li, L. et al., 2020. Global trends in water and sediment fluxes of the world's large rivers. 65, 62-69.

Li, S., Bush, R.T., 2015. Rising flux of nutrients (C, N, P and Si) in the lower Mekong River. Journal of Hydrology, 530, 447-461.

Liu, C., He, Y., Des Walling, E., Wang, J., 2013. Changes in the sediment load of the Lancang-Mekong River over the period 1965–2003. Science China Technological Sciences, 56, 843-852.

Liu, C., Wang, Z., Sui, J., 2007. Analysis on variation of seagoing water and sediment load in main rivers of China. Journal of Hydraulic Engineering, 38, 1444-1452.

Lu, X., Kummu, M., Oeurng, C.J.E.S.P., Landforms, 2014a. Reappraisal of sediment dynamics in the Lower Mekong River, Cambodia. 39, 1855-1865.

Lu, X., Li, S., Kummu, M., Padawangi, R., Wang, J.J.Q.I., 2014b. Observed changes in the water flow at Chiang Saen in the lower Mekong: Impacts of Chinese dams? , 336, 145-157.

Lu, X., Siew, R., 2005. Water discharge and sediment flux changes in the Lower Mekong River. Hydrology and Earth System Sciences Discussions, 2, 2287-2325.

Ludwig, W., Probst, J.-L.J.A.J.o.S., 1998. River sediment discharge to the oceans; present-day controls and global budgets. 298, 265-295.

Ly, K., Metternicht, G., Marshall, L.J.S., 2020. Linking Changes in Land Cover and Land Use of the Lower Mekong Basin to Instream Nitrate and Total Suspended Solids Variations. 12, 2992.

Mangiarotti, S. et al., 2013. Discharge and suspended sediment flux estimated along the mainstream of the Amazon and the Madeira Rivers (from in situ and MODIS Satellite Data). 21, 341-355.

Manh, N.V., Dung, N.V., Hung, N.N., Merz, B., Apel, H., 2014. Large-scale suspended sediment transport and sediment deposition in the Mekong Delta. Hydrology and Earth System Sciences, 18, 3033.

Mann, H.B., 1945. Nonparametric tests against trend. Econometrica: Journal of the Econometric Society, 245-259.

Martinez, J.-M., Guyot, J.-L., Filizola, N., Sondag, F.J.C., 2009. Increase in suspended sediment discharge of the Amazon River assessed by monitoring network and satellite data. 79, 257-264.

Masumoto, T., 2000. Modelling of multi-functional hydrologic roles of tonle sap lake and its vicinities, Proceedings of the Workshop on Hydrologic & Environmental Modelling in the Mekong Basin, Mekong River Commission, 2000, pp. 181-192.

Meade, R.H., Moody, J.A.J.H.P.A.I.J., 2010. Causes for the decline of suspended-sediment discharge in the Mississippi River system, 1940–2007. 24, 35-49.

Meade, R.H. et al., 1979. Sediment loads in the Amazon River. 278, 161-163.

Mertes, L.A., Dunne, T., Martinelli, L.A.J.G.S.o.A.B., 1996. Channel-floodplain geomorphology along the Solimões-Amazon river, Brazil. 108, 1089-1107.

Milliman, J.D., Farnsworth, K.L., 2013. River discharge to the coastal ocean: a global synthesis. Cambridge University Press.

Milliman, J.D., Meade, R.H.J.T.J.o.G., 1983. World-wide delivery of river sediment to the oceans. 91, 1-21.

Milliman, J.D., Syvitski, J.P.J.T.j.o.G., 1992. Geomorphic/tectonic control of sediment discharge to the ocean: the importance of small mountainous rivers. 100, 525-544.

MRC, 2019. State of the basin report 2018.

Murphy, J.C.J.H., Sciences, E.S., 2020. Changing suspended sediment in United States rivers and streams: linking sediment trends to changes in land use/cover, hydrology and climate. 24, 991-1010.

Nittrouer, J.A., Allison, M.A., Campanella, R.J.J.o.G.R.E.S., 2008. Bedform transport rates for the lowermost Mississippi River. 113.

Partheniades, E.J.J.o.t.h.d., 1977. Unified view of wash load and bed material load. 103.

Peng, J., Chen, S., Dong, P.J.C., 2010. Temporal variation of sediment load in the Yellow River basin, China, and its impacts on the lower reaches and the river delta. 83, 135-147.

Perdue, P.C.J.T.J.o.A.S., 1982. Official goals and local interests: Water control in the Dongting Lake region during the Ming and Qing periods. 747-765.

Pietroń, J., Jarsjö, J., Romanchenko, A.O., Chalov, S.R.J.J.o.H., 2015. Model analyses of the contribution of in-channel processes to sediment concentration hysteresis loops. 527, 576-589.

Pokhrel, Y. et al., 2018. A review of the integrated effects of changing climate, land use, and dams on Mekong river hydrology. 10, 266.

Rahman, M. et al., 2018. Recent sediment flux to the Ganges-Brahmaputra-Meghna delta system. Science of the total environment, 643, 1054-1064.

Robinson, R.A.J. et al., 2007. The Irrawaddy river sediment flux to the Indian Ocean: the original nineteenth-century data revisited. The Journal of Geology, 115, 629-640.

Runkel, R.L., Crawford, C.G., Cohn, T.A., 2004. Load Estimator (LOADEST): A FORTRAN program for estimating constituent loads in streams and rivers. 2328-7055.

Saito, Y., Chaimanee, N., Jarupongsakul, T., Syvitski, J.P., 2007. Shrinking megadeltas in Asia: Sea-level rise and sediment reduction impacts from case study of the Chao Phraya Delta. Inprint Newsletter of the IGBP/IHDP Land Ocean Interaction in the Coastal Zone, 2, 2007.

Shrestha, B. et al., 2013. Impact of climate change on sediment yield in the Mekong River basin: a case study of the Nam Ou basin, Lao PDR. Hydrology and Earth System Sciences, 17, 1-20.

Siev, S., Paringit, E.C., Yoshimura, C., Hul, S.J.H., 2016. Seasonal changes in the inundation area and water volume of the Tonle Sap River and its floodplain. 3, 33.

Stevaux, J.C., Martins, D.P., Meurer, M.J.G., 2009. Changes in a large regulated tropical river: The Paraná River downstream from the Porto Primavera Dam, Brazil. 113, 230-238.

Syvitski, J., Higgins, S., 2012. Going under: The world's sinking deltas. New Scientist, 216, 40-43.

Syvitski, J.P., Kettner, A.J.P.T.o.t.R.S.A.M., Physical, Sciences, E., 2011. Sediment flux and the Anthropocene. 369, 957-975.

Syvitski, J.P., Vörösmarty, C.J., Kettner, A.J., Green, P.J.s., 2005. Impact of humans on the flux of terrestrial sediment to the global coastal ocean. 308, 376-380.

Ta, T.K.O. et al., 2002. Holocene delta evolution and sediment discharge of the Mekong River, southern Vietnam. Quaternary Science Reviews, 21, 1807-1819.

Vinhteang, K. et al., 2019. Temporal Variation of Sediment and Nutrients (Nitrate and Phosphorus) Dynamics in the Mekong River in Cambodia, The 4th International Symposium On Conservation and Management of Tropical Lakes "Featuring Environmental Health and Lake Basin Management", Phnom Penh.

Vörösmarty, C.J. et al., 2003. Anthropogenic sediment retention: major global impact from registered river impoundments. 39, 169-190.

Walling, D., Fang, D., 2003. Recent trends in the suspended sediment loads of the world's rivers. Global and planetary change, 39, 111-126.

Walling, D., Fang, D.J.G., change, p., 2003. Recent trends in the suspended sediment loads of the world's rivers. 39, 111-126.

Walling, D.E., 2009. The impact of global change on erosion and sediment transport by rivers: current progress and future challenges. Unesco.

Walling, D.E.J.A.A.J.o.t.H.E., 2008. The changing sediment load of the Mekong River. 37, 150-157.

Walling, D.J.G., 2006. Human impact on land–ocean sediment transfer by the world's rivers. 79, 192-216.

Walling, D.J.R.p.f.t.M.R.C., 2005. Evaluation and analysis of sediment data from the Lower Mekong River.

Wang, J.J., Lu, X., Kummu, M.J.R.R., Applications, 2011. Sediment load estimates and variations in the Lower Mekong River. 27, 33-46.

Wei, X. et al., 2021. A modelling-based assessment of suspended sediment transport related to new damming in the Red River basin from 2000 to 2013. 197, 104958.

Wild, T.B., Loucks, D.P., 2014. Managing flow, sediment, and hydropower regimes in the Sre Pok, Se San, and Se Kong Rivers of the Mekong basin. Water Resources Research, 50, 5141-5157.

Wild, T.B., Loucks, D.P., 2015. Mitigating dam conflicts in the Mekong River Basin, Conflict resolution in water resources and environmental management. Springer, pp. 25-48.

Williams, G.P.J.J.o.H., 1989. Sediment concentration versus water discharge during single hydrologic events in rivers. 111, 89-106.

Wittmann, H. et al., 2011. Sediment production and delivery in the Amazon River basin quantified by in situ–produced cosmogenic nuclides and recent river loads. Bulletin, 123, 934-950.

Yue, S., Wang, C.Y., 2002. Applicability of prewhitening to eliminate the influence of serial correlation on the Mann-Kendall test. Water Resources Research, 38.

CHAPTER IV

Nutrient Flux Variabilities Mekong-Tonle Sap

This chapter was submitted in the Ecological Engineering Journal, and it is under review process. The work of this chapter is aligned with the previous chapter. The purpose of this chapter is to present the annual and monthly dynamic of nutrient flux (Nitrate and Total Phosphorus) in the Mekong in Cambodia connecting with Tonle Sap River in Cambodia and to quantify nitrate and total phosphorus flux contributed by the Mekong River and Tonle Sap Lake to the Mekong Delta through hydrological reversal system.

Sok, T., Oeurng, C., Kaing, V., Sauvage, S., Lu, X.X. and Sánchez-Pérez, J.M. Nutrient Transport and Exchange between Mekong River and Tonle Sap Lake in Cambodia. Ecological Engineering. Under review.

4. Chapter IV. Nutrient Flux Variabilities Mekong-Tonle Sap

4.1. Scientific Context and Objectives

The sediment and nutrient linkage between the Mekong mainstream and the Tonle Sap Lake would be necessary to better understand, as the sediment input from the Mekong is crucial for the Tonle Sap's ecosystem functions. The sediment exchange between Tonle Sap Lake and Mekong River was previously estimated. However, the study of the long-term nutrient transport dynamics as a baseline and information between the Mekong mainstream and the Tonle Sap River is still lacking. To address the problem mentioned above and the aforementioned gaps, understanding and changing nutrient flux in the Lower Mekong River is crucially required. The nutrient exchange between the Tonle Sap Lake and Mekong River through Tonle Sap River and their nutrient input to the Mekong Delta for a long-term period in different hydrological conditions. The study firstly presented the annual and monthly dynamic and flux of nutrient transports (Nitrate and Total Phosphorus) in the Mekong in Cambodia connecting with Tonle Sap River in Cambodia, and secondly, the study presented a quantification of annual and monthly nitrate. Total phosphorus flux contributed by the Mekong River and Tonle Sap Lake to the Mekong Delta through hydrological reversal system.

4.2. Materials and Methods

The monitoring sites started from the upstream site of the Mekong River of Cambodia at Kratie, moving to the Chroy Changva (near Chatumuk confluence) to capture the water discharge and quality before the water changing the curse to the Tonle Sap River and Mekong Delta. Prek Kdam station, located along the Tonle Sap River, was included in the study since it can represent the Mekong-Tonle Sap system's reverse system. Nitrate (NO_3^-) and total phosphorus (TP) concentration was obtained from water quality sampling conducted monthly by MOWRAM from 1995 to 2018 at Kratie station and 1993 to 2017 Chroy Changvar station. For Tonle Sap River, the monthly basis water sampling (once every month) also carried out from 1995 to 2018. Sediment Loads were estimated at Kratie, Chroy Changvar, and Prek Kdam Station using the LOAD ESTimator (LOADEST) (Runkel et al., 2004).

4.3. Results and Discussions

For the Mekong River, the peak value of nitrate and total phosphorus flux occurred in August, and September corresponds to the peak runoff period. The maximum monthly nitrate flux at Kratie and Chroy Changva was about 85 $\times 10^3$ tons and 138 $\times 10^3$ tons (kt), respectively. Maximum TP flux was approximately 28 $\times 10^3$ tons at Kratie and 18 $\times 10^3$ tons at Chroy Changva. Moreover, the lowest fluxes appeared in low runoff periods from February to March with less than 5 $\times 10^3$ tons of nitrate and 2 $\times 10^3$ tons of TP flux. The annual total phosphorus flux in Kratie and Chroy Changva was fluctuated over the study period from 77 to 137 $\times 10^3$ tons/yr for Kratie and 46 to 116 $\times 10^3$ tons/yr for Chroy Changva. On average, nitrate flux was estimated at 364 and 557 $\times 10^3$ tons/yr, and total phosphorus was approximately 100 $\times 10^3$ tons/yr and 73 $\times 10^3$ tons/yr at Kratie and Chroy Changva, respectively.

In terms of flow from Tonle Sap Lake towards Mekong River, nitrate and total phosphorus flux were estimated to be 0.4-1.84 kt/month and 0.06-0.18 kt/month. August is the peak month of nutrients flux that Tonle Sap Lake contributes to the Mekong River or delta. Otherwise, the estimation of nitrate and total phosphorus flux from the Mekong to the lake was 0.88-1.72 kt/month and 0.04-1.14 kt/month. These values showed that the Mekong provided nitrate to Tonle Sap Lake more than the lake provided to the Mekong; in contrast, the lake shared total phosphorus to the Mekong in a year**.** The amount of annual nitrate and TP flux from Tonle Sap Lake to the Mekong was approximately 33.96±13.77 kt/yr and 6.55±1.37 kt/yr on average.

Furthermore, the amount of inflow nutrients to the Mekong river was estimated at about 35.76±12.47 kt/yr of nitrate and 8.67±3.34 kt/yr of total phosphorus. This result points out that annually Tonle Sap received a higher amount of both nitrate and total phosphorus from the Mekong system than its amount provided to the Mekong. The study has emphasized the interaction role of Tonle Sap Lake and Mekong in nutrient supply. Based on the analysis during the study period (1997-2016 for nitrate and 2005-2016 for TP), Tonle Sap Lake contributed 34 kt/year of nitrate and 6.6 kt/year of total phosphorus to the Mekong system or Mekong Delta. At the same time, Mekong River shared nitrate flux 35.8 kt/year and 8.7 kt/year of TP to Tonle Sap Lake and its floodplain during high flow season. This result can lead to a conclusion that Tonle Sap Lake gain flux (nitrate and total phosphorus) from the Mekong. In other words, the Mekong River plays the role of the source of nutrients, especially total phosphorus, to Tonle Sap Lake and its floodplain.

4.4. Conclusion and Perspectives

The study firstly assessed the dynamic of nutrient transport in the Mekong in Cambodia and secondly to quantify the nutrient (nitrate and total phosphorus) fluxes contributed by the Mekong River to Tonle Sap Lake and its hydrological reversal system. We estimated annual nitrate flux of 364±45 kt/yr at Kratie and 557±109 kt/yr at Chroy Changva from the hydrological year 1995-2016. The total phosphorus flux was found 100±16 kt/yr at Kratie and 73±19 kt/yr at Chroy Changva from 2005-2017. For the nutrient exchanging between Tonle Sap Lake and Mekong River, the amount of annual nitrate and TP flux from Tonle Sap Lake to the Mekong on average was approximately 34±13.8 kt/yr and 6.6±1.4 kt/yr. Furthermore, the amount of inflow nutrients to the lake from the Mekong amounted to 35.8±12.5 kt/yr of nitrate and 8.7±3.3 kt/yr of total phosphorus, respectively. The study also pointed out that Tonle Sap Lake was the nitrate sinks during the period 2000-2012 and 2007-2015 for total phosphorus. The study has emphasized the interaction role of Tonle Sap Lake and Mekong in nutrient supply. This result can lead to conclude that Tonle Sap Lake gains in the amount of nutrients from the Mekong; in other words, the Mekong River plays the role of the source to Tonle Sap Lake and its floodplain.

Further, beyond this part of the work, the study on nutrient flux in the Mekong Tonle Sap system need to investigated, and modelling required.

4.5. Full paper: Sok, T., Oeurng, C., Kaing, V., Sauvage, S., Lu, X.X. and Sánchez-Pérez, J.M. Nutrient Transport and Exchange between Mekong River and Tonle Sap Lake in Cambodia. Ecological Engineering. Under review.

Nutrient Transport and Exchange between Mekong River and Tonle Sap Lake in Cambodia

Ty SOK[1,2,*], Chantha OEURNG[1], Vinhteang KAING[1], Sabine SAUVAGE[2], Lu Xi Xi[3], José Miguel SANCHEZ PEREZ[2]

[1]Faculty of Hydrology and Water Resources Engineering, Institute of Technology of Cambodia, Russian Federation Blvd., P.O.BOX 86, Phnom Penh Cambodia.
[2]Laboratoire Ecologie Fonctionnelle et Environnement, UMR 5245 CNRS/UPS/INPT ENSAT, Avenue de l'Agrobiopole, BP 32607, Auzeville Tolosane, 31326 CASTANET TOLOSAN, France
[3] Department of Geography, National University of Singapore, Singapore 119260
[*]Corresponding author: sokty@itc.edu.kh

Abstract: The Mekong River, one of the world's great rivers in Asia, has significant biodiversity and productivity in the region; however, recently, the water quality of the basin has been reported deteriorating as a consequence of land-use change, dam reservoir construction, population growth, and climate change. This study provided the first attempt to estimate inter-annual and intra-annual (monthly) variability of nutrients fluxes (nitrate (NO_3^-) and total phosphorus (TP)) of the Lower Mekong River and Tonle Sap River in Cambodia. It assessed the nutrients linkage between the Mekong River and Tonle Sap Great Lake. Long-term monitoring data from three stations were used in this study, from the Mekong at Kratie (upstream), downstream to the Mekong at Chroy Changva (just upstream of the Tonle Sap confluence), and the Tonle Sap River at Prek Kdam (about 40 km upstream of the Mekong confluence and 70 km downstream the Tonle Sap Lake). We estimated inter-annual nitrate flux about 364±45 kt/yr at Kratie and 557±109 kt/yr at Chroy Changva from 1995-2017. The total phosphorus flux was found 100±16 kt/yr at Kratie and 73±19 kt/yr at Chroy Chnagva from 2005-2017. We noticed that the annual nitrate flux along the Mekong is strongly seasonal as a result of 80-88% of the annual nitrate occurring from May to October. A similar pattern to total phosphorus, approximately 90% of the annual total phosphorus flux occurring between May to October. The result of nutrients exchange between the Mekong River and Tonle Sap River showed that Tonle Sap Lake gained in the nutrients flux from the Mekong by receiving from the Mekong about 35.8±12.5 kt/yr of nitrate flux and 8.7±3.3 kt/yr of TP flux while contributing to the Mekong only about 34±13.8 kt/yr of nitrate and 6.6±1.4 kt/yr of TP flux. The result authenticated that the Mekong River plays a vital role in supplying nutrient source, especially during flood season, to Tonle Sap Lake and its floodplain.

Keywords: Nutrient Transport, Mekong River, Tonle Sap Lake

1. Introduction

One of the largest transboundary rivers in Asia and the world, the Mekong River, originates in the Tangelo mountain range of the Tibetan region of China. It flows through six nations: China, Cambodia, Lao PDR, Myanmar, Thailand, and Vietnam before it enters the South China Sea in Vietnam. The physical diversity, tropical location, and high productivity of the Mekong fostered it to become the second most species richness after the Amazon River (Froese and Pauly, 2010). There are at least 1200 species of fish and possibly up to 1700, living in the Mekong Basin as the potential of its geological and hydrological heterogeneity (Coates et al., 2005). The Lower Mekong

River is the most essential region both economically and environmentally and while there are about 60 million living and depend on the water resources in the region (MRC, 2010). Located in Lower Mekong in Cambodia, the Tonle Sap Great Lake is the productive ecosystem and the most diverse and highest yielding in inland fisheries in the world, which supported by the sediment and sediment-bound nutrients from the annual flood pulse of the Mekong (Lamberts, 2006). The Mekong Delta is an Asian center of biodiversity and rice production and supports a population of more than 17 million people (Szabo et al., 2016). The seasonal delivery of water, sediments, and nutrients of the Mekong is the core attributed to agricultural, ecological, and fish productivity of the Lower Mekong, particularly Tonle Sap Lake and Mekong Delta (Arias et al., 2014; Kummu et al., 2008; Lamberts, 2006).

Despite the significance of the Mekong River to biodiversity and productivity of regions, recently, water quality has deteriorated consequence of land-use change, reservoir construction, population growth, and meteorological extremes (Campbell, 2009; Chea et al., 2016b; Dudgeon, 2005). The construction of the dams in Upstream Mekong has led to significant trapping of sediment and nutrients (Kummu and Varis, 2007; Lu and Siew, 2006), e.g Manwan dam in 1992 and Dachaoshan in 2003. The Mekong River is experiencing dramatic land surface disturbance such as forest clearing, arable land expansion, as a result of rapid population growth and expanding urbanization (Lu and Siew, 2005). Land-use change in the region is accelerating element cycling and appreciably altering ecosystems the riverine, estuarine systems, which is evident by dramatic shifts in the supply of nutrients (Li and Bush, 2015). Changes in sediment and nutrient are of particular concern in tropical regions undergoing rapid development (change of land cover and dams development) since the 1990s, which have impacted on biodiversity and long-term stability of Tonle Sap lake and the Mekong Delta (Campbell, 2007; Tamura et al., 2007).

Compared to other rivers in Asia such as the Ganges and the Yangtze, the annual nitrogen load in the Mekong was still low in twenty-century (Seitzinger et al., 2005). However, the Mekong is facing the disruption of its nutrient balance as large increases of nutrient inputs to surface water are expected in the twenty-first century due to increases in agricultural production and infrastructure development (Galloway et al., 2004; Liljeström et al., 2012; MRC, 2003b)., Iida et al. (2011) and Iida et al. (2011) and Ribolzi et al. (2011) pointed out high concentrations of nutrients (NO_3 and P), nitrogenous matter, and TSS in upstream Mekong located in northern of Laos PDR. Watanabe et al. (2003) also raised the disturbance of nitrogen balance in Southern

Vietnam that was likely affected by agricultural development. Li and Bush (2015) examined a whole-of-system scale, the spatial, monthly, and inter-annual flux of nutrients and stoichiometric ratios in the Mekong River using a data-set (1985–2011). Kummu and Varis (2007) revealed that the construction of dams in Upstream Mekong has led to significant trapping of sediment and nutrients and could reduce the fertility of Tonle Sap system. The sediment and nutrient linkage between the Mekong mainstream and the Tonle Sap Lake would be necessary to better understand, as the sediment input from the Mekong is crucial for the Tonle Sap's ecosystem functions (Arias et al., 2014). The sediment exchange between Tonle Sap Lake and Mekong River was previously estimated by Kummu et al. (2008), Lu et al. (2014a), and Sok et al. (2020c) (under review). The study of sediment load by Kummu et al. (2008) showed that Tonle Sap is the sink of the Mekong River over the period 1997-2003. Lu et al. (2014a) revealed that Tonle Sap is the sediment source of the Mekong river from 2008–2010. A recent study by Sok et al. (2020c) indicates that Tonle Sap Lake provided 0.65±0.6 Mt/year of sediment annually to the Lower Mekong River from 1995 to 2000 and from 2001-2018, Tonle Sap Lake had become a sink for sediment load. However, the study of the long-term nutrient transport dynamics as a baseline and information between the Mekong mainstream and the Tonle Sap River is still lacking.

To address the problem mentioned above and the aforementioned gaps, the understanding and the changing of nutrient flux in the Lower Mekong River is crucially required. Particularly, the nutrient exchange between the Tonle Sap Lake and Mekong River through Tonle Sap River and their nutrient input to the Mekong Delta for a long-term period in different hydrological conditions. The study firstly presented the annual and monthly dynamic and flux of nutrient transports (Nitrate and Total Phosphorus) in the Mekong in Cambodia connecting with Tonle Sap River in Cambodia and secondly the study presented a quantification of annual and monthly nitrate, and total phosphorus flux contributed by the Mekong River and Tonle Sap Lake to the Mekong Delta through hydrological reversal system.

2. Materials and Methods

Study area

The Mekong River spans a total length of 4800 km and drains an area of 795 000 km^2, with a mean annual water discharge of 470 km^3, making it one of the largest rivers in the world (Lu and Siew, 2006). By convention, the Mekong River basin is divided into two sub-basins: The Upper Mekong

basin (24% of the total drainage area) and the Lower Mekong basin (76% of the total drainage area). The basin distinguishes two main sub-basins are illustrated in **Figure 4-1**.a. The climate of the Mekong Basin is dominated by the Southwest Monsoon, which generates rainy and dry seasons of more or less equal length. The monsoon season usually lasts from May until October. Annual average rainfalls over the Cambodian floodplain and the Vietnamese delta are equally low and less than 1,500 mm. Elsewhere, the highest rainfalls are as expected-in the Central Highlands and within the mainstream valley at the middle part of Lao. In the warmest months of March and April, the average temperature ranges from 30°C to 38°C. Rainy season means temperatures decrease significantly from south to north, from 26°-27°C in Phnom Penh to 21°-23°C in Thailand northern part. The Mekong's average discharge to the sea is about 15,000 m^3/s (Adamson et al., 2009; Gupta and Liew, 2007).

The Tonle Sap Lake and River are located in the central part of Cambodia (**Figure 4-1**.b). It is an integral part, a sub-catchment of the Mekong River system. It is the largest permanent freshwater body in Southeast Asia and an important natural reservoir for the Mekong River. It covers the area of 2,500 km^2 in the dry season and 16,000 km^2 in the wet season. It extends over 300 km from northwest Cambodia to Mekong River at Phnom Penh by Tonle Sap River. Tonle Sap Lake has a unique hydrological system characterized by a flood pulse from the Mekong River. The Tonle Sap River flows from the southeastern end of Tonle Sap Lake, joins the Mekong River at Chaktomuk confluence at Phnom Penh (**Figure 4-1**.c). The water from the Mekong River flows up to the Tonle Sap River to fill the Tonle Sap Lake and its floodplain during the rainy season from May. In reverse, from October to April, the water starts flowing back from Tonle Sap Lake to Mekong River by crossing Tonle Sap River. This phenomenon occurs annually in late May/early June. In September/October, when the water level in the Mekong starts to recede, this stored water starts to drain back into the lower Mekong and Bassac Rivers (Fujii et al., 2003; Masumoto et al., 2001). The lake receives most of its water from the Mekong mainstream and, as the lake's water level is directly controlled by the water level of the Mekong (Kummu et al., 2014).

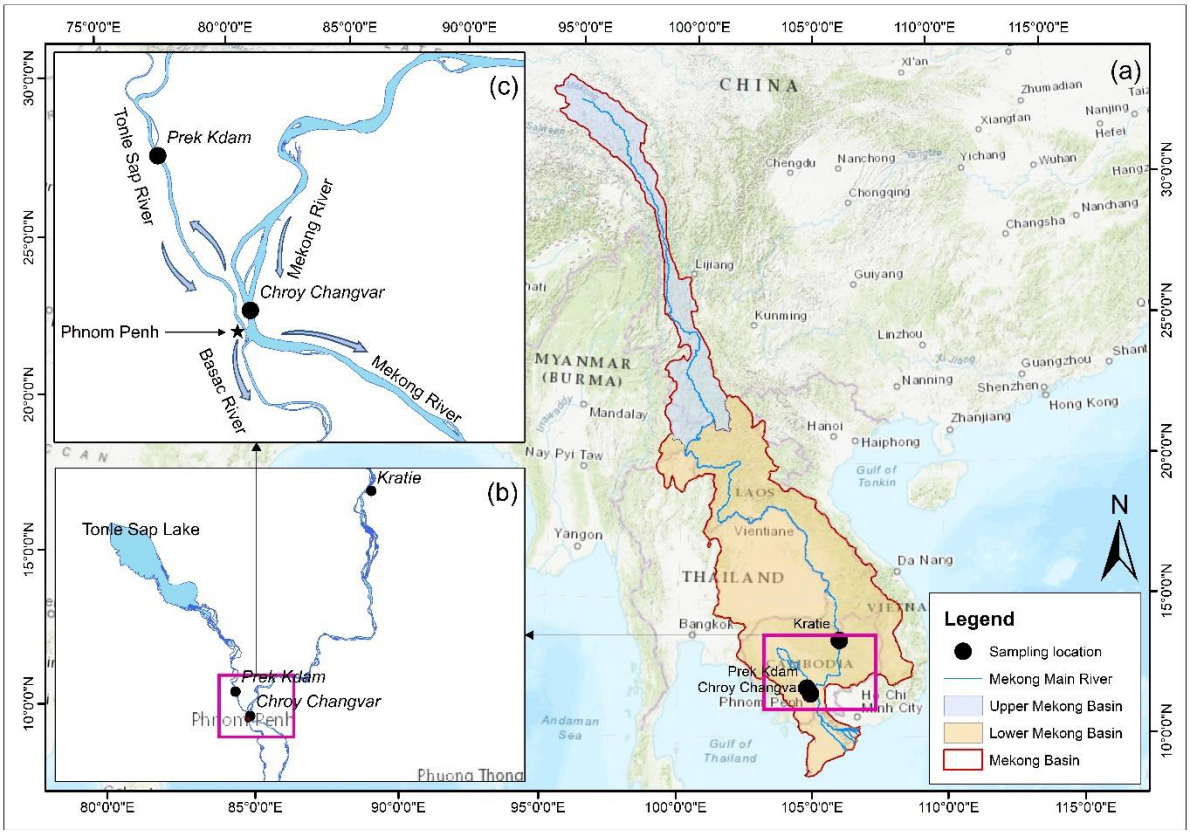

Figure 4-1: *Map of the study sites: (a) Mekong River basin, (b) sampling sites along the Mekong River and the Tonle Sap River, and (c) the flow directions and revers flow at the Chroy Changva site near the Chaktomuk confluence at Phnom Penh*

Water discharge and nutrient data

Nutrient data and daily water discharge were obtained from the Ministry of Water Resources and Meteorology (MOWRAM) of Cambodia under the Mekong River Commission framework: Water Quality Monitoring Network (WQMN) at the three sites in the Lower Mekong of Cambodia (Table 1). The monitoring sites started from the upstream site of the Mekong River of Cambodia at Kratie moving to the Chroy Changva (near Chatumuk confluence) to capture the water discharge and quality before the water changing the curse to the Tonle Sap River and Mekong Delta. Prek Kdam station, located along the Tonle Sap River, was included in the study since this station can represent the reverse system of the Mekong-Tonle Sap system (Figure 1c).

Nitrate (NO_3^-), and total phosphorus (TP) concertation have been available and were used in this study (**Table 4-1**). In WQMN database, the water samples were collected at 0.3 m-0.5 m below the water surface in the middle of the river cross-section where free flowing water is observable

at each station. For consistency, the sampling of water quality on a monthly basis (once every month) between the 13th and 18th day of each month (Kongmeng and Larsen, 2016). The water sampling, sample preservation, sample transportation and storage, would be carried out in accordance (Kongmeng and Larsen, 2016) with methods outlined in the 20th edition of the Standard Methods for the Examination of Water and Wastewater (Clesceri et al., 1998). The samples were analyzed at the designated laboratories by MRC and by recommended analytical methods (2540-D-TSS-SM) for TSS, 4500-NO_{2-3}/SM for NO_3 and 4500-P/SM for TP (Kongmeng and Larsen, 2014). Data from MRC was confirmed satisfactory data quality and laboratory by Hedlund et al. (2005) , and Li and Bush (2015).

The studies of the nutrient flux of the Asian Monsoon Rivers also used data monthly and satisfied to use monthly data. For example, Gong et al. (2015) study the seasonal variation of dissolved nutrient of the Yellow River; the sampling data was done in monthly frequency. Nutrient discharge of Yangtze River by Tong et al. (2017a) based on a monthly basis either. Even the studies of many rivers' nutrient fluxes and budget of China's estuaries, the analysis was based on the monthly data, for example, the study of Liu et al. (2009) and Wu et al. (2019). These some authentications revealed the satisfactory and reliable in using nutrients monthly data in the estimation of nutrients flux and budget even annually and seasonally of riverine experienced in Mekong River and other major rivers.

Flow and nutrient analysis had been calculated based on the hydrological year: from 1st of May to 30th of April next year (Kummu and Sarkkula, 2008; Kummu et al., 2014). Thus, our period of record analyzed by hydrological year is one year shorter than period of available data expressed in calendar years (i.e., the calendar year is 1995-2017; thus, the study expressed as the hydrological year 1995-2016). At Prek Kdam, the observed value of water discharge and water quality parameters were distinguished to positive and negative responses to the two opposite flow directions of Tonle Sap River. In this study, the negative values of water discharge and water quality parameters are inflow into the Tonle Sap Lake from Mekong River, while positive values correspond to the outflow from the Tonle Sap Lake towards the Mekong River.

Table 4-1: *Data coverage period and the number of nutrient (nitrate and total phosphorus) records and water discharge data used in the study.*

Locations		Nitrate (NO_3^-)		Total Phosphorus (TP)		Discharge
		Number of samples	Data coverage	Number of samples	Data coverage	Data coverage
Kraite		235	1995-2017	133	2005-2017	1995-2017
Chroy Changva		243	1995-2017	136	2005-2017	2005-2017
Prek Kdam	Tonle Sap towards Mekong	153	1997-2017	95	2005-2017	1997-2017
	Mekong towards Tonle Sap	64	1997-2017	40	2005-2017	1997-2017

Nutrient flux estimation

Nutrient fluxes were estimated by using the LOAD ESTimator (LOADEST) model (Runkel et al., 2004). LOADEST incorporates daily discharge, seasonality, and measured constituent data to parameterize a multiple-regression model that allows a continuous time series to be estimated from discrete measurements (Bouraoui and Grizzetti, 2011b; Hanley et al., 2013). LOADEST calculates fluxes by applying the method of adjusted maximum likelihood estimation while eliminating collinearity by centering discharge and concentration data. The regression model is automatically selected from one of nine predefined regression models to fit the data based on the Akaike Information Criterion (Johnston et al., 2018). Flux estimation considers datasets of at least 120 observations (Hirsch, 2014), thus our dataset is validated. The use of LOADEST to estimate the flux in the major river such as the Mekong can be found at Sun et al. (2013) in Yangtze River using monthly Nitrogen and TP concentration data, as well as daily streamflow, Hanley et al. (2013) in temperate rivers of North America using monthly measurement of water quality, Bouraoui and Grizzetti (2011a) used for rivers discharging in European seas using monthly nutrient data collection. In our study, LOADEST was used to extrapolate the monthly nitrate concentration measurements to daily nutrient load as follow regression models:

(1) $\ln L = a_0 + a_1 \ln Q$

(2) $\ln L = a_0 + a_1 \ln Q + a_2 \mathrm{dtime}$

(3) $$\ln L = a_0 + a_1 \ln Q + a_2 \ln Q^2 + a_3 \mathrm{Sin}(2\pi.\mathrm{dtime}) + a_4 \mathrm{Cos}(2\pi.\mathrm{dtime}) + a_5 \mathrm{dtime} + a_6.\mathrm{dtime}^2$$

where, L is the constituent load, $a_{0\text{-}6}$ are coefficients obtaining from LOADEST; Q is streamflow (as daily).

3. Results

Nutrient concertation variations in the Lower Mekong River

The hydrograph of the daily water discharge and observed monthly water quality at Kratie and Chroy Changva showed obvious variation during the study period from 1995-2017 (**Figure 4-2**) for nitrate concentrations and 2005-2017 for total phosphorus concentrations (**Figure 4-3**). At Kratie, the maximum discharge reached about 58,000 m^3/s in the rainy season of 1996, while minimum discharge was 1,073 m^3/s in the dry season of 1995. At Chroy Changva, the maximum discharge was 40,500 m^3/s in the rainy season of 2014, and the minimum lowest discharge was 405 m^3/s in the dry season of 1995. The concentration of nitrate and total phosphorus observed at both stations was nearly equal (**Table 4-2**). Nitrate concentration was averagely 0.67±0.43 mg/L (from 0.02-1.86 mg/L) at Kratie and 0.67±0.47 mg/L (from 0.01-2.21 mg/L) at Chroy Changva. Total phosphorus concentration was 0.11±0.09 mg/L (from 0.01-0.32 mg/L) at Kratie and 0.10±0.08 mg/L (from 0.01-0.35 mg/L) at Chroy Changva. The concentration of both nitrate and total phosphorus was generally high during high discharge and low during low discharge; thus, concentrations exhibit strong seasonal variations.

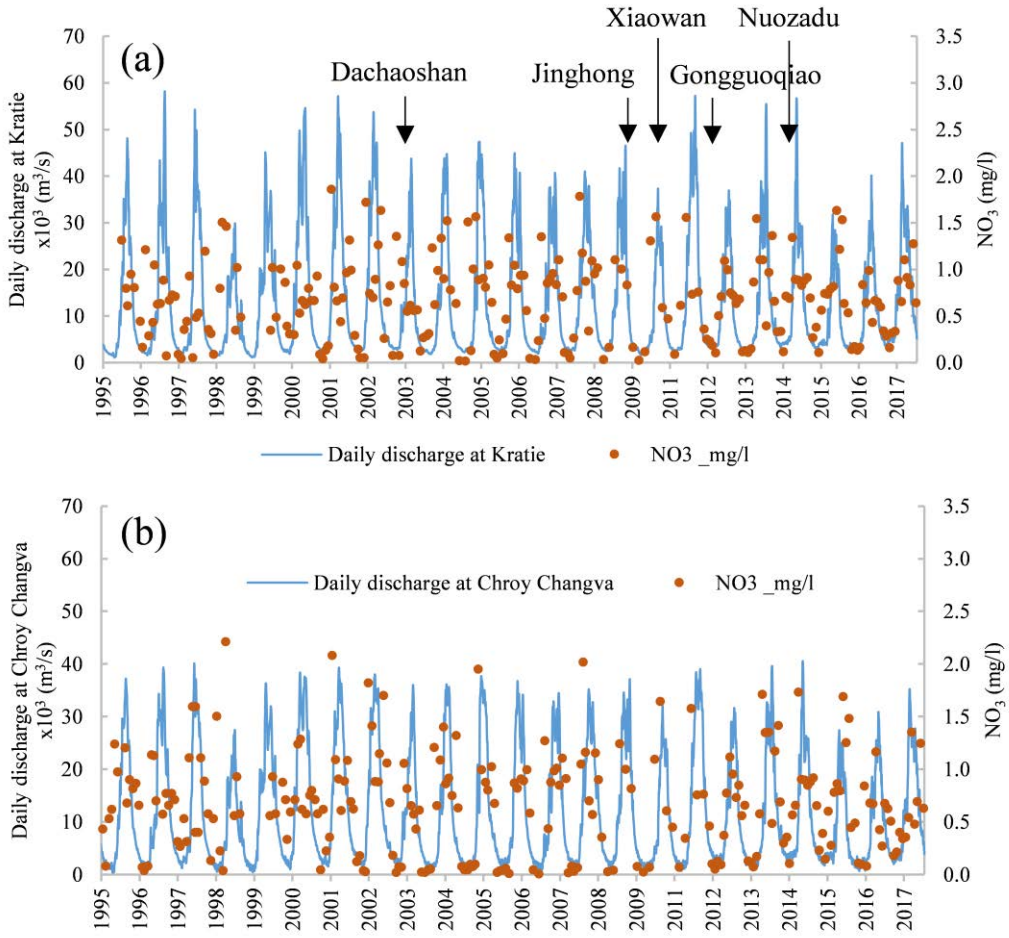

Figure 4-2: *Variation of daily water discharge and nitrate concentration (NO_3^-) at (a) Kratie and (b) Chroy Changva from 1995 to 2017. Data from MOWRAM of Cambodia. The arrow indicates the major dams operating year in the Upper Mekong part.*

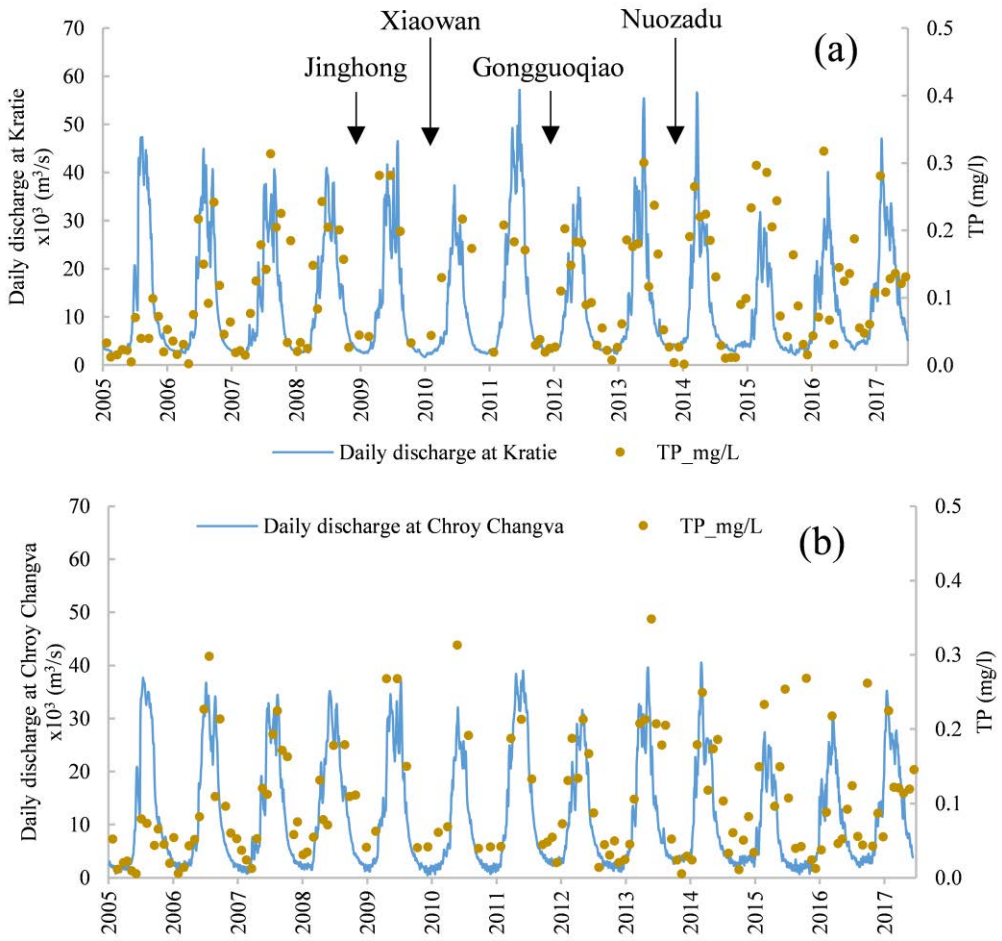

Figure 4-3: *Variation of daily water discharge and total phosphorus concentration (TP) concentration at (a) Kratie and (b) Chroy Changva from 2005 to 2017. Data from MOWRAM of Cambodia. The arrow indicates the major dams operating year in the Upper Mekong part.*

Table 4-2: *Nitrate (NO_3^-) and total phosphorus (TP) concentration at Kratie and Chroy Changva*

	Kratie		Chroy Changva	
	NO_3^- (mg/l)	TP (mg/l)	NO_3^- (mg/l)	TP (mg/l)
Min	0.02	0.01	0.01	0.01
Max	1.86	0.32	2.21	0.35
Mean	0.67	0.11	0.67	0.10
STDEV	0.43	0.09	0.47	0.08

Nutrient concentration variations in the Tonle Sap River

Prek Kdam station recorded flow and nutrient concentration for the Tonle Sap River, connecting Tonle Sap Lake and Mekong River (**Figure 4-4**). The water discharge and water quality that represent the reverse system of Tonle Sap River was recorded at Prek Kdam station. From the observed water discharge at Prek Kdam, the reverse system started to change direction from Tonle Sap Lake towards the Mekong River in October. Generally, water flow from Mekong River into Tonle Sap Lake counted from 70 to 157 days per year and, on average 118 days per year between late May to end of September whereas the opposite direction from Tonle Sap Lake towards Mekong River varies annually from 209 days to 295 days on average 247 days per year in between October and April/May. The peak inflow discharge into the lake generally occurred in July and August, while the periods of peak discharge of Mekong River occurred in August and September at Chroy Changva station. Otherwise, peak outflow from the lake to Mekong River mainly took place a few months later, the peak inflow from October to December. During the observed period from January 1997 to 2017, maximum inflow discharge into the lake accounted for 10,680 m^3/s. Regarding the outflow water from the Tonle Sap Lake, the maximum water flowing out from the lake was 10,100 m^3/s. The lowest water discharge flowing into the lake regularly appeared in late May when the water level in Mekong River higher than Tonle Sap Lake. The water started to change flow direction from the Mekong to the lake and happened in September when the water in the lake reaches the highest level and the biggest volume, therefore, the lake's water level quite equal the Mekong's and the lake received less inflow water from the Mekong through Tonle Sap River.

To understand the behavior of nutrient concentrations inflow/outflow the lake, the observed nutrient concentrations were calculated basic statistic inflow and outflow separately. Due to data availability, we used observed NO_3^- concentration covering from 1997-2017, while observed TP concentration covering from 2005-2017. In terms of water quality concentration of flow direction from Tonle Sap Lake towards the Mekong River, nitrate concentration was 0.81±0.77 mg/L (from 0.02-3.4 mg/L), and total phosphorus concentration was 0.11±0.07 mg/L (from 0.01-0.33 mg/L). For flow from Mekong toward Tonle Sap Lake, nitrate concentration was 0.98±0.67 mg/L (from 0.04-2.9 mg/L) and for total phosphorus was 0.16±0.1 mg/L (from 0.02-0.43 mg/L). On average, the nutrient concentration from Mekong River to Tonle Sap Lake was higher than from the lake to Mekong (**Table 4-3**).

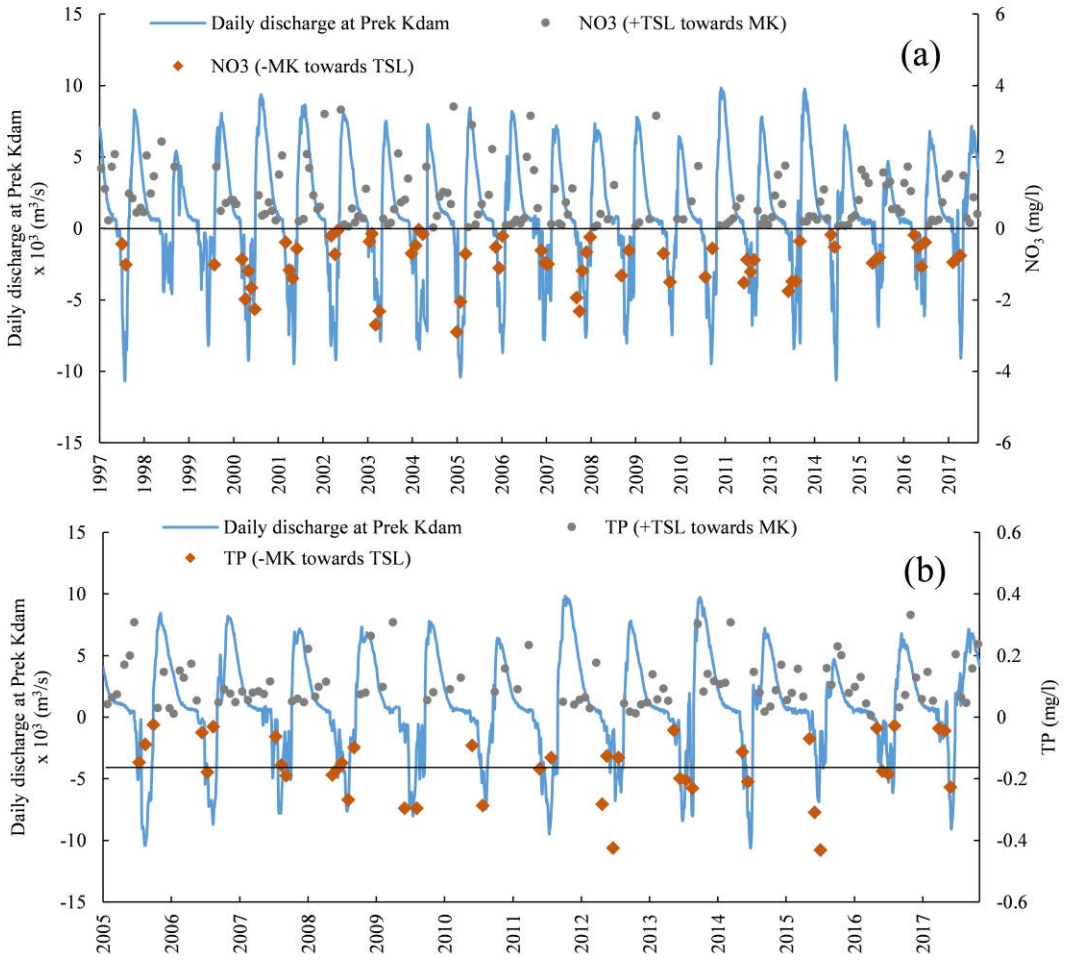

Figure 4-4: *Variation of daily water discharge and nutrient concentration at Prek Kdam, (a) Nitrate concentration from 1997-2017, and (b) Total Phosphorus concentration from 2005-2017. Positive values correspond to the outflow from the lake towards Mekong River, while negative values are (reverse) inflow into the lake from Mekong River. Data from MOWRAM of Cambodia.*

Table 4-3: *Nitrate and total phosphorus concentration at Prek Kdam.*

	Tonle Sap Lake towards Mekong		Mekong towards Tonle Sap Lake	
	NO_3^- (mg/l)	TP (mg/l)	NO_3^- (mg/l)	TP (mg/l)
Min	0.02	0.01	0.04	0.02
Max	3.40	0.33	2.90	0.43
Mean	0.81	0.11	0.98	0.16
STDEV	0.77	0.07	0.67	0.10

Temporal variability of nutrient flux in the Mekong River

The variability of monthly (accumulation per month) nitrate and total phosphorus flux have been employed at both Kratie and Chroy Changva station (**Figure 4-5** and **Figure 4-6**). The peak value of nitrate and total phosphorus flux occurred in August, and September corresponds to the peak runoff period. The maximum monthly nitrate flux at Kratie and Chroy Changva was about 85 $\times 10^3$ tons and 138 $\times 10^3$ tons (kt), respectively. Maximum TP flux was approximately 28 $\times 10^3$ tons at Kratie and 18 $\times 10^3$ tons Chroy Changva. Moreover, the lowest fluxes appeared in low runoff periods from February to March with less than 5 $\times 10^3$ tons of nitrate and 2 $\times 10^3$ tons of TP flux. Overall, monthly nitrate flux at Chroy Changva was higher than at Kratie, whereas monthly TP flux at Chroy Changva was lower than at Kratie. Furthermore, the monthly runoff in the rainy season at Kratie was higher than Chroy Changva. The downstream reduction in gauged flow at Kratie and Chroy Changvar occurred mainly at higher flows and can be attributed to overland flow from the Mekong River traversing the floodplain to the Tonle Sap Lake and by flow into major distributaries between Kratie and Chroy Changva.

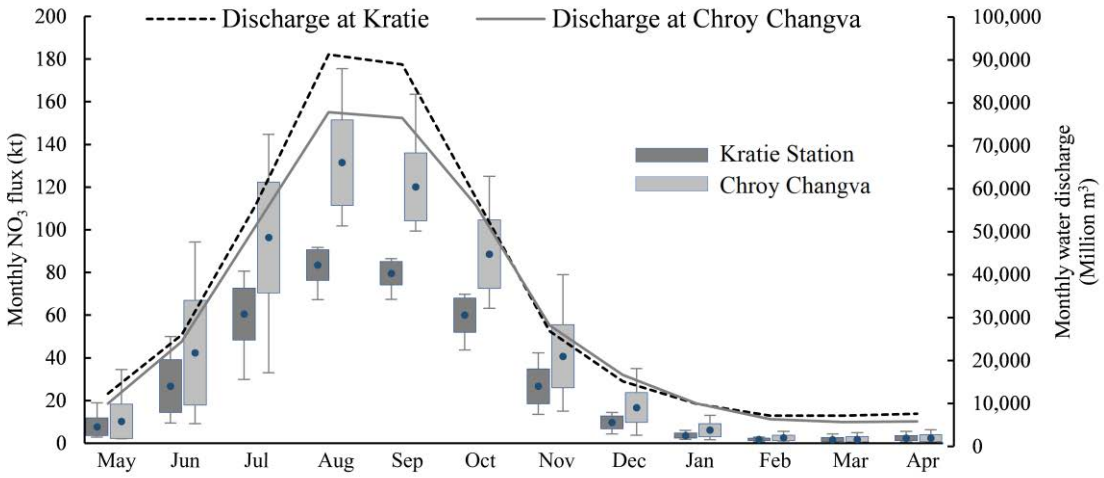

Figure 4-5: *Monthly variation of nitrate flux and monthly water discharge at Kratie and Chroy Changva. Point inside box: mean, lower and upper box boundaries: standard deviation value, lower and upper lines: minimum and maximum, respectively.*

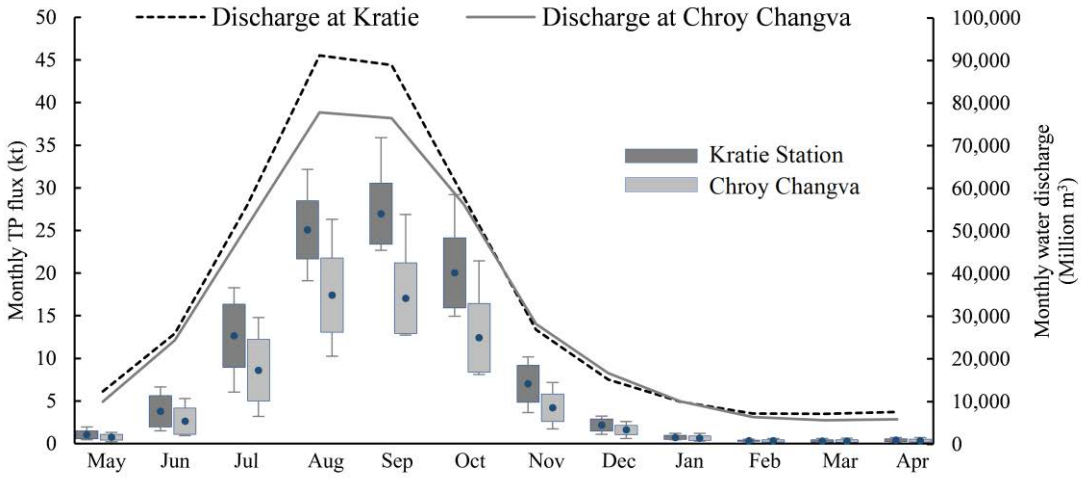

Figure 4-6: *Monthly variation of TP flux and monthly water at Kratie and Chroy Changva. Point inside box: mean, lower and upper box boundaries: standard deviation value, lower and upper lines: minimum and maximum, respectively.*

The annual water discharges at Kratie and Chroy Changva were presented in **Figure 4-7**. On average, the annual water yield in Kratie was 40,400 million m^3/yr (Mm^3) and was higher than the annual water discharge at Chroy Changva (3,700 Mm^3). A similar pattern of water discharge for both stations was obtained. The factor involved in the water discharge in the upstream higher than downstream could be described as the overland flow from the Mekong via the floodplains to the Tonle Sap Lake and major distributaries in between Kratie and Chroy Changva as previously mentioned.

Nitrate flux was calculated over the hydrological year 1995-2016 and hydrological year 2005-2016 for total phosphorus flux based on the available data (**Figure 4-7**). The results of nitrate flux demonstrate two things. Firstly, nitrate flux in Kratie keeps a slightly constant pattern, in particular, from the year 2002 to 2016. Second, nitrate flux in Chroy Changva maintaining the fluctuation over the study period 1995-2017. Nitrate flux at Kratie has low variability (272 to 441 $\times 10^3$ tons/yr) compared to Chroy Changva station (380 to 739 $\times 10^3$ tons/yr). The annual total phosphorus flux in Kratie and Chroy Changva was fluctuated over the study period from 77 to 137 $\times 10^3$ tons/yr for Kratie and 46 to 116 x10^3 tons/yr for Chroy Changva (**Figure 4-8**). On average, nitrate flux was estimated at about 364 and 557 $\times 10^3$ tons/yr, and total phosphorus was approximately 100 $\times 10^3$ tons/yr and 73 $\times 10^3$ tons/yr at Kratie and Chroy Changva, respectively (**Table 4-4**). It is interesting to note that annual nitrate flux at Chroy Changva was higher than flux at Kratie, even though the

water discharge at Chroy Changva acquired water discharge less Kratie. However, total phosphorus flux showed in different values to nitrate, and its amount was found at Chroy Changva less than at Kratie. To be discussed, the result of nitrate and total phosphorus flux showed an opposite tendency in the flux between Kratie and Chroy Changva, for this contrast it denoted two things; the nitrate and phosphorus are different in dynamic across the basin, and a large amount of water discharge does not always transport in a large amount of nutrient.

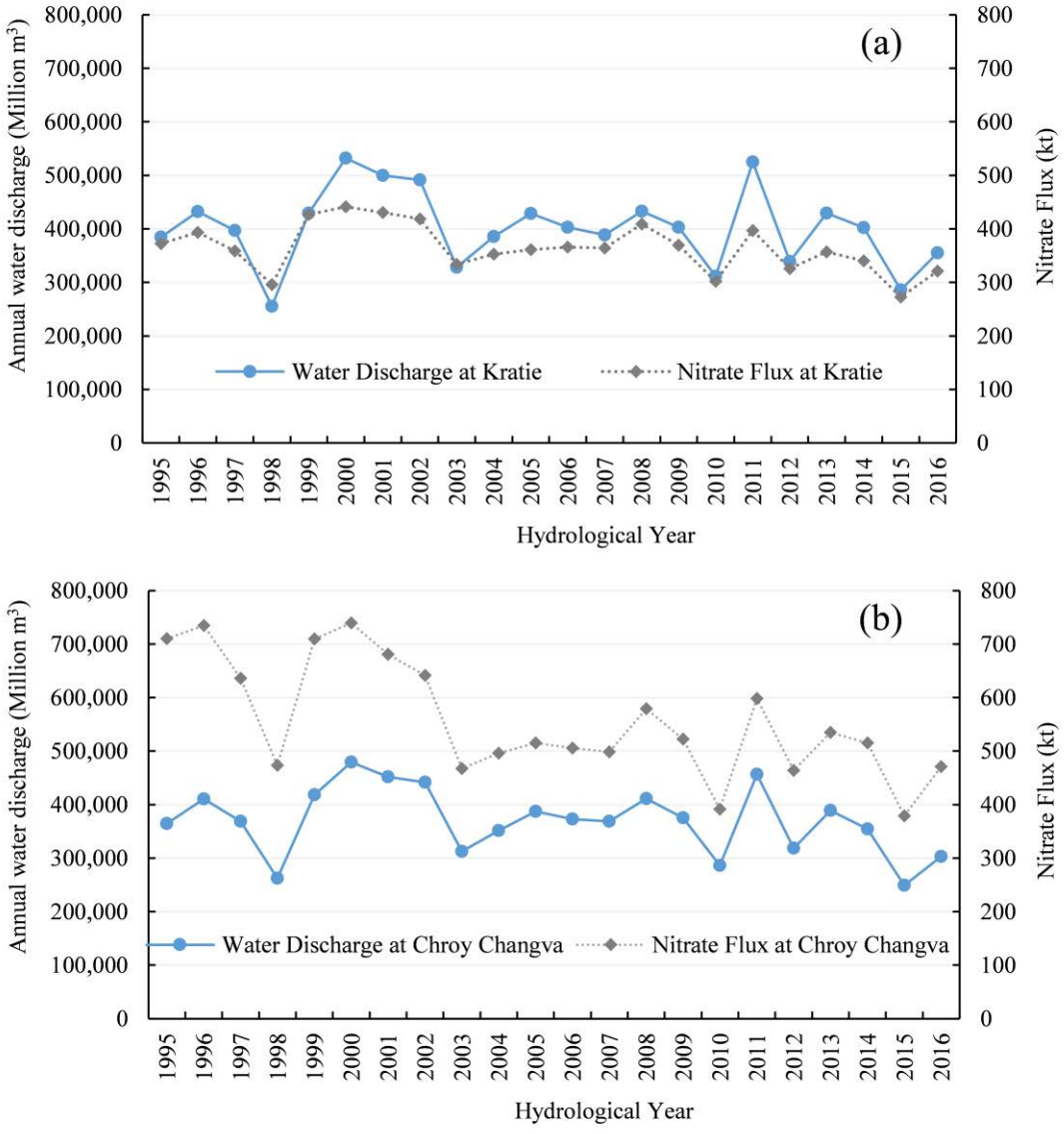

Figure 4-7: *Annual nitrate flux dynamics in the Mekong River for the period of hydrological year 1995 to 2016 (a). at Kratie and (b). at Chroy Changva.*

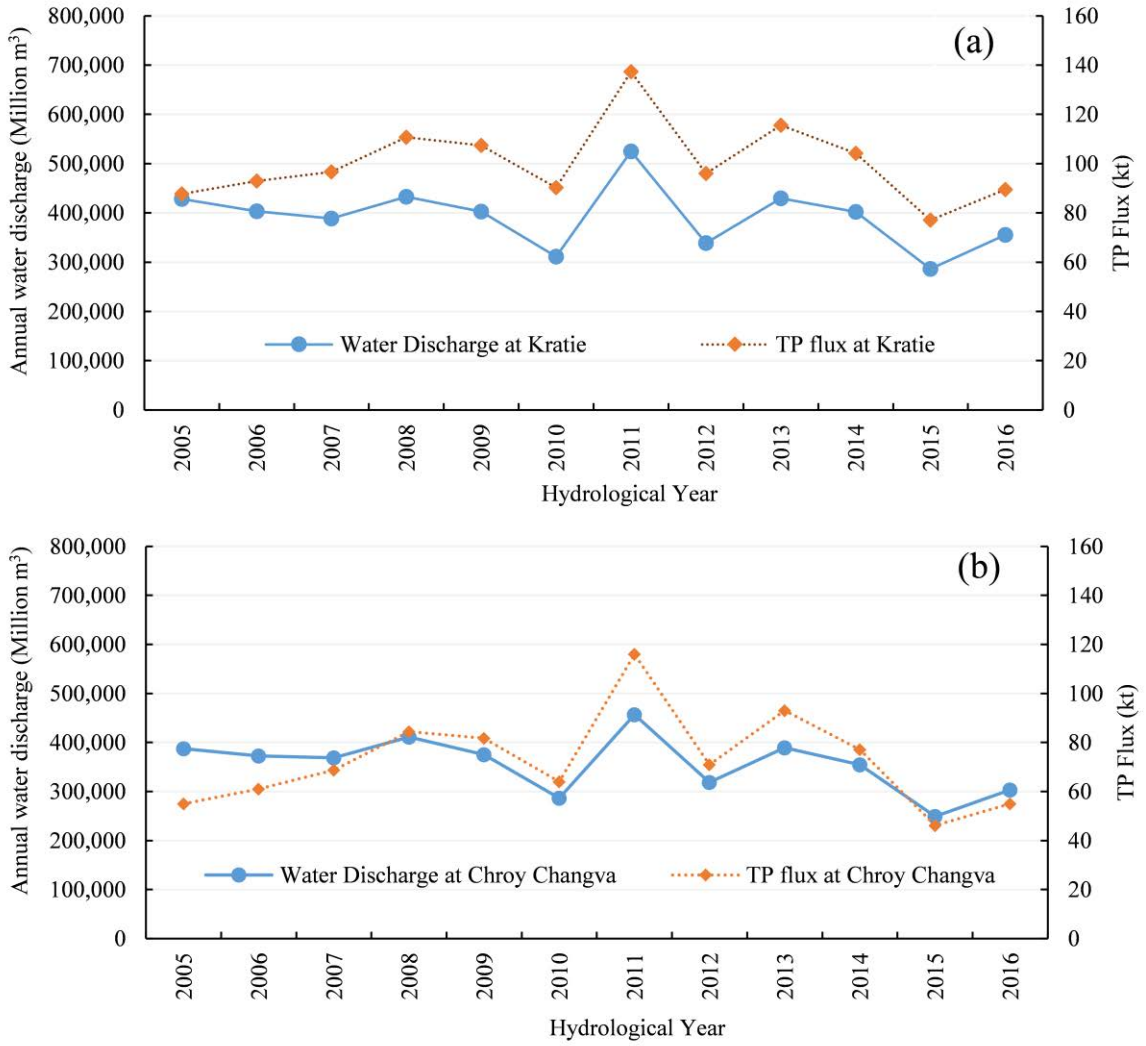

Figure 4-8: *Annual total phosphorus flux dynamics in the Mekong River for the period of hydrological year through hydrological year 2005 to 2016 (a). at Kratie and (b). at Chroy Changva.*

Table 4-4: *Annual nitrate and total phosphorus flux dynamics in the Mekong River for the period of hydrological year 1995 to 2016 at Kratie and Chroy Changva*

	Kratie			Chroy Changva		
	Water Discharge	NO_3^- Flux	TP Flux	Water Discharge	NO_3^- Flux	TP Flux
	(Million m^3/year)	(kt/year)		(Million m^3/year)	(kt/year)	
Mean	401 812	364.08	100.45	369 762	557.38	72.74
Min	255 561	272.46	77.06	249 279	378.72	46.08
Max	531 813	441.31	137.27	479 066	739.15	116.06
STDEV	72 106	45.39	15.89	62 099	109.47	19.37

Temporal variations of water and nutrient flux inflow and outflow from the Tonle Sap Lake

To assess the temporal variations of input to and output from the Tonle Sap Lake linkage with the Mekong River, it is very important to understand the discharge input/output from the lake associating with the Mekong River. In general, with timing and magnitude of flow, the Mekong River provided less water to Tonle Sap Lake than its receiving. Inflow to the lake from Mekong River starts from May or very early of June, and reverse flow occurred in October (**Figure 4-9**). The results of intra-annual variation of nitrate and TP fluxes of Tonle Sap River was separately calculated to represent opposite flow direction, from Tonle Sap Lake towards the Mekong River and from Mekong River towards Tonle Sap Lake (**Figure 4-10**). Generally, the nitrate and TP flux to the Tonle Sap Lake was found in the rainy season from May to October corresponding to flow discharge from the Mekong to the lake and the reverse flux from the lake to the Mekong was in the dry season from October to May. In terms of flow from Tonle Sap Lake towards Mekong River, nitrate and total phosphorus flux was estimated to be 0.4-1.84 kt/month and 0.06-0.18 kt/month. August is the peak month of nutrients flux that Tonle Sap Lake contributes to the Mekong River or delta. Otherwise, the estimation of nitrate and total phosphorus flux from Mekong to the lake was 0.88-1.72 kt/month and 0.04-1.14 kt/month. These values showed that the Mekong provided nitrate to Tonle Sap Lake more than the lake provided to the Mekong; in contrast, the lake shared total phosphorus to the Mekong in a year.

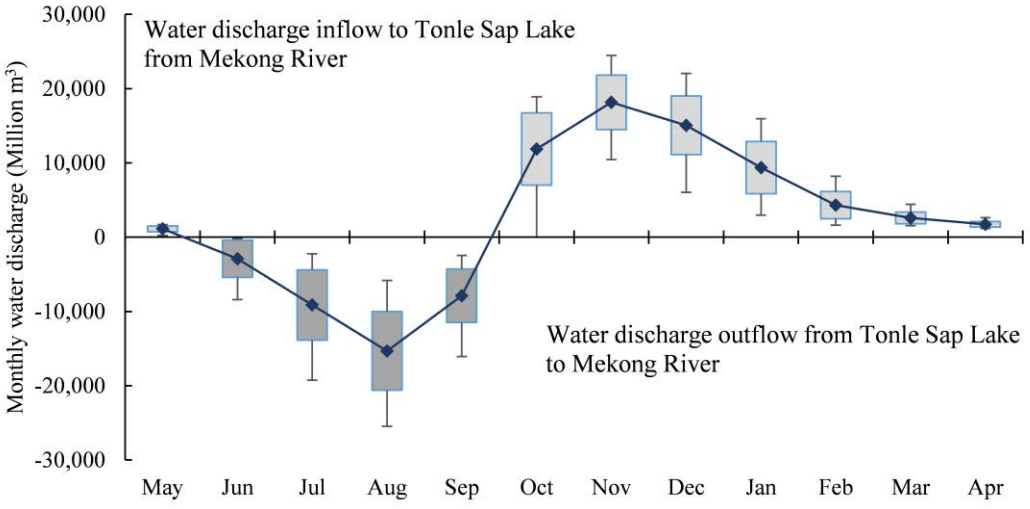

Figure 4-9: *The monthly variation of water discharge connecting between Mekong River and Tonle Sap Lake at Prek Kdam from 1997-2017. Negative values reflect the inflow to the lake from the Mekong River, while positive values correspond to outflow from the lake to the Mekong River. Point inside box: mean, lower and upper box boundaries:*

standard deviation value, lower and upper lines: minimum and maximum, respectively.

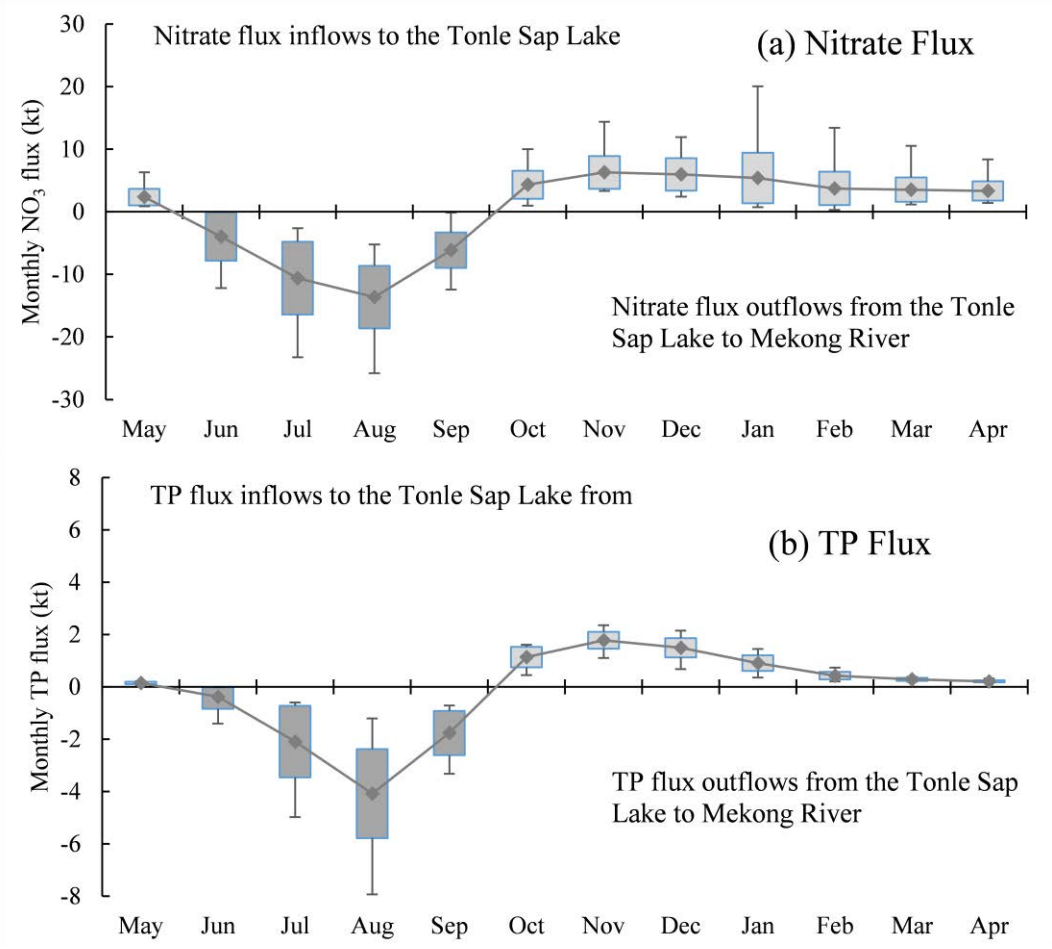

Figure 4-10: *The monthly variation of nutrient flux. (a). Nitrate flux from 1997-2017 and (b). Total Phosphorus flux from 2005-2017, at Prek Kdam. Negative values reflect inflow to the lake from Mekong River, while positive values correspond to outflow from the lake to the Mekong River. Point inside box: mean, lower and upper box boundaries: standard deviation value, lower and upper lines: minimum and maximum, respectively.*

On the annual scale, the results of the annual water balance revealed that Tonle Sap Lake generally contributes an amount of water 36,000 Mm^3 during the low flow season to the Mekong River from October to May. Cumulative seasonal water volumes are presented in **Figure 4-11**, with negative values indicating reverse flow from the Mekong to Tonle Sap Lake, and positive values for outflow from the lake to the Mekong River. The seasonal outflow from the lake averaged 68,000 Mm^3, equivalent to 18% of the annual discharge of Mekong River at Chroy Changva. The seasonal reverse flow into the lake from the Mekong River averaged 36,000 Mm^3, about 10% of the annual discharge of the Mekong River at Chroy Changva. Thus, the outflow from the lake was almost twice the reverse flow from the Mekong River.

The amount of annual nitrate and TP flux from Tonle Sap Lake to the Mekong was approximately 33.96±13.77 kt/yr and 6.55±1.37 kt/yr on average. Furthermore, the amount of inflow nutrients to the lake from Mekong was estimated about 35.76±12.47 kt/yr of nitrate and 8.67±3.34 kt/yr of total phosphorus (**Figure 4-12**). This result points out that annually Tonle Sap received a higher amount of both nitrate and total phosphorus from the Mekong system than its amount provided to Mekong.

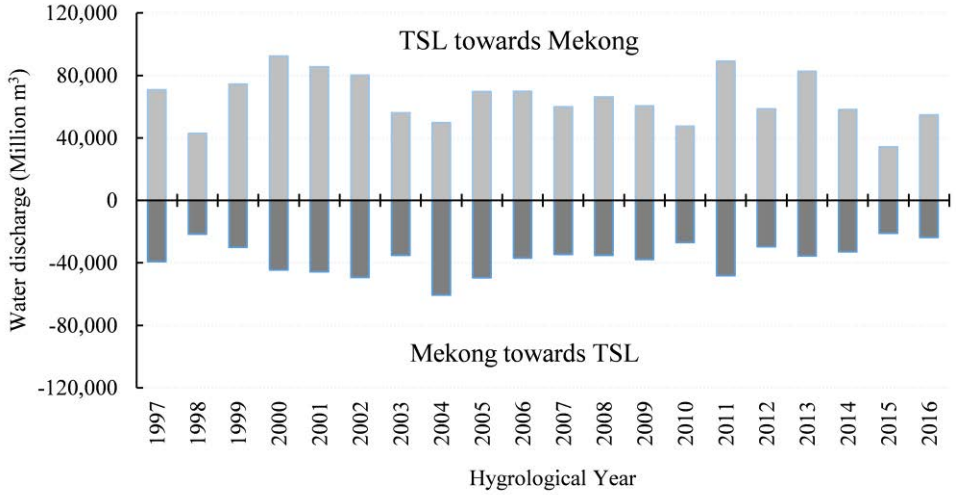

Figure 4-11: *Seasonal water discharge exchanging between Tonle Sap Lake (TSL) and Mekong River through Tonle Sap River at Prek Kdam station over the hydrological year 1997 to 2017.*

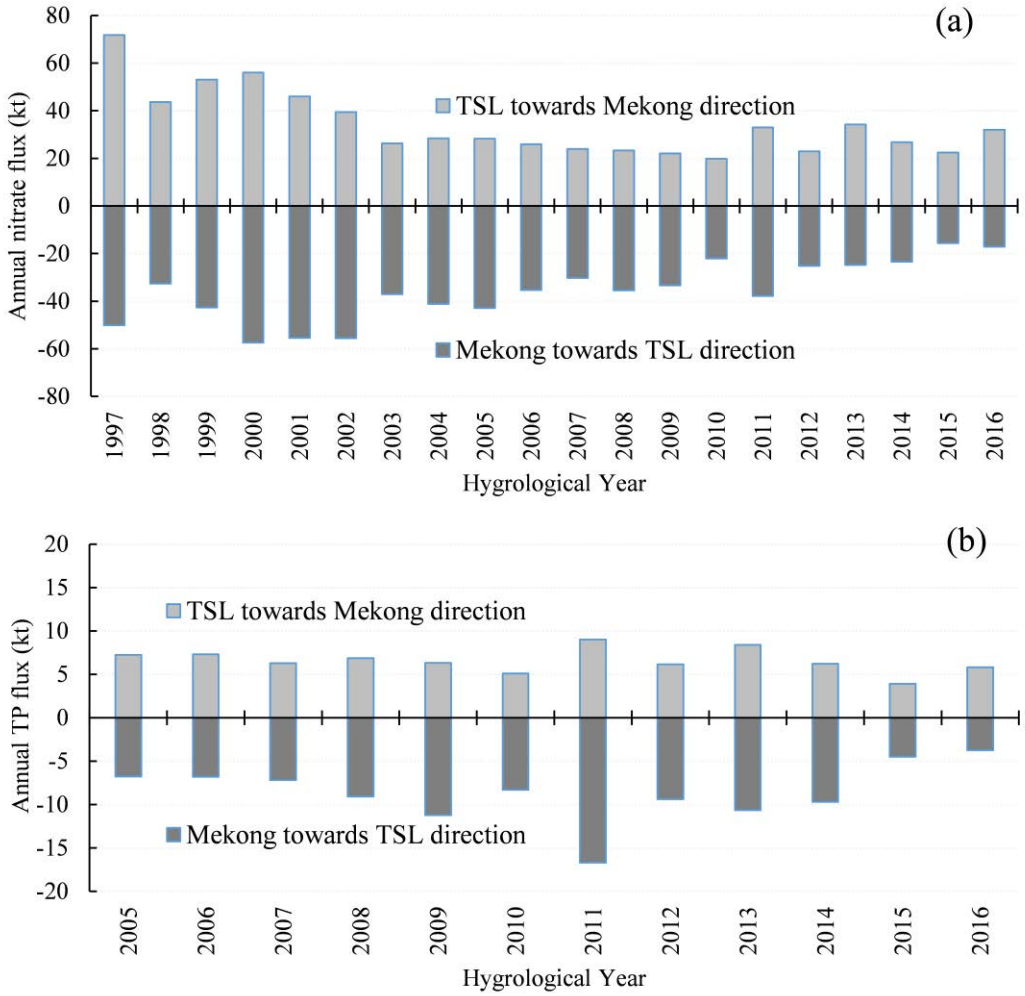

Figure 4-12: *Seasonal nitrate and total phosphorus flux exchange between Tonle Sap Lake and Mekong River through Tonle Sap River at Prek Kdam station. (a). seasonal nitrate flux for hydrological year 1997-2016, (b). seasonal total phosphorus flux for hydrological year 2005-2016. The negative values of total phosphorus flux are inflow into the lake from Mekong River, while the positive values correspond to the outflow from the lake towards Mekong River.*

Changes of nutrient exchange between the Tonle Sap Lake and the Mekong River

Tonle Sap Lake received an amount of water less than its contribution to the Mekong River system, except for the hydrological year 2004. This was due to the hydrological year 2004, the Mekong River at Chroy Changva reached its maximum discharge of 60,000 Mm^3, while on average, and it was 36,000 Mm^3. On the annual scale, it is worth discussing these interesting facts revealed by the results of the annual water balance that Tonle Sap generally contributes an amount of water 65,000 Mm^3 or equal 18% during the low flow season of the Mekong River and Mekong Delta (**Figure 4-13**).

To comprehensively understand whether the lake gains or losses of nutrient flux during each hydrological year, the subtraction of seasonal nitrate and total phosphorus flux for the Tonle Sap was employed. Lake's inflow nitrate flux from the Mekong River was higher than the lake's outflow flux towards the Mekong during the time interval 2000-2012 (**Figure 4-13**). Moreover, in the early study period 1997-1999 and the late study period 2013-2016, outflow nitrate flux was more than the inflow nitrate flux. However, the transportation amount of total phosphorus flux that Mekong delivered to the lake higher than the lake delivered back was from 2007-2015. It means that Tonle Sap Lake was the nitrate sinks during the period 2000-2012 and 2007-2015 for total phosphorus. Before and after this period, Tonle Sap Lake play a role as the source of nutrients for the Mekong System, particularly Mekong delta. The study has emphasized the interaction role of Tonle Sap Lake and Mekong in nutrient supply. Base on the analysis during the study period (1997-2016 for nitrate and 2005-2016 for TP), Tonle Sap Lake contributed 34 kt/year of nitrate and 6.6 kt/year of total phosphorus to the Mekong system or Mekong Delta. While Mekong River shared nitrate flux 35.8 kt/year and 8.7 kt/year of TP to Tonle Sap Lake and its floodplain during high flow season. **Table 4-5** summarized the inflow/outflow of nitrate and phosphorus flux Tonle Sap Lake comparing the Mekong River. This result can lead to conclude that Tonle Sap Lake gain in the amount of nutrient flux (nitrate and total phosphorus) from the Mekong. In other words, the Mekong River plays the role of the source of nutrients, especially total phosphorus, to Tonle Sap Lake and its floodplain.

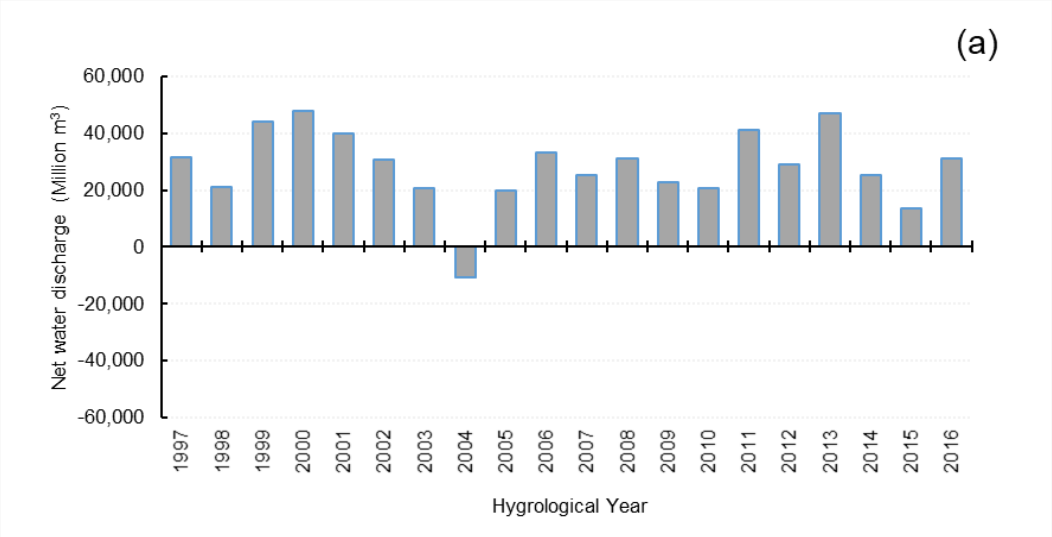

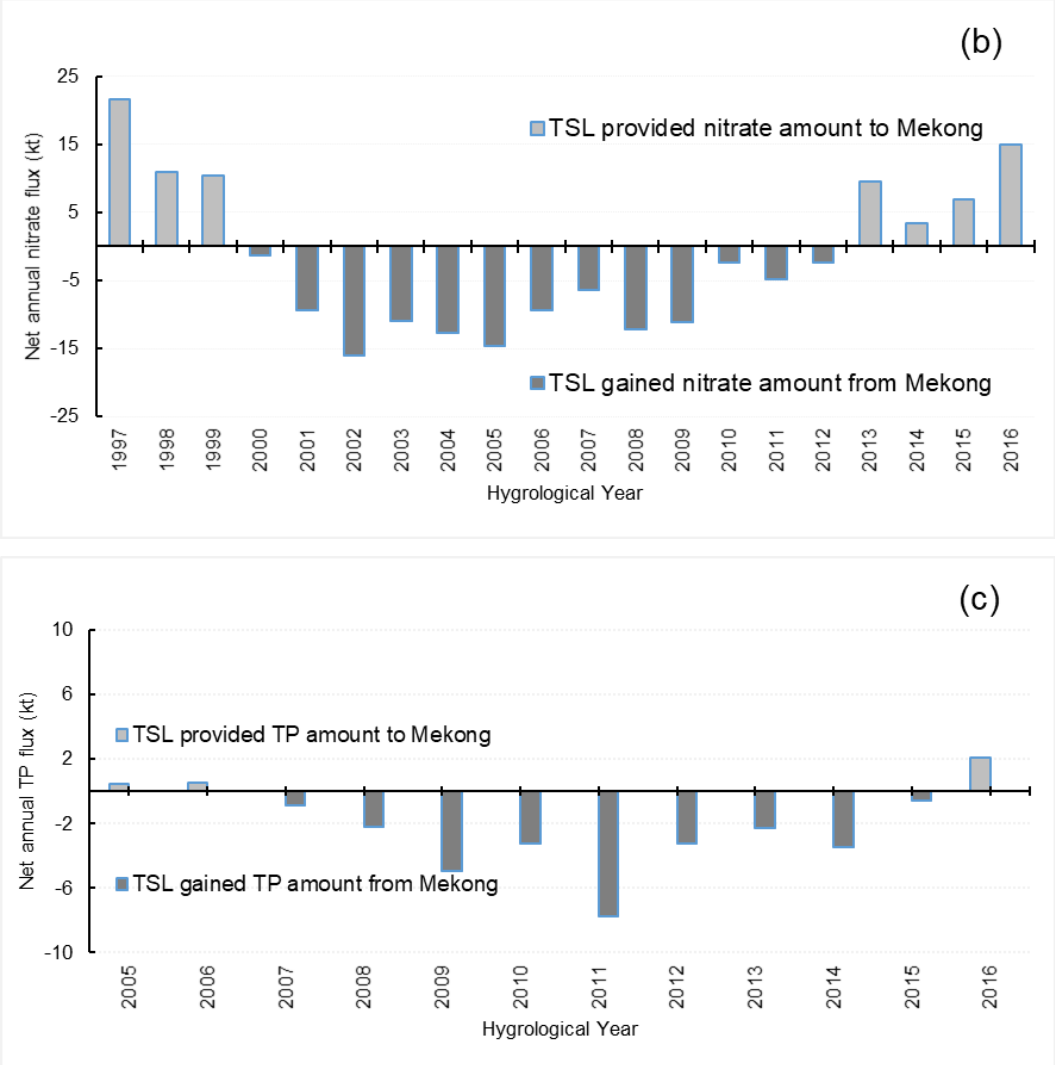

Figure 4-13: *Water discharge and nutrient fluxes balance between Tonle Sap Lake and Mekong River through Tonle Sap River at Prek Kdam station from the hydrological year 1997 to 2016. (a). Net water discharge, (b). Net nitrate flux and (c). Net total phosphorus flux. Annual water discharge and nutrient flux obtaining from subtracting seasonal water discharge and fluxes inflow and outflow Tonle Sap Lake. The negative values of net discharge and nutrient flux: outflow from the lake lower than inflow, while the positive values: outflow from the lake higher than inflow.*

Table 4-5: *Nitrate (NO_3^-), and total phosphorus (TP) flux exchange between Tonle Sap Lake and the Mekong River through Tonle Sap River at Prek Kdam.*

Nutrient Flux		Flux of Mekong mainstem at Chroy Changva (kt/yr)	Flux from Tonle Sap Lake towards Mekong (kt/yr)	Flux from Mekong towards Tonle Sap Lake (kt/yr)
NO_3^-	Mean	557	34.0	35.8
	STDEV	109	13.8	12.5

TP	Mean	73	6.6	8.7
	STDEV	19	1.4	3.3

4. Discussion

This study is the first attempt to quantifying nutrient transport linkage between the Mekong mainstream and the Tonle Sap Lake. The study also estimated the nutrient flux in the lower Mekong River at Kratie and Chroy Changva. The annual nitrate flux along the Mekong is strongly seasonal as a result of 80-88% of the annual nitrate occurring from May to October. A similar pattern to total phosphorus, approximately 90% of the annual total phosphorus flux occurring between May to October. The peak of nitrate flux in both Kratie and Chroy Changva has been observed in August, while total phosphorus reached its peaks in September. We estimated annual nitrate flux 364±45 kt/yr at Kratie and 557±109 kt/yr at Chroy Changva. The total phosphorus flux was found 100±16 kt/yr at Kratie and 73±19 kt/yr at Chroy Changva. The total phosphorus flux from the Mekong River basin to the South-China Sea was accounted for 55 kt/year for 3-years data (2003-2005) (Liljeström et al., 2012). Liljeström et al. (2012) described both total inorganic nitrogen and total phosphorus fluxes increased for 1985–2005. Yoshimura et al. (2009) predicted nutrient (total nitrogen and total phosphorus) levels in the Lower Mekong mainstream were expected to increase of 13-25% by the 2020s compared to the 1990s. The long-term average nitrate fluxes (1985-2005) from the 3S to the Mekong River was estimated to be 57.6 kt/year and is about 30% of the total annual nitrate flux of the Mekong River at Pakse (Oeurng et al., 2016). The results of fluxes estimation could be associated with agricultural expansion in the last two decades, (i.e., increases from 50,000 ha in 1997 to 120,000 ha in 2007 for in Laos part of the Mekong basin) (Li and Bush, 2015; MRC, 2003b).

Nitrogen (N) and phosphorus (P) in the river are mainly from two sources; non-point sources (i.e., fertilizer use in agriculture, basin soil erosion, precipitation) and point sources (i.e. wastewater from the sewage system and industries) (Seitzinger et al., 2005). At the global scale the major attribute of dissolved inorganic nitrogen (DIN) reported from 62% of anthropogenic non-point sources (Seitzinger et al., 2005) and precipitation and agricultural sources dominate the nitrate and DIN in the Mekong basin, a less developed area with intensive agricultural practices. The analysis of nitrate flux and total phosphorus flux in this study illustrated the relation with water discharge;

this demonstrates the continuous transport of nitrate and phosphorus from basin runoff. Nitrogen and phosphorus mainly from agricultural non-point sources (Jarvie et al., 1998; MRC, 2003b), reported massive use of fertilizer in Thailand (100 kg mineral fertilizer per hectare), this can lead to increase of nutrient in the Lower Mekong. Estimates of nitrate loading from concentration and discharge data; however, these do not provide much information about sources, the further deep analysis would be required to identify nutrient sources (e.g., stable isotopes) might be useful (Chang et al., 2002b). Anthropogenic activities also significantly increase concentrations and fluxes of nutrients in Mekong River Basin (Li and Bush, 2015). Dam construction could somehow affect the nutrient transport processes in the rivers (Supit and Ohgushi, 2012). Dam construction can also reduce the amount of downstream nutrient fluxes, thereby changing the spatial distribution of river nutrients; these variations eventually result in changes in the river ecosystem (Chai et al., 2009; Paul, 2003). From the mid-1990s to early 2000s dam development accelerated in China and Vietnam with the construction of mainstream dams on the Lower Lancang and tributary dams (Kondolf et al., 2018). The basin's hydropower reservoir storage, which may rise from ~2% of its mean annual flow in 2008 to ~20% in 2025, is attenuating seasonal flow variability downstream of many dams with integral powerhouses and large storage reservoirs (Hecht et al., 2019). Under a scenario of 38 dams built and under construction (main river and tributary), approximately sediment load 77 Mt/year ~50% of long-term load would be reached Lower Mekong at Kratie from upstream which significantly affecting sediment delivery to downstream reaches (Kondolf et al., 2018). Dams are known to affect nutrient fluxes in rivers (Bosch, 2008). Water impoundments by dam construction increase both depth and residence times compared to pre-dam conditions. Phosphorus, which is mainly attached to soil particles inflow, is heavily influenced by trapping of sediment in reservoirs (Oeurng et al., 2016). A study on the effects of dams on nutrients in the Huron and Raisin Rivers, for instance, demonstrated that dams played a vital role in effectively removing excess nutrients (Bosch, 2008). The eight main rivers flowing into the coastal waters of China include the Yangtze River, Huanghe River, Liaohe River, Haihe River, Huaihe River, Qiangtangjiang River, Minjiang River, and Zhujiang River. The eight rivers accounted for the majority of water discharge into the coastal waters in China. This emerge of nutrient also found in other East Asian monsoon rivers such as Yangtze Shen and Liu (2009), and for Red River by Li and Bush (2015). Nutrient fluxes compare of Mekong compare to other Asian Monsoon Rivers are summarized in **Table 4-6**.

Table 4-6: *Nutrient fluxes of Mekong comparing to others Asian Monsoon Rivers.*

River	Region	Basin area (10^6 km^2)	River length (km)	Water Discharge (km^3/yr)	Nitrate flux (kt/yr)	TP flux (kt/yr)	Reference
Yellow	East Asia	0.77	5464	49	214.8	0.21 (DIP)	Wu et al. (2019)
Yangtze	East Asia	1.94	6300	900	5516.2	110	Hua et al. (2019b)
Pearl	East Asia	0.44	2129	302	559 (DIN)	10 (DIP)	Hu and Li (2009)
Red	East Asia	0.12	1139	123	296 (TIN)	46	Le et al. (2015)
Mekong	Southeast Asia	0.79	4800	404	557	73	This study

Note: DIN: dissolve inorganic nitrogen. (DIP): dissolved inorganic phosphorus. TIN: total inorganic nitrogen

5. Conclusions

The study firstly assessed the dynamic of nutrient transport in the Mekong in Cambodia and secondly to quantify the nutrient (nitrate and total phosphorus) fluxes contributed by the Mekong River to Tonle Sap Lake and its hydrological reversal system. We estimated annual nitrate flux of 364±45 kt/yr at Kratie and 557±109 kt/yr at Chroy Changva from the hydrological year 1995-2016, respectively. The total phosphorus flux was found 100±16 kt/yr at Kratie and 73±19 kt/yr at Chroy Changva from 2005-2017. For the nutrient exchanging between Tonle Sap Lake and Mekong River, the amount of annual nitrate and TP flux from Tonle Sap Lake to the Mekong on average was approximately 34±13.8 kt/yr and 6.6±1.4 kt/yr. Furthermore, the amount of inflow nutrients to the lake from Mekong was amounted to 35.8±12.5 kt/yr of nitrate and 8.7±3.3 kt/yr of total phosphorus, respectively. The study also pointed out that Tonle Sap Lake was the nitrate sinks during the period 2000-2012 and 2007-2015 for total phosphorus. The study has emphasized the interaction role of Tonle Sap Lake and Mekong in nutrient supply. This result can lead to conclude that Tonle Sap Lake gains in amount of nutrients from the Mekong; in other words, the Mekong River plays the role of source to Tonle Sap Lake and its floodplain. This study provided the first findings regarding nutrient exchanges between Mekong River and Tonle Sap Lake and set up the baseline result for the long-term nutrient dynamics and load in Tonle Sap River.

Data availability statement

The data that support the findings of this study are available from the corresponding author upon reasonable request.

Acknowledgement:

The authors also thank the Ministry of Water Resources and Meteorology (MOWRAM) of Cambodia for providing the data. Ty SOK would like to acknowledge Les Bourses du Gouvernement Français (BGF) and Laboratoire Ecologie Fonctionnelle et Environnement for hosting during his Ph.D. study.

Reference:

Adamson, P. T., Rutherfurd, I. D., Peel, M. C., & Conlan, I. A. (2009). The hydrology of the Mekong River. In The Mekong (pp. 53-76): Elsevier.

Arias, M., Piman, T., Lauri, H., Cochrane, T., & Kummu, M. (2014). Dams on Mekong tributaries as significant contributors of hydrological alterations to the Tonle Sap Floodplain in Cambodia. Hydrology and Earth System Sciences, 18(12), 5303.

Bosch, N. S. (2008). The influence of impoundments on riverine nutrient transport: An evaluation using the Soil and Water Assessment Tool. Journal of Hydrology, 355(1-4), 131-147.

Bouraoui, F., & Grizzetti, B. (2011). Long term change of nutrient concentrations of rivers discharging in European seas. Science of the Total Environment, 409(23), 4899-4916.

Bouraoui, F., & Grizzetti, B. J. S. o. t. T. E. (2011). Long term change of nutrient concentrations of rivers discharging in European seas. 409(23), 4899-4916.

Campbell, I. (2007). Perceptions, data, and river management: Lessons from the Mekong River. Water Resources Research, 43(2).

Campbell, I. (2009). The challenges for Mekong River management. In The Mekong (pp. 403-419): Elsevier.

Chai, C., Yu, Z., Shen, Z., Song, X., Cao, X., & Yao, Y. (2009). Nutrient characteristics in the Yangtze River Estuary and the adjacent East China Sea before and after impoundment of the Three Gorges Dam. Science of the Total environment, 407(16), 4687-4695.

Chang, C. C., Kendall, C., Silva, S. R., Battaglin, W. A., Campbell, D. H. J. C. J. o. F., & Sciences, A. (2002). Nitrate stable isotopes: tools for determining nitrate sources among different land uses in the Mississippi River Basin. 59(12), 1874-1885.

Chea, R., Grenouillet, G., & Lek, S. (2016). Evidence of water quality degradation in lower Mekong basin revealed by self-organizing map. PloS one, 11(1).

Clesceri, L., Greenberg, A., & Eaton, A. J. A., WEF, Monrovia, USA. (1998). Standard Methods for the Examination of Water and Wastewater APHA.

Coates, D., Poeu, O., Suntornratnana, U., Nguyen, T., & Viravong, S. (2005). Biodiversity and fisheries in the Mekong River Basin. Mekong development series(2).

Dudgeon, D. (2005). River rehabilitation for conservation of fish biodiversity in monsoonal Asia. Ecology and Society, 10(2).

Fujii, H., Garsdal, H., Ward, P., Ishii, M., Morishita, K., & Boivin, T. (2003). Hydrological roles of the Cambodian floodplain of the Mekong River. International Journal of River Basin Management, 1(3), 253-266.

Galloway, J. N., Dentener, F. J., Capone, D. G., Boyer, E. W., Howarth, R. W., Seitzinger, S. P., . . . Holland, E. A. (2004). Nitrogen cycles: past, present, and future. Biogeochemistry, 70(2), 153-226.

Gong, Y., Yu, Z., Yao, Q., Chen, H., Mi, T., & Tan, J. (2015). Seasonal variation and sources of dissolved nutrients in the Yellow River, China. International journal of environmental research and public health, 12(8), 9603-9622.

Gupta, A., & Liew, S. C. (2007). The Mekong from satellite imagery: A quick look at a large river. Geomorphology, 85(3-4), 259-274.

Hanley, K. W., Wollheim, W. M., Salisbury, J., Huntington, T., & Aiken, G. (2013). Controls on dissolved organic carbon quantity and chemical character in temperate rivers of North America. Global biogeochemical cycles, 27(2), 492-504.

Hecht, J. S., Lacombe, G., Arias, M. E., Dang, T. D., & Piman, T. (2019). Hydropower dams of the Mekong River basin: A review of their hydrological impacts. Journal of hydrology, 568, 285-300.

Hedlund, U., Manusthiparom, C., Jirayoot, K., Modeller, , & Campbell, I. C. (2005). Water Statistics in the Mekong River Basin. IWG-Env, International Work Session on Water Statistics, Vienna.

Hirsch, R. M. J. J. J. o. t. A. W. R. A. (2014). Large biases in regression-based constituent flux estimates: Causes and diagnostic tools. 50(6), 1401-1424.

Hu, J., & Li, S. (2009). Modeling the mass fluxes and transformations of nutrients in the Pearl River Delta, China. Journal of Marine Systems, 78(1), 146-167.

Hua, W., Huaiyu, Y., Fengnian, Z., Bao, L., Wei, Z., & Yeye, Y. (2019). Dynamics of nutrient export from the Yangtze River to the East China sea. Estuarine, Coastal and Shelf Science, 229, 106415.

Iida, T., Inkhamseng, S., Yoshida, K., & Tanji, H. (2011). Characterization of water quality variation in the Mekong River at Vientiane by frequent observations. Hydrological Processes, 25(23), 3590-3601.

Jarvie, H., Whitton, B., & Neal, C. (1998). Nitrogen and phosphorus in east coast British rivers: speciation, sources and biological significance. Science of The Total Environment, 210, 79-109.

Johnston, S. E., Shorina, N., Bulygina, E., Vorobjeva, T., Chupakova, A., Klimov, S. I., . . . Podgorski, D. C. (2018). Flux and seasonality of dissolved organic matter from the Northern Dvina (Severnaya Dvina) River, Russia. Journal of Geophysical Research: Biogeosciences, 123(3), 1041-1056.

Kondolf, G. M., Schmitt, R. J., Carling, P., Darby, S., Arias, M., Bizzi, S., . . . Kummu, M. (2018). Changing sediment budget of the Mekong: Cumulative threats and management strategies for a large river basin. Science of The Total Environment, 625, 114-134.

Kongmeng, L., & Larsen, H. (2014). Lower Mekong Regional water quality monitoring report. MRC Technical Paper No, 60.

Kongmeng, L., & Larsen, H. (2016). Lower Mekong Regional water quality monitoring report. In: Vientiane, Lao PDR: Mekong River Commission.

Kummu, M., Penny, D., Sarkkula, J., & Koponen, J. (2008). Sediment: curse or blessing for Tonle Sap Lake? AMBIO: A Journal of the Human Environment, 37(3), 158-163.

Kummu, M., & Sarkkula, J. (2008). Impact of the Mekong River flow alteration on the Tonle Sap flood pulse. AMBIO: A Journal of the Human Environment, 37(3), 185-192.

Kummu, M., Tes, S., Yin, S., Adamson, P., Józsa, J., Koponen, J., . . . Sarkkula, J. (2014). Water balance analysis for the Tonle Sap Lake–floodplain system. Hydrological Processes, 28(4), 1722-1733.

Kummu, M., & Varis, O. (2007). Sediment-related impacts due to upstream reservoir trapping, the Lower Mekong River. Geomorphology, 85(3-4), 275-293.

Lamberts, D. (2006). The Tonle Sap Lake as a productive ecosystem. International Journal of Water Resources Development, 22(3), 481-495.

Le, T. P. Q., Billen, G., & Garnier, J. (2015). Long-term biogeochemical functioning of the Red River (Vietnam): past and present situations. Regional Environmental Change, 15(2), 329-339.

Li, S., & Bush, R. T. (2015). Rising flux of nutrients (C, N, P and Si) in the lower Mekong River. Journal of Hydrology, 530, 447-461.

Liljeström, I., Kummu, M., & Varis, O. (2012). Nutrient Balance Assessment in the Mekong Basin: nitrogen and phosphorus dynamics in a catchment scale. International Journal of Water Resources Development, 28(2), 373-391.

Liu, S., Hong, G.-H., Zhang, J., Ye, X., & Jiang, X. (2009). Nutrient budgets for large Chinese estuaries. Biogeosciences, 6(10).

Lu, X., Kummu, M., & Oeurng, C. (2014). Reappraisal of sediment dynamics in the Lower Mekong River, Cambodia. Earth Surface Processes and Landforms, 39(14), 1855-1865.

Lu, X., & Siew, R. (2005). Water discharge and sediment flux changes in the Lower Mekong River.

Lu, X. X., & Siew, R. (2006). Water discharge and sediment flux changes over the past decades in the Lower Mekong River: possible impacts of the Chinese dams.

Masumoto, T., Kubota, T., & Matsuda, S. (2001). Preliminary analysis of the 2000-flood in the Lower Mekong River basin. Annual Report of Japan Research Society of Practical Hydrology System, 4, 103-122.

MRC. (2003). State of the basin report: Mekong River Commission.

MRC. (2010). State of the basin report: Mekong River Commission (MRC).

Oeurng, C., Cochrane, T. A., Arias, M. E., Shrestha, B., & Piman, T. (2016). Assessment of changes in riverine nitrate in the Sesan, Srepok and Sekong tributaries of the Lower Mekong River Basin. Journal of Hydrology: Regional Studies, 8, 95-111.

Paul, L. (2003). Nutrient elimination in pre-dams: results of long term studies. Hydrobiologia, 504(1-3), 289-295.

Ribolzi, O., Cuny, J., Sengsoulichanh, P., Mousquès, C., Soulileuth, B., Pierret, A., . . . Sengtaheuanghoung, O. (2011). Land use and water quality along a Mekong tributary in Northern Lao PDR. Environmental management, 47(2), 291-302.

Seitzinger, S. P., Harrison, J. A., Dumont, E., Beusen, A. H., & Bouwman, A. (2005). Sources and delivery of carbon, nitrogen, and phosphorus to the coastal zone: An overview of Global Nutrient Export from Watersheds (NEWS) models and their application. Global Biogeochemical Cycles, 19(4).

Shen, Z.-L., & Liu, Q. (2009). Nutrients in the changjiang river. Environmental monitoring and assessment, 153(1-4), 27-44.

Sok, T., Oeurng, C., Kaing, V., Sauvage, S., G KONDOLF, M., & PEREZ, J. M. S. (2020). Assessment of Sediment Load Variabilities in the Tonle Sap and Lower Mekong Rivers, Cambodia. Manuscript submitted for publication.

Sun, C., Shen, Z., Liu, R., Xiong, M., Ma, F., Zhang, O., . . . Chen, L. (2013). Historical trend of nitrogen and phosphorus loads from the upper Yangtze River basin and their responses to the Three Gorges Dam. Environmental Science and Pollution Research, 20(12), 8871-8880.

Supit, C., & Ohgushi, K. (2012). Dam construction impacts on stream flow and nutrient transport in Kase River Basin. International Journal of Civil & Environmental Engineering, 12(3), 1-5.

Szabo, S., Brondizio, E., Renaud, F. G., Hetrick, S., Nicholls, R. J., Matthews, Z., . . . Foufoula-Georgiou, E. (2016). Population dynamics, delta vulnerability and environmental change: comparison of the Mekong, Ganges–Brahmaputra and Amazon delta regions. Sustainability science, 11(4), 539-554.

Tamura, T., Saito, Y., Sieng, S., Ben, B., Kong, M., Choup, S., & Tsukawaki, S. (2007). Depositional facies and radiocarbon ages of a drill core from the Mekong River lowland near Phnom Penh, Cambodia: evidence for tidal sedimentation at the time of Holocene maximum flooding. Journal of Asian Earth Sciences, 29(5-6), 585-592.

Tong, Y., Bu, X., Chen, J., Zhou, F., Chen, L., Liu, M., . . . Mi, Z. (2017). Estimation of nutrient discharge from the Yangtze River to the East China Sea and the identification of nutrient sources. Journal of hazardous materials, 321, 728-736.

Watanabe, T., Nagumo, T., & Hung, N. (2003). Estimation of changes in nitrogen flow accompanying agricultural development in Cantho Province, Vietnam predicted for 2010. Estimation of changes in nitrogen flow accompanying agricultural development in Cantho Province, Vietnam predicted for 2010., 22-23.

Wu, G., Cao, W., Wang, F., Su, X., Yan, Y., & Guan, Q. (2019). Riverine nutrient fluxes and environmental effects on China's estuaries. Science of The Total Environment, 661, 130-137.

Yoshimura, C., Zhou, M., Kiem, A. S., Fukami, K., Prasantha, H. H., Ishidaira, H., & Takeuchi, K. (2009). 2020s scenario analysis of nutrient load in the Mekong River Basin using a distributed hydrological model. Science of The Total Environment, 407(20), 5356-5366.

Chapter V

Spatial and Temporal Sediment Fluxes and Yield in Mekong River Basin

This chapter was published in the Journal of Water. The work of this chapter is the base of the following works in the following chapters. This chapter aims to assess long-term basin hydrology focusing on the water balance components and contribution of the different basin compartments to water yield and quantify the sediment load and spatial sediment yield through the modelling method.

Sok, T.; Oeurng, C.; Ich, I.; Sauvage, S.; Sánchez-Pérez, J.M. Assessment of Hydrology and Sediment Yield in the Mekong River Basin Using SWAT Model. Water 2020, 12, 3503. https://doi.org/10.3390/w12123503

5. Chapter V. Spatial and Temporal Sediment Fluxes and Yield in Mekong River Basin

5.1. Scientific Context and Objectives

Sediment in the Mekong River is important to sustain the geomorphology of the floodplains and particularly the Tonle Sap Lake and provide essential nutrients for its productive ecosystem. Due to the limited sediment monitoring data for both suspended and bed loads in the Mekong Rivers and their tributaries, the spatial and temporal resolution to accurately determine how much of the sediment load is from tributaries entering the Mekong mainstream is still lacking. As a result, no consensus was reached on sediment baselines amongst the countries in the Mekong Basin. The Mekong River basin spreads across six countries has made studying the system a complex task. Much importance is given to modelling in terms of developing sustainable management of water resources at the river basin scale. As mentioned previously, prior studies have applied the SWAT model to parts of the basin. In this study, the SWAT model was applied for the Mekong River Basin to (i) assess long-term basin hydrology focusing on the water balance components and contribution of the different compartments of the basin to water yield, and (ii) quantify the sediment load and spatial sediment yield.

5.2. Materials and Methods

The SWAT model has been set up to cover the total area of 748,000 km2 from the most upstream (80%) of the total Mekong River Basin. The SWAT application of this study in the Mekong Basin can be split into eight zones, as availability of recorded streamflow and sediment used in this study for SWAT setup. The model was set up with the following major sub-basins: (1) from most upstream to China/Laos Border, (2) China/Laos Border to Chiang Saen, (3) Chiang Saen to Luang Prabang, (4) Luang Prabang to Vientiane, (5) Vientiane to Mukdahan, (6) Mukdahan to Pakse, (7) Pakse to Stung Treng and (8) Stung Treng to Kratie. The Kratie station was selected as the most downstream for the model setup since this location is not affected by the tidal influence and the flood wave's buffering in the Tonle Sap Lake system. The hydrology model was calibrated and validated using eight locations, and the sediment model was calibrated and validated using six locations.

5.3. Results and Discussions

For all the gauge stations, the result of monthly streamflow and sediment performance of the SWAT model shows the adequate capability to process hydrology and sediment modelling process.

During the study period, the mean annual rainfall was 1540 mm; 67% (1032 mm) of the average annual rainfall was removed by evapotranspiration and 33% (508 mm) for the streamflow. A water yield of 508 mm has come from surface runoff (proportion of 34%), lateral flow (proportion of 21%), and groundwater (proportion of 45%). The overall proportion of streamflow in the Mekong River in the study modelled by SWAT was 34% from surface runoff, 21% from lateral flow, 45%from the contribution of groundwater. Sediment load yields by major area, the highest sediment yield (1295 t/km^2/year) can be found in Chiang Saen to Luang Prabang in the northern part of Laos. This area is covered by mixed land use and high topography with steep slopes. In the upper Mekong part in China (where the river is called Lancang River), despite high topography and steep slope, the sediment load is lower than Chiang Saen to Luang Prabang due to covering by the forest type (evergreen and mixed forest). It is noticed that in the Mekong Basin in Thailand (Mukdahan to Pakse), despite the high agricultural activity, the sediment yield is low (78 t/km^2/year) since most of the area covers by gentle slope. In between Pakse and Kratie (including 3S, the largest tributary of Mekong), the average sediment yield was found 138 t/km^2/year; however, we found high yields at the upstream part of the 3S basin (>500 t/km^2/year).

5.4. Conclusion and Perspectives

The overall proportions of streamflow in the Mekong River were 34% from surface runoff, 21% from lateral flow, 45% from groundwater contribution. The average annual sediments yield presented 1,295 t/km^2/year in the upper part of the basin, 218 t/km^2/year in the middle, 78 t/km^2/year in the intensive agricultural area and 138 t/km^2/year in the highland area in the lower part. The Mekong River's annual average sediment yield was 310 t/km²/year from the upper 80% of the total MRB before entering the delta. This study also supplies a sediment loading map in the Mekong River Basin, which could limit storage capabilities, increase the risk for ageing infrastructure, and lead to proper management strategies of this region. The outcome of the study could also be the baseline information of sediment studies for the sustainable watershed management plan.

Based on this part of the work, the study on nitrate assessment using the SWAT model in the Mekong River can be carried on.

5.5. Full paper: Sok, T.; Oeurng, C.; Ich, I.; Sauvage, S.; Sánchez-Pérez, J.M. Assessment of Hydrology and Sediment Yield in the Mekong River Basin Using SWAT Model. Water 2020, 12, 3503. *https://doi.org/10.3390/w12123503*

water

MDPI

Article

Assessment of Hydrology and Sediment Yield in the Mekong River Basin Using SWAT Model

Ty Sok[1,2,*], Chantha Oeurng[1,*], Ilan Ich[1], Sabine Sauvage[2], José Miguel Sanchez-Perez[2]

[1] Faculty of Hydrology and Water Resources Engineering, Institute of Technology of Cambodia, Russian Federation Blvd., P.O.BOX 86, Phnom Penh Cambodia;
[2] Laboratoire Ecologie Fonctionnelle et Environnement, UMR 5245 CNRS/UPS/INPT ENSAT, Avenue de l'Agrobiopole, BP 32607, Auzeville Tolosane, 31326 CASTANET TOLOSAN, France;
* Correspondence: sokty@itc.edu.kh , chantha@itc.edu.kh

Received: 6 November 2020; Accepted: 10 December 2020; Published: 13 December 2020

Abstract: The Mekong River Basin (MRB) in Southeast Asia is among the world's ten largest rivers, both in terms of its discharge and sediment load. The spatial and temporal resolution to accurately determine the sediment load/yield from tributaries and sub-basin that enters the Mekong mainstream still lacks from the large-scale model. In this study, the SWAT model was applied to the MRB to assess long-term basin hydrology and to quantify the sediment load and spatial sediment yieldin the MRB. The model was calibrated and validated (1985-2016) at a monthly time step. The overall proportions of streamflow in the Mekong River were 34% from surface runoff, 21% from lateral flow, and 45% from groundwater contribution. The average annual sediments yield presented 1,295 t/km^2/year in the upper part of the basin, 218 t/km^2/year in the middle, 78 t/km^2/year in the intensive agricultural area and 138 t/km^2/year in the highland area in the lower part. The annual average sediment yield for the Mekong River was 310 t/km^2/year from upper 80% of the total MRB before entering the delta. The derived sediment yield and a spatial soil erosion map can explicitly illustrate the identification and prioritization of the critical soil erosion-prone areas of the MR sub-basins.

Keywords: SWAT, hydrology, sediment yield, Mekong River

1. Introduction

Sediment transport, as one of natural components of river geomorphology, plays an overarching role for the maintenance of fluvial environments such as channel systems, floodplains, wetlands and estuaries, and equilibrium between deposition and erosion, which usually occurs along a river in natural and undisturbed systems. Over the past few decades, dynamic river conditions have been noticed to be under the influence of anthropogenic activities, leading to considerable changes in water discharge and sediment loads [1-4]. Major rivers in the world such as the Nile and Congo in Africa, Colorado in America, the Ebro in Europe, and the Yangtze, Yellow, and Mekong River in Asia have been reported to supply less sediment following anthropogenic activities [5-12]. This has resulted in catastrophic morphological changes, not only in the river itself but also in the delta [13].

There is a recent trend of building new large hydropower dams in developing countries, particularly in mega biodiversity river basins, such as the Amazon, the Congo, and the Mekong, although substantial losses in these ecologically important regions are being observed [11,14,15]. The transboundary Mekong River Basin, which is ranked the 21st largest river basin worldwide, distributed between five countries: China, Myanmar, Lao People's Democratic Republic, Thailand, Cambodia, and Vietnam. The river basin can be separated into two sections: the Upper Mekong Basin in China (UMB), where the river is called Lancang) and the Lower Mekong Basin (LMB) from Yunnan (China) downstream to the South China Sea in Vietnam. The Mekong is considered one of the last unregulated great rivers in the world, as the flow regime is still close to its natural state [16]. The Mekong could potentially produce over 30,000 MW of electricity; however, only about 10% of this potential has been developed to date [17,18]. Since the 1990s, the Mekong River has been undergoing dam construction. One of the most evident transformations in the construction of large hydropower dams in the upstream Mekong, is that has reduced the sediment discharge into the floodplain and estuaries at an alarming rate [19]. The sediment could limit storage capabilities and increases the risk for ageing infrastructure, in particular the reservoir impoundment in the Mekong River Basin. For example, the main dams in the Lancang River

occupy sediment trapping efficiencies between 30% and 70% because of the high sediment yield in the Lancang-Mekong River's mainstream and sub-basins [20]. Some estimate the sediment flux of the Mekong, the pre-dam sediment flux into the South China Sea, has been estimated from 40 to 160 Mt/year [21-24].

Sediment in Mekong River is important to sustain the geomorphology of the floodplains and particularly the Tonle Sap Lake and to provide essential nutrients for the lake's productive ecosystem [25]. As a requisite part of the Mekong River system, the Tonle Sap Lake in central Cambodia is the Southeast Asia's largest permanent freshwater body and the essential natural reservoir from which the Mekong River benefits [25]. Further, the Tonle Sap Lake and its floodplains connecting with the Mekong mainstream through the Tonle Sap River rely as well upon the Mekong sediment regimes since the primary source of sediment supply to the Tonle Sap Lake is of sediment transport from the Mekong [25-26]. The Mekong River is responsible for the majority (more than 70%) of the sediment delivered to Tonle Sap Lake [25-27].

Due to the limited sediment monitoring data for both suspended and bed loads in the Mekong Rivers and their tributaries, the spatial and temporal resolution to accurately determine how much of the sediment load is from tributaries entering the Mekong mainstream is still lacking. As a result, no consensus was reached on sediment baselines amongst the countries in the Mekong Basin [28]. The fact that the Mekong River basin spreads across six countries has made studying the system a complex task. Much importance is given to modelling in terms of the development of sustainable management of water resources at the river basin scale, which can help evaluate current water resources, identify pollution sources, and improve sustainable development [29]. The Soil and Water Assessment Tool (SWAT) model [30-32] has emerged as one of the most extensively used eco-hydrological models worldwide. The SWAT model has been quite reliable in Southeast Asia (SEA), with most of the studies reporting above the satisfactory statistical values. Applications of SWAT in Southeast Asia (SEA) were for hydrologic analyses of the Mekong River basin [33]. Partial analyses of the Mekong system with SWAT are ongoing, as a rising number of studies have been conducted for specific catchments based in different SEA countries [33]. Several recent studies have attempted to perform a SWAT model in parts of Mekong river for various objectives from hydrology, sediment to water quality, land use/climate scenarios, and others, e.g. [34,35,36,37]. As mentioned previously, prior studies have applied the SWAT model to parts of the basin. In this study, the SWAT model was applied for the Mekong River Basin to (i) assess

long-term basin hydrology focusing on the water balance components and contribution of the different compartments of the basin to water yield, and to (ii) quantify the sediment load and spatial sediment yield.

2. Materials and Methods

2.1. Study area

Located in Asia, the Mekong River, measuring a length of 4,800 km, is the 12th longest river in the world, and has a basin area ranked 21st (795,000 km^2), with an average annual runoff ranked 8th in the world (475,000 million m^3). The basin area is shared by China (21%), Myanmar (3%), Lao PDR (25%), Thailand (23%), Cambodia (20%), and Vietnam (8%). The Mekong River Basin is politically divided into two parts, the Upper Mekong Basin in China (Lancang River) and the Lower Mekong Basin from downstream of China/Laos Border to the South China Sea in Vietnam. The Lower Mekong River Basin mainly overlays the areas in the four downstream riparian countries (Lao PDR, Thailand, Cambodia, and Vietnam) accounting for 620,000 km^2 of the basin area (Figure 5-1.a). The water resources and productivity of the river and its basin benefit a population of over 60 million people. That part of the basin is occupied by Northeast Thailand and currently undergoes considerable irrigation development and the potential for future development. Cambodia has a significant part of the basin that includes the Great Lake and Tonle Sap. The lake area varies from 3,000 km^2 in the dry season to 15,000 km^2 in the wet season. The lake becomes the biggest source of freshwater fish in Southeast Asia. Tonle Sap River with an approximate length of 120 km adjoins the lake to the Mekong River. The reverse flow from the Mekong River to the lake complicates the understanding of the hydraulic and ecological processes pertinent to this area. The Mekong Delta, mostly in Vietnam and partly in Cambodia, is affected by the tidal process and can impact as far as Phnom Penh of Cambodia [38].

Remaining undeveloped until 1990, The Mekong River is now witnessing dam construction at a rapid pace. The seven dams' construction is in progress on the mainstream in China, and 133 are proposed for the Lower Mekong River, including 11 on the Lower Mekong mainstream [39]. The active volume of the existing dams in the UMB in China measures between 120 and 12,300 million m3; on the other hand, the 11 dams to be proposed in the LMB would contain the volume of 115-1,450 million m^3. The operation of dams in the UMB will be either seasonal or yearly, but

all those 11 proposed dams in the LMB are intended for daily operation. However, recently the Upper Mekong River in China is governed by a number of dams and reservoirs, all of which have laid dramatic changes in navigation patterns, the flow of water as well as sediment to the Mekong Delta [40].

2.2. Discharge and sediment data used in the study

The streamflow data (recorded daily) and sediment data (recorded monthly) used in this study were obtained from the metadata of the Mekong River Commission (MRC). There are eight discharge gauge stations along the main Mekong River in this study (Table 1). The total suspended sediment (TSS) concentration from the MRC-WQMN (MRC-Water Quality Monitoring Network) dataset has been widely used in sediment load estimation in the Mekong River Basin study, e.g. [25,41,42]. TSS concentrations were obtained from the water quality sampling conducted monthly by respective member countries. The TSS samples were collected at 0.30 m below the water surface in the middle of the mainstream cross-section at each station. The samples were analyzed at designated laboratories by MRC and recommended analytical method for TSS analysis (2540-D-TSS-SM) were employed [43]. Sediment loads were estimated at six locations using the LOAD ESTimator (LOADEST) program [44]. It should be noted that our study did not include the bed-load, which is approximately 1.40% of suspended sediment load [45]. The sediment record use in this study is also detailed in **Table 5-1**.

Table 5-1: *Recorded streamflow and sediment used in this study. Data from MRC.*

Name of station	Basin coverage		Streamflow record used		Sediment record used	
	(km^2)	(%) of total basin	Period	Time step of measurement	Period	Time step of measurement
China/Laos Border	164,226	18%	1985-2007			
Chiang Saen	199,008	21%	1985-2016		1995-2011	
Luang Prabang	288,380	31%	1985-2016		1995-2011	
Vientiane	323,027	34%	1985-2016	Daily	1995-2011	Monthly
Mukdahan	429,210	46%	1985-2016		2001-2011	
Pakse	621,404	66%	1985-2016		1995-2011	
Stung Treng	728,828	78%	1985-2016			
Kratie	747,958	80%	1985-2016		1995-2016	

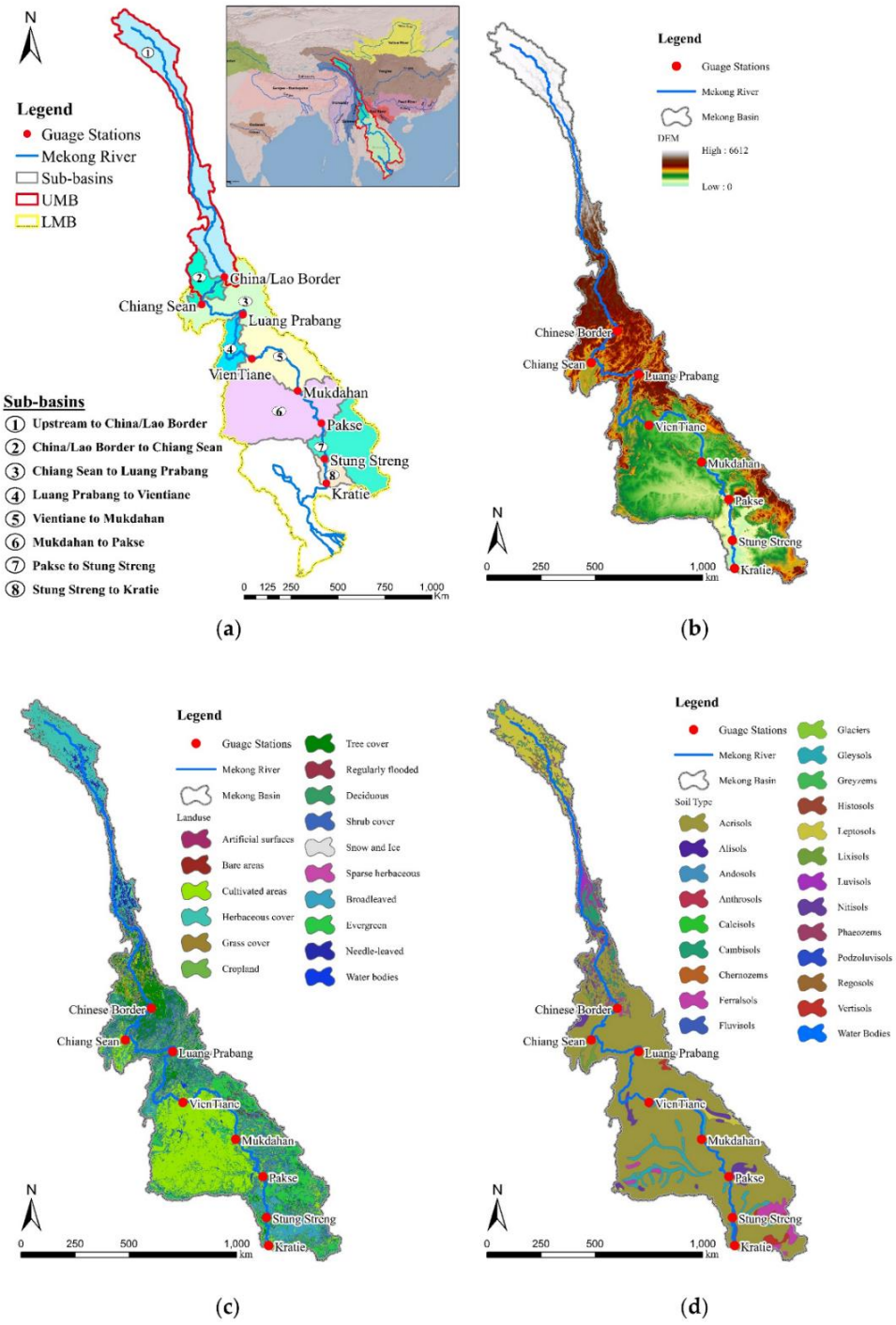

Figure 5-1: *Spatial Maps of the Mekong River Basin.* ***(a)*** *Study area: Mekong River Basin (including the Upper and Lower Mekong Basin) sharing of the basin area includes Southern part of China and major sub-basin identifications based on the gauge stations,* ***(b)*** *DEM,* ***(c)*** *Land use distribution, and* ***(d)*** *Soil type distribution.*

2.3. SWAT conceptual model

SWAT is a physically-based, semi-distributed, agro-hydrological simulation model that operates on a sub-daily to annual scale time step on a watershed scale. SWAT was developed with the aim of predicting the impact of management on water, sediment, and agricultural chemical yields in ungauged catchments [31]. The model's capability lies in continuous simulation for dissolved and particulate elements in large complex catchments with varying weather, soils, and management conditions over long periods. Small or expansive catchments can be analyzed using SWAT through discretizing into sub-basins, which are then further subdivided into hydrological response units (HRUs) with homogeneous land use, soil type, and slope.

The prediction streamflow of the SWAT model is based on the water balance equation:

$$SW_t = SWL_0 + \sum_{i=0}^{t}(R_{day} - Q_{surf} - E_a - W_{seep} - Q_{gw}) \quad (1)$$

SW_t is the final soil water content (mm H_2O)
t is the time (day)
SWL_0 is the initial water content on day $i\,(mm)$
R_{day} is the amount of precipitation on day i (mm H_2O)
Q_{surf} is the amount of surface runoff on day i (mm H_2O)
E_a is the amount of evaporanspiration on day i (mm H_2O)
W_{seep} is the amount of water entring the vadose zone from the soil profile on i (mm H_2O)
Q_{gw} is the amount of return flow on day i (mm H_2O)

The prediction of the sediment of the SWAT model is based on modified universal soil loss (MUSLE) equation where rainfall and runoff are the main reason for soil loss.

$$sed = 11.8\,(Q_{surf} \times q_{peak} \times area_{hru})^{0.56} \times (K_{USLE} \times C_{USLE} \times P_{USLE} \times LS_{USLE} \times CFRG) \quad (2)$$

sed is the sediment yield on a given day (metric tons)
Q_{surf} is the surface runoff volume (mm H_2O / ha)
q_{peak} is the peak runoff rate (m^3/s)
$area_{hru}$ is the area of the HRU (ha)
K_{USLE} is the USLE soil erodibility factor (0.13 metric ton m^2 hr/(m^3 metric ton cm))
C_{USLE} is the USLE cover and management factor
P_{USLE} is the USLE support practice factor
LS_{USLE} is the USLE topographic factor
$CFRG$ is the coarse fragment factor

2.4. SWAT model setup and data inputs for the Mekong River Basin

The SWAT model has been set up to cover the total area of 748,000 km^2 from the most upstream (80%) of the total Mekong River Basin (Figure 5-1.a). The SWAT application of this study in the Mekong Basin can be split into eight zones, as seen in Figure 1a, as availability of recorded streamflow and sediment used in this study for SWAT setup. The model was set up with the following major sub-basins: (1) from most upstream to China/Laos Border, (2) China/Laos Border to Chiang Saen, (3) Chiang Saen to Luang Prabang, (4) Luang Prabang to Vientiane, (5) Vientiane to Mukdahan, (6) Mukdahan to Pakse, (7) Pakse to Stung Treng and (8) Stung Treng to Kratie. The Kratie station was selected as the most downstream for the model setup since this location is not affected by the tidal influence [38] and the buffering of the flood wave in the Tonle Sap Lake system [46].

Each data input was obtained from different sources, which is summarized in **Table 5-2**. The precipitation used for this study was obtained from the Global Precipitation Climatology Centre (GPCC) (www.gcmd.nasa.gov), and daily temperatures were downloaded from NASA Earth Exchange (NEX) (www.nasa.gov/nex). The study used the Multi-Error-Removed Improved-Terrain DEM (MERIT DEM) (www.hydro.iis.u-tokyo.ac.jp/~yamadai/). The MERIT DEM was developed through the removal of multiple error components (absolute bias, stripe noise, speckle noise, and tree height bias) from the existing space-borne DEMs (SRTM3 v2.1 and AW3D-30m v1) [47]. The distribution of elevation varies from 8 m to 6612 m as representing the topographic condition of the SWAT Model setup for the Mekong River Basin (**Figure 5-1**.b). The acquisition of land use distribution in the Mekong River Basin was from the Global Land Cover 2000 Database (www.usgs.gov) at a 1 km resolution (**Figure 5-1**.c). Soil type distribution was downloaded from Global Soil data by FAO (www.fao.org/) (**Figure 5-1**.d). The watershed had been discretized into small 345 sub-basins, which is equal to 345 HRUs from 14 land uses, 20 soils and five slopes classes (0%-1%, 1%-2%, 2%-5%, 5%-20%, and >20%). The SWAT model included six major dams based in the Upper Mekong Basin, the Manwan Dam operating in 1993, Dachaoshan in 2001, Jinghong in 2008, Xiaowan in 2009, Gongguoqiao in 2011, and Nuozhadu in 2012. All of these reservoirs quantify an accumulated total and active reservoir storage capacity of approximately 400×10^8 m^3 and 230×10^8 m^3, respectively [48].

Table 5-2: *Data input and sources in the SWAT model in the study.*

Data type	Description	Spatial resolution	Temporal resolution	Data sources
Topography map	DEM	90 m		MERIT DEM: Multi-Error-Removed Improved-Terrain DEM http://hydro.iis.u-tokyo.ac.jp/~yamadai/MERIT_DEM/
Land use map	Land use classification	250 m × 250 m	2002	Global Land Cover Characterization (GLCC): https://www.usgs.gov/
Soil Map	Soil types	250 m × 250 m	2002	Global Soil data: http://www.fao.org/
Meteorological data	Gridded daily rainfall	1°	Daily, 1982-2016	Global Precipitation Climatology Centre: https://gcmd.nasa.gov/
Meteorological data	Temperature	0.25°	Daily, 1982-2016	NASA Earth Exchange (NEX) https://www.nasa.gov/nex
Hydrological data	Observed streamflow	8 stations	Daily, 1980-2016[1]	MoWRAM and MRC
Sediment data	Observed TSS	6 stations	Monthly, 1980-2016[1]	MoWRAM and MRC

[1] Data used to depend on data available to this study for each station.

2.5. SWAT model calibration and validation

The SWAT simulates the overall hydrologic balance for each HRU (hydrologic response units), and model output is available in daily, monthly, and annual time steps. The SWAT version used in this study is SWAT2012 rev. 664 (http://swat.tamu.edu/ software/arcswat/) [30,31]. The calibration was executed manually with the comparison of observed data and literature review information for overall hydrology components and sediment. The Penman-Monteith method was selected to calculate potential evapotranspiration. Parameters controlling the groundwater behaviour in the model and depending on spatial data have been calibrated with literature at the monthly time step (**Table 5-3**). The parameters were calibrated/validated for each sub-basin (based in the gauge stations). The results of calibration showed the importance of parameters, such as Soil_AWC, Soil_K, and ALPHA_BF (groundwater parameter) in the studied flow of the analyzed Mekong Basin (**Table 5-3**). The parameter CN2 is pertinent to the quantity of runoff and is based on soil use. Soil_K and Soil_AWC are related to the quantity of soil-water relationships in various soil types of the region. For sediment load calibration, the parameter PRF_BSN has been calibrated to reduce the impact of streamflow peaks on erosion rate and sediment load at reaches while the USLE_K parameter has been calibrated depending on the permafrost type to slow down erosion comparing to literature reviews.

The model performance was subjected to evaluate by means of comparison between the simulated and the observed constituents using Nash-Sutcliffe efficiency (NSE) [49] and Coefficient of determination (R^2). NSE was used to indicate how well the plot of observed versus simulated data fits the 1:1 line. A calibrated model could be deemed satisfactory if NSE And R^2 are higher than 0.60 for mean behavior [50-53].

Table 5-3: *Calibrated values of SWAT parameters.*

Parameter	Name	Input File	Literature range	Calibrated value
Hydrology:				
ALPHA_BF	Baseflow alpha factor (days)	.gw	0-1	0.005
CANMX	Maximum canopy storage (mm H_2O)	.hru	0-100	100
CN2	Curve number	.mgt	35-98	35-70
ESCO	Soil evaporation compensation factor	.bsn	0-1	0.35
GW_DELAY	Groundwater delay (days)	.gw	0-500	31
GW_REVAP	Groundwater "revap" coefficient	.gw	0.02-0.20	0.05
REVAPMN	Threshold depth of water in the shallow aquifer for "revap" to occur (mm)	.gw	0-500	150
SOL_AWC	Available water capacity of the soil layer (mm H_2O/mm soil)	.sol	0-1	0.20-0.40
SOL_K	Depth soil surface to bottom of layer (mm/hr)	.sol	0-2000	50; 90; 100
SOL_Z	Saturated hydraulic conductivity (mm/hr)	.sol	0-3500	495
Sediment:				
PRF_BSN	Peak rate adjustment factor for sediment routing	.bsn	0-10	0.80
USLE_K	USLE equation soil erodibility factor	.sol	0-0.65	0.20-0.60
SPCON	Linear factor for channel sediment routing	.bsn	0.0001-0.01	0.0025
SPX	Exponential factor for channel sediment routing	.bsn	1-2	1.15

3. Results and Discussion

3.1. Streamflow calibration and validation for the SWAT model

The mean annual rainfall during the study period was 1540 mm; 67% (1032 mm) of the average annual rainfall was removed by evapotranspiration and 33% (508 mm) for the streamflow. A water yield of 508 mm has come from surface runoff (proportion of 34%), lateral flow (proportion of 21%), and groundwater (proportion of 45%). The graphical results of streamflow simulation performance during the calibration and validation periods are shown in **Figure 5-2**. In addition to the monthly comparison of simulated and observation streamflow, we also evaluated the average monthly simulated and observed streamflow of our model for the eight-gauge stations, respectively (**Figure 5-3**). **Figure 5-4** illustrates the monthly observed and simulated streamflow for the study watershed during study periods. The result of calibration periods covers 1985-1999 at monthly time steps, except at Chiang Saen (1985-1994). The validation period covers from 2000-2016, except at Chiang Saen (1995-2007). The statistical performance of monthly streamflow simulation suggested that these SWAT models were well-calibrated/validated and are in a very good range in the lower part of the Mekong Basin from Luang Prabang to Kratie (**Table 5-4**). The NSE values were over 0.80, and R^2 values were over 0.75, respectively. For the two stations at China/Laos Border and Chiang Saen, the statistical indicators were found to be higher than 0.70 (NSE>0.70, $0.65 < R^2 < 0.75$) for results of SWAT monthly streamflow calibration and validation, which suggested that the SWAT model was well-calibrated/validated and was in a good range. For all the gauge stations, the result of monthly streamflow performance of the SWAT model shows the adequate capability to process sediment calibration and further process. In general, graphical results (**Figure 5-2**) indicated good calibration and validation over the range of streamflow discharge, although the calibration and validation results are not differentiated. The model simulated the timing and end of seasonal streamflow but was slightly off in some estimates of peak flows. The result of the statistical performance of streamflow simulation during both calibration and validation are summarized in **Table 5-4**.

Table 5-4: *Monthly flow calibration and validation at eight-gauge stations along the Mekong mainstream.*

Name of station	Calibration			Validation		
	Period	Performance indicators		Period	Performance indicators	
		NSE	R^2		NSE	R^2
China/Laos Border	1985-1994	0.64	0.66	1995-2007	0.65	0.75
Chiang Saen	1985-1999	0.63	0.65	2000-2016	0.67	0.72
Luang Prabang	1985-1999	0.80	0.83	2000-2016	0.80	0.85

Vientiane	1985-1999	0.79	0.84	2000-2016	0.80	0.85
Mukdahan	1985-1999	0.89	0.91	2000-2016	0.87	0.92
Pakse	1985-1999	0.88	0.89	2000-2016	0.90	0.92
Stung Treng	1985-1999	0.88	0.89	2000-2016	0.90	0.92
Kratie	1985-1999	0.88	0.89	2000-2016	0.90	0.92

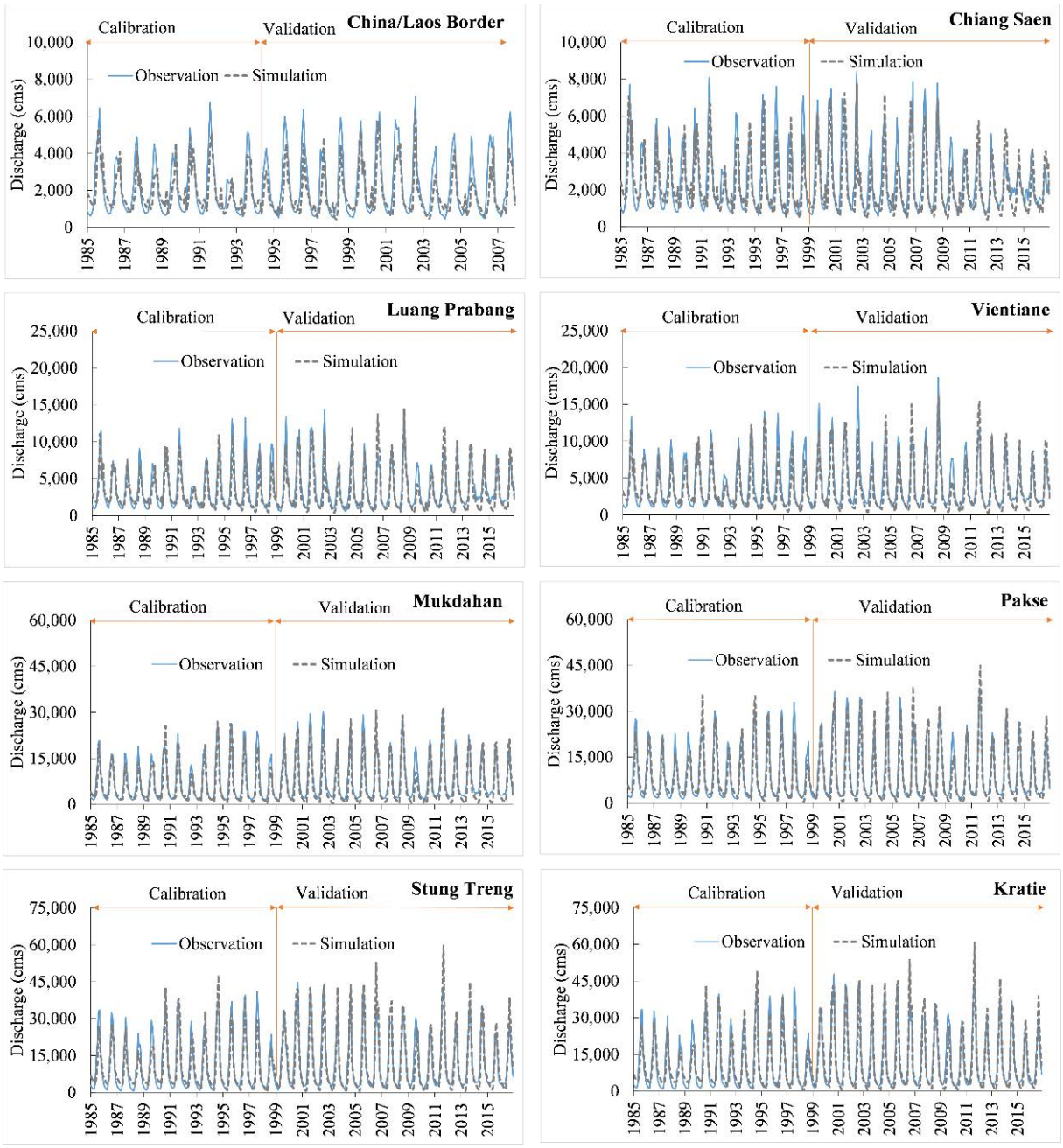

Figure 5-2: *Observed and simulated monthly streamflow during the period 1985 to 2016 for Mekong River Basin during calibration and validation at China/Laos Border, Chiang Saen, Luang Prabang, Vientiane, Mukdahan, Pakse, Stung Treng, Kratie.*

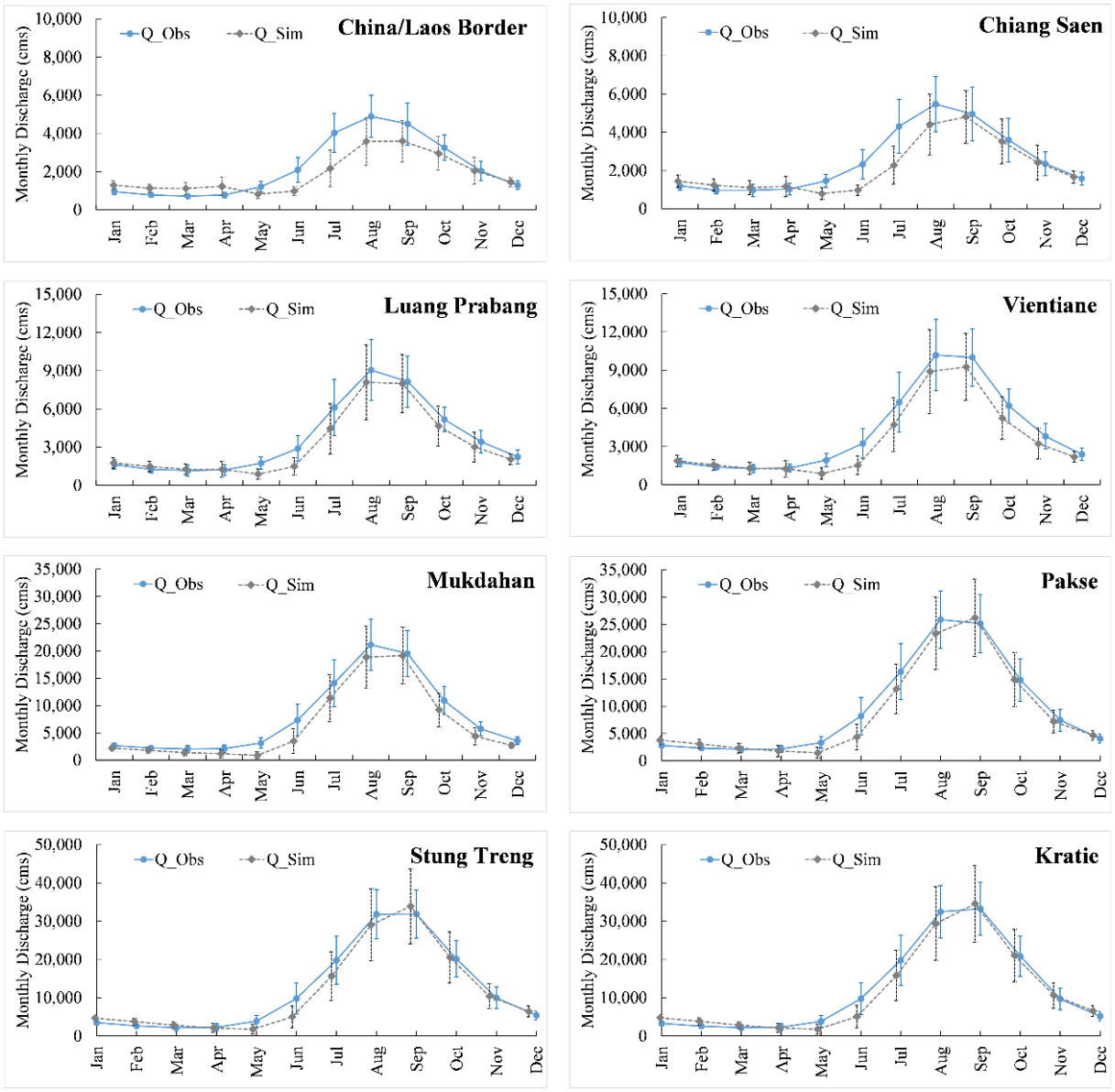

Figure 5-3: *Average monthly observed and simulated streamflow (with standard deviations) for Mekong River Basin from the eight sub-basins: China/Laos Border, Chiang Saen, Luang Prabang, Vientiane, Mukdahan, Pakse, Stung Treng, Kratie.*

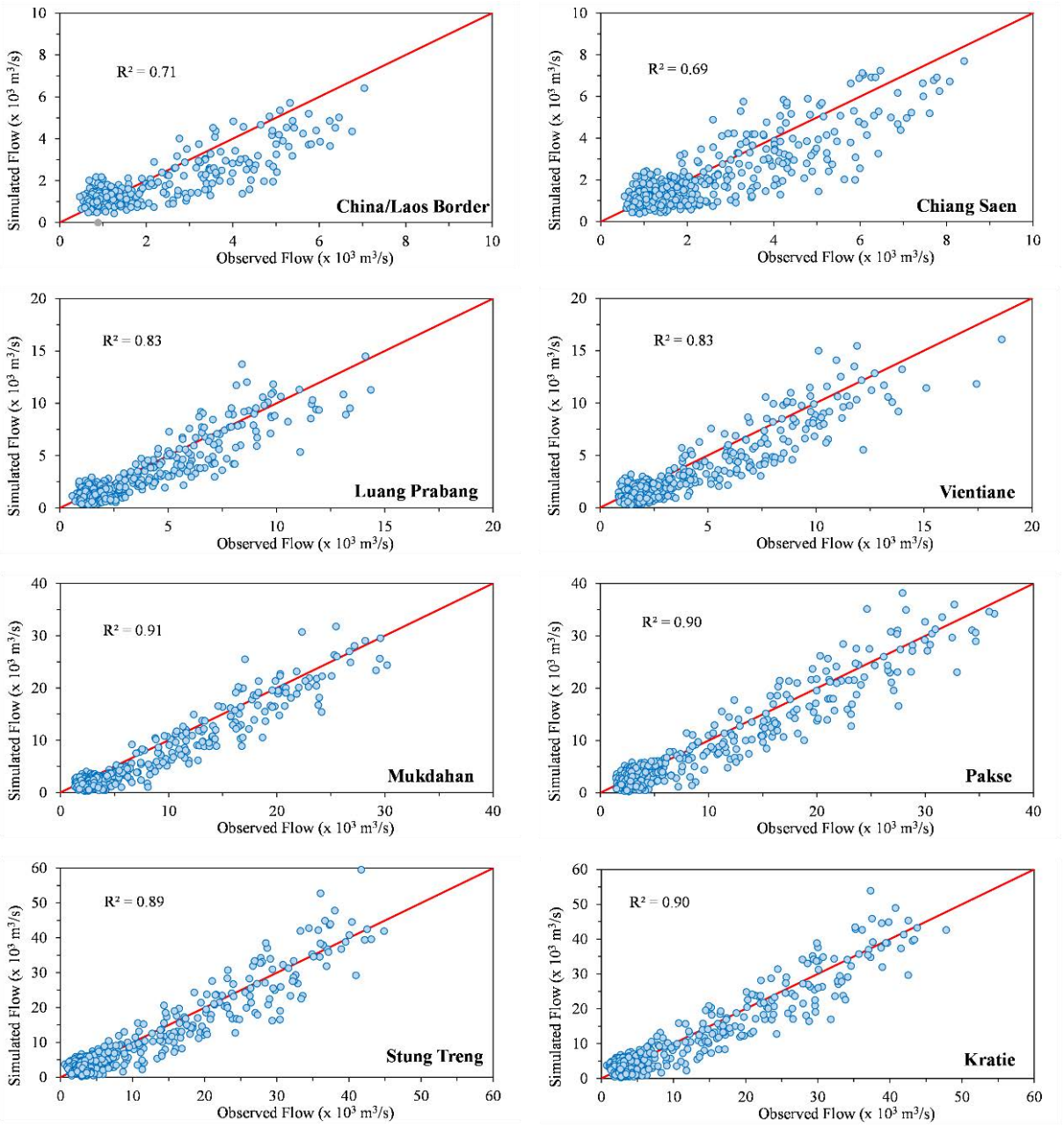

Figure 5-4: *Scatterplot of monthly observed and simulated discharge for eight-gauge stations along the main river from 1985-2016.*

3.2. Sediment loads calibration and validation for the SWAT model

Figure 5-5 shows the visual comparisons between simulated and observed sediment loads in the calibration and validation years at the Chiang Saen, Vientiane, Mukdahan, Pakse, Kratie stations. The results authenticated that SWAT is satisfactory for use in the sediment study. However, the model does not be able to apprehend the peak sediment loads well for both

calibration and validation years. This can be attributed to the bias of precipitation data and errors in stream gauges [54]. In addition, the result of mismatch in low-flows may be have caused by unaccounted flow control from upstream hydropower dams in the dry season, as recommended by [55].

The result of calibration periods covers from 1985-1999, except at Chiang Saen (1985-1994), and the validation period covers from 2000-2016, except at Chiang Saen (1995-2007). The statistical performance of monthly sediment load simulation suggested that the SWAT model was well-calibrated/validated and is in a good range in the lower part of the Mekong Basin from Luang Prabang to Kratie (**Table 5-5**). The NSE values were over 0.50, and R^2 values were above 0.50, for most of the stations during both calibration and validation periods. For two stations, the most upstream at Chiang Saen and the lowest station at Kratie, the statistical indicators were found to be 0.30 of NSE (Chiang Saen) at the calibration period and 0.30 of NSE (Kratie) in the validation period. The low performance of the model in the upstream part could be due to the six dams affecting the upstream at Chiang Saen. Overall, the result of the monthly streamflow performance of the SWAT model shows the adequate capability to process sediment calibration and further process. This can be caused by the scarcity of sediment data in the upstream, moreover the precision of the SWAT performance in simulating sediment load could be reduced at the steep slope area. Walling [23] has acknowledged that the number of gauging stations, reliability, and the spatial and temporal resolutions of data are crucial information in investigations on the load in Chiang Saen station. The lowest station at Kratie seems to be problematic in modelling due to the wetlands (at Stung Treng). On the whole, the perceptible comparisons and the estimations of statistical indices represent acceptable fits between simulated and measured load.

In general, graphical visual and statistical indices indicated good calibration and validation over the range of sediment load. The model simulated the timing and end of seasonal streamflow but was slightly off in some estimates of peak flows. In addition to the monthly comparison of simulated and observation streamflow, we also evaluated the average monthly simulated and observed streamflow of our model for the six-gauge stations, respectively (**Figure 5-6**). It demonstrated the underestimate in monthly sediment load in two upstream stations at Chiang Saen and Luang Prabang. The upstream underestimation can be confirmed and found in **Figure 5-7**, which is the scatter plot of the monthly comparison of simulated and observation sediment load.

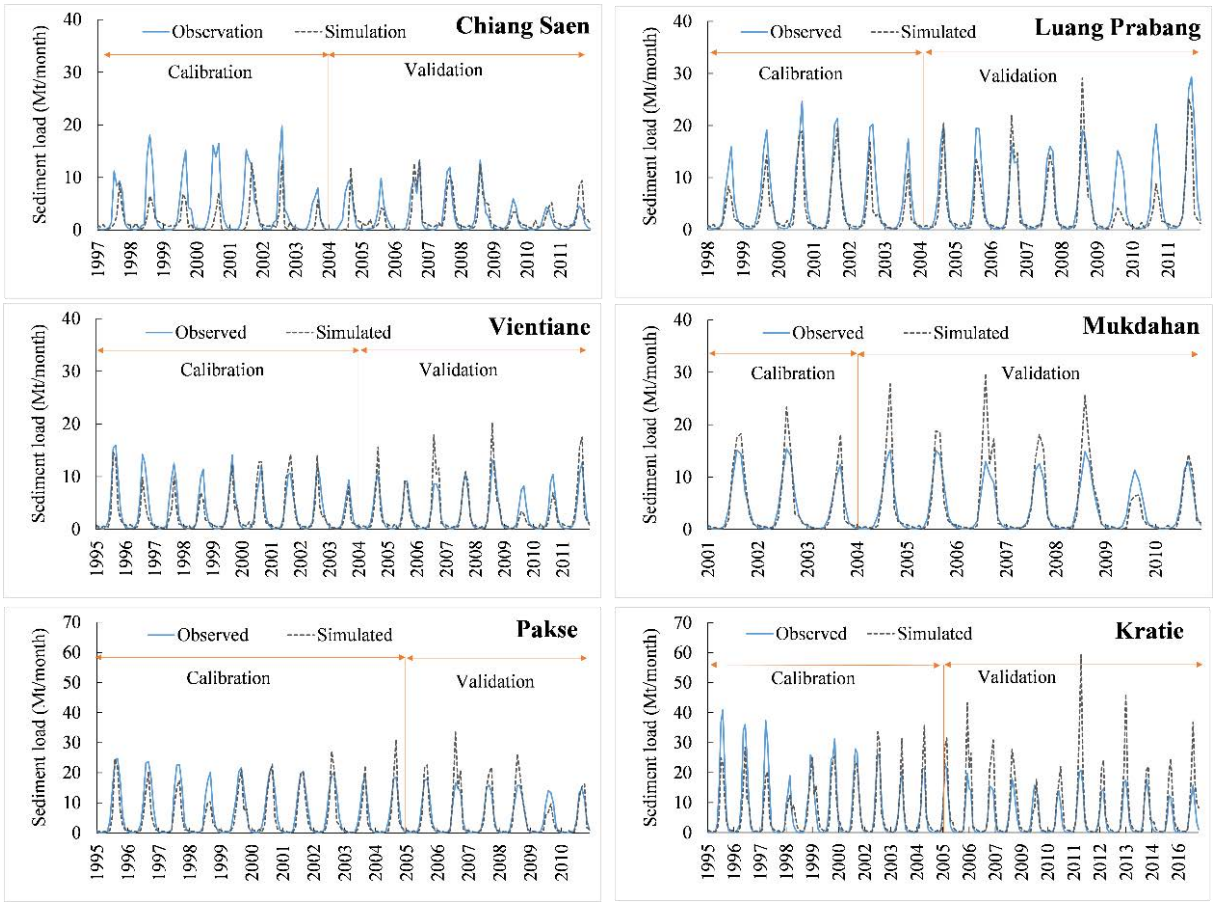

Figure 5-5: *Observed and simulated monthly sediment for Mekong River Basin during calibration and validation at Chiang Saen, Luang Prabang, Vientiane, Mukdahan, Pakse and Kratie.*

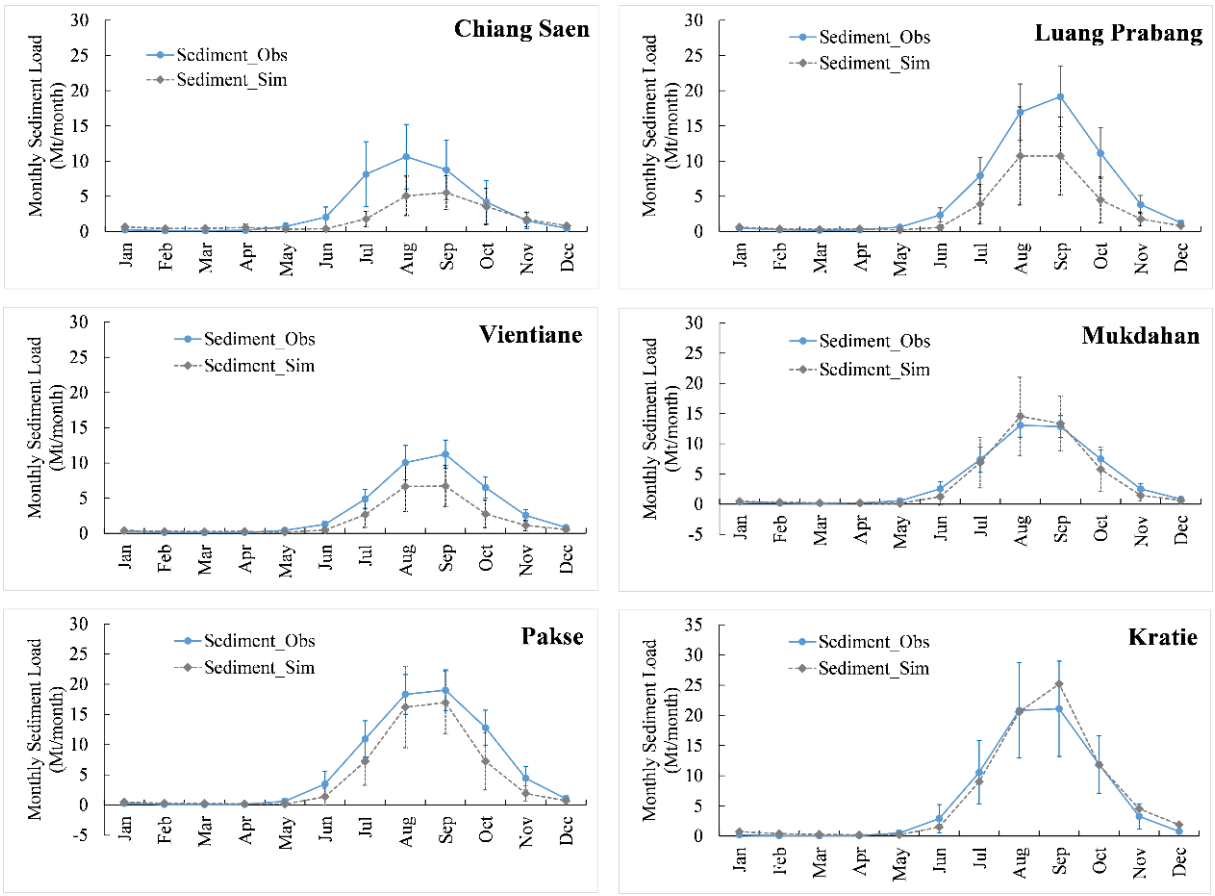

Figure 5-6: *Monthly average observed and simulated sediment load (with standard deviations) for Mekong River Basin from the six locations: Chiang Saen, Luang Prabang, Vientiane, Mukdahan, Pakse, Kratie.*

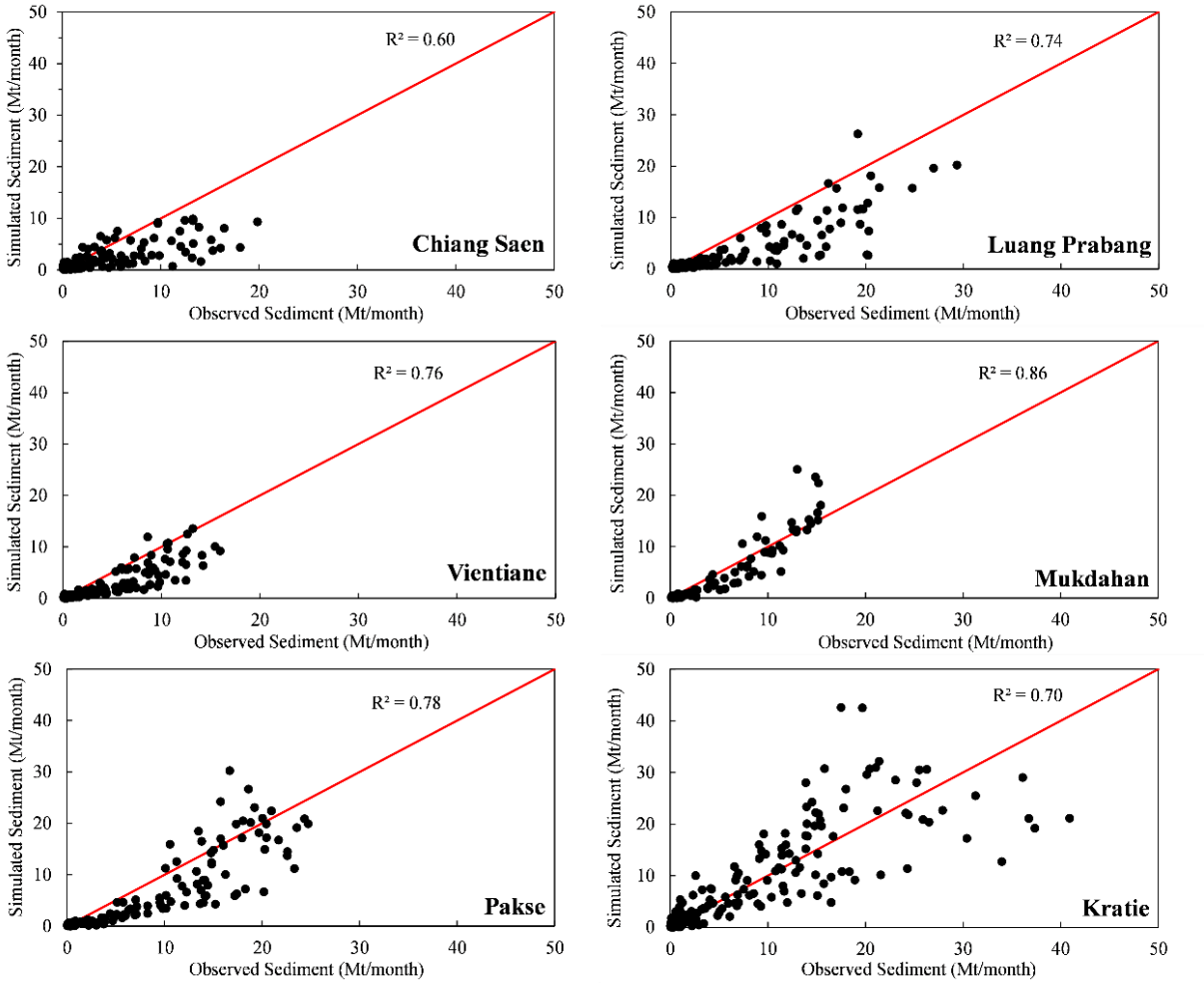

Figure 5-7: *Scatterplot of monthly observed and simulated sediment for six monitoring stations along the main river.*

Table 5-5: *Mean monthly sediment load calibration and validation of the SWAT model in Mekong River Basin.*

Name of station	Calibration			Validation		
	Period	Performance indicators		Period	Performance indicators	
		NSE	R^2		NSE	R^2
Chiang Saen	1997-2003	0.30	0.60	2004-2011	0.69	0.74
Luang Prabang	1998-2003	0.46	0.74	2004-2011	0.57	0.7
Vientiane	1995-2003	0.55	0.79	2004-2011	0.71	0.78
Mukdahan	2001-2003	0.82	0.89	2004-2011	0.66	0.82
Pakse	1995-2004	0.72	0.80	2005-2011	0.58	0.77
Kratie	1995-2004	0.77	0.80	2005-2016	0.30	0.86

3.3. Water balance and hydrological component in the Mekong River Basin

Water balance components on the Mekong Basin have been illustrated in **Figure 5-8**. The system in the Mekong Basin can be divided and can be identified in three major groups. The first upper group in the Upper Mekong River Basin (sub-basin #1 and #2) have low rainfall in the annual scale; however, snowmelt contributes to its streamflow during the dry season. The left bank tributaries group (sub-basin #3, #5, #7 and #8) drains the high-rainfall areas of Lao DPR, Central Highland of Vietnam and the Northeast of Cambodia. The right bank tributaries (mainly the Mun and Chi Rivers, the sub-basin #4 and #6) drain a large part of northeast Thailand [56].

In the Upper Basin (Lancang), the climate varies from tropical and subtropical monsoons in the south of Yunnan to temperate monsoons in the north as the elevation rises from a mean of 2,500 to 4,000 m above MSL in the most upstream part. The seasonal distribution of rainfall is similar to the Lower Basin; however, annual precipitation decreases towards the north (the most upstream of the basin) to as little as 400-600 mm. Snow at higher elevations is the major source of water during the dry season and spring flows (April, May) in the upper part of mainstream. The rainfall distribution can reach a double peak over the Lower Mekong Basin in Central of Laos, Central highland of Vietnam, and the Upper part of Cambodia (from Vientiane to Kratie) comparing to the Upper Mekong Basin. The highest precipitation (>2,000 mm/year) occurs in the left bank of the river in Lao DPR and the central highland of Vietnam.

The overall proportion of streamflow in the Mekong River in the study modelled by SWAT was 34% from surface runoff, 21% from lateral flow, 45%from the contribution of groundwater. The detail in each sub-basin is summarized in **Table 5-6**. The high average water yield was noticed at the sub-basin #5 in between Vientiane to Mukdahan following by sub-basin #7 from Pakse to Stung Streng, which is the highland area in Vietnam. The detail of water yield, which is contributed by surface runoff, lateral flow, and groundwater to the streamflow (total water yield) in the Mekong River at eight stations are detailed in **Table 5-7**. Comparing to Kratie, the upper Mekong Basin at China/Laos Border and Chiang Saen contribute average flows of 18% and 21%, respectively. At Luang Prabang and Vientiane, the flow contribution to the Mekong flow at Kratie was 30% and 34%. At the downstream of Vientiane, the station at Mukdahan and Pakse contributes a large part of the flow, with the average flow 65% and 79% of total flow at Kratie. At the same time, average flow at Stung Treng to Kratie was close to each other (1% difference of the total

flow at Kratie). Apart from the upstream flow, the large part of the average flow at Stung Treng comes from the 3S basin (Se San, Sekong, and Sre Pok), which is the largest tributary of the Mekong River and originates from the central highland of Vietnam.

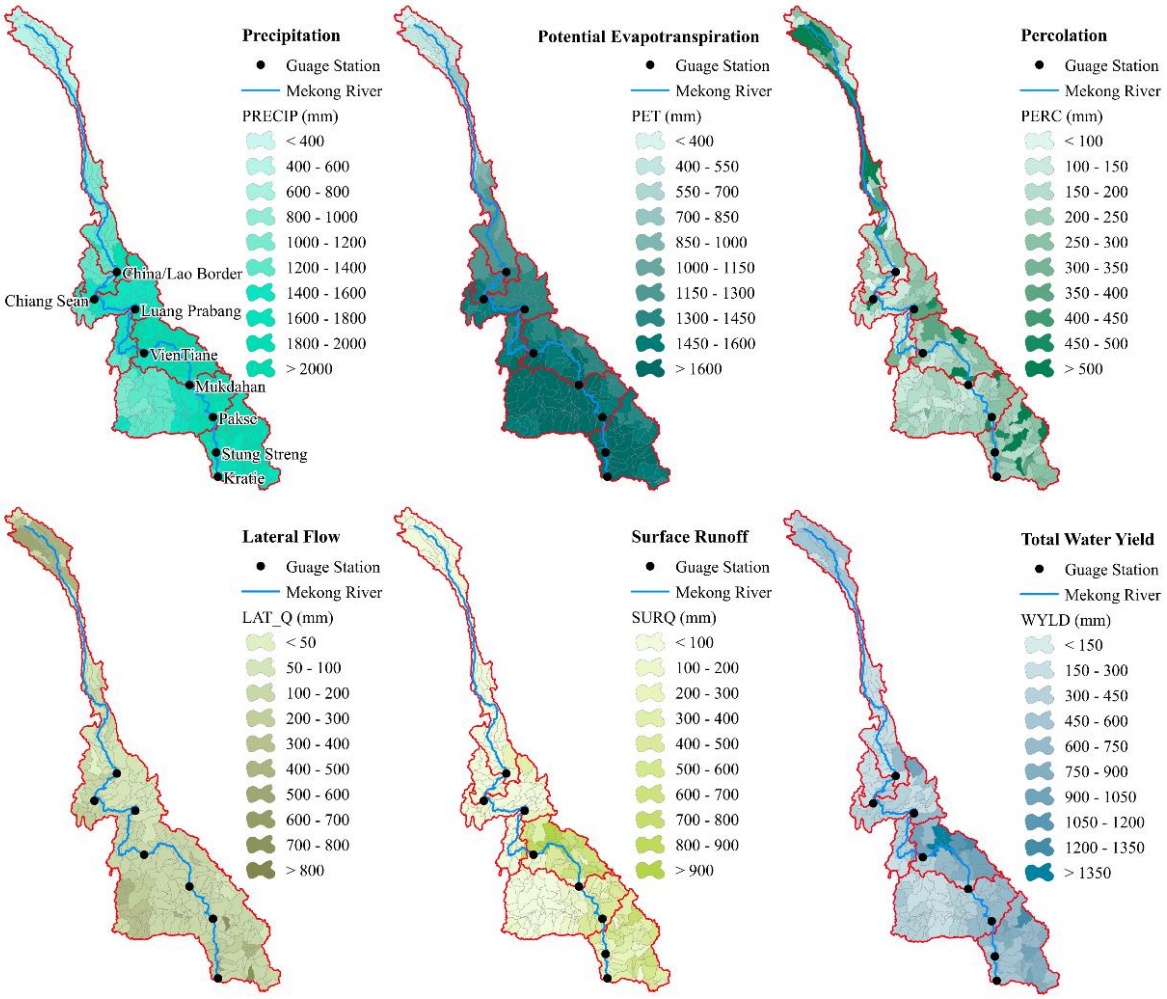

Figure 5-8: *Water balance components on the Mekong river basin and its sub-basin: Precipitation, Potential Evapotranspiration, Percolation, Lateral flow, Surface runoff, and water yield from 1985-2016.*

Table 5-6: *Water balance components in mm/year (Potential Evapotranspiration, Actual Evapotranspiration, Percolation, and Water Yield) of the Mekong river basin for each sub-basin from 1985-2016.*

Area	Gauge name	Precipitation		PET	ET	PERC	Total water yield
		Range	Average				
		mm per year					
1	Upstream to China/Laos Border	462-1805	954	890	604	229	325
2	China/Laos Border to Chiang Sean	1256-1632	1435	1404	1073	185	311

3	Chiang Sean to Luang Prabang	1380-2082	1559	1439	1121	166	385
4	Luang Prabang to Vientiane	1274-2281	1517	1527	1110	194	348
5	Vientiane to Mukdahan	1482-3189	2265	1549	1179	231	1024
6	Mukdahan to Pakse	1148-1930	1523	1650	1034	284	424
7	Pakse to Stung Streng	1676-2420	1925	1625	1116	296	736
8	Stung Streng to Kratie	1386-1744	1624	1751	1039	322	507

Note: PET: Potential Evapotranspiration, ET: Actual Evapotranspiration, PERC: Percolation

Table 5-7: *Contribution of surface runoff, lateral flow, and groundwater to the streamflow (total water yield) in mm/year in the Mekong River at eight stations from 1985-2016.*

Area	Gauge name	Surface runoff		Lateral flow		Ground water flow		Total water yield
		(mm/year)	%	(mm/year)	%	(mm/year)	%	(mm/year)
1	Upstream to China/Laos Border	16	5%	112	34%	197	61%	325
2	China/Laos Border to Chiang Sean	45	14%	139	45%	127	41%	311
3	Chiang Sean to Luang Prabang	99	26%	179	46%	107	28%	385
4	Luang Prabang to Vientiane	120	34%	100	29%	128	37%	348
5	Vientiane to Mukdahan	706	69%	156	15%	162	16%	1024
6	Mukdahan to Pakse	184	43%	33	8%	207	49%	424
7	Pakse to Stung Streng	216	29%	304	41%	216	29%	736
8	Stung Streng to Kratie	248	49%	24	5%	235	46%	507

3.4. Spatio-temporal sediment load and yield of Mekong River Basin

The variation of the annual water discharge, annual sediment load, and yield at Chiang Saen, Luang Prabang, Vientiane, Mukdahan, Pakse, and Kratie along the Lower Mekong River have been illustrated in **Figure 5-9** and **Table 5-8**. Key factors affecting the amount of sediment yield include vegetation cover, topography, soil, and climate. From **Table 5-8** which describe general characteristic and sediment load yields by major area, the highest sediment yield (1295 t/km^2/year) can be found in Chiang Saen to Luang Prabang in the northern part of Laos. This area is covered by mixed land use and high topography with steep slopes. In the upper Mekong part in China (where the river is called Lancang River), despite high topography and steep slope, the sediment load is lower than Chiang Saen to Luang Prabang due to covering by the forest type (evergreen and mixed forest). It is noticed that the Mekong Basin in Thailand (Mukdahan to Pakse), despite

the high agricultural activity, the sediment yield is low (78 t/km^2/year) since most of the area covers by gentle slope. In between Pakse and Kratie (including 3S, the largest tributary of Mekong), the average sediment yield was found 138 t/km^2/year; however, we found high yields at the upstream part of 3S basin (>500 t/km^2/year). Even though Tonle Sap and its basin were not included in this study; it is worthy of mentioning that the Tonle Sap Lake at flood stage receives substantial sediment in backwater flooding upstream from the Mekong River mainstem and its net deposition [25,27,57], thus zero sediment yield assumption was commonly mentioned in this apart. The delta is naturally a sediment sink, so it also has a zero-sediment yield [39].

Our result of sediment loads in various stations along the main river align with some previous studies that suggest sediment discharge to the South China Sea varies from 40 to 160 Mt/year such as [34], [26], [58], [59] and [60]. However, some studies found higher sediment loads, such as [61], [62], and [63]. Sediment load have been started to decrease continuously due to the fact of sediment trapping by hydropower dams was confirmed in most research [20,39,41,64,65]. The reduction of sediment loads in the Mekong could be aligned with the global context. e.g [1], [66], [67], and [12]. In the Mekong River Basin, one of the recent studies on the effects of rapid development dams on sediment transport was conducted by [64], which found that more than 50% of the total Mekong River sediment load would be trapped annually (between 1993 and 2003). Before 2003 and after 2009, average suspended loads reduced at Chiang Saen station from 60 to 10 Mt/year (83% reduction), at Pakse from 120 to 60 Mt/year (50% reduction), and at Kratie from 160 to 90 Mt/year (43 % reduction) [28]. The concern stems not only from dam development on Mekong mainstem but also on its main tributaries. For example, Wild and Loucks [68] found a substantial portion of the sediment reduction from the 3S basin, where there is a rich source of sediment. Beside the dam development in Mekong River Basin, climate change and land use change are also the crucial factors of sediment transport throughout the basin [69]. The instream sediment load and yield in the lower part of the Mekong River are likely influenced by the interaction between land use/land cover, rainfall-runoff, and anthropogenic activities within the basin [70]. Deforestation and agriculture expansion could change the landcover and alters basin erosion of the Mekong River [71]. Shrestha et al. [69] also indicate large unreliability of Mekong River's watershed in the direction and magnitude of variability of flow and sediment yields due to climate change. The variability of sediment can be from the accumulation of upstream and localized erosion agricultural activities [72].

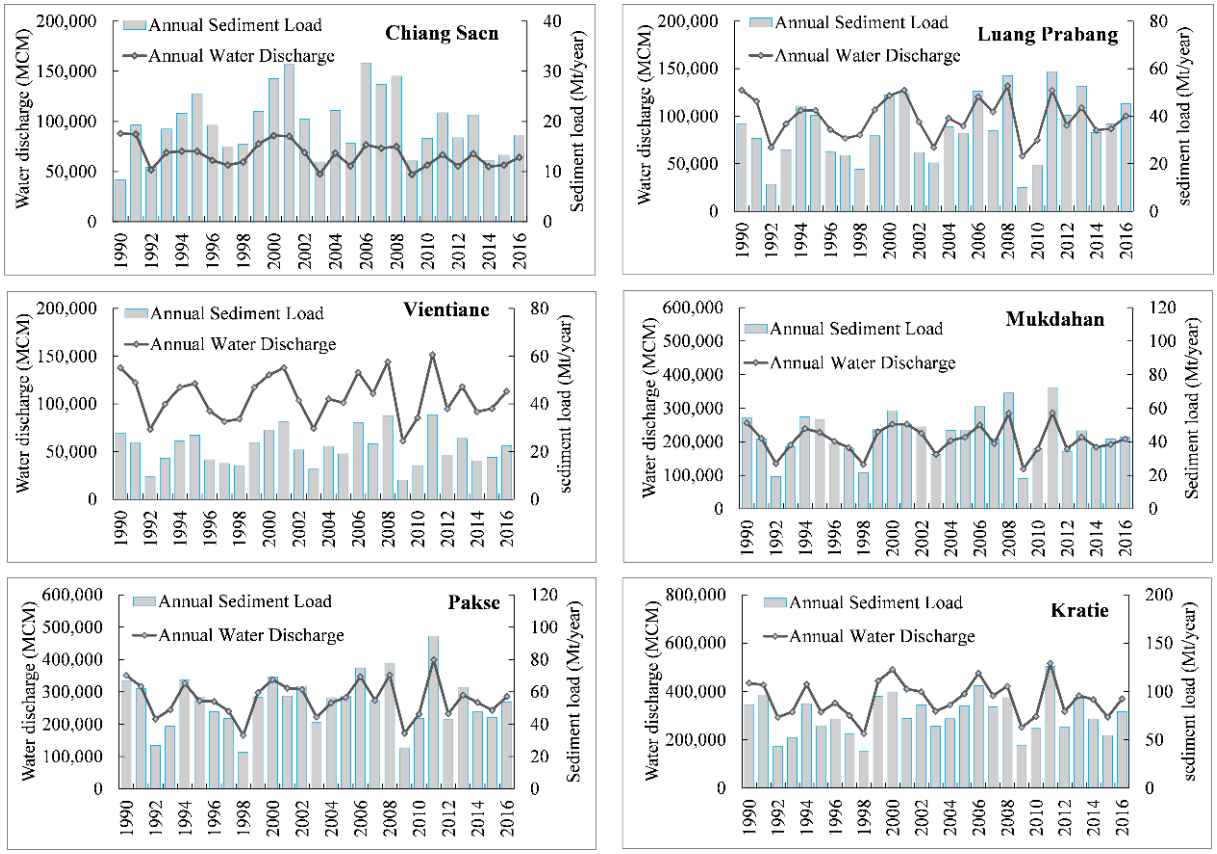

Figure 5-9: *Variations of the annual water discharge and annual sediment load from 1990-2016 along the Mekong River. Stations are Chiang Saen, Luang Prabang, Vientiane, Mukdahan, Pakse, and Kratie.*

Table 5-8: *Mekong River Sediment Yields by major sub-basins in the study from 1990-2016.*

Area	Description of sub-basin general characteristic	Average annual sediment yield (t/km^2/year)	Average annual sediment load in main Mekong River (Mt/year)
China/Laos Border to Chiang Saen	In upper Mekong part in China. Covered by the forest type (evergreen and mixed forest) and range grasses (more than 80% of the total area. High topography and steep slope.	340	20±7
Chiang Saen to Luang Prabang	The northern part of Laos. Mixed land use (forest and grasses more than 50% and agriculture type 25%). High topography and steep slope	1295	35±14
Luang Prabang to Vientiane	Mixed land use between grasses type (more than 50%) and agriculture (30%). Steep (40%) and medium slope (60%)	49	22±8
Vientiane to Mukdahan	In the central of Laos. Dominated by agriculture type (more than 80%) and grasses type (20%). Gentle slope (more than 50%) and medium slope (20%) and some steep hill at the north and far-right bank	218	44±14

Mukdahan to Pakse	The area cover is in Thailand. It is dominated by agriculture type (70%) and some grass type. Gentle slope (70%) and some medium slope.	78	54±17
Pakse to Kratie	In central highland of Vietnam and some part in Cambodia. Covered by forest type (evergreen forest, 60%) and some agricultural type. The gentle slope in Laos and Cambodia and some high slope in the far-right bank in Central of Vietnam.	138	75±21

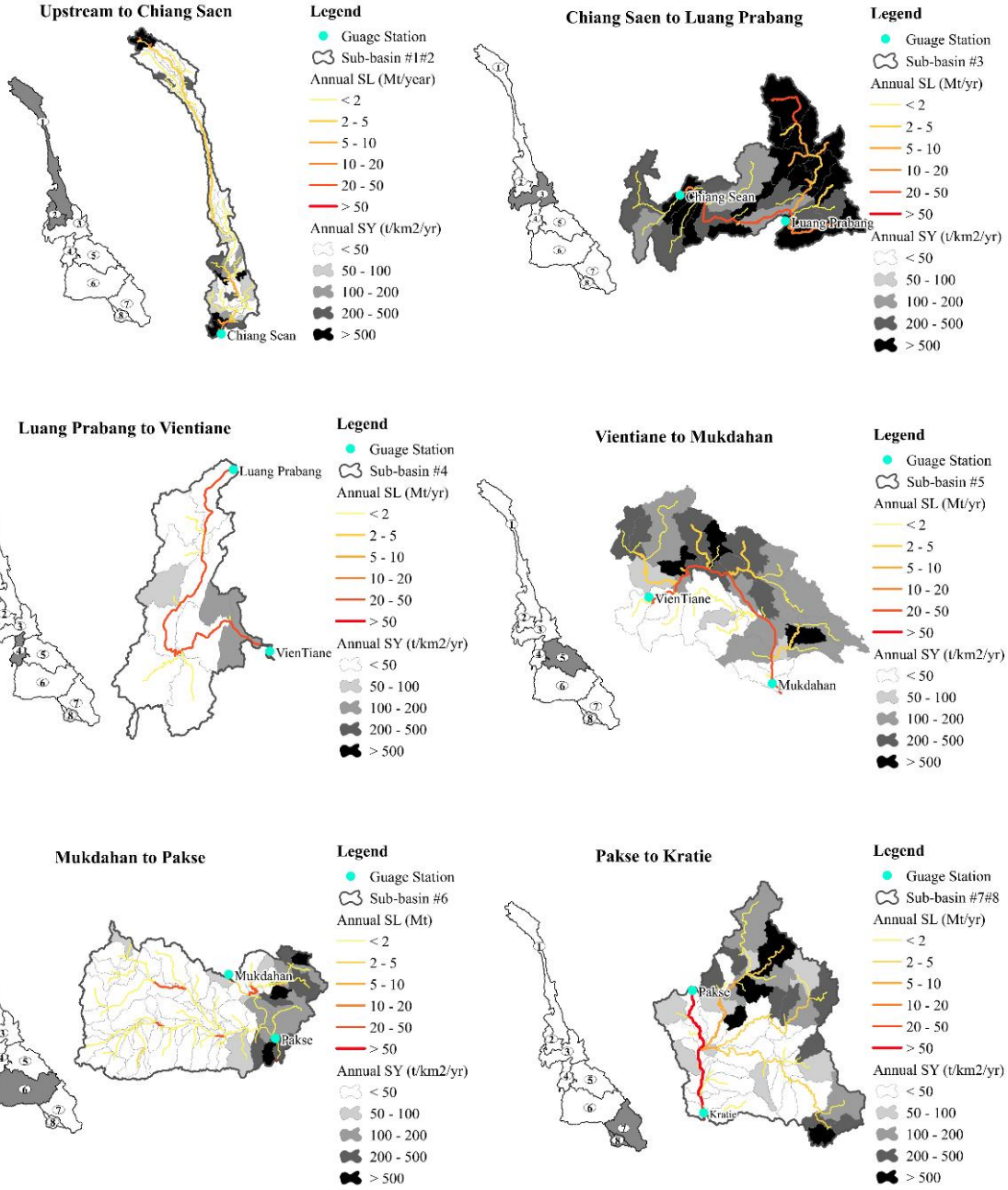

Figure 5-10: *Mean annual fluvial sediment load (SL, Mt/year) and annual sediment yield (SY, t/km^2/year) for the Mekong river major sub-basins from 1985 to 2016.*

The empirical relationship between sediment load and water discharge will be used for sediment load estimation along the Mekong River (**Figure 5-11**). The monthly sediment load correlated well to the monthly discharge (notably high values of R^2). The R^2 values of these correlations were generally over 0.90. According to the results of R^2 values suggested that these correlations were well-closely and are in a very good relationship between sediment load and water discharge in the Mekong Basin from Chiang Saen to Kratie.

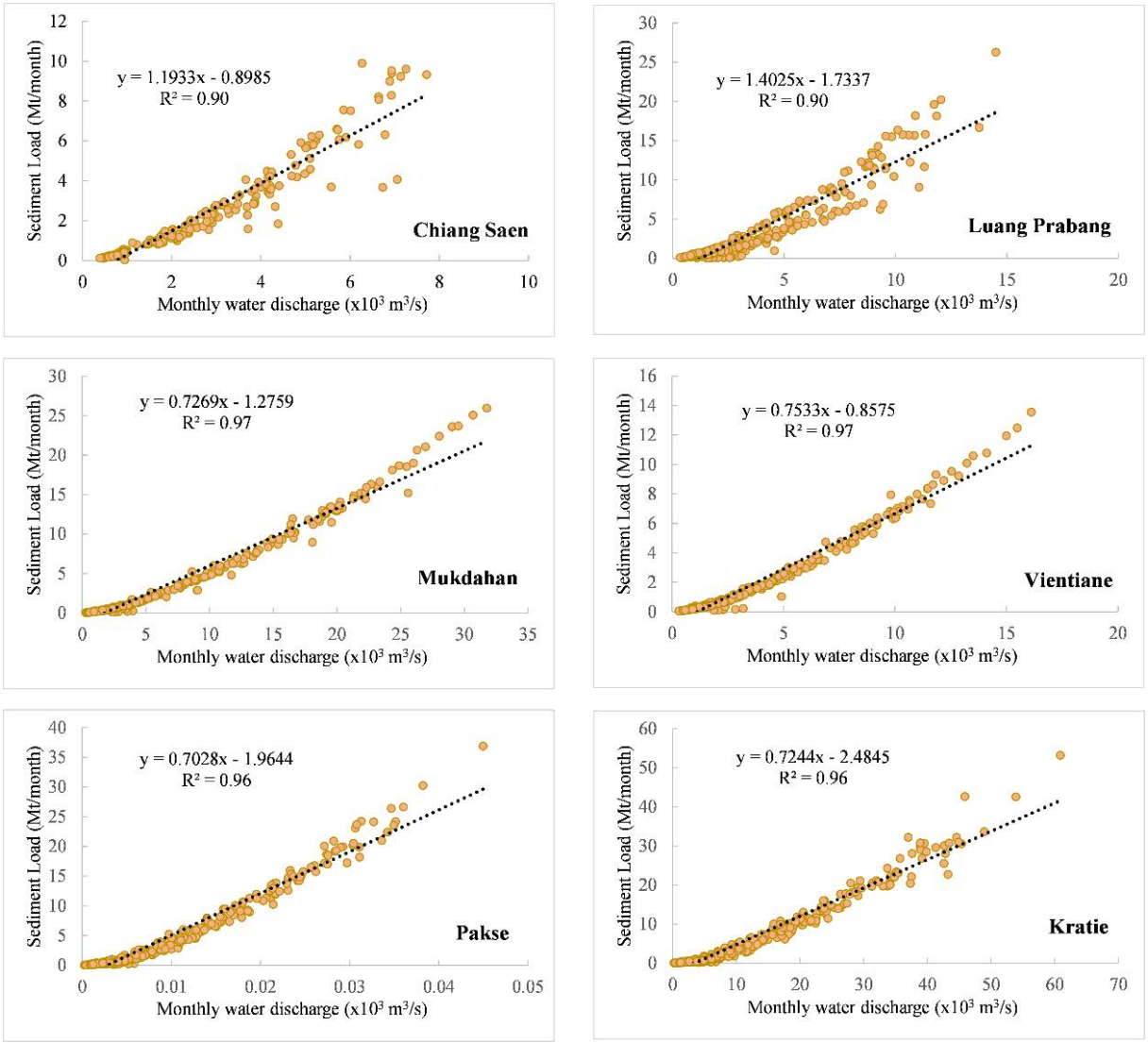

Figure 5-11: *Empirical relationship between monthly sediment load and monthly water discharge at six locations along the main river from 1985-2016.*

Figure 5-10 illustrated the overall spatial mapping of average sediment yields and mean annual sediment load for the Mekong River Basin from 1985 to 2016. To understand in detail sediment yield in the Mekong related to basin characteristic, the annual mean of the sediment yield in the Mekong River Basin for the simulation period 1990-2016 by divided into land use/land cover types, slope class, and area sub-basin class. The mean annual sediment of land use/land cover types, and its percentage over the basin ware divided into seven types as agricultural land generic, forest evergreen, range grasses, forest deciduous, pasture, forest mixed, and range brush (Figure 12). The highest and lower erosion sediment yield of the basin compared to other are range grasses and forest deciduous about 610 t/km^2/year and 28 t/km^2/year, respectively. For the erosion sediment yield of the pasture about 397 t/km^2/year, range brush 217 t/km^2/year, forest evergreen was found to be less sediment yield with approximately 193 t/km^2/year; for agricultural land generic was found even lower averagely 135 t/km^2/year, and the lowest forest cover erosion was forest mixed with 62 t/km^2/year.

The annual sediment yield classification related to slope class and its percentage over the basin was separated into five classes such as 0-1, 1-2, 2-5, 5-20, and higher than 20 described in **Figure 5-12**. The highest slope class covered area about 48% of the whole basin, was highly erosion sediment yield about 539 t/km^2/year, and the gentle slope classes (0-1% and 1-2%) were low erosion sediment yield approximately 90 t/km^2/year and 49 t/km^2/year, respectively. The steep slope classes (2-5% and 5-20%) were covered about 24% of the whole basin, which were erosion sediment yield about 137 t/km^2/year and 317 t/km^2/year, respectively.

The sediment yield of sub-basin area class and its percentage over the basin by divided into five classes (less than 1000 km^2, 1000-2000 km^2, 2000-4000 km^2, 4000-6000 km^2, and higher than 6000 km^2) were also presented and can be found in **Figure 5-12**. The most significant erosion sediment yield of the sub-basin area class is sub-basin area less than 1000 km^2 covered area only 3% of the whole Mekong River Basin about 376 t/km^2/year. The lowest erosion sediment yield of the sub-basin area class about 110 t/km^2/year in the sub-basin 4000-6000 was 110 t/km^2/year, which covered an area of about 20% of the whole Mekong River Basin. For the sub-basin area class 1000-2000 km^2, 2000-4000 km^2, and higher than 6000 km^2 were covered in a total area of about 50% of the whole Mekong River Basin, which was erosion sediment yield about 267 t/km^2/year, 372 t/km^2/year, and 352 t/km^2/year, respectively.

Unlike some other large alluvial rivers such as the Amazon, little sediment exchange occurs between channel and floodplain in the Lower Mekong River, except in downstream reaches below Kratie in the Cambodian lowlands and the Mekong Delta [22]. In this area of basin, Mekong river is essentially a conduit cut in rock that transfers sediment derived from the upper basin and tributaries draining nearby hillslopes and the sediment appears to be stored almost entirely within the channel [22]. The annual sediment yield of the Mekong River is comparable with sediment yields reported for other major rivers in Asia and elsewhere (**Figure 5-13**).

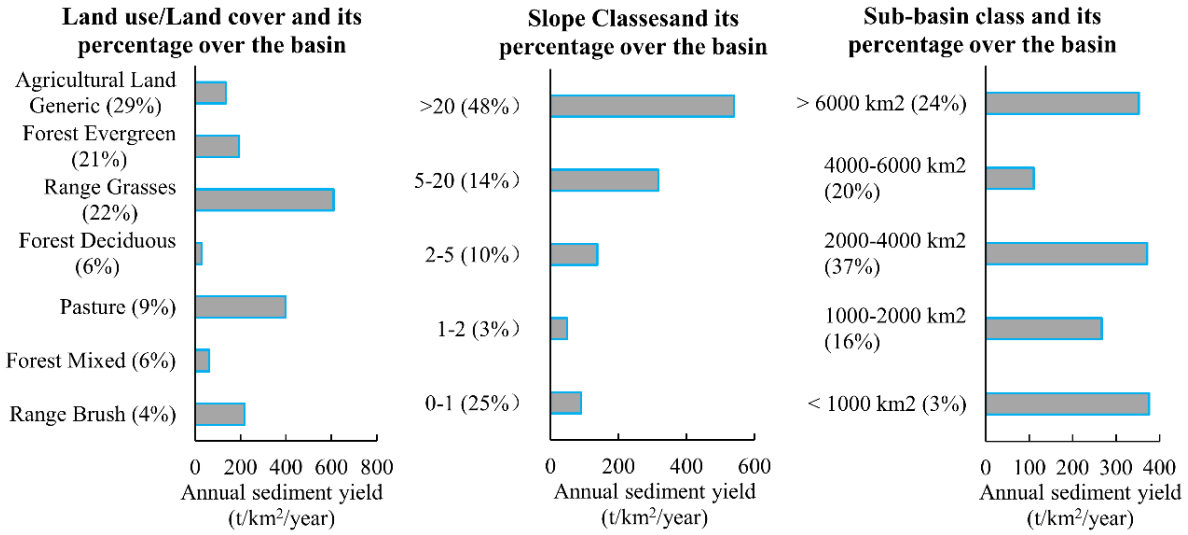

Figure 5-12: *Distribution of mean annual sediment yields (t/km^2/year) in the Mekong River Basin for the simulation period 1995-2016, divided by main land use types, slope classes and basin sizes.*

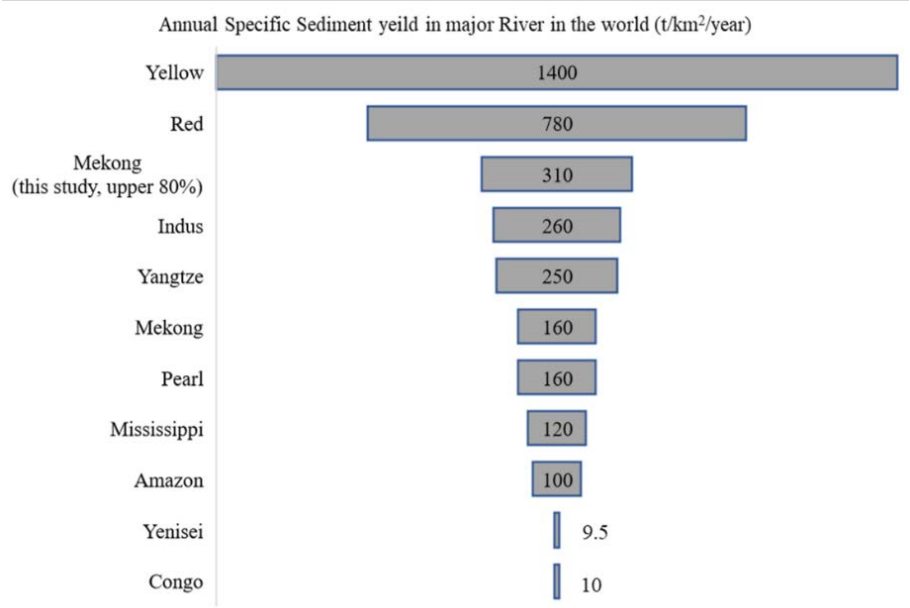

Note: The value from [23], [58], [73], [74], [75], [76]

Figure 5-13: *Annual mean of sediment yield of Mekong River with other major rivers in Asia and continents.*

4. Conclusions

The SWAT model was applied to assess the water balance components and sediment erosion yield in the Mekong River Basin. The model was calibrated and validated against eight hydrological stations and six sediment stations along the Mekong mainstream. The calibration and valuation results authenticated the model performance to be very good in monthly flow performance and acceptable in monthly sediment performance. In the overall proportion of streamflow in the Mekong River, groundwater played a key role and contributed to almost half of the streamflow. At the same time, surface runoff took part in 1/3 of streamflow. The high average water yield was noticed in between Vientiane to Mukdahan from Pakse to Stung Streng, which is in the highland area in Vietnam. The Upper Mekong Basin contributed 20% of the average flow and is especially important during the dry season due to snowmelt. Apart from the upstream flow, the large part of the average flow from the 3S basin (Se San, Sekong, and Sre Pok), which is the largest tributary of the Mekong River and originates from the central highland of Vietnam, contributed 20% of the flow. The annual average sediment yield for the Mekong River was 312 t/km²/year from upper 80% of the total MRB before entering the delta. The highest sediment yield (1,295 t/km^2/year) can be found in Chiang Saen to Luang Prabang in the northern part of Laos due

to covering by the mixed land use and high topography with steep slopes. The middle part of Mekong Basin, located in Thailand (Mukdahan to Pakse), despite the high agricultural activity, has a low sediment yield (78 t/km^2/year) since most of the area is covered by gentle slope. It is important to note that slope and land-use type in the Mekong could be the main factors related to sediment yield in the basin. The results of this study would be useful for understanding the derived sediment yield, and a spatial soil erosion map that can explicitly illustrate the identification and prioritization of the critical soil erosion-prone areas of Mekong River's sub-basins. This study also supplies a sediment loading map in the Mekong River Basin, which could help to limit storage capabilities, increases the risk for ageing infrastructure, and lead to proper management strategies of this region. The outcome of the study could also be the baseline information of sediment studies for the sustainable watershed management plan.

It is also important to note that the assessment of hydrology and sediment in the Mekong River Basin accomplished in our study was mainly based on a dataset with only monthly water sampling at some stations along the main river. Given the large size of the Mekong River Basin, refinement of the basin monitoring network is necessary to improve assessments and future modelling work. The sediment load and yield have been influenced by land-use change, which is likely to alter the upland erosion process and not to mention climate change. The future dam development of some major tributaries will continue to cause a change in sediment load dynamics through sediment trapping of water impoundment. The combined effect of climate change, agricultural, and hydropower development requires further study, as complex interactions could cause drastic changes of sediment as well as water quality like nutrients, which can affect downstream ecosystems, delta, and the South China Sea.

Author Contributions: T.S. conducted the modelling, analyzed the results and wrote the paper. C.O., S.S., and J.M.S.-P. supervised the research, advised on the methodologies, gave comments, improved the manuscript, and corrected the manuscript. I.I. assisted in modelling and data processing from the model. All authors have read and agreed to the published version of the manuscript.

Funding: This research received no external funding.

Acknowledgements: The authors also thank the Ministry of Water Resources and Meteorology (MOWRAM) of Cambodia for providing the data. Ty SOK would like to acknowledge Les

Bourses du Gouvernement Français (BGF) and Laboratoire Ecologie Fonctionnelle et Environnement for hosting during his Ph.D. study. Authors would like to thank Cody J. Stewart for English editing this paper.

Conflicts of Interest: The authors declare no conflict of interest.

References:

1. Vörösmarty, C.J.; Meybeck, M.; Fekete, B.M.; Sharma, K.; Green, P.; Syvitski, J.P. Anthropogenic sediment retention: Major global impact from registered river impoundments. *Glob. Planet. Chang.* **2003**, *39*, 169–190, doi:10.1016/s0921-8181(03)00023-7.
2. Syvitski, J.P.; Vörösmarty, C.J.; Kettner, A.J.; Green, P. Impact of humans on the flux of terrestrial sediment to the global coastal ocean. *Science* **2005**, *308*, 376–380, doi:10.1126/science.1109454.
3. Walling, D. Human impact on land–ocean sediment transfer by the world's rivers. *Geomorphology* **2006**, *79*, 192–216, doi:10.1016/j.geomorph.2006.06.019.
4. Walling, D.E.; Fang, D. Recent trends in the suspended sediment loads of the world's rivers. *Glob. Planet. Chang.* **2003**, *39*, 111–126, doi:10.1016/s0921-8181(03)00020-1.
5. Khafagy, A.; Naffaa, M.; Fanos, A.; Dean, R. Nearshore Coastal Changes Along the Nile Delta Shores. In *Coastal Engineering 1992*; American Society of Civil Engineers (ASCE): Reston, VA, USA, 1993; pp. 3260–3272.
6. Fanos, A.M. The impact of human activities on the erosion and accretion of the nile delta coast. *J. Coast. Res.* **1995**, *11*, 821–833.
7. Carriquiry, J.; Sánchez, A. Sedimentation in the colorado river delta and upper gulf of california after nearly a century of discharge loss. *Mar. Geol.* **1999**, *158*, 125–145, doi:10.1016/s0025-3227(98)00189-3.
8. Mikhailova, M.V. Transformation of the ebro river delta under the impact of intense human-induced reduction of sediment runoff. *Water Resour.* **2003**, *30*, 370–378, doi:10.1023/a:1024963911893.

9. Yang, S.L.; Li, M.; Dai, S.B.; Liu, Z.; Zhang, J.; Ding, P.X. Drastic decrease in sediment supply from the yangtze river and its challenge to coastal wetland management. *Geophys. Res. Lett.* **2006**, *33*, doi:10.1029/2005gl025507.
10. Wang, H.; Yang, Z.; Saito, Y.; Liu, J.P.; Sun, X.; Wang, Y. Stepwise decreases of the Huanghe (yellow river) sediment load (1950–2005): Impacts of climate change and human activities. *Glob. Planet. Chang.* **2007**, *57*, 331–354, doi:10.1016/j.gloplacha.2007.01.003.
11. Moran, E.F.; Lopez, M.C.; Moore, N.; Müller, N.; Hyndman, D.W. Sustainable hydropower in the 21st century. *Proc. Natl. Acad. Sci.USA* **2018**, *115*, 11891–11898, doi:10.1073/pnas.1809426115.
12. Kondolf, G.M.; Schmitt, R.J.; Carling, P.; Darby, S.; Arias, M.; Bizzi, S.; Castelletti, A.; Cochrane, T.A.; Gibson, S.; Kummu, M.; et al. Changing sediment budget of the Mekong: Cumulative threats and management strategies for a large river basin. *Sci. Total. Environ.* **2018**, *625*, 114–134, doi:10.1016/j.scitotenv.2017.11.361.
13. Peng, J.; Chen, S.; Dong, P. Temporal variation of sediment load in the yellow river basin, China, and its impacts on the lower reaches and the river delta. *Catena* **2010**, *83*, 135–147, doi:10.1016/j.catena.2010.08.006.
14. Galipeau, B.A.; Ingman, M.; Tilt, B. Dam-induced displacement and agricultural livelihoods in China's Mekong Basin. *Hum. Ecol.* **2013**, *41*, 437–446, doi:10.1007/s10745-013-9575-y.
15. Rex, W.; Foster, V.; Lyon, K.; Bucknall, J.; Liden, R. *Supporting hydropower: An overview of the world bank group's engagement*.; The World Bank: Washington, WA, USA, 2014.
16. Adamson, P.T.; Rutherfurd, I.D.; Peel, M.C.; Conlan, I.A. The Hydrology of the Mekong River. In *The Mekong Biophysical Environment of an International River Basin*; Campbell, I.C., Ed.; Elsevier Inc.: Amsterdam, The Netherlands, 2009; pp. 53–76.
17. Hecht, J.S.; Lacombe, G.; Arias, M.E.; Dang, T.D.; Piman, T. Hydropower dams of the Mekong River basin: A review of their hydrological impacts. *J. Hydrol.* **2019**, *568*, 285–300, doi:10.1016/j.jhydrol.2018.10.045.
18. Mekong River Commission, MRC. Assessment of Basin-Wide Development Scenarios—Main Report. Mekong River Commission Vientiane, MRC: Phnom Penh, Cambodia, 2011.
19. Schmitt, R.; Rubin, Z.; Kondolf, G. Losing ground-scenarios of land loss as consequence of shifting sediment budgets in the Mekong Delta. *Geomorphology* **2017**, *294*, 58–69, doi:10.1016/j.geomorph.2017.04.029.

20. Fu, K.; He, D.; Chen, W.; Ye, C.; Li, Y. Impacts of dam constructions on the annual distribution of sediment in Lancang-Mekong River Basin. *Acta Geogr. Sin.-Chin. Ed*. **2007**, *62*, 14.
21. Milliman, J.D.; Syvitski, J.P. Geomorphic/tectonic control of sediment discharge to the ocean: The importance of small mountainous rivers. *J. Geol.* **1992**, *100*, 525–544, doi:10.1086/629606.
22. Gupta, A.; Liew, S. The Mekong from satellite imagery: A quick look at a large river. *Geomorphology* **2007**, *85*, 259–274, doi:10.1016/j.geomorph.2006.03.036.
23. Walling, D.E. The changing sediment load of the Mekong River. *AMBIO: J. Hum. Environ.* **2008**, *37*, 150–157, doi:10.1579/0044-7447(2008)37[150:tcslot]2.0.co;2.
24. Stephens, J.; Allison, M.; di Leonardo, D.; Weathers, H., III; Ogston, A.; McLachlan, R.; Xing, F.; Meselhe, E. Sand dynamics in the Mekong River channel and export to the coastal ocean. *Cont. Shelf Res*. **2017**, *147*, 38–50.
25. Kummu, M.; Penny, D.; Sarkkula, J.; Koponen, J. Sediment: curse or blessing for Tonle Sap Lake? *Ambio: A J. Hum. Environ.* **2008**, *37*, 158–163.
26. Lu, X.; Kummu, M.; Oeurng, C. Reappraisal of sediment dynamics in the lower Mekong River, Cambodia. *Earth Surf. Process. Landforms* **2014**, *39*, 1855–1865, doi:10.1002/esp.3573.
27. Sok, T.; Oeurng, C.; Kaing, V.; Sauvage, S.; Kondol, G.M.; Perez, J.M. Assessment of sediment load variabilities in the tonle sap and lower Mekong Rivers, Cambodia. Manuscript submitted for Publication. *Authorea* **2020**, doi:10.22541/au.157901475.50635048
28. Piman, T.; Shrestha, M. *Case Study on Sediment in the Mekong River Basin: Current State and Future Trends*; Stockholm Environment Institute: Stockholm, Sweden, 2017.
29. Bouraoui, F.; Benabdallah, S.; Jrad, A.; Bidoglio, G. Application of the SWAT model on the Medjerda river basin (Tunisia). *Phys. Chem. Earth Parts A/B/C* **2005**, *30*, 497–507, doi:10.1016/j.pce.2005.07.004.
30. Arnold, J.G.; Srinivasan, R.; Muttiah, R.S.; Williams, J.R. Large area hydrologic modeling and assessment part I: Model development. *JAWRA J. Am. Water Resour. Assoc.* **1998**, *34*, 73–89, doi:10.1111/j.1752-1688.1998.tb05961.x.

31. Arnold, J.G.; Moriasi, D.N.; Gassman, P.W.; Abbaspour, K.C.; White, M.J.; Srinivasan, R.; Santhi, C.; Harmel, R.D.; van Griensven, A.; van Liew, M.W.; et al. SWAT: Model use, calibration, and validation. *Trans. ASABE* **2012**, *55*, 1491–1508, doi:10.13031/2013.42256.
32. Bieger, K.; Arnold, J.G.; Rathjens, H.; White, M.J.; Bosch, D.D.; Allen, P.M.; Volk, M.; Srinivasan, R. Introduction to SWAT+, A completely restructured version of the soil and water assessment tool. *JAWRA J. Am. Water Resour. Assoc.* **2016**, *53*, 115–130, doi:10.1111/1752-1688.12482.
33. Tan, M.L.; Gassman, P.W.; Raghavan, S.; Arnold, J.G.; Yang, X. A Review of SWAT studies in southeast Asia: Applications, challenges and future directions. *Water* **2019**, *11*, 914, doi:10.3390/w11050914.
34. Al-Soufi, R. Soil erosion and sediment transport in the Mekong basin. In Proceedings of the 2nd Asia Pacific Association of Hydrology and Water Resources Conference, Suntec International Convention and Exhibition Center, Singapore, 5–8 July 2004; pp. 47–56.
35. Shrestha, B.; Cochrane, T.A.; Caruso, B.S.; Arias, M.E.; Piman, T. Uncertainty in flow and sediment projections due to future climate scenarios for the 3S Rivers in the Mekong Basin. *J. Hydrol.* **2016**, *540*, 1088–1104, doi:10.1016/j.jhydrol.2016.07.019.
36. Mohammed, I.N.; Bolten, J.; Srinivasan, R.; Lakshmi, V. Satellite observations and modeling to understand the lower Mekong River Basin streamflow variability. *J. Hydrol.* **2018**, *564*, 559–573, doi:10.1016/j.jhydrol.2018.07.030.
37. Trung, L.D.; Duc, N.A.; Nguyen, L.T.; Thai, T.H.; Khan, A.; Rautenstrauch, K.; Schmidt, C. Assessing cumulative impacts of the proposed lower Mekong Basin hydropower cascade on the Mekong River floodplains and Delta-Overview of integrated modeling methods and results. *J. Hydrol.* **2020**, *581*, 122511, doi:10.1016/j.jhydrol.2018.01.029.
38. Ogston, A.; Allison, M.; McLachlan, R.; Nowacki, D.; Stephens, J.D. How tidal processes impact the transfer of sediment from source to sink: mekong river collaborative studies. *Oceanography* **2017**, *30*, 22–33, doi:10.5670/oceanog.2017.311.
39. Kondolf, G.M.; Rubin, Z.K.; Minear, J.T. Dams on the Mekong: Cumulative sediment starvation. *Water Resour. Res.* **2014**, *50*, 5158–5169, doi:10.1002/2013wr014651.
40. Yoshida, Y.; Lee, H.S.; Trung, B.H.; Tran, H.-D.; Lall, M.K.; Kakar, K.; Xuan, T.D. Impacts of mainstream hydropower dams on fisheries and agriculture in lower Mekong Basin. *Sustainability* **2020**, *12*, 2408, doi:10.3390/su12062408.

41. Kummu, M.; Varis, O. Sediment-related impacts due to upstream reservoir trapping, the lower Mekong River. *Geomorphology* **2007**, *85*, 275–293, doi:10.1016/j.geomorph.2006.03.024.
42. Wang, J.-J.; Lu, X.X.; Kummu, M. Sediment load estimates and variations in the lower Mekong River. *River Res. Appl.* **2011**, *27*, 33–46, doi:10.1002/rra.1337.
43. Kongmeng, L.; Larsen, H. *Lower Mekong Regional Water Quality Monitoring Report*; Mekong River Commission: Vientiane, Lao, 2016.
44. Runkel, R.L.; Crawford, C.G.; Cohn, T.A. Load Estimator (LOADEST): A FORTRAN Program for Estimating Constituent Loads in Streams and Rivers; USGS Colorado Water Science Center: Herndon, VA, USA, 2004.
45. Koehnken, L. IKMP Discharge and Sediment Monitoring Program Review, Recommendations and Data Analysis. In *Part 2: Data Analysis and Preliminary Results*; MRC: Phnom Penh, Cambodia, 2012.
46. Hung, N.N.; Delgado, J.M.; Tri, V.K.; Hung, L.M.; Merz, B.; Bárdossy, A.; Apel, H. Floodplain hydrology of the Mekong Delta, Vietnam. *Hydrol. Process.* **2011**, *26*, 674–686, doi:10.1002/hyp.8183.
47. Yamazaki, D.; Ikeshima, D.; Tawatari, R.; Yamaguchi, T.; O'Loughlin, F.; Neal, J.C.; Sampson, C.C.; Kanae, S.; Bates, P.B. A high-accuracy map of global terrain elevations. *Geophys. Res. Lett.* **2017**, *44*, 5844–5853, doi:10.1002/2017gl072874.
48. Lu, X.; Li, S.; Kummu, M.; Padawangi, R.; Wang, J. Observed changes in the water flow at Chiang Saen in the lower Mekong: Impacts of Chinese dams? *Quat. Int.* **2014**, *336*, 145–157.
49. Nash, J.E.; Sutcliffe, J.V. River Flow forecasting through conceptual models-Part I: A discussion of principles. *J. Hydrol.* **1970**, *10*, 282–290.
50. Benaman, J.; Shoemaker, C.A.; Haith, D.A. Calibration and validation of soil and water assessment tool on an agricultural watershed in Upstate New York. *J. Hydrol. Eng.* **2005**, *10*, 363–374, doi:10.1061/(asce)1084-0699(2005)10:5(363).
51. Gupta, H.V.; Kling, H.; Yilmaz, K.K.; Martinez, G.F. Decomposition of the mean squared error and NSE performance criteria: Implications for improving hydrological modelling. *J. Hydrol.* **2009**, *377*, 80–91, doi:10.1016/j.jhydrol.2009.08.003.

52. Moriasi, D.N.; Arnold, J.G.; Van Liew, M.W.; Bingner, R.L.; Harmel, R.D.; Veith, T.L. Model evaluation guidelines for systematic quantification of accuracy in watershed simulations. *Trans. ASABE* **2007**, *50*, 885–900, doi:10.13031/2013.23153.
53. Hydrologic and water quality models: Performance measures and evaluation criteria. *Trans. ASABE* **2015**, *58*, 1763–1785, doi:10.13031/trans.58.10715.
54. Shrestha, D.L.; Robertson, D.E.; Wang, Q.J.; Pagano, T.C.; Hapuarachchi, H.A.P. Evaluation of numerical weather prediction model precipitation forecasts for short-term streamflow forecasting purpose. *Hydrol. Earth Syst. Sci.* **2013**, *17*, 1913–1931, doi:10.5194/hess-17-1913-2013.
55. Lauri, H.; de Moel, H.; Ward, P.J.; Räsänen, T.A.; Keskinen, M.; Kummu, M. Future changes in Mekong River hydrology: Impact of climate change and reservoir operation on discharge. *Hydrol. Earth Syst. Sci. Discuss.* **2012**, *9*, 6569–6614, doi:10.5194/hessd-9-6569-2012.
56. M.R.C. Overview of the Hydrology of the Mekong Basin. In *Mekong River Commission, Vientiane*; M.R.C: Vientiane, Lao, 2005.
57. Tsukawaki, S. Sedimentation rates in the northern part of Lake Tonle Sap, Cambodia, during the last 6,000 years. *Sam. Res. AMS* **1997**, *8*, 125–133.
58. Milliman, J.D.; Meade, R.H. World-wide delivery of River Sediment to the oceans. *J. Geol.* **1983**, *91*, 1–21, doi:10.1086/628741.
59. Nowacki, D.J.; Ogston, A.S.; Nittrouer, C.A.; Fricke, A.T.; Van, P.D.T. Sediment dynamics in the lower M ekong River: Transition from tidal river to estuary. *J. Geophys. Res. Oceans* **2015**, *120*, 6363–6383, doi:10.1002/2015jc010754.
60. Jordan, C.; Tiede, J.; Lojek, O.; Visscher, J.; Apel, H.; Nguyen, H.Q.; Quang, C.N.X.; Schlurmann, T. Sand mining in the Mekong Delta revisited-current scales of local sediment deficits. *Sci. Rep.* **2019**, *9*, 1–14, doi:10.1038/s41598-019-53804-z.
61. Manh, N.V.; Dung, N.V.; Hung, N.N.; Merz, B.; Apel, H. Large-scale suspended sediment transport and sediment deposition in the Mekong Delta. *Hydrol. Earth Syst. Sci.* **2014**, *18*, 3033–3053, doi:10.5194/hess-18-3033-2014.
62. Ta, T.; Nguyen, V.; Tateishi, M.; Kobayashi, I.; Tanabe, S.; Saito, Y. Holocene delta evolution and sediment discharge of the Mekong River, southern Vietnam. *Quat. Sci. Rev.* **2002**, *21*, 1807–1819, doi:10.1016/s0277-3791(02)00007-0.

63. Liu, C.; He, Y.; Walling, E.D.; Wang, J. Changes in the sediment load of the Lancang-Mekong River over the period 1965–2003. *Sci. China Technol. Sci.* **2013**, *56*, 843–852, doi:10.1007/s11431-013-5162-0.
64. Kummu, M.; Lu, X.X.; Wang, J.J.; Varis, O. Basin-wide sediment trapping efficiency of emerging reservoirs along the Mekong. *Geomorphology* **2010**, *119*, 181–197, doi:10.1016/j.geomorph.2010.03.018.
65. Fu, K.; He, D.; Lu, X.X. Sedimentation in the Manwan reservoir in the Upper Mekong and its downstream impacts. *Quat. Int.* **2008**, *186*, 91–99, doi:10.1016/j.quaint.2007.09.041.
66. Liu, C.; Wang, Z.; Sui, J. Analysis on variation of seagoing water and sediment load in main rivers of China. *J. Hydraul. Eng.* **2007**, *38*, 1444–1452.
67. Gupta, H.; Kao, S.-J.; Dai, M. The role of mega dams in reducing sediment fluxes: A case study of large Asian rivers. *J. Hydrol.* **2012**, *464*, 447–458, doi:10.1016/j.jhydrol.2012.07.038.
68. Wild, T.B.; Loucks, D.P. Managing flow, sediment, and hydropower regimes in the Sre Pok, Se San, and Se Kong Rivers of the Mekong basin. *Water Resour. Res.* **2014**, *50*, 5141–5157, doi:10.1002/2014wr015457.
69. Shrestha, B.; Babel, M.S.; Maskey, S.; van Griensven, A.; Uhlenbrook, S.; Green, A.; Akkharath, I. Impact of climate change on sediment yield in the Mekong River basin: A case study of the Nam Ou basin, Lao PDR. *Hydrol. Earth Syst. Sci.* **2013**, *17*, 1–20, doi:10.5194/hess-17-1-2013.
70. Ly, K.; Metternicht, G.; Marshall, L. Linking changes in land cover and land use of the lower Mekong Basin to instream nitrate and total suspended solids variations. *Sustainability* **2020**, *12*, 2992, doi:10.3390/su12072992.
71. Kaura, M.; Arias, M.E.; Benjamin, J.A.; Oeurng, C.; Cochrane, T.A. Benefits of forest conservation on riverine sediment and hydropower in the Tonle Sap Basin, Cambodia. *Ecosyst. Serv.* **2019**, *39*, 101003, doi:10.1016/j.ecoser.2019.101003.
72. Chea, R.; Grenouillet, G.; Lek, S. Evidence of water quality degradation in lower Mekong Basin revealed by self-organizing map. *PLoS ONE* **2016**, *11*, e0145527, doi:10.1371/journal.pone.0145527.
73. Fabre, C.; Sauvage, S.; Tananaev, N.; Noël, G.E.; Teisserenc, R.; Probst, J.-L.; Sánchez-Pérez, J.M. Assessment of sediment and organic carbon exports into the Arctic ocean: The

case of the Yenisei River basin. *Water Res.* **2019**, *158*, 118–135, doi:10.1016/j.watres.2019.04.018.

74. Wittmann, H.; von Blanckenburg, F.; Maurice, L.; Guyot, J.-L.; Filizola, N.; Kubik, P.W. Sediment production and delivery in the Amazon River basin quantified by in situ-produced cosmogenic nuclides and recent river loads. *GSA Bull.* **2010**, *123*, 934–950, doi:10.1130/b30317.1.
75. Meade, R.H. River-Sediment Inputs to Major Deltas. In *Coastal Systems and Continental Margins*; Springer: Berlin/Heidelberg, Germany, 1996; pp. 63–85.

    Wei, X.; Sauvage, S.; Le, T.P.Q.; Ouillon, S.; Orange, D.; Herrman, M.; Sánchez-Pérez, J.-M. A drastic decrease of suspended sediment fluxes in the Red River related to climate variability and dam constructions. *Catena* **2020**, *197*, doi:10.1016/j.catena

CHAPTER VI

Evaluation of Nitrate Transport and Yield in the Mekong River Basin

This chapter was submitted in the Ecological Engineering Journal, and it is under review process. The work of this chapter is aligned with the previous chapter. This chapter aims to evaluate the nitrate flux and determine the spatial variability of nitrate yields in the Mekong River Basin through modelling approaches.

Sok, T., Oeurng, C., Ich. I. Kaing, V., Sauvage, S., Lu, X.X. and Sánchez-Pérez, J.M. Nutrient Transport and Exchange between Mekong River and Tonle Sap Lake in Cambodia. Echohydrology. To be submitted in Echohydrology.

6. Chapter VI. Evaluation of Nitrate Transport and Yield in the Mekong River Basin

6.1. Scientific Context and Objectives

Global nutrient inputs from major rivers into the oceans have tripled during the second half of the last century. Changes in nutrient loading are a particular concern in tropical regions undergoing rapid development, and the Mekong basin is one of the major rivers of concern. Some large-scale studies on nutrients in the Mekong Basin have been conducted. However, a more detailed study on nitrate flux from major tributaries and spatial nutrient sources for the Mekong Basin is still limited and deserves regional scientific knowledge and basin management. Otherwise, the sediment, nutrient transport, and responses throughout the basin are critical and urgently needed for perspective plans for basin development and management for the present and future. Long-term and spatial watershed monitoring data are rare due to the expense involved; however, long-term simulations are possible using water quality models. Understanding and modelling the nutrient flux dynamic and its source in the Mekong River are crucially for addressing the problem mentioned above and the aforementioned gaps. This study presented the nitrate flux modelling and determined the spatial variability of nitrate yields in the Mekong River Basin.

6.2. Materials and Methods

The SWAT model has been set up to cover the total area of 748,000 km^2 from the most upstream (80%) of the total Mekong River Basin. The SWAT application of this study can be split into eight zones. The model was set up with the following major sub-basins: (1) from most upstream to China/Laos Border, (2) China/Laos Border to Chiang Saen, (3) Chiang Saen to Luang Prabang, (4) Luang Prabang to Vientiane, (5) Vientiane to Mukdahan, (6) Mukdahan to Pakse, (7) Pakse to Stung Treng and (8) Stung Treng to Kratie. The hydrology model was calibrated and validated using eight locations, and the sediment model was calibrated and validated using six locations, while nitrate flux was calibrated and validated with 5 stations. The study also included Nitrate Net Balance (NNB) and nitrate Net Balance Rate (NNBR) for main rivers and majors reaches of the Mekong Rivers.

6.3. Results and Discussions

River flow, sediment and nitrate flux showed large differences from year to year, a strong seasonality, and clear variability patterns in both nitrate flux and yield. The average annual nitrate

yield presented 49±96 kg/km^2/year in the upper part of the basin, 245±257 kg/km^2/year in the middle, 473±526 kg/km^2/year in the intensive agricultural area (gentle slope area in the lower part) and 181±276 kg/km^2/year in a highland area in the lower part of Mekong River Basin, respectively, which is comparable with other forested catchments, but much lower than agriculture dominated catchments in the tropics. The Mekong River's annual average nitrate yield was 202 kg/km^2/year with 361.8±83.5×10^3 t of annual nitrate flux for 80% of the Mekong River basin before entering the delta. Nitrate Production reaches covered 19% of total reach numbers while Nitrate Removal reaches covered 61% of total reach numbers of the Mekong Basin. Net Nitrate Balance rate (NNBR) shows the negative value for most reaches (91% of Mekong) with a higher rate for smaller reaches, while major reaches and main rivers show the low rate of NNBR. The removal rates of nitrate are higher during the dry season with median values of -0.05 m^{-2} than during the rainy season, with median values of -0.04 m^{-2}.

6.4. Conclusion and Perspectives

The annual average nitrate yield for the Mekong River Basin was estimated at approximately 202 kg/km^2/year for the upper 80% of the total MRB before entering the delta. The Mekong land-use type could be the main factor determining nitrate yield in the basin. As a distributed and physical model, SWAT model has considered many processes in the watershed such as topography, soil, meteorology and land use/cover, and can effectively simulate the catchment scale nitrate transport and evaluate the changing trend, which provides a basic model for further simulations in a long-time scale. The removal rates of nitrate are higher during the dry season with median values of -0.05 m^{-2} than during the rainy season, with the median value of -0.04 m^{-2}. This study could also serve as baseline information of nitrate studies for the sustainable watershed management plan. Finding a relationship between these variables, river hydro-morphological characteristics, and land management could be a good way to help stakeholders in water management decisions and boost awareness and involvement of people for sustainable management of water resources.

The establish model could include the Tonle Sap Lake region located in the lower part of the Mekong to evaluate its roles to the Mekong river parts and its delta.

6.5. Full paper: Sok, T., Oeurng, C., Ich. I. Kaing, V., Sauvage, S., and Sánchez-Pérez, J.M. Evaluation of Nitrate Transport and Yield in the Mekong River Basin using SWAT Model. Echohydrology. To be submitted.

Evaluation of Nitrate Transport and Yield in the Mekong River Basin using SWAT Model

Ty SOK[1,2,*], Chantha OEURNG[1,*], Ilan ICH[1], Vinhteang KAING[1], Sabine SAUVAGE[2], José Miguel SANCHEZ PEREZ[2]

[1]*Faculty of Hydrology and Water Resources Engineering, Institute of Technology of Cambodia, Russian Federation Blvd., P.O.BOX 86, Phnom Penh Cambodia.*

[2]*Laboratoire Ecologie Fonctionnelle et Environnement, UMR 5245 CNRS/UPS/INPT ENSAT, Avenue de l'Agrobiopole, BP 32607, Auzeville Tolosane, 31326 CASTANET TOLOSAN, France*

**Corresponding author: sokty@itc.edu.kh, chantha@itc.edu.kh*

Abstract

One of the world's great rivers in Asia, the Mekong River, has significant biodiversity and productivity in the region and crucially required understanding the behaviour of its nutrient dynamic and sources. However, long-term spatial watershed monitoring data related to nutrients are rare due to the expense and complexities. This study evaluated the spatial and temporal variability in nitrate flux and yield of the Mekong River basin. The SWAT model performance for monthly nitrate flux was assessed from 1985-2016 and provided good performance to simulate the Mekong basin nitrate output. Nitrate flux showed large differences from year to year, a strong seasonality, and clear variability patterns in both nitrate flux and yield. The average annual nitrate yield presented 49±96 kg/km^2/year (±standard deviation) in the upper part of the basin, 245±257 kg/km^2/year in the middle, 473±526 kg/km^2/year in the lower part of the basin and 181±276 kg/km^2/year in a highland area in the Lower Mekong River Basin. The Mekong River annual average nitrate yield was 202 kg/km^2/year with 361.8±83.5×10^3 t of annual nitrate flux from the upper 80% of the Mekong River basin before entering the delta. Nitrate Production reaches covered 19% of total reach numbers, while Nitrate Removal reaches covered 61% of total reach numbers of the Mekong Basin. Most reaches (91% of Mekong) indicated nitrate removal. The

higher rate that occurred, the more minor reaches, while major reaches and main rivers show the low rate of nitrate removal. The removal rates of nitrate were higher during the dry season (median values of -0.05 m^{-2}) than during the rainy season (with median values of -0.04 m^{-2}). This study establishes that SWAT is a useful model for temporally and spatially nitrate flux simulation and yield of the Mekong River basin for long-term, which now can be used for further study related to a global context such as climate change.

Keywords: SWAT; hydrology; nitrate yield; Mekong River

1. Introduction

2. Materials and Methods

2.1. Study Area

The Mekong River is the 12th longest river globally, with a length of 4,800 km, a basin area of 795,000 km^2, ranked 21st, and an average annual runoff of 475,000 m^3, ranked 8th in the world. The basin area is transboundary share includes China 21%, Myanmar 3%, Lao PDR 25%, Thailand 23%, Cambodia 20%, and Vietnam 8%. The Lower Mekong River Basin mainly covers the four downstream riparian countries, i.e., Lao PDR, Thailand, Cambodia, and Vietnam, with a total basin area of about 620,000 km^2 (Figure 6-1). In Cambodia, the Mekong River connects with Tonle Sap Lake (TSL) (the largest permanent freshwater lake in Southeast Asia) via Tonle Sap River at Chaktomuk confluence at Phnom Penh. The Great Lake and Tonle Sap and the lake area vary from 3,000 km^2 in the dry season to 15,000 km^2 in the wet season. The Mekong River's reverse flow to the lake causes hydraulic and ecological processes to be quite complicated.

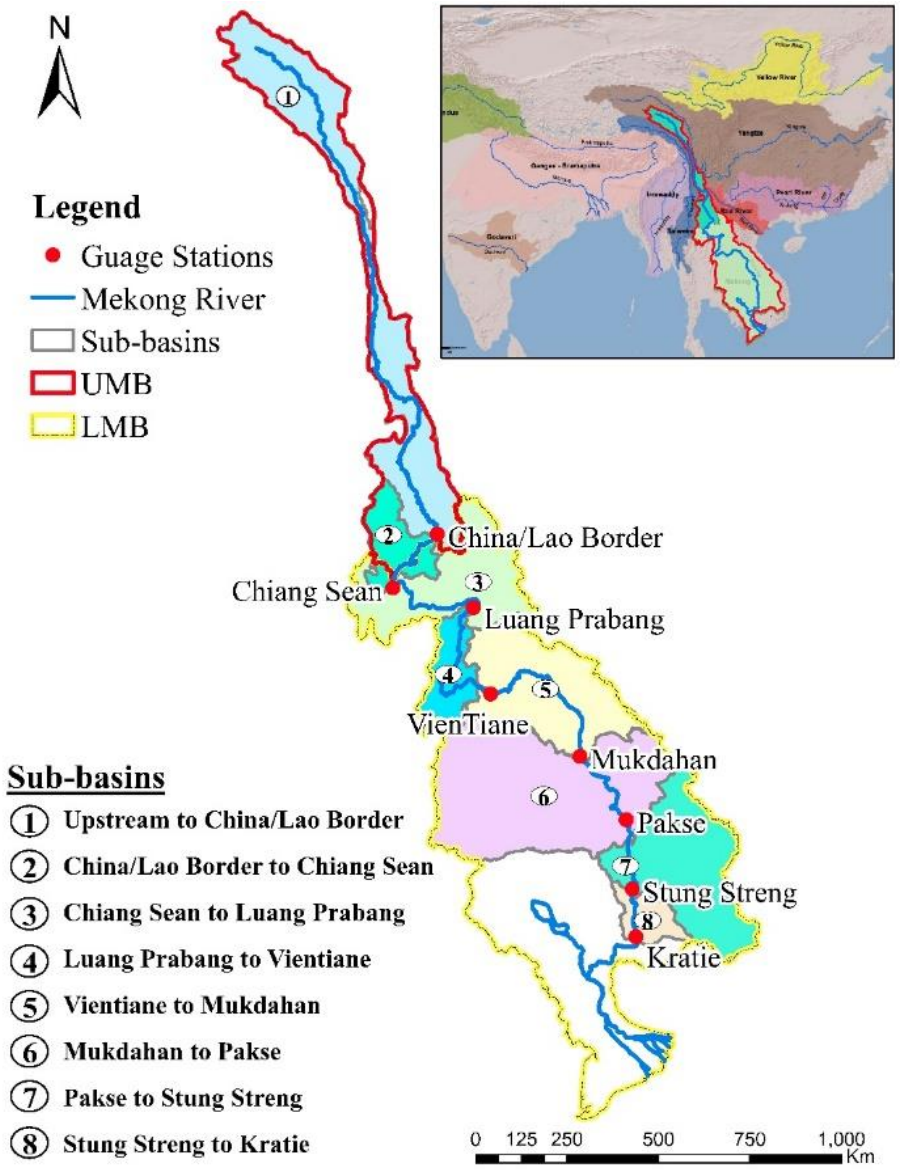

Figure 6-1: *Spatial Maps of the Mekong River Basin, including the Upper and the Lower Mekong Basin sharing of the basin area includes the Southern part of China and major sub-basin identifications based on the gauge stations.*

2.2. Sediment and Nitrate Data Used in SWAT Modeling

Eight discharge gauge stations along the main Mekong River were used in this study (**Table 6-1**). Nitrate (NO_3) data was obtained from the Water Quality Monitoring Network (WQMN) of the Mekong River Commission (MRC). This dataset has been widely used for flux estimations in Mekong River Basin studies, e.g., (Kummu et al., 2008a; Kummu and Varis, 2007; Wang et al., 2011). Total suspended sediment and nitrate concentrations were obtained from the water quality sampling conducted monthly. The variability of NO_3 differs from suspended sediments in that the

concentration levels do not vary significantly daily within a month in large rivers (Li and Bush, 2015a). Nitrate fluxes were calculated using the LOAD ESTimator (LOADEST) program (Runkel et al., 2004). In the study, no investigation will be made for the consistency of the nitrate data. Information on nitrate record used in this study is summarized in **Table 6-1**.

Table 6-1: *Nitrate data used in this study. Data from MRC.*

Name of station	Basin Coverage		Nitrate record used
	(km^2)	(%) of total basin	
Luang Prabang	288,380	31%	1995-2011
Vientiane	323,027	34%	1995-2011
Mukdahan	429,210	46%	2001-2011
Pakse	621,404	66%	1995-2011
Kratie	747,958	80%	1995-2016

2.3. SWAT Model Set-Up and Data Inputs for the Mekong River Basin

The SWAT model has been set up to cover a total area of about 748,000 km^2 from the most upstream (80%) of the total Mekong River basin (**Figure 6-1**). The SWAT application of this study in the Mekong Basin can be divided into eight zones based on the stream flow record used, as seen in Figure 1 as the availability of recorded streamflow and sediment used in this study for SWAT set-up. The set-up model was subjected to be studied as separate major sub-basins as follows: (1) from Most Upstream to Chinese Border, (2) Chinese Border to Chiang Saen, (3) Chiang Saen to Luang Prabang, (4) Luang Prabang to Vientiane, (5) Vientiane to Mukdahan, (6) Mukdahan to Pakse, (7) Pakse to Stung Treng and (8) Stung Treng to Kratie. The model set up was referred to Sok et al. (2020).

The streamflow and sediment load calibration were done manually. The nitrate model parameters were fitted through a semi-auto calibration procedure for the six locations using SWAT-CUP, a sequential uncertainty fitting algorithm (SUFI-2) (Abbaspour, 2013). This method was more reliable in comparison to observed data and literature review information for water and sediments. **Table 6-2** shows the fitted values of parameters used to calibrate nitrate flux calibration and validation.

The model performance was evaluated by comparing the simulations with the nitrate flux using Nash-Sutcliffe efficiency (NSE) (Nash and Sutcliffe, 1970) and Coefficient of determination (R^2). A calibrated model could be judged satisfactory if NSE and R^2 are higher than 0.35 for monthly scale nitrate simulation for mean behaviour, while higher than 0.65 is considered good performance (Benaman et al., 2005; Gupta et al., 2009; Moriasi et al., 2007; Moriasi et al., 2015).

Table 6-2: *Calibrated values of SWAT parameters for nitrate.*

Parameter	Name	Input File	Literature range	Calibrated value
Nitrate:				
ERORGN	Organic N enrichment ratio	.hru	1-5	3.9
RSDCO	Residue decomposition coefficient	.bsn	0.03-0.06	0.058
SOL_NO_3	Initial NO_3 concentration in the soil layer [mg/kg]	.chm	0-100	23.1
CMN	Rate factor for humus mineralization of active organic nitrogen	.bsn	0.0001-0.002	0.0018
SHALLST_N	Concentration of nitrate in groundwater contribution to streamflow from subbasin (mg N/l)	.gw	0-500	454.5
AI1	Fraction of algal biomass that is nitrogen	.wwq	-0.5-0.5	-0.317
BC2_BSN	Rate constant for biological oxidation NO_2 to NO_3 (1/day)	.bsn	0.3-1.5	0.618
CH_ONCO	Organic nitrogen concentration in the channel (ppm)	.rte	0-30	25.83
SOL_ORGN	Initial organic N concentration in the soil layer [mg/kg]	.chm	10-30	28.78
NPERCO	Nitrogen percolation coefficient	.bsn	-0.5-0.5	-0.467
LAT_ORGN	Organic N in the baseflow (mg/l)	.gw	0-50	1.95

2.4. Nitrate Net Balance (NNB) and Nitrate Net Balance Rate (NNBR)

Nitrate net balance is the difference between input and output of a reach, the instream nitrate evolution at the scale of the reach. *NNB* is calculated with the reach scale by dividing the in-out nitrate flux difference by the wetted area. If the value of the *NNB* is negative, nitrate is removed from the surface water, which indicates *Nitrate Removal (NR).* NR describes the amount of nitrate that is retained or withdrawn from the river system either by denitrification, aquatic plant assimilation or sediment retention. If the NNB is positive, it indicates that nitrate inputs are higher than sinks, meaning that *Nitrate Production (NP)* occurs. NNBR is a weighting of *NNB* by nitrate flux that enters the reach. This indicator removes the discharge effect that has a significant impact on seasonal analysis and compares the NR capacity of each reach.

The indicator of *NNB* and *NNBR* is defined as Cakir et al. (2020):

$$NNB = \frac{\left[NO_{3\ Flux}OUT\right] - \left[NO_{3\ Flux}IN\right]}{\text{Reach wetted area}} \quad (1)$$

$$NNBR = \frac{NNB}{\left[NO_{3\ Flux}IN\right]} \quad (2)$$

Where $NO_{3\ Flux}$OUT is the Nitrate transported with water into reach (kg/month), $NO_{3\ Flux}$IN is Nitrate transported with water out of reach (kg/month), Reach wetted area is wet cross-section area (m^2), NNB indicator is in $kg.m^{-2}.day^{-1}$ and NNBR is removal rate in m^{-2}.

Nitrate Net Balance (NNB) and nitrate Net Balance Rate (NNBR) is adapted from Cakir et al. (2020). The indicator of *NNB* and *NNBR* is defined as:

$$NNB = \frac{\left[NO_{3\ Flux}OUT\right] - \left[NO_{3\ Flux}IN\right]}{\text{Reach wetted area}} \quad (1)$$

$$NNBR = \frac{NNB}{\left[NO_{3\ Flux}IN\right]} \quad (2)$$

Where $NO_{3\ Flux}$OUT is the Nitrate transported with water into reach (kg/month), $NO_{3\ Flux}$IN is Nitrate transported with water out of reach (kg/month), Reach wetted area is wet cross-section area (m^2), NNB indicator is in $kg.m^{-2}.day^{-1}$ and NNBR is removal rate in m^{-2}.

3. Results and Discussion

3.1. Nitrate Calibration and Validation for SWAT Model

The monthly streamflow simulation statistical performance suggested that these SWAT models were well-calibrated/validated and are in a very good range (NSE > 0.80, and R^2 > 0.75 in the lower part of the basin and NSE>0.7, 0.65<R^2<0.75 for two most upper stations) (Sok et al., 2020). The result of the monthly streamflow performance of the SWAT model shows it has adequate capability to process sediment calibration and nitrate modelling process. The statistical performance of monthly sediment flux simulation suggested that these SWAT models were well-calibrated/validated and are in a good range. The NSE values were over 0.5, and R^2 values were over 0.5 for most of the stations and both calibration and validation period (Sok et al. (2020). The statistical performance of nitrate flux simulation during both calibration and validation is summarized in **Table 6-3**. Calibration and validation of nitrate flux for monthly estimates were

carried out at five monitoring stations and provided the adequately estimated monthly variations in nitrate flux (**Figure 6-2**).

Table 6-3: *Streamflow, sediment and nitrate flux calibration and validation at the monthly scale of SWAT model in the Mekong River basin.*

Stations	Nitrate flux Calibration			Nitrate flux Validation		
	Period	NSE	R^2	Period	NSE	R^2
Luang Prabang	1995-2004	0.72	0.77	2005-2011	0.31	0.57
Vientiane	1995-2004	0.71	0.73	2005-2011	0.6	0.71
Mukdahan	2001-2006	0.59	0.66	2007-2011	0.54	0.69
Pakse	1995-2005	0.2	0.58	2006-2011	0.2	0.56
Kratie	1995-2005	0.66	0.71	2006-2016	0.52	0.67

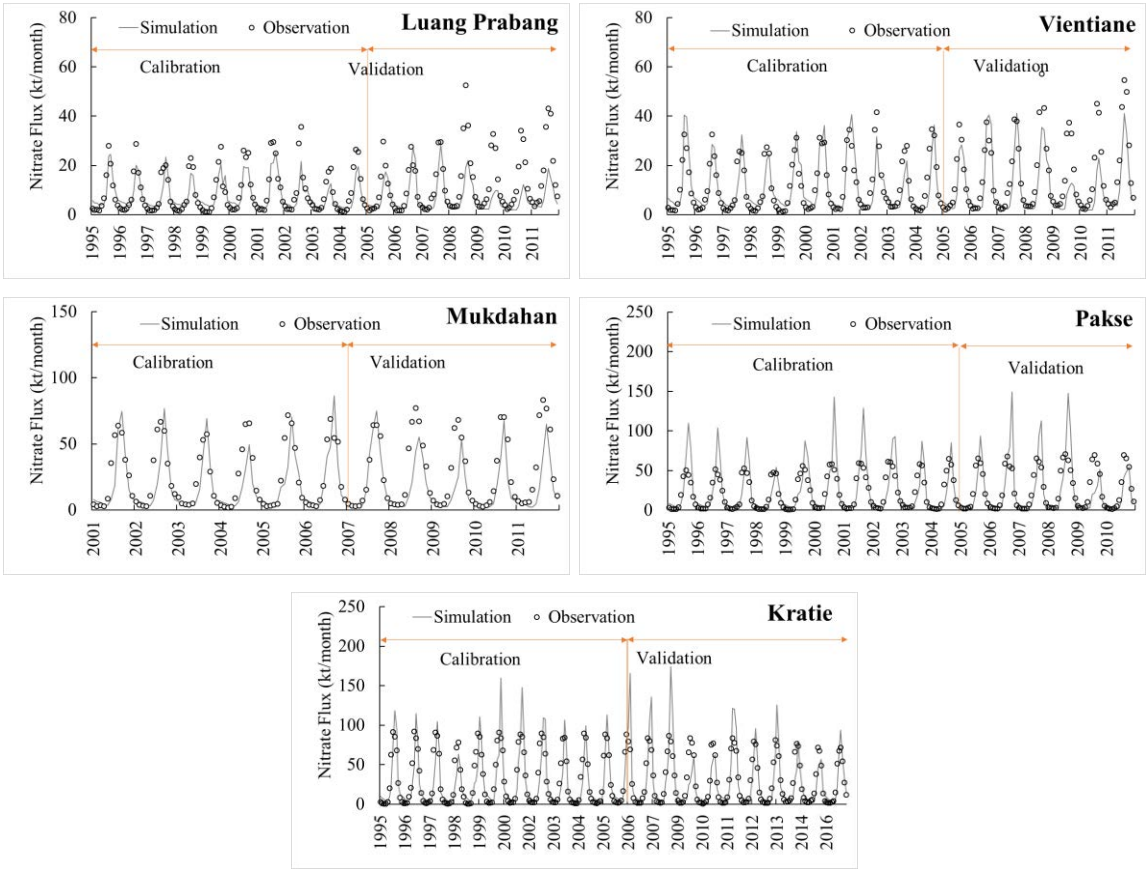

Figure 6-2: *Observed and simulated monthly nitrate flux from 1985 to 2016 for Mekong River Basin during calibration and validation at Luang Prabang, Vientiane, Mukdahan, Pakse and Kratie.*

3.2. Spatio-Temporal Variability of Nitrate Flux Transport in the Mekong River Basin

The Mekong River monthly nitrate flux for five main stations along the main Mekong River, where multiple years of continued nitrate sampling had taken place, distinguished a strong seasonality and clear variability patterns (**Table 6-4**). Monthly flux during the rainy season months of July, August, September and October at Kratie were 31.8 (SD ± 11.9) $\times 10^3$ t/month, 63.6 (SD ± 24.1) $\times 10^3$ t/month, 104.1 (SD ± 32.9) $\times 10^3$ t/month, and 71.3 (SD ± 28.2) $\times 10^3$ t/month, respectively. In contrast, both magnitude and variability are low during the dry season months of January, February, March and April. The simulation of nitrate flux (1985–2016) at Chiang Saen, Luang Prabang, Vientiane, Mukdahan, Pakse and Kratie showed a large difference in inter-annual nitrate fluxes, assuming no change in land use and land cover through time (**Figure 6-3**). The rainy season flux accounted for 70-80% of the total annual flux, while the dry season delivered 20-30% of total annual fluxes. Even though the spatial variability of riverine nitrate fluxes at different reaches in the Mekong river basins follow the magnitudes of flow, the spatial variability of nitrate indicates a more complex relationship as a function of HRU characteristics (**Figure 6-3**).

Table 6-4: *Mean monthly and annual average of nitrate flux along the main river of Mekong.*

Month	Luang Prabang	Vientiane	Mukdahan	Pakse	Kratie
	Monthly nitrate flux with Standard Deviation ($\times 10^3$ t)				
January	5.2±1.9	6.3±2.3	7.7±2.7	8.9±3.6	11.4±3.8
February	4.3±1.5	5±1.9	6±2.2	6.7±2.9	8.5±3.1
March	4.3±1.6	4.7±1.9	5.4±2.3	5.9±2.9	7.2±3.2
April	3.9±2.2	4.1±2.4	4.4±2.8	4.6±3.4	5.2±3.7
May	3.9±1.9	4±2.2	4.5±2.6	4.9±3.4	5.7±4.0
June	4.5±2.1	5.5±3.0	9.3±5.1	11.3±6.5	13.1±7.5
July	9.7±5.3	14.5±7.6	22.6±9.6	27.5±10.9	31.8±11.9
August	16.9±6.0	27.6±9.6	45.4±16.7	54.6±21.1	63.6±24.1
September	19±6.1	31.1±8.4	62.9±17.3	89.4±29.4	104.1±32.9
October	14.4±5.6	20.8±7.5	35.4±11.4	60.9±25.4	71.3±28.2
November	8.7±3.9	11.4±5.3	15.6±6.4	20.6±7.3	25.1±7.8
December	5.6±2.0	7.1±2.4	9.1±2.7	11±3.3	14.4±3.6
Annual	100.8±32.1	142.6±40.2	228.9±56.6	309.1±75.9	361.8±83.5

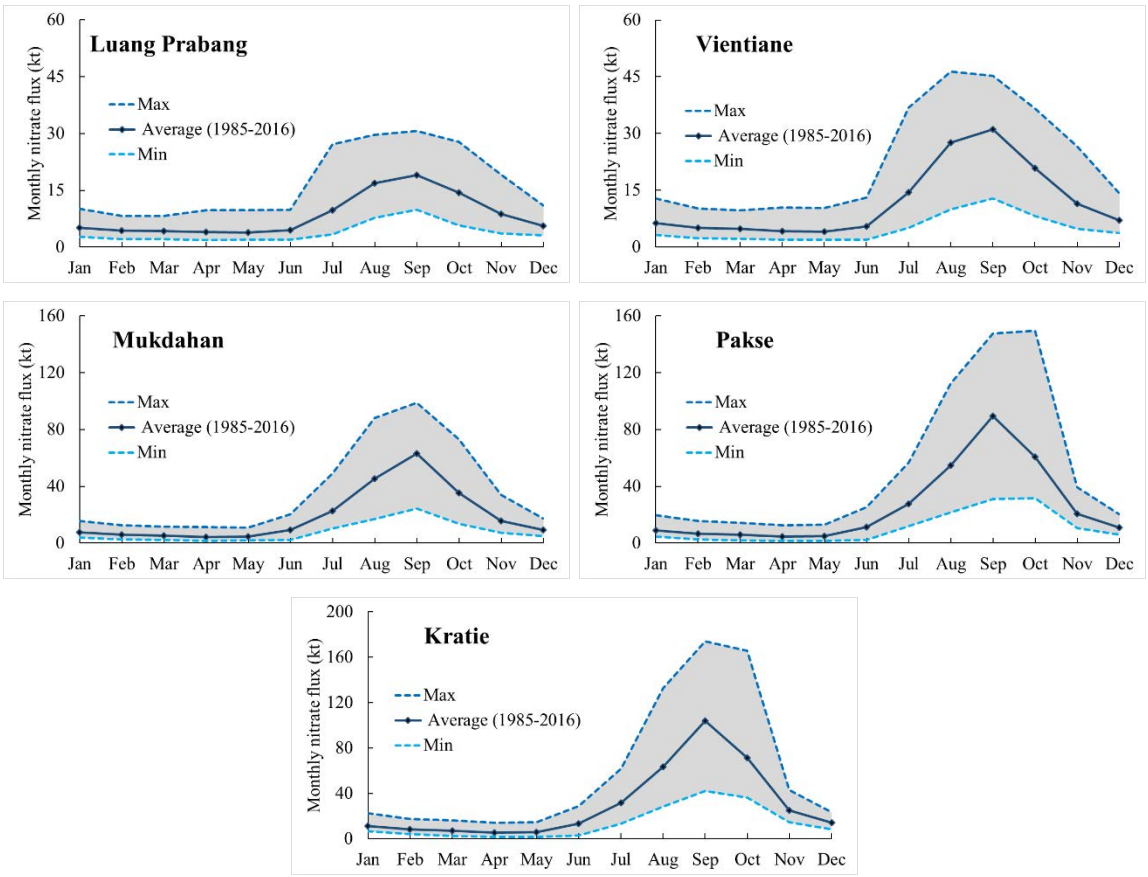

Figure 6-3: *Variability (mean, minimum and maximum) in monthly river nitrate flux for 31 years of simulation (1985-2016) and mean annual water flow at major locations of the Mekong River (1985–2016).*

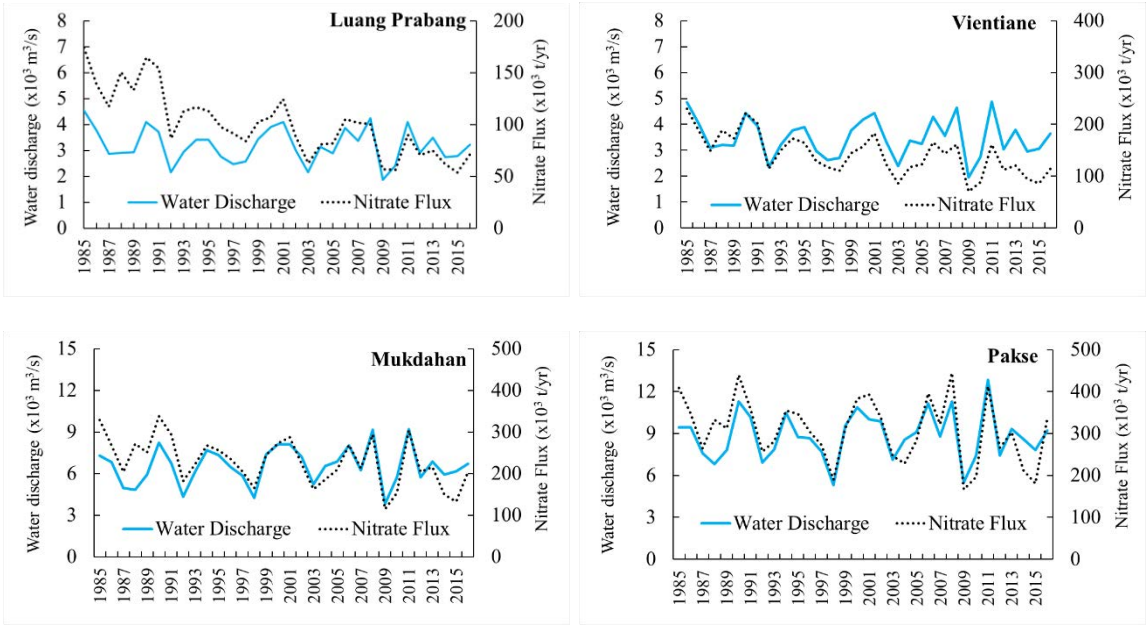

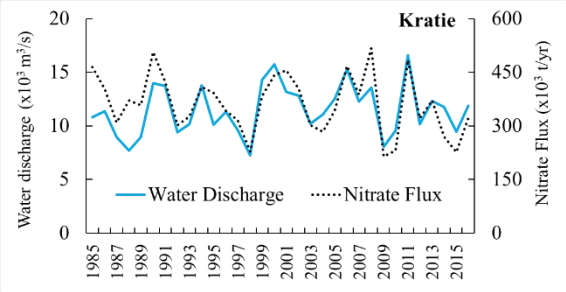

Figure 6-4: *Temporal variability of annual nitrate flux and mean annual water flow at the major locations of the Mekong River (1985–2016).*

The temporal variability of nitrate fluxes in the Mekong River at multiple locations is correlated with river flow (**Figure 6-4**). For instance, the lowest annual nitrate flux at Kratie outlet of the study over 32 years was 214×10^3 t with a mean annual water discharge of 8063 m^3/s observed in 2009, while the highest load was of 518 $\times10^3$ t with a mean annual water discharge of 13565 m^3/s, observed in 2008.

The plans to build various large reservoirs to the Mekong mainstream and tributaries might trap a large part of the nutrients, particularly those bound to suspended sediments (Kummu et al., 2010). Yet, the MRC (2010) maintains that the dams may critically change the nutrient flushing conditions. Within the existing dams, the nitrate fluxes have dropped significantly aligned with water discharge in some specific years, which could be a consequence of sediment and nitrate flux being stored behind hydropower construction and operation of dams. For example, the Manwan Dam operating in 1993, Dachaoshan in 2001, Jinghong in 2008, and Xiaowan in 2009. The impact to lower sediment load can be seen from upper stations, Chiang Saen, Luang Prabang, Vientiane, Mukdahan, and the lowermost part at Pakse and Kratie.

The mean annual nitrate flux of the Mekong at Kratie River from 1985-2015 was estimated to be $361.8\pm83.5\times10^3$ t/year, which could be comparable to other major Asian main rivers flowing into the coastal waters of China such as the Yangtze River (5516.2×10^3 t/year), Yellow (214.8×10^3 t/year), Red River (296 $\times10^3$ t/year of total inorganic nitrogen) and Pearl (559 $\times10^3$ t/year of dissolved inorganic nitrogen) (Hu and Li, 2009; Hua et al., 2019; Le et al., 2015; Wu et al., 2019).

The analysis of annual nitrate flux in this study illustrated annual water discharge relation. This demonstrates the continuous transport of nitrate from basin runoff (**Figure 6-4**). However, estimates of nitrate loading from flux and discharge data do not provide much information about

sources. Further in-depth analysis to identify nutrient sources (e.g., stable isotopes) might be useful (Chang et al., 2002a). Anthropogenic activities also significantly increase concentrations and fluxes of nutrients in the Mekong River Basin (Li and Bush, 2015a). Dam construction could somehow affect riverine nutrient transport processes (Supit and Ohgushi, 2012). From the mid-1990s to the early 2000s, dam development accelerated in China and Vietnam with the construction of mainstream dams on the Lower Lancang and tributary dams (Kondolf et al., 2018a). The nutrient emergence was also found in other East Asian monsoon rivers such as Yangtze (Shen and Liu, 2009) and Red River (Li and Bush, 2015a).

The monthly nitrate flux correlated well to the monthly water discharge (high values of R^2) (**Figure 6-5**). Based on this strong relationship, monthly water discharge could be used to estimate monthly nitrate flux. The empirical relationship could be used to estimate monthly nitrate flux for long-term periods within the basin, but only under conditions where current land use does not change drastically (Oeurng et al., 2016).

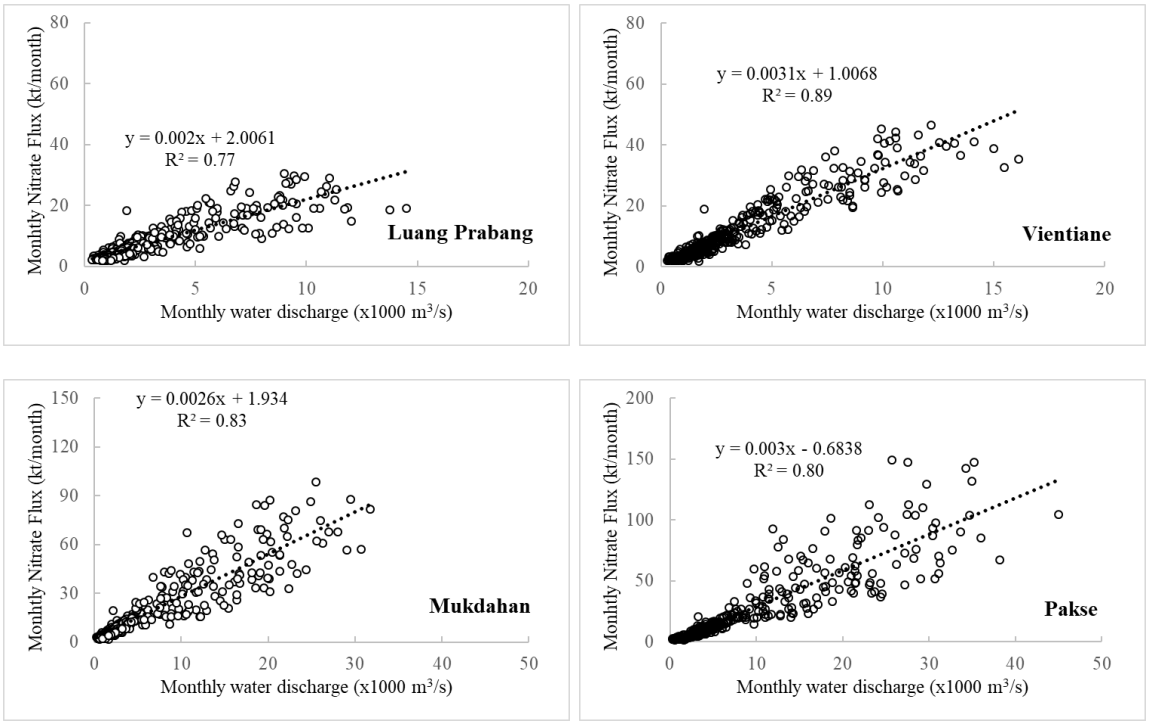

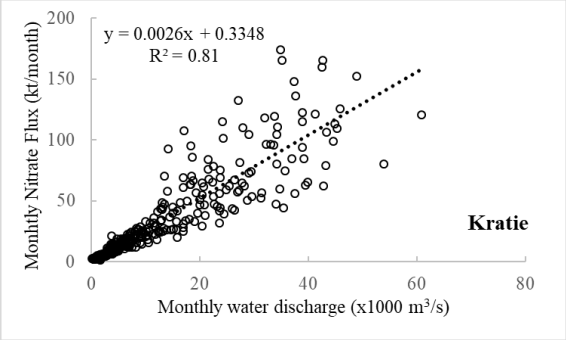

Figure 6-5: *Empirical relationship between monthly nitrate flux and monthly water discharge at six locations along the main river from 1985-2016*

3.3. Spatial patterns of sub-basin nitrate yield

To understand nitrate yield in detail in the Mekong related to basin characteristic, the mean annual nitrate yield in the Mekong River Basin for the simulation by major sub-basins present in

Table 6-5. The large variability of annual spatial nitrate yields noticed at the sub-basin level in the study area is shown in **Figure 6-6**. **Figure 6-6** also illustrates the overall spatial mapping of average nitrate yields and mean annual nitrate flux for the Mekong River Basin from 1985 to 2016. The highest nitrate yield (473±526 kg/km^2/year) can be found in Vientiane to Mukdahan in the northern part of Laos. This area is in Laos's central part and is dominated by agriculture (more than 80%) and grasses (20%). It is characterized by the gentle slope (more than 50%) and medium slope (20%), and some steep hill at the north and far-right bank. In the upper part of Mekong in China (where the river is called Lancang River), covered by the forest type (evergreen and mixed forest) and range grasses (more than 80% of this total area) and high topography and steep slope, the nitrate yield is as low (49±96 kg/km^2/year). In the Mekong Basin in Thailand (Mukdahan to Pakse), with high agricultural activity, the nitrate yield is 245±257 kg/km^2/year. In between Pakse and Kratie (including 3S, the largest tributary of Mekong), the average nitrate yield was found to be 181±276 kg/km^2/year; however, we found high yields at the upstream part of the 3S basin (>1000 kg/km^2/year).

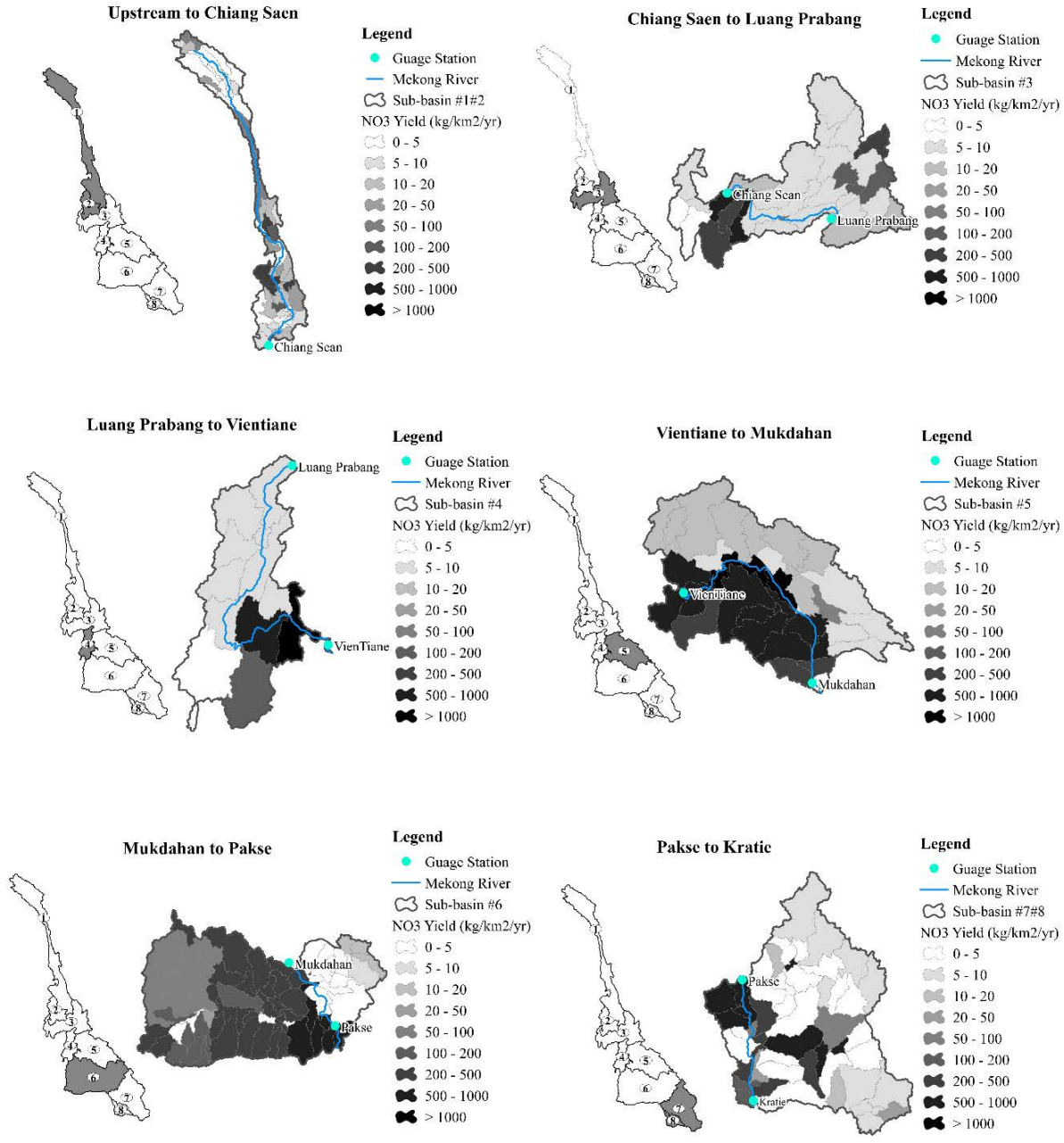

Figure 6-6: *Spatial variability of mean nitrate flux and yields.*

Table 6-5: *Average annual nitrate yields by major sub-basins in the study from 1985–2016 in the Mekong River basin.*

Area	Description of Sub-Basin General Characteristic	Average Annual Nitrate Yield ($kg.km^{-2}.year^{-1}$)
China/Laos Border to Chiang Saen	In upper Mekong part in China. Covered by the forest type (evergreen and mixed forest) and range grasses (more than 80% of the total area. High topography and steep slope.	49 ± 96
Chiang Saen to Luang Prabang	The northern part of Laos. Mixed land use (forest and grasses more than 50% and agriculture type 25%). High topography and steep slope	131 ± 225
Luang Prabang to Vientiane	Mixed land use between grasses type (more than 50%) and agriculture (30%). Steep (40%) and medium slope (60%)	152 ± 356
Vientiane to Mukdahan	In the central of Laos. Dominated by agriculture type (more than 80%) and grasses type (20%). Gentle slope (more than 50%) and medium slope (20%) and some steep hill at the north and far-right bank	473 ± 526
Mukdahan to Pakse	The area cover is in Thailand. It is dominated by agriculture type (70%) and some grass type. Gentle slope (70%) and some medium slope.	245 ± 257
Pakse to Kratie	In central highland of Vietnam and some part in Cambodia. Covered by forest type (evergreen forest, 60%) and agricultural type (33%). The gentle slope in Laos and Cambodia and some high slope in the far-right bank in Central of Vietnam.	181 ± 276

The effects or contributions from each land-use class were then quantitatively determined in this study. The average nitrate yield for each land use are detailed in **Table 6-6**. The average annual nitrate yield in the upper 80% of the total Mekong River Basin was an estimated 202 $kg/km^2/year$; however, average agricultural sub-basins have nitrate yields higher than 472 $kg/km^2/year$, and some forested sub-basins have yielded lower than 50 $kg/km^2/year$. As expected, the forests had the lowest yield (less than 26 $kg/km^2/year$). The grass had a medium value from 150 and 256 $kg/km^2/year$. As for effects of agricultural activities, the Agricultural Land Generic yielded averagely 472 $kg/km^2/year$, which was almost 20 times higher than the forest, and could be regarded as one of the nitrate exports sources. The major source of this high yield resulted from fertilization. However, other factors such as spatial variability in slope and surface runoff also affect nitrate yields.

Table 6-6: *Annual nitrate yield for the land use classes in the Mekong River basin.*

Landuse class	Percentage over the basin (%)	Average	Standard deviation	Max	Min
		kg. km^{-2}.year^{-1}			
Weatern Wheatgrass	1	151	54	233	100
Crested Wheatgrass	2	256	77	380	184
Range Brush	4	4	3	13	1
Forest Mixed	6	13	8	37	5
Forest Deciduous	6	3	2	6	1
Pasture	9	11	23	84	0
Range Grasses	22	11	13	66	3
Forest Evergreen	21	26	73	438	0
Agricultural Land Generic	29	472	361	1946	1

The effects of agricultural activities, which was almost 20 times higher than the forest, could be regarded as one of the nitrate exports sources. The timing of fertilizer application is a main cause of N leaching, in particular for nitrate, with respect to soil moisture and crop uptake (Edwards, 1973). MRC, (2003) reported massive use of fertilizer in Thailand (100 kg mineral fertilizer per hectare); this can lead to increase of nutrient in the Lower Mekong.

The nutrient load of the river was particularly high in the settlement and agricultural segments, where fertilizer usage is a common practice like in other river catchments, e.g. the Yangtze River of China, the Mississippi River of the North American, and the Pamba River in India (David and Gentry, 2000; David et al., 2016; Qu and Kroeze, 2012; Wang et al., 2009). The TN yield of the Yangtze River was estimated to be about 1400 kg/km^2/yr (Tong et al., 2017) and haft of total nutrient flux to the coastal water of China (Qu and Kroeze, 2012), this not only the Yangtze is the largest basin area and river discharge in China but also the basin includes intensive agriculture. The second largest river in China, the Yellow River, also reported a considerably increasing quantity of nutrient inputs (with 25 kg/km^2/year of total nitrogen) to the basin due to economic development and fast population growth during the past 40 years (Wang et al., 2009).

River nutrients come from natural process and anthropogenic sources such as from agricultural practices (synthetic fertilizers and manure) and anthropogenic pollutants from sewage. Those factors cause different nutrient loads and yields in many world river basins. From the study of global nutrient export to the coastal zone by Dumont et al. (2005), DIN yields are 113.2 kgN/km^2/yr in the Amazon River, 172.5 kgN/km^2/yr in the Amur River, 136.9 kgN/km^2/yr in the

Indus River, 43.1 kgN/km^2/yr in theYenisei, and 43.9 kgN/km^2/yr in the Parana River. Our result of mean annual nitrate yield (45.6 kgN/km^2/yr) of the Mekong River is comparable to reported yield for other major rivers in Asia and elsewhere.

Future trends in nitrate flux are likely to be influenced by changes in the climate and mainly by nitrogen sources in cultivated areas such as fertilizer additions (Martínková et al., 2011). Fertilizer use has not been widespread among farmers in the region's basins in the last few decades, but this is likely to change to achieve higher agricultural yields. In the Lower Mekong traditional farming practices are mostly used rather than commercial farming (MRC, 2010). Nevertheless, the agricultural area makes up the largest nutrient fluxes in the basin. Commercial farming and increasing fertilizer use have recently become more common, and this trend is expected to continue (MRC, 2010). In Thailand and Vietnam, high fertilizer applications are already occurring, and the Lao PDR and Cambodia will definitely follow. Under impacts by factors including climate change, population increase, land cover change, fertilizer use, and industrial wastewater, the Mekong mainstream will expect an increase of 13–25% in nutrient levels by the 2020s (Yoshimura et al., 2009).

Other important considerable factors impacting nutrients of the Mekong Basin are population and economy. The population of the Mekong is expected to increase from the current 65 million to more than 82 million by 2030 (based on medium variant projection, UN Population Division 2006), and the proportion of urban dwellers from about 20% to 40%, reaching approximately 33 million with 4.5% per annum of economic growth. Total food demand will increase at a rate greater than that of population alone, due to rising incomes and changing diet preferences consequent upon urbanization. These factors will drive great change in the Mekong Basin. Significant future land cover changes in the basins are likely to cause the most remarkable change in future nitrate flux and yield, led by deforestation of native rain forests, expansion of agricultural and urban areas, and expansion of commercial plantations such as rubber trees (Takamatsu et al., 2014).

3.4. Nitrate Net Balance and Nitrate Net Balance Rate in the Mekong River basin

We can distinguish between two types of reaches: production reaches and removal reaches. Along the Main River and major downstream tributaries, NNB is positive and show *Nitrate Production (NP)*. Upstream and small reaches in the basin shows *Nitrate Removal (NR)* (**Figure 6-7**). NP reaches covered 19% of total reach numbers, while NR reaches made up 61% of the Mekong

Basin's total reach numbers. NNBR show the negative value for most of the reach (91% of total reach numbers), with the higher rate occurring in smaller reaches, while major reaches and main rivers show a low rate of NNB, as shown in **Table 6-7**.

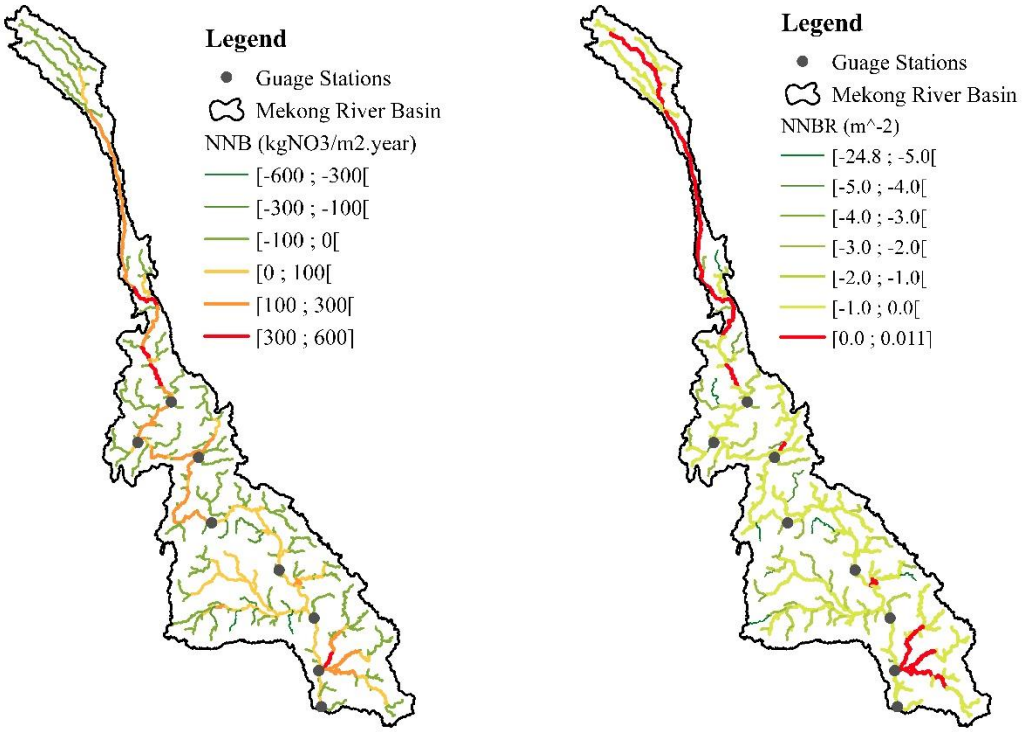

Figure 6-7: *The annual average simulation by reaches of (A) Nitrate Net Balance (NNB) in kg.m^{-2}.year^{-1}; (B) Nitrate Net Balance Rate (NNBR) in. m^{-2}.month^{-1} over the Mekong River Basin. Negative NNB values indicate Nitrate Removal (NR). If the NNB is positive, it indicates that Nitrate Production (NP) occurs.*

Table 6-7: *Annual average simulation of Nitrate Net Balance (NNB) and Nitrate Net Balance Rate (NNBR) over the Mekong River Basin.*

	NNB ($kgNO_3.m^{-2}.year^{-1}$)	NNBR ($.m^{-2}.year$)
Max	624.8	0.0
Min	-634.5	-24.8
Mean	25.1	-0.8
Median	-0.4	-0.1
SD	101.0	2.3

Comparing the seasonal monthly average NNB and NNBR variations (Table 7) shows that the removal rates are higher during the dry season with median values of -0.05 m^{-2} than during the rainy season with median values -0.04 m^{-2}, respectively. The NNB and NNBR in reaches vary

along the watershed and among the seasons (**Figure 6-8**). The NNB spatial variation, ranging from -400 to +600 kg.m^{-2}.month^{-1}, is similar to the temporal variation (ranging from -390 to 675 kg.m^{-2}.month^{-1}). The positive NNB and NNBR, which is the Nitrate Production (NP) occurrence, could be found for the major tributaries and main river in the Mekong River Basin. The result expresses the same condition at Garonne River of southwest France and northern Spain that the hot spots of NP are located downstream in the main rivers, whereas NR strongly occurs in small reaches of lowlands and intermediate streams (Cakir et al., 2020)

Table 6-8: *Seasonal variations of simulated Nitrate Net Balance and Nitrate Net Balance Rates.*

	Nitrate Net Balance (kg. m^{-2}. month^{-1})		Nitrate Net Balance Rate m^{-2}.month^{-1}	
	Dry Season	Rainy Season	Dry Season	Rainy Season
Max	575	675	0.02	0.01
Min	-390	-126	-8.60	-44.95
Mean	-24	35	-0.72	-0.83
Median	-0.17	-0.77	-0.05	-0.04
SD	319	97	1.43	3.38

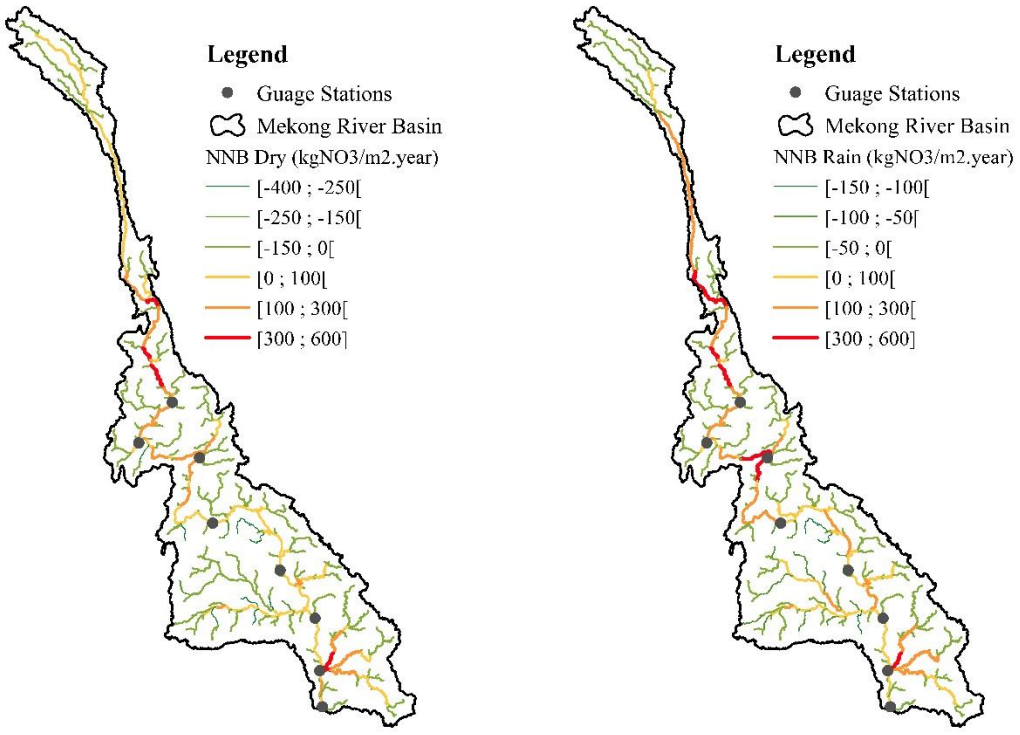

Figure 6-8: *Seasonal variations of simulated Nitrate Net Balance (NNB) in reaches of Mekong river basin during the dry season and rainy season.*

4. Conclusion

The SWAT model was applied to assess the streamflow, sediment yield and nitrate yield in the Mekong River Basin. The model was calibrated and validated against eight hydrological stations, six sediment, and five nitrate stations along the Mekong mainstem. The annual average nitrate yield for the Mekong River Basin was estimated at approximately 202 kg/km^2/year for the upper 80% of the total MRB before entering the delta. It is important to note that the Mekong land-use type could be the main factor determining nitrate yield in the basin. As a distributed and physical model, the SWAT model has considered many processes in the watershed such as topography, soil, meteorology and land use/cover, and can effectively simulate the catchment scale nitrate transport and evaluate the changing trend, which provides a basic model for further simulations in a long-time scale. The removal rates of nitrate are higher during the dry season with median values of -0.05 m^{-2} than during the rainy season, with a median value of -0.04 m^{-2}. This study could also serve as baseline information of nitrate studies for the sustainable watershed management plan. Finding a relationship between these variables, river hydro-morphological characteristics, and land management could be a good way to help stakeholders in water management decisions and boost awareness and involvement of people for sustainable management of water resources.

Data Availability Statement

The data that support the findings of this study are available from the corresponding author upon reasonable request.

Acknowledgement:

The authors also thank the Ministry of Water Resources and Meteorology (MOWRAM) of Cambodia for providing the data. Ty SOK would like to acknowledge Les Bourses du Gouvernement Français (BGF) and Laboratoire Ecologie Fonctionnelle et Environnement for hosting during his PhD study.

References:

Abbaspour, K.C., 2013. Swat-cup 2012. SWAT Calibration and uncertainty program—a user manual.

Arias, M., Piman, T., Lauri, H., Cochrane, T., Kummu, M., 2014. Dams on Mekong tributaries as significant contributors of hydrological alterations to the Tonle Sap Floodplain in Cambodia. Hydrology and Earth System Sciences, 18, 5303.

Benaman, J., Shoemaker, C.A., Haith, D.A., 2005. Calibration and validation of soil and water assessment tool on an agricultural watershed in upstate New York. Journal of Hydrologic Engineering, 10, 363-374.

Cakir, R., Sauvage, S., Gerino, M., Volk, M., Sánchez-Pérez, J.M., 2020. Assessment of ecological function indicators related to nitrate under multiple human stressors in a large watershed. Ecological Indicators, 111, 106016.

Campbell, I., 2009. The challenges for Mekong River management, The Mekong. Elsevier, pp. 403-419.

Chang, C.C., Kendall, C., Silva, S.R., Battaglin, W.A., Campbell, D.H., 2002. Nitrate stable isotopes: tools for determining nitrate sources among different land uses in the Mississippi River Basin. Canadian Journal of Fisheries and Aquatic Sciences, 59, 1874-1885.

Chea, R., Grenouillet, G., Lek, S., 2016. Evidence of water quality degradation in lower Mekong basin revealed by self-organizing map. PloS one, 11, e0145527.

Conley, D.J. et al., 2009. Controlling eutrophication: nitrogen and phosphorus. Science, 323, 1014-1015.

David, M.B., Gentry, L.E.J.J.o.E.Q., 2000. Anthropogenic inputs of nitrogen and phosphorus and riverine export for Illinois, USA. 29, 494-508.

David, S.E., Chattopadhyay, M., Chattopadhyay, S., Jennerjahn, T.C.J.S.o.t.T.E., 2016. Impact of human interventions on nutrient biogeochemistry in the Pamba River, Kerala, India. 541, 1420-1430.

Duan, S. et al., 2008. Seasonal changes in nitrogen and phosphorus transport in the lower Changjiang River before the construction of the Three Gorges Dam. Estuarine, coastal and shelf science, 79, 239-250.

Duan, S., Xu, F., Wang, L.-J., 2007. Long-term changes in nutrient concentrations of the Changjiang River and principal tributaries. Biogeochemistry, 85, 215-234.

Dudgeon, D., 2005. River rehabilitation for conservation of fish biodiversity in monsoonal Asia. Ecology and Society, 10.

Dumont, E., Harrison, J., Kroeze, C., Bakker, E., Seitzinger, S.J.G.B.C., 2005. Global distribution and sources of dissolved inorganic nitrogen export to the coastal zone: Results from a spatially explicit, global model. 19.

Galloway, J.N. et al., 2004. Nitrogen cycles: past, present, and future. Biogeochemistry, 70, 153-226.

Gupta, H.V., Kling, H., Yilmaz, K.K., Martinez, G.F., 2009. Decomposition of the mean squared error and NSE performance criteria: Implications for improving hydrological modelling. Journal of hydrology, 377, 80-91.

Hu, J., Li, S., 2009. Modeling the mass fluxes and transformations of nutrients in the Pearl River Delta, China. Journal of Marine Systems, 78, 146-167.

Hua, W. et al., 2019. Dynamics of nutrient export from the Yangtze River to the East China sea. Estuarine, Coastal and Shelf Science, 229, 106415.

Iida, T., Inkhamseng, S., Yoshida, K., Tanji, H., 2011. Characterization of water quality variation in the Mekong River at Vientiane by frequent observations. Hydrological Processes, 25, 3590-3601.

Jennerjahn, T. et al., 2004. Biogeochemistry of a tropical river affected by human activities in its catchment: Brantas River estuary and coastal waters of Madura Strait, Java, Indonesia. Estuarine, Coastal and Shelf Science, 60, 503-514.

Kondolf, G.M. et al., 2018. Changing sediment budget of the Mekong: Cumulative threats and management strategies for a large river basin. Science of the total environment, 625, 114-134.

Kuenzer, C. et al., 2013. Understanding the impact of hydropower developments in the context of upstream–downstream relations in the Mekong river basin. Sustainability science, 8, 565-584.

Kummu, M., Lu, X., Wang, J., Varis, O.J.G., 2010. Basin-wide sediment trapping efficiency of emerging reservoirs along the Mekong. 119, 181-197.

Kummu, M., Penny, D., Sarkkula, J., Koponen, J., 2008. Sediment: curse or blessing for Tonle Sap Lake? AMBIO: A Journal of the Human Environment, 37, 158-163.

Kummu, M., Varis, O., 2007. Sediment-related impacts due to upstream reservoir trapping, the Lower Mekong River. Geomorphology, 85, 275-293.

Lamberts, D., 2006. The Tonle Sap Lake as a productive ecosystem. International Journal of Water Resources Development, 22, 481-495.

Lane, R.R. et al., 2004. Changes in stoichiometric Si, N and P ratios of Mississippi River water diverted through coastal wetlands to the Gulf of Mexico. Estuarine, Coastal and Shelf Science, 60, 1-10.

Le, T.P.Q., Billen, G., Garnier, J., 2015. Long-term biogeochemical functioning of the Red River (Vietnam): past and present situations. Regional Environmental Change, 15, 329-339.

Li, S., Bush, R.T., 2015. Rising flux of nutrients (C, N, P and Si) in the lower Mekong River. Journal of Hydrology, 530, 447-461.

Li, Y., Chen, B.-M., Wang, Z.-G., Peng, S.-L., 2011. Effects of temperature change on water discharge, and sediment and nutrient loading in the lower Pearl River basin based on SWAT modelling. Hydrological Sciences Journal, 56, 68-83.

Liljeström, I., Kummu, M., Varis, O., 2012. Nutrient Balance Assessment in the Mekong Basin: nitrogen and phosphorus dynamics in a catchment scale. International Journal of Water Resources Development, 28, 373-391.

Liu, S.M. et al., 2003. Nutrients in the Changjiang and its tributaries. Biogeochemistry, 62, 1-18.

Ludwig, W., Bouwman, A., Dumont, E., Lespinas, F., 2010. Water and nutrient fluxes from major Mediterranean and Black Sea rivers: Past and future trends and their implications for the basin-scale budgets. Global biogeochemical cycles, 24.

Ludwig, W., Dumont, E., Meybeck, M., Heussner, S., 2009. River discharges of water and nutrients to the Mediterranean and Black Sea: major drivers for ecosystem changes during past and future decades? Progress in oceanography, 80, 199-217.

Martínková, M., Hesse, C., Krysanova, V., Vetter, T., Hanel, M., 2011. Potential impact of climate change on nitrate load from the Jizera catchment (Czech Republic). Physics and Chemistry of the Earth, Parts A/B/C, 36, 673-683.

Meybeck, M., 1982. Carbon, nitrogen, and phosphorus transport by world rivers. Am. J. Sci, 282, 401-450.

Moriasi, D.N. et al., 2007. Model evaluation guidelines for systematic quantification of accuracy in watershed simulations. Transactions of the ASABE, 50, 885-900.

Moriasi, D.N., Gitau, M.W., Pai, N., Daggupati, P., 2015. Hydrologic and water quality models: Performance measures and evaluation criteria. Transactions of the ASABE, 58, 1763-1785.

MRC, 2003. State of the Basin report. Mekong River Commission.

Müller, B., Berg, M., Pernet-Coudrier, B., Qi, W., Liu, H., 2012. The geochemistry of the Yangtze River: Seasonality of concentrations and temporal trends of chemical loads. Global biogeochemical cycles, 26.

Nash, J.E., Sutcliffe, J.V., 1970. River flow forecasting through conceptual models part I—A discussion of principles. Journal of hydrology, 10, 282-290.

Oeurng, C., Cochrane, T.A., Arias, M.E., Shrestha, B., Piman, T., 2016. Assessment of changes in riverine nitrate in the Sesan, Srepok and Sekong tributaries of the Lower Mekong River Basin. Journal of Hydrology: Regional Studies, 8, 95-111.

Qu, H.J., Kroeze, C.J.R.E.C., 2012. Nutrient export by rivers to the coastal waters of China: management strategies and future trends. 12, 153-167.

Raymond, P.A., Oh, N.-H., Turner, R.E., Broussard, W., 2008. Anthropogenically enhanced fluxes of water and carbon from the Mississippi River. Nature, 451, 449-452.

Ribolzi, O. et al., 2011. Land use and water quality along a Mekong tributary in Northern Lao PDR. Environmental management, 47, 291-302.

Runkel, R.L., Crawford, C.G., Cohn, T.A., 2004. Load Estimator (LOADEST): A FORTRAN program for estimating constituent loads in streams and rivers. 2328-7055.

Santhi, C. et al., 2001. Validation of the swat model on a large rwer basin with point and nonpoint sources 1. JAWRA Journal of the American Water Resources Association, 37, 1169-1188.

Seitzinger, S.P., Harrison, J.A., Dumont, E., Beusen, A.H., Bouwman, A., 2005. Sources and delivery of carbon, nitrogen, and phosphorus to the coastal zone: An overview of Global Nutrient Export from Watersheds (NEWS) models and their application. Global Biogeochemical Cycles, 19.

Seitzinger, S.P. et al., 2010. Global river nutrient export: A scenario analysis of past and future trends. Global Biogeochemical Cycles, 24.

Shen, Z.-L., Liu, Q., 2009. Nutrients in the changjiang river. Environmental monitoring and assessment, 153, 27-44.

Sok, T., Oeurng, C., Ich, I., Sauvage, S., Miguel Sánchez-Pérez, J., 2020a. Assessment of Hydrology and Sediment Yield in the Mekong River Basin Using SWAT Model. Water, 12, 3503.

Stevens, C.J., Dise, N.B., Mountford, J.O., Gowing, D.J., 2004. Impact of nitrogen deposition on the species richness of grasslands. Science, 303, 1876-1879.

Supit, C., Ohgushi, K., 2012. Dam construction impacts on stream flow and nutrient transport in Kase River Basin. International Journal of Civil & Environmental Engineering, 12, 1-5.

Takamatsu, M., Kawasaki, A., Rogers, P.P., Malakie, J.L., 2014. Development of a land-use forecast tool for future water resources assessment: case study for the Mekong River 3S Sub-basins. Sustainability science, 9, 157-172.

Tong, Y. et al., 2017. Estimation of nutrient discharge from the Yangtze River to the East China Sea and the identification of nutrient sources. 321, 728-736.

Turner, B.L., Chudek, J.A., Whitton, B.A., Baxter, R., 2003. Phosphorus composition of upland soils polluted by long-term atmospheric nitrogen deposition. Biogeochemistry, 65, 259-274.

Turner, R.E., Rabalais, N.N., 1994. Coastal eutrophication near the Mississippi river delta. Nature, 368, 619-621.

Voss, M., Bombar, D., Loick, N., Dippner, J.W., 2006. Riverine influence on nitrogen fixation in the upwelling region off Vietnam, South China Sea. Geophysical Research Letters, 33.

Wang, J.J., Lu, X., Kummu, M., 2011. Sediment load estimates and variations in the Lower Mekong River. River Research and Applications, 27, 33-46.

Wang, X. et al., 2009. Simulation of nitrogen contaminant transportation by a compact difference scheme in the downstream Yellow River, China. 14, 935-945.

Wassen, M.J., Venterink, H.O., Lapshina, E.D., Tanneberger, F., 2005. Endangered plants persist under phosphorus limitation. Nature, 437, 547-550.

Wu, G. et al., 2019. Riverine nutrient fluxes and environmental effects on China's estuaries. Science of The Total Environment, 661, 130-137.

Wu, Y., Chen, J., 2009. Simulation of nitrogen and phosphorus loads in the Dongjiang River basin in South China using SWAT. Frontiers of Earth Science in China, 3, 273-278.

Yoshimura, C. et al., 2009. 2020s scenario analysis of nutrient load in the Mekong River Basin using a distributed hydrological model. Science of the total Environment, 407, 5356-5366.

CHAPTER VII

General discussion

This chapter aims to estimate provide the general discussion of hydrology, sediment and nutrient flux in the Mekong River and Tonle Sap River and in the global context. This chapter also provide the discussion on the role of Tonle Sap and its uniqueness.

7. Chapter VII. General Discussion

7.1. Hydrological Regime

For the Mekong river basin before entering the floodplain area and delta, the mean annual rainfall from 1985-2016 was 1540 mm; 67% (1032 mm) of the average annual rainfall was removed by evapotranspiration and 33% (508 mm) for the streamflow. In Asia, the annual rainfall of the tropical river basins is higher than others in the subtropical and temperate zones. Compared to other large tropical river basins, the mean annual rainfall of the Mekong River basin is lower than Amazon (2 095 mm yr^{-1} during 1973-2013, Almeida et al., 2017) and is similar to the Congo (1560 mm yr^{-1} during 1951-1989, Alsdorf et al., 2016) and Red River (1494 mm yr^{-1} from 2000 to 2013) (Wei et al., 2019).

For streamflow, the model estimated a mean annual water yield of 404 km^3 yr^{-1} (with a mean annual water depth of 508 mm yr^{-1} and mean annual discharge of 12 684 m^3 s^{-1}, Table 7-1), of which 58% was the groundwater, 39% was surface runoff accounted and 3% was the lateral flow. The water yield of 508 mm has come from surface runoff (proportion of 34%), lateral flow (proportion of 21%), and groundwater (proportion of 45%). The groundwater is the main component for the river flow in the Mekong River basin, especially during the dry season.

Table 7-1: *Mean annual rainfall and hydrology for major Asian River and other tropical rivers.*

River	Basin Area (10^3 km^2)	Precipitation		Hydrology				References
		Period	Rainfall (mm yr^{-1})	Period	Yield (km^3 yr^{-1})	Discharge (m^3 s^{-1})	Depth (mm yr^{-1})	
Mekong	795	1980-2016	1470	1980-2016	404	12684	503	This study
Red	137	2000-2013	1494	2000-2013	95	3003	697	Wei et al 2020
Pearl	452	2000-2009	1650	2000-2009	268	8498	593	Wu et al., 2012
Yangtze	1830	1980-2015	1086	2003-2013	838	26573	466	Yang et al., 2015
Yellow	752	1981-2013	466	n.a.	58	1839	77	Wu et al., 2016
Irrawaddy	413	n.a.	n.a.	1991-2012	380	12054	1057	Sirisena er al., 2018
Congo	3500	1951-1989	1560	2000-2010	1282	40662	347	Alsdorf et al., 2016
Amazon	5960	1973-2013	2095	n.a.	6591	209000	1099	Moreira et al., 2003

The mean water yield of major Asia river originated from the Tibetan Plateau, the Mekong is 404 km^3 yr^{-1} (with a mean annual water depth of 508 mm yr^{-1} and mean annual discharge of 12 684 m^3 s^{-1} during 2985-2018), Pearl is 268 km^3 yr^{-1} (with a mean annual water depth of 593 mm yr^{-1} and mean annual discharge of 8 498 m^3 s^{-1} during 2000-2009, Wu et al., 2012), Yangze river is 838

$km^3\ yr^{-1}$ (with a mean annual water depth of 466 mm yr^{-1} and mean annual discharge of 26 573 $m^3\ s^{-1}$ during 2003-2012, Yang et al., 2015), Yellow river 58 $km^3\ yr^{-1}$ (with a mean annual water depth of 77 mm yr^{-1} and mean annual discharge of 1839 $m^3\ s^{-1}$, Wu et al., 2016), Irrawady is 380 $km^3\ yr^{-1}$ (with a mean annual water depth of 1057 mm yr^{-1} and mean annual discharge of 12 054 $m^3\ s^{-1}$ during 1991-2010, Sirisena et al., 2018). Other part of the world, the mean annual water yield for the Congo river is 1282 $km^3\ yr^{-1}$ (with a mean annual water depth of 347 mm yr^{-1} and mean annual discharge of 40,662 $m^3\ s^{-1}$ during 2000-2010, Alsdorf et al., 2016) and Amazon is 6591 $km^3\ yr^{-1}$ (with a mean annual water depth of 1099 mm yr^{-1} and mean annual discharge of $209\times10^3\ m^3\ s^{-1}$, period not mentioned in Moreira-Turcq et al., 2003). Comparing to major rivers from the Tibetan Plateau, though the annual water discharge and yield of the Mekong river basin are lower than the Yangtze Yellow, its annual water depth is the highest among these rivers but lower than Irrawaddy.

Within the Mekong river itself, annually, 80% of the annual flow occurred during the rainy season (from May to October), while 20% of the annual flow occurred during dry season (from November to April). It is interesting that at the same time, on average, the annual water discharge in Kratie was 404,000 (Mm^3/yr), 36,000 Mm^3/yr higher than the annual water discharge at Chroy Changvar (368,000 Mm^3/yr). This pattern is similar to the pattern of the flow in Kratie and Stung Treng (Cambodia-Laos border, about 150 km upstream of Kratie). MRC (2019) reported in their observed flows for the Mekong mainstream stations over the period 2000-2017, Stung Treng discharge is found higher than the downstream at Kratie. Water flow in this reach is very complex (due to downstream backwater effects, overbank flows and temporary water storage on the floodplain) especially during the flood season when hydraulic conditions define the flow distribution between different river branches. The downstream reduction in gauged flow at Kratie and Chroy Changvar occurred mainly at higher flows and can be attributed to overbank flow from the Mekong River traversing the floodplain to TSL and by flow into major distributaries between Kratie and Chroy Changvar. During the flood season, water starts to spillover both banks of the Mekong River between upstream of Kompong Cham (150 km upstream of Chroy Changvar) and Chroy Changvar station. The bypass discharge by this river has not been previously reported in the literature. Part of the water spilling over the right bank reaches the Tonle Sap Lake as overland flow. It is clearly indicated that from the Kratie downward, After Kratie the Mekong reaches extensive floodplains and then delta and Kratie is selecting for the outlet of the hydrological model.

7.2. Sediment and Nitrate Dynamic of the Mekong River

Of the total natural global sediment flux to the oceans of about 12.6 to 18 Gt/year, Asia exported the most sediments (~4.8 Gt/year) among continents (Gordeev, 2006; Syvitski et al., 2011; Syvitski et al., 2005). High sediment loads are a common feature of many Asian rivers, especially those originating from the Himalayan-Tibetan Plateau, such as the Yellow Rivers, the Yangtze, the Red and the Mekong, and due to the pronounced topographic relief of the region (Evans et al., 2012; Ludwig and Probst, 1998; Milliman and Syvitski, 1992).

Rivers, draining the Asian continent, mainly flow to the Arctic, the Pacific Ocean and the Indian Ocean. Water discharge and sediment load. Rivers from the Asian continent transport the total water discharge of 6,362 km^3, and contribute the total sediment load of 4,145 Mt to the oceans (Liu et al., 2001). Distribution of sediment load in Asia continent is non-uniform. Sediment loads in rivers of Southeast Asia are larger than in the Northwest. Asian rivers can be divided into three categories in terms of their values of water and sediment discharges. There are rivers carry little sediment, but they have large water discharge which can be found in rivers draining into the Arctic Ocean. Rivers contribute tremendous sediment load, but they are of low water discharge for example Yellow draining into the Yellow Sea. The last category is rivers transport very large sediment load and have very large water discharge. These rivers are the Yangtze and Pearl rivers, Mekong River, Ganges, Brahmaputra, and Indus River. The rivers in the last category which is high sediment loads originate from the Qinghai-Tibet Plateau (Table 7-2).

However, Africa and Asia showed the largest reduction in sediment flux to the coast in rivers (such as the Nile, Orange, Niger, and the Zambezi in Africa and the Yangtze, Indus, and Yellow in Asia), and 31% of the total sediment load retained in reservoirs were indicated in Asia and 25% in Africa (Syvitski et al., 2005). The world's largest river, the Amazon, exports around ~550–1500 Mt/yr of sediment to the Atlantic (Dunne et al., 1998; Gaillardet et al., 1997; Guyot et al., 2005; Martinez et al., 2009; Meade et al., 1979).

Table 7-2: *The annual mean of sediment is comparable with other major rivers in Asia*

River	Region	Basin area (10^6 km^2)	River length (km)	Water Discharge km^3/yr	Sediment yield t/km^2/yr	Sediment load (Mt/yr)	References
Yenisei	North Asia	2.5	4800	630	9.54	23.85	Fabre et al., (2019)
Yellow	East Asia	0.77	5464	49	1400	1080	Wang et al., (2011)
Yangtze	East Asia	1.94	6300	900	250	480	Wang et al., (2011)
Pearl	East Asia	0.44	2129	302	88.6	39	Chalov et al., (2018); Lai et al., (2016)
Red	East Asia	0.12	1139	123	780	107	Wei et al., (2021)
Mekong	Southeast Asia	0.79	4800	ND 404	202 102	160 78	Walling, (2008) (This study)
Irrawaddy	Southeast Asia	0.43	2210	410	846	364	Robinson et al., (2007)
Brahmaputra	South Asia	0.61	2900	625	819	500	Rahman et al., (2018)

Estimation of the sediment flux of Mekong to the delta is complicated by interactions with the Tonle Sap system (Kummu and Varis, 2007) since large volumes of flood water enter the Tonle Sap floodplain, where a part of the sediment loads deposited. However, the study presented the sediment load along the Main River in various location (Figure 7-2). Our estimated loads at Kratie (75± 21 Mt from 1993-2017, Figure 7-1) is similar to those proposed by prior authors, such as Dang et al. (2016), who reported suspended sediment flux of 87±28 Mt/year (1981–2005), Lu et al. (2014a), who reported 50-91 Mt/year of suspended sediment load from 2008 to 2010, and Manh et al. (2014), who estimated 106 Mt/year at Kratie (2010-2011). However, the more recent estimates cover relatively short periods after major dam construction in the upper Mekong mainstem. Looking over longer time scales reflected in stratigraphic analysis of Holocene sediment cores, Ta et al. (2002) proposed 144±34 Mt/year of long-term mean sediment load to the sea, which is consistent with pre-dam estimate of 145 Mt/year by Liu et al. (2013).

The Mekong River and majority of regions of Asia continent, sediment flux are controlled by monsoon. Seasonal variation of water discharge and sediment load depends on variation of runoff to a great extent; therefore, seasonal variations have a large change rate. At this stage, it shall be noted that about 80% of the total annual sediment in Mekong River is delivered during flood season. The sediment hydrograph is similar to the discharge hydrograph. The peaks of sediment concentration and discharge of the majority of rivers appear in the flood period, when the peak of flood appears from May to October when during the monsoon season.

The sediment loads and yield of the Mekong River, same as the rest of Asian rivers (Liu et al., 2001), are mainly controlled by the climate, hydrology, vegetation, soil and geomorphology. Some studies on soil erosion and sedimentation claim that the geographical features of the Mekong River basin, such as its steep slopes and the slope length of its hills and mountains, are affected directly by the occurrence of soil erosion in specific areas, and these sediments are transformed when transported along the river (Hua-rong et al., 2006; Peng et al., 2007; Yao et al., 2005; Yu et al., 2006). However, the influence factors issue need to be improved correctly for understanding the influencing factor on soil erosion in each feature of the Mekong river basin. In addition, our study on confirm and agree that that natural vegetation covers, such as the forests in Laos PDR and Cambodia, can decrease soil erosion at rates greater than those of agricultural areas in Thailand (Chuenchum et al., 2020). Hence, if forested areas are transformed into agricultural activities, then the soil erosion rate will increase remarkably, especially in upstream areas (Peng et al., 2007). On one hand sediment load and yield depend on basic variation tendency of precipitation and runoff; on the other hand, they relate to geological construction, terrain, soil and vegetation. Sediment loads and yields in Mekong River are majorly influenced by land cover and land use, which alters upland erosion processes.

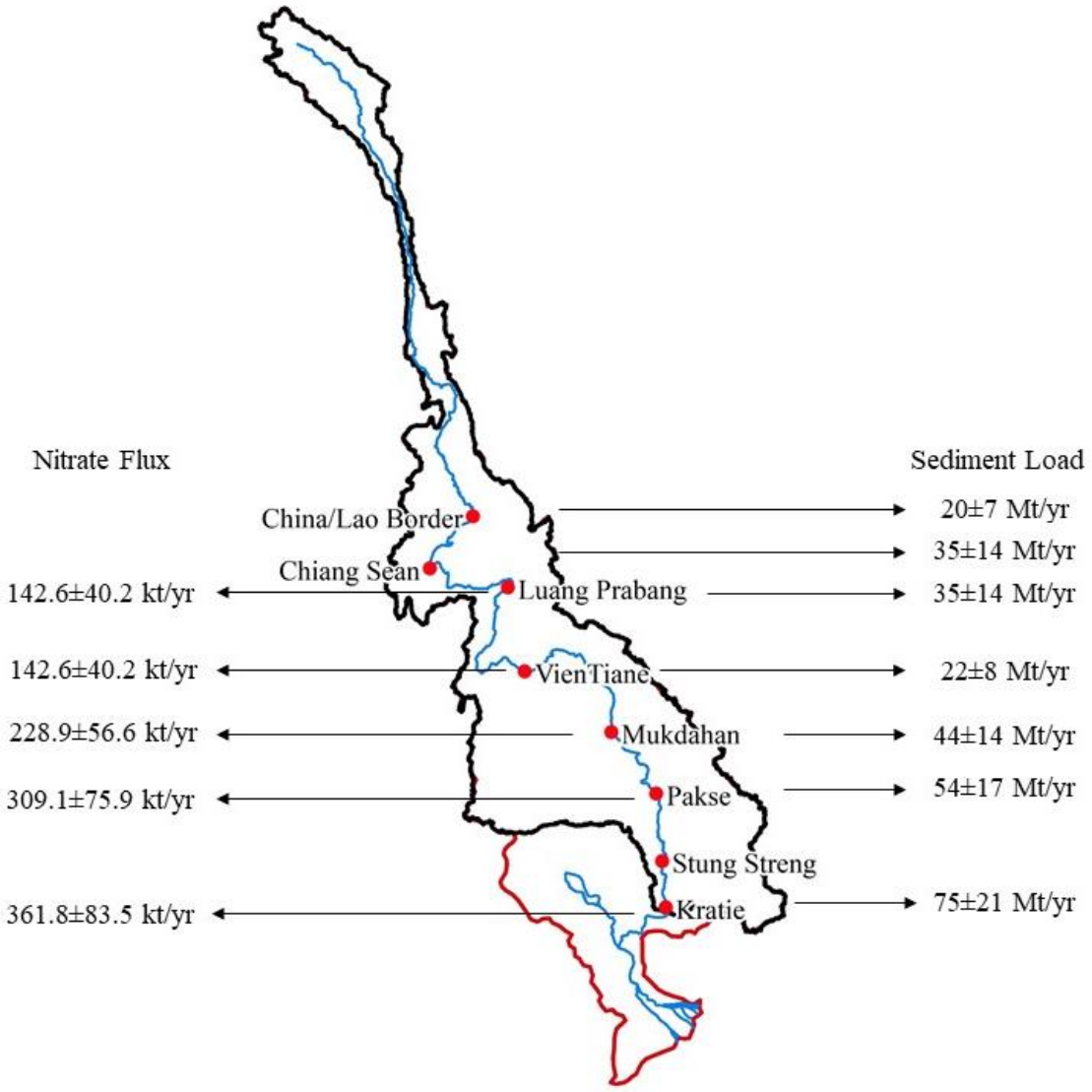

Figure 7-1: *Sediment and Nutrient flux of Mekong River at different sites from the Upper Mekong before entering the floodplain area including Tonle Sap region and Delta from 1985-2016*

The mean annual nitrate flux of the Mekong River before entering the floodplain and delta (at Kratie) from 1985-2016 was estimated to be 361.8±83.5×10^3 t/year, which could be comparable to other major Asian main rivers flowing into the coastal waters of China such as the Yangtze River (5516.2×10^3 t/year), Yellow (214.8×10^3 t/year), Red River (296 ×10^3 t/year of total inorganic nitrogen) and Pearl (559 ×10^3 t/year of dissolved inorganic nitrogen) (Hu and Li, 2009; Hua et al., 2019; Le et al., 2015; Wu et al., 2019). While the total phosphorus flux from the Mekong River basin to the South-China Sea was accounted for 55 kt/year for 3-years data (2003-2005) (Liljeström et al., 2012). The intra annual nitrate flux within the Mekong basin is strongly seasonal

as a result of 80-88% of the annual nitrate occurring from May to October. A similar pattern to total phosphorus, approximately 90% of the annual total phosphorus flux occurring between May to October. The peak of nitrate flux in both Kratie and Chroy Changva has been observed in August, while total phosphorus reached its peaks in September.

At the global scale, the major attribute of dissolved inorganic nitrogen (DIN) reported from 62% of anthropogenic non-point sources (Seitzinger et al., 2005b) while precipitation and agricultural sources dominate the nitrate in the Mekong basin, a less developed area with intensive agricultural practices. The analysis of nitrate flux and total phosphorus flux in this study illustrated water discharge relation; this demonstrates the continuous transport of nitrate and phosphorus from basin runoff. Nitrogen and phosphorus, mainly from agricultural non-point sources (Jarvie et al., 1998; MRC, 2003). Estimates of nitrate loading from concentration and discharge data; however, these do not provide much information about sources. Further deep analysis would be required to identify nutrient sources (e.g., stable isotopes) that might be useful (Chang et al., 2002b).

The plans to build various large reservoirs to the Mekong mainstream and tributaries might trap a large part of the nutrients, particularly those bound to suspended sediments (Kummu et al., 2010). Yet, the MRC (2010) maintains that the dams may critically change the nutrient flushing conditions. Within the existing dams, the nitrate fluxes have dropped significantly aligned with water discharge in some specific years, which could be a consequence of sediment and nitrate flux being stored behind hydropower construction and operation of dams. For example, the Manwan Dam operating in 1993, Dachaoshan in 2001, Jinghong in 2008, and Xiaowan in 2009. The impact to lower sediment load can be seen from upper stations, Chiang Saen, Luang Prabang, Vientiane, Mukdahan, and the lowermost part at Pakse and Kratie.

The average annual nitrate yield in the upper 80% of the total Mekong River Basin was an estimated 202 kg/km^2/year. The major source of this high yield resulted from fertilization. However, other factors such as spatial variability in slope and surface runoff also affect nitrate yields. The nutrient load of the river was particularly high in the settlement and agricultural segments, where fertilizer usage is a common practice like in other river catchments, e.g. the Yangtze River of China, the Mississippi River of the North American, and the Pamba River in India (David and Gentry, 2000; David et al., 2016; Qu and Kroeze, 2012; Wang et al., 2009). The

TN yield of the Yangtze River was estimated to be about 1400 kg/km^2/yr (Tong et al., 2017) and haft of total nutrient flux to the coastal water of China (Qu and Kroeze, 2012), this not only the Yangtze is the largest basin area and river discharge in China but also the basin includes intensive agriculture. The second largest river in China, the Yellow River, also reported a considerably increasing quantity of nutrient inputs (with 25 kg/km^2/year of total nitrogen) to the basin due to economic development and fast population growth during the past 40 years (Wang et al., 2009).

From the overview of global nutrient export to the coastal zone by Dumont et al. (2005), DIN yields are 113.2 kgN/km^2/yr in the Amazon River, 172.5 kgN/km^2/yr in the Amur River, 136.9 kgN/km^2/yr in the Indus River, 43.1 kgN/km^2/yr in theYenisei, and 43.9 kgN/km^2/yr in the Parana River. Our result of mean annual nitrate yield (45.6 kgN/km^2/yr) of the Mekong River is comparable to reported yield for other major rivers in Asia and elsewhere.

7.3. Hydrology, Sediment and Nutrient Flux of the Mekong River-Tonle Sap System

The water discharge and water quality that represent the reverse system of Tonle Sap River was recorded at Prek Kdam station. From the observed water discharge at Prek Kdam, the reverse system started to change direction from Tonle Sap Lake towards the Mekong River in October. Generally, water flow from Mekong River into Tonle Sap Lake counted from 70 to 157 days per year and, on average 118 days per year between late May to end of September whereas the opposite direction from Tonle Sap Lake towards Mekong River varies annually from 209 days to 295 days on average 247 days per year in between October and April/May. The peak inflow discharge into the lake generally occurred in July and August, while the periods of peak discharge of Mekong River occurred in August and September at Chroy Changva station. Otherwise, peak outflow from the lake to Mekong River mainly took place a few months later, the peak inflow from October to December

From 1995 to 2000, the Tonle Sap contributed more sediment load to Mekong River than was deposited in the lake, on the average 0.65 Mt annually. However, the rate decreased, and then since 2001, an average net 1.35±0.7 Mt of sediment has been deposited in the lake annually. An assessment of water discharge and sediment loads variability of Mekong River and Tonle Sap system presented in this study helps clarify the exchange annual discharge and sediment load toward the Mekong River that Tonle Sap Lake provided sediment load to the Mekong system and delta annually 0.65±0.6 Mt from 1995 to 2000. However, since 2001 Tonle Sap Lake has become

a sediment sink for about 1.35±0.7 Mt annually, thereby reducing the annual sediment transport to the Mekong delta. This reduction in sediment supply compounds the threat to the delta from accelerated subsidence and sea-level rise (Pokhrel et al., 2018; Syvitski and Higgins, 2012). Decreased sediment loads to the delta and altered sediment transport processes will impact numerous livelihoods which depend on ecosystem services (Kondolf et al., 2018). The sudden change appears to be due to increased TSS concentrations from the Mekong to Tonle Sap Lake. The concentration of TSS in Kratie appears to have been largely unchanged. However, the river could have picked up sediment as it overflowed the wide floodplain, used for agriculture and thus exposed to erosion without the protection of native vegetation (Chea et al., 2016). The instream TSS levels in the lower part of the Mekong River are likely influenced by the interaction between land use/land cover, rainfall-runoff, and anthropogenic activities within the basin (Ly et al., 2020).

For the nutrient exchanging between Tonle Sap Lake and Mekong River, the amount of annual nitrate and TP flux from Tonle Sap Lake to the Mekong on average was approximately 34±13.8 kt/yr and 6.6±1.4 kt/yr. Furthermore, the amount of inflow nutrients to the lake from the Mekong amounted to 35.8±12.5 kt/yr of nitrate and 8.7±3.3 kt/yr of total phosphorus, respectively. The study also pointed out that Tonle Sap Lake was the nitrate sinks during 2000-2012 and 2007-2015 for total phosphorus. The amount of the nutrient input and output mentioned about, it would lead to conclude that Tonle Sap Lake gains in the amount of nutrients from the Mekong; in other words, the Mekong River plays the role of the source to Tonle Sap Lake and its floodplain.

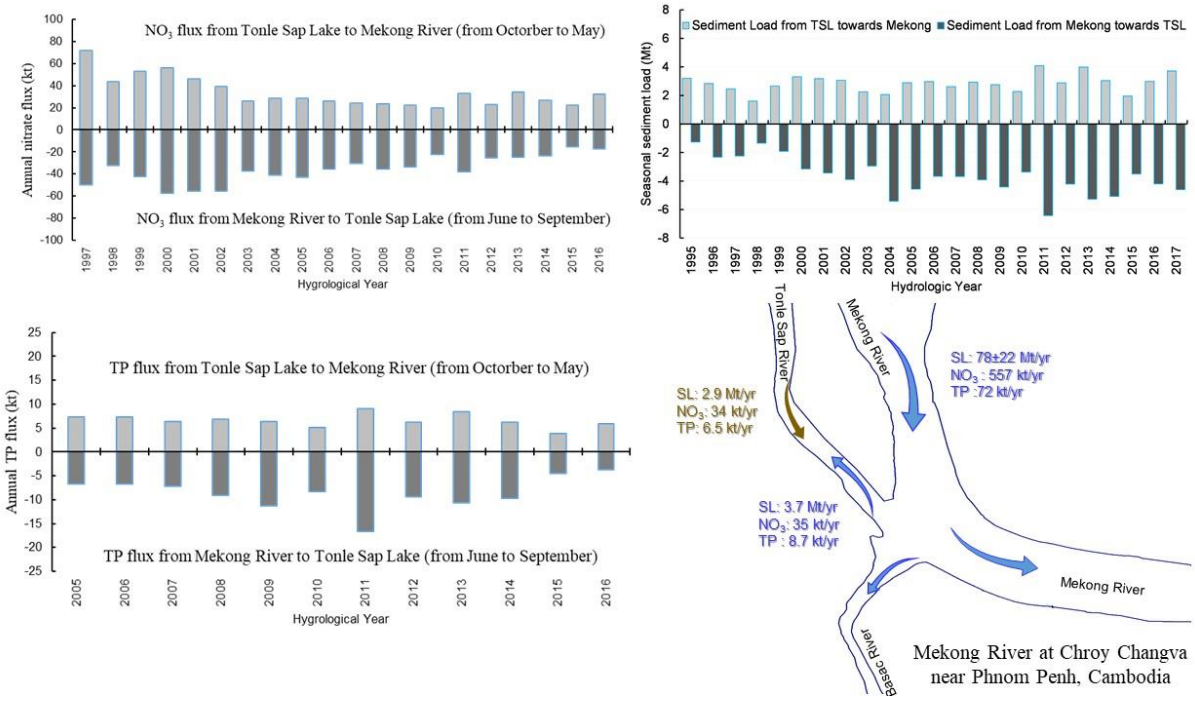

Figure 7-2: *Sediment and Nutrient flux (NO_3 and TP) of Mekong River at Chroy Changvar and the exchanging of Nutrient flux between Mekong River and Tonle Sap Lake through Tonle Sap River.*

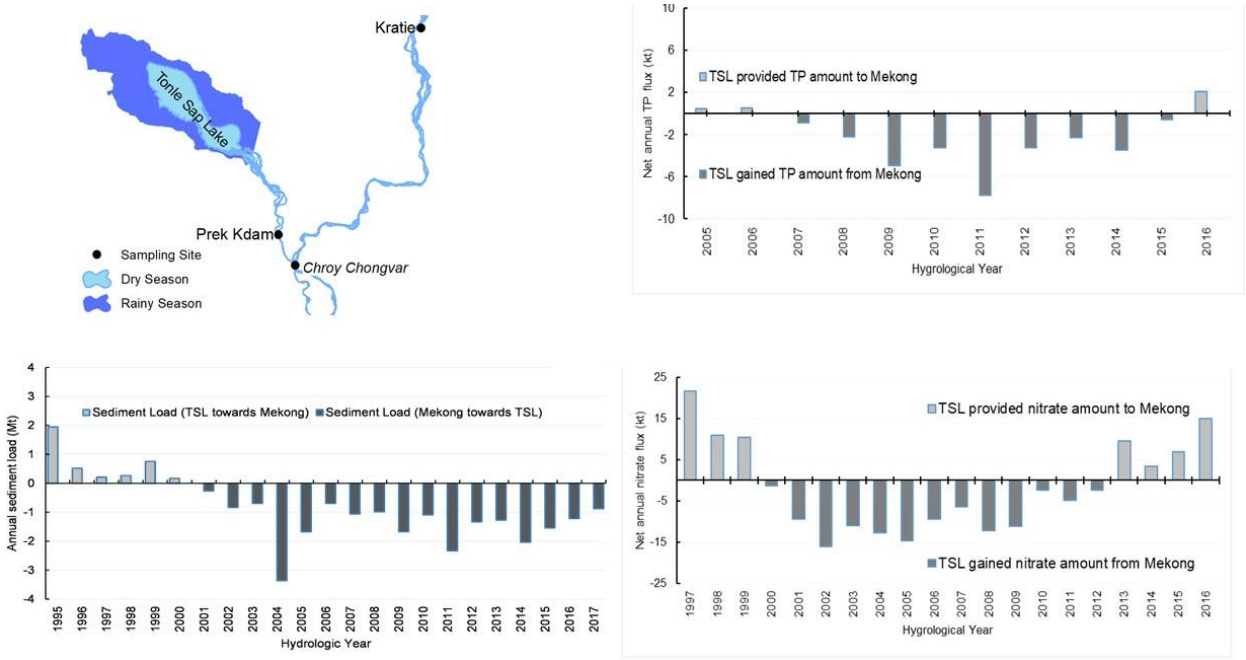

Figure 7-3: *Net balance of Sediment and Nutrient flux (NO_3 and TP) between Mekong River and Tonle Sap Lake through Tonle Sap River. The negative values is the annual source of sediment and nutrient while and negative value is the sink.*

The Tonle Sap is an example of a lake-channel system, a lake (usually on a floodplain) that connects with the main river (via defined channels and overbank flow), and that absorbs flood peaks and releases waters gradually back into the main river as flood stage recedes. Retaining floodwaters in the lake for extended periods can substantially deposition sediment from suspension, potentially impacting the riverine sediment budget. With its channel sized reverse flow pattern, combined with broad, shallow lateral inundation of floodplains during the wet season, the Tonle-Sap-Mekong exchange represents a uniquely developed and important channel-floodplain exchange. The Mekong-Tonle-Sap exchange is arguably among the best developed such river-floodplain-lake exchange systems in the world, and it supports a fishery that is globally exceptional in many respects (Campbell et al., 2009).

7.4. Role of Tonle Sap in the Mekong River

7.4.1. Hydrology Role

The role of Tonle Sap to the Mekong River can be in different context. The main themes for the hydrological roles of the Cambodian floodplain are (1) Mekong River Flood Reduction and (2) dry season flow augmentation. The study found the annual water inflow to the lake via reverse flow was 36 km^3, while outflow to the Mekong was 68 km^3. The great water outflow can be attributed to runoff from the Tonle Sap Lake basin and also flows across the floodplain lying to the west of the Mekong River. The outflow of the lake to Mekong play great important contribution to the base flow (~18% of the Mekong River flow) in the Mekong Delta downstream of Chaktumuk confluence from June to May of the year (Campbell et al., 2009).

As water levels fall following the end of the wet season, the water stored on the floodplain during the flood season augments the dry season flows. Following the end of the wet season rains, and as the Mekong River recedes from its flood levels, water again begins to flow from the Great Lake and the floodplains down the Tonle Sap River toward the sea, supplementing water flowing down from the upper Mekong. As the river level in the Mekong rises during the annual wet season, it eventually exceeds the water level in the Tonle Sap Great Lake causing the famous flow reversal in the Tonle Sap River. As water levels rise further in the Mekong upstream of Phnom Penh water also begins to flow overland across the floodplain toward the Tonle Sap Lake.

The storage of water around the lake and elsewhere on the floodplain during the wet season ameliorates flood levels from Phnom Penh downstream in the Mekong Delta (Campbell et al.,

2009). The annual water inflow to the lake via reverse flow was 36 km^3 (~10% of the Mekong River flow), began in late May to early June of the year which is during the flood season of the Mekong River. Moreover, during the flood season, there is overbank flow from the Mekong mainstem across floodplains into the lake with an estimated annual average of 2.6 km^3 (Lu et al., 2014b). Hydrologically the lake plays a key role in the lower Mekong as the regulator of the Mekong flood.

7.4.2. Sediment and Nutrient Supply Role

The Lower Mekong River showed a significant decrease in sediment load, consistent with trends documented in other major rivers in the region and globally. The seasonal and annual sediment load linkage between the Mekong mainstem and Tonle Sap Lake are controlled principally by suspended sediment concentrations and water discharge, in both the reverse flows into the lake and outflows from the lake, both via the Tonle Sap River. We can get the first estimates for the sediment dynamics between Mukdahan and the upstream boundary of the Mekong Delta. Moreover, part of that sediment might still end up in the floodplains from Phnom Penh towards the South China Sea. This is estimated to be approximately 6-10% of the sediment load transported in the river in Cambodian – Vietnam border (Manh et al., submitted).

The seasonal relationship between water flow and suspended sediment concentration in the Mekong River offers interesting insights into temporal patterns of sediment load. Sediment transport in most of the large river systems increases with precipitation and water discharge (Dionne, 1998) . For the Mekong River, since most of the sediment load was transported during the peak flood in August and September. The Tonle Sap Lake can absorb high sediment thought the peak flood of Mekong. The temporal variability of sediment transport in the Mekong River can be well explained by the variability of the water flow in the river.

Tonle Sap River contributed more sediment load to Mekong River than it received via reverse flows. While from the hydrological year 2001-2017, the Lake received more sediment from the Mekong River than it contributed. However, the sediment does not settle out evenly throughout the Tonle Sap system, but, instead, it is primarily trapped by the vegetation at the lake edge and in the floodplain (Kummu et al., 2008b). Among the international, national, and local observers, it is often stated that Tonle Sap Lake is rapidly filling up with the sediment. However, the rapid rates

of infilling are needed further study such as load from tributary, the re-suspension of sediment and dynamic phenomena within the lake itself for study detail sediment budget.

In terms of water quality, on average the nutrient concentration from Tonle Sap Lake to the Mekong River was lower than from Mekong to the lake. During flow direction from Tonle Sap Lake towards the Mekong River, nitrate concentration was 0.81±0.77 mg/L, and total phosphorus concentration was 0.11±0.07 mg/L. For flow from Mekong toward Tonle Sap Lake, nitrate concentration was 0.98±0.67 mg/L and for total phosphorus was 0.16±0.1 mg/L. Similarly, the Mekong shares the nitrate and total phosphorus flux to the lake higher than those from the lake to the Mekong. This result can conclude that Tonle Sap Lake gains in the amount of nutrients from the Mekong; in other words, the Mekong River plays the role of the source to Tonle Sap Lake and its floodplain.

As the role of the Mekong River in sediment nutrient supply to the lake, it also means that the Mekong River provides the primary element of lives for this world's productive ecosystem lake. On the other hand, if the nutrient concentration and flux in the Mekong River escalate, it can accelerate the environmental problem to the Tonle Sap Lake (i.e., eutrophication, causing by the excessive nutrient in the lake water column, that leads to imbalances among different biological processes and also on ecosystem function). Regarding these, the development and changes in the Mekong River Basin are also the concern and threat of the Tonle Sap Lake ecosystem, and it can be massive concern to the lake. While the changing in the lake basin consequently disturbs the downstream water quality, particularly the Mekong Delta, in somehow lower level that Mekong to the Tonle Sap Lake.

7.4.3. Tonle Sap Lake System, a Unique a Lake-Channel System

The Tonle Sap is an example of a lake-channel system, a lake (usually on a floodplain) that connects with a main river (via defined channels as well as overbank flow), and that absorbs flood peaks and releases waters gradually back into the main river as flood stage recedes. Retaining floodwaters in the lake for extended periods of time can result in substantial deposition of sediment from suspension, with potentially significant influences on the riverine sediment budget. Thus, we can ask how the Tonle Sap system compares with other major lake-channel systems, such as Dongting Lake on the Yangtze River floodplain, the second largest freshwater lake in China, and the channel-floodplain systems of the Amazon River. The Dongting Lake- Yangtze River system

is similar to the floodplain lake-channel exchanges of TSL and Mekong River, in that Dongting Lake plays an important role in regulating flood stage and is an important sink of sediments. The Amazon is characterized by strong exchanges of water, sediment, nutrients, and biota between channel and its extensive floodplains. The channel-floodplain systems of the Amazon River can act as important sinks of sediments, not only via channelized flow to the Lago Grand de Curuaı complex, but also via diffuse overbank flow. However, unlike the Amazon, most of the Mekong's course follows a narrow bedrock-controlled path, so there is very limited exchange of sediment between channel and floodplain, until the reach downstream at the Delta, where the floodplains of the Cambodian lowlands and the Mekong delta are inundated, allowing important fluxes of material and energy between the floodplain and mainstem river channel (Gupta and Liew, 2007). With its channel sized reverse flow pattern, combined with broad, shallow lateral inundation of floodplains during the wet season, the Tonle-Sap-Mekong exchange represents a uniquely developed and important channel-floodplain exchange. In fact, the Mekong-Tonle-Sap exchange is arguably among the best developed such river-floodplain-lake exchange systems in the world, and it supports a fishery that is globally exceptional in many aspects (Campbell et al., 2009).

The flood pulse system of Tonle Sap Lake is a unique system that control mainly by reverse flow of seasonal flood from Mekong River both by channel and by path, and its local tributaries. The reverse flow from the Mekong River enhances the magnitude and extent of the lake floods creating extensive floodplain areas. There is significant variation of inflow, outflow, surface area, and water volume in every hydrological year. The variation of the floodplain size (excluding the permanent lake area) is vary from 7190 km^2 to 12,720 km^2 (Kummu and Sarkkula, 2008). The water volume greatly differs seasonally, approximately 20-fold larger during the rainy season than the dry season (approx. 1.8 km^3 during the driest month to 58.3 km^3 during the peak water level) (Kummu and Sarkkula, 2008). These factors make the hydrodynamic behaviour of the lake to be highly dynamic and become a unique. Moreover, this unique hydrodynamic process is a critical factor in inducing active sediment-nutrient distribution throughout the lake and its floodplain. Intern of lake area and volume derive the Tonle Sap Lake become the largest freshwater lake in Southeast Asia and well known as a productive ecosystem lake in term of species richness.

7.5. Conceptual model for sediment and nutrient of Mekong Tonle Sap system

The management of sediment in large watershed such Mekong river facing a series of water impoundment requires the integration of various effective sediment management approaches and tools. There is a need to better understand integrated sediment management on reservoir sustainability for a large basin. The use of integrated or coupling sediment and water quality modelling frameworks can introduce model error due to the different theoretical assumptions and how the model is integrated or coupling. Therefore, there is a need to develop a single tool under the SWAT modelling framework for sediment, water quality, reservoir management, and other output, which can evaluate both catchment-level and reservoir-level sediment management options watershed development scenarios. A conceptual model that can be deal with the sediment and nutrient of Mekong Tonle Sap system from the study and ideal for further study.

7.5.1. Proposed Mekong-Tonle Sap system conceptual model

The Tonle Sap Lake acts as a natural reservoir for the Lower Mekong River Basin, regulating the floods downstream from Phnom Penh during the wet season and makes an important addition to the dry season flow to the Mekong Delta in Vietnam. Due to this unique phenomenon that the downstream of Kratie affected by the tidal influence and the buffering of the flood wave in the Tonle Sap Lake system, it would be necessary to set up the Mekong-Tonle Sap system conceptual model such as SWAT.

The implementation of hydrology and water quality requires continuous monitoring data and/or result, computational models being one of them to produce such result. Computational models offer many possibilities to enhance the understanding of ecosystems processes as well as enabling the investigation of the cause and consequences in various development scenarios. However, such model requires not only an understanding of cause and consequences of water quality change but also the capability of model and application technique. Integration of these very different technique can be aided by computational modelling. This is certainly the case for the Tonle Sap Lake where the complexity of the system. Driven by these challenges, the objectives of this conceptual model are to:

- Present and cover the current understanding of Mekong River. The certain outlet of the model will be used as the boundary input for Tonle Sap Lake hydrology, sediment and nutrient flux.
- Present the hydrological modelling tools developed for the Tonle Sap Lake, aiming to increase the understanding of exchanging figure of sediment and nutrient flux.
- Be able to create tools for predictions by hydrological model results with anthropogenic activities for further study under the global context.

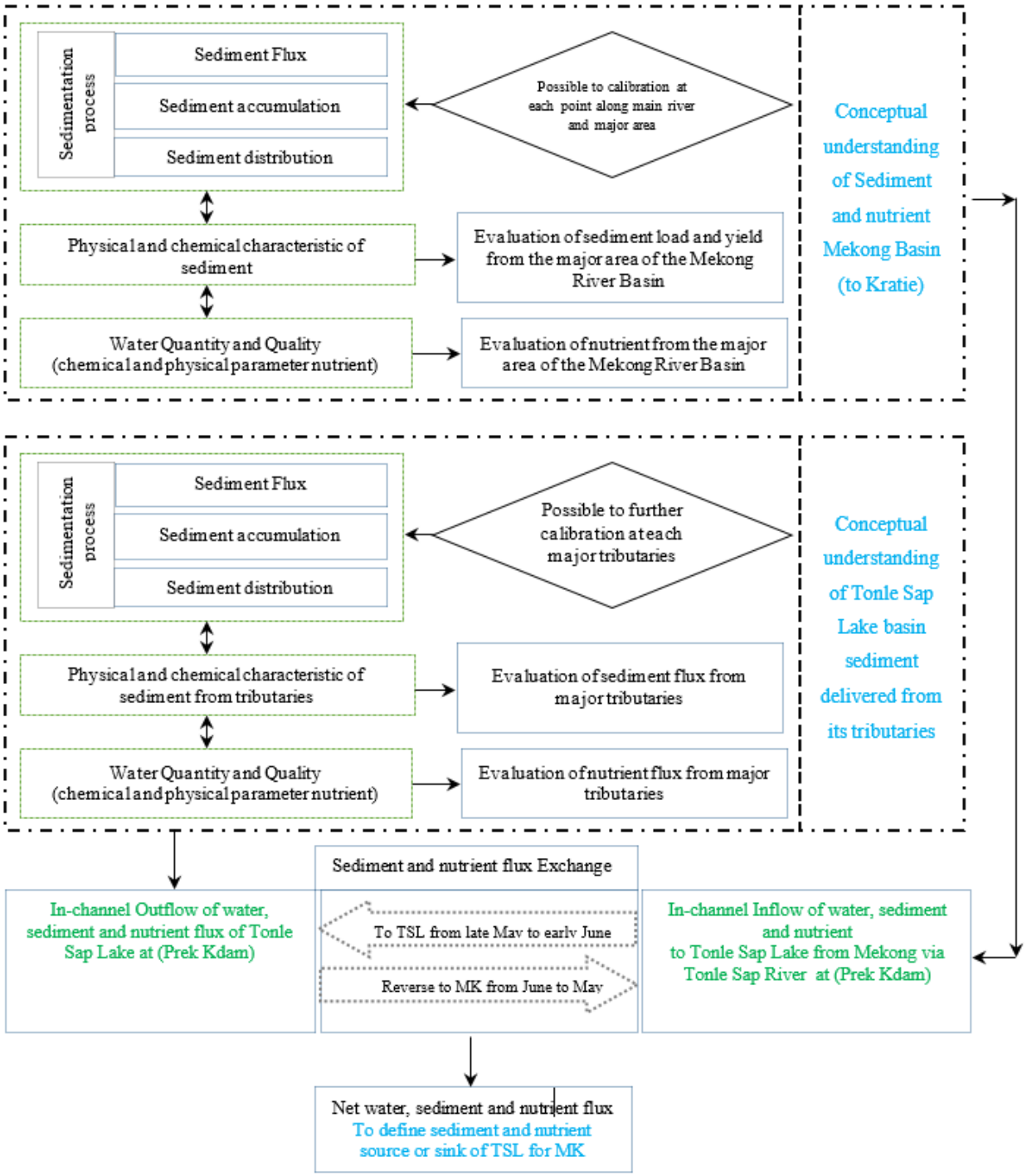

***Figure 7-4**: Proposed Mekong-Tonle Sap system conceptual model*

7.5.2. Proposed Process for SWAT Sediment Transport Model in Mekong River

To calibrate the SWAT sediment transport model for the area covered from Upper Mekong to down to Kratie, a new calibration process was proposed in this study as displayed in **Figure 7-5**. The idea, firstly the appropriate values for USLE_C in crop.dat file and USLE_P in *.mgt files will be assigned based on sound information, for example as reported in soil erosion in Forest area in Upper Mekong, extensive agricultural in Thailand, Central highland in Vietnam and overall sediment yield in whole basin based in the land use/land cover, slope…etc., and should not be later changed. However, due to the SWAT allows only one value of USLE_C to be assigned for the whole watershed, its appropriate value may be also obtained through calibration to represent for the average condition of crop management in the watershed. At this stage after the appropriate values of USLE_C have been applied, some calibration point will be skipped for further calibration unless the volume ratio of simulated and observed sediment loads is not sufficient close to 100%. The next step is to calibrate for the values of PRF, ADJ_PKR, SPCON and SPEXP in basins.bsn and the SWAT considers only one value per each parameter for the whole watershed. The R2 or COE may be improved and volume ratio may get closer to 100% by changing the values of USLE_K in *.sol and BIOMIX in *.mgt files. After this step if R^2 or volume ratio (less than 100%) still not be satisfied, the parameters concerning channel degradation i.e. CH_EROD and CH_COV in *.rte files will be considered in the final stage of model calibration. However, the maximum values of these two parameters will be limited by field experience.

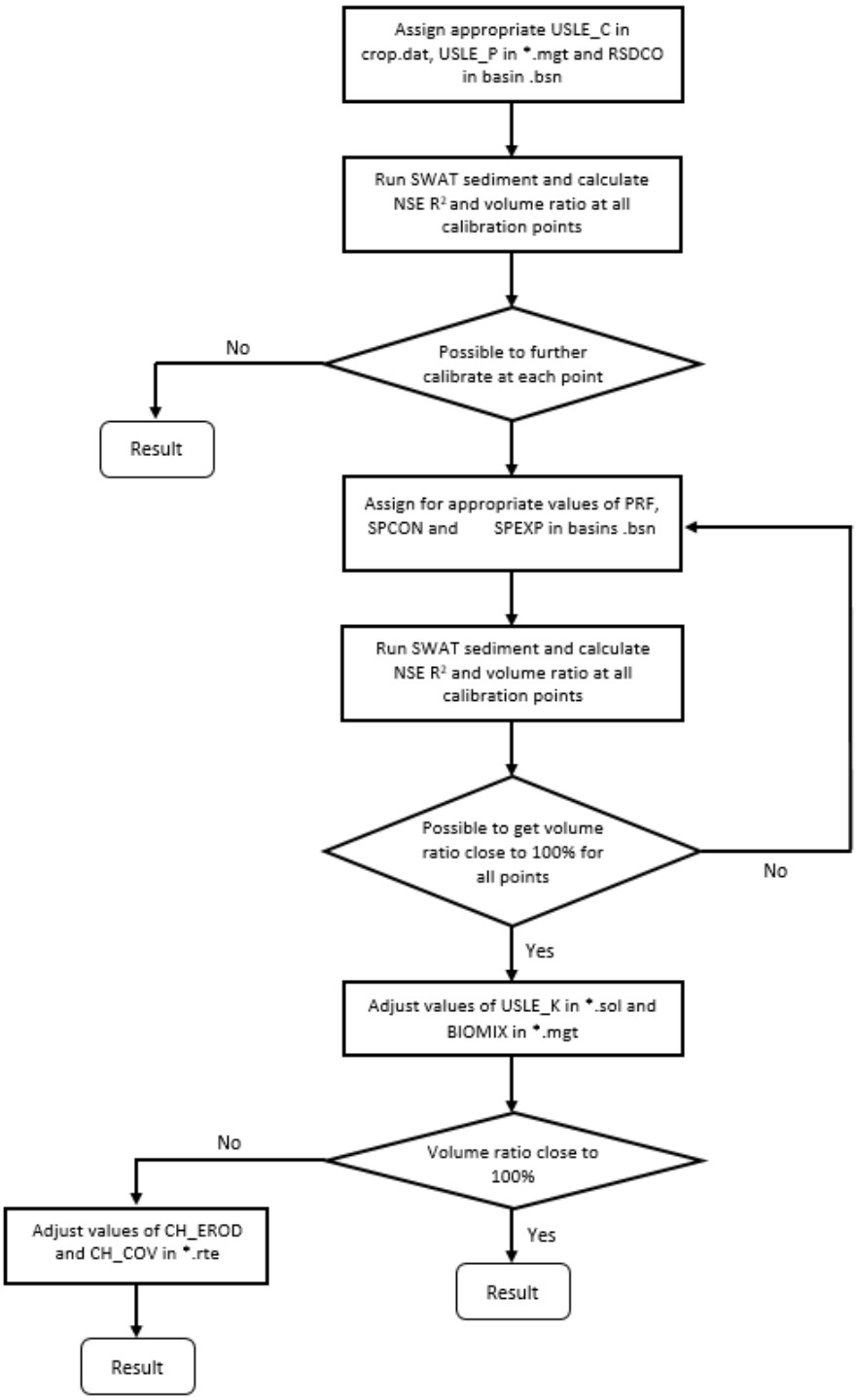

Figure 7-5: *New proposed process to calibrate the SWAT sediment transport model for the area covered from Upper Mekong to Kratie*

CHAPTER VIII

Conclusion and Perspectives

8. Chapter XIII. Conclusion and Perspectives

8.1. Conclusion

The study aims to understand the dynamic transport of the sediment and nutrient in the Mekong River Basin and the Tonle Sap's role through assessment coupling data and modelling approaches. This work improves and provides a better understanding of the sediment and nutrient in the Mekong River and the role of the Lake channel Role such as Tonle Sap Lake.

8.1.1. Hydrology, Sediment and Nutrient Flux of the Mekong River

For the Mekong river basin before entering the floodplain area and delta, the mean annual rainfall from 1985-2016 was 1540 mm; 67% (1032 mm) of the average annual rainfall was removed by evapotranspiration and 33% (508 mm) for the streamflow. The mean annual water yield of 404 $km^3\ yr^{-1}$ (with a mean annual water depth of 508 mm yr^{-1} and mean annual discharge of 12 684 $m^3\ s^{-1}$). The water yield of 508 mm has come from surface runoff (proportion of 34%), lateral flow (proportion of 21%), and groundwater (proportion of 45%). The groundwater is the main component for the river flow in the Mekong River basin, especially during the dry season. Compared to major rivers from the Tibetan Plateau, though the Mekong river basin's annual water discharge and yield are lower than the Yangtze Yellow, its annual water depth is the highest among these rivers but lower than Irrawaddy.

Mekong River is among the rivers that transport very large sediment load and have very large water discharge like the Yangtze and Pearl Rivers, Ganges, Brahmaputra, and Indus River originate from the Qinghai-Tibet Plateau. The recent sediment load of Mekong River before entering the Tonle Sap lake floodplain and Delta (75± 21 Mt from 1993-2017 at Kratie from 1985-2016) is lower than sediment load over longer time scales (144±34 Mt/year of long-term mean sediment load to the sea) which is consistent with pre-dam estimate. The sediment loads and yield of the Mekong River, same as the rest of Asian rivers, are mainly controlled by the climate, hydrology, vegetation, soil and geomorphology. In addition, the sediment dynamic in the Mekong River is majorly influenced by land cover and land use, which alters upland erosion processes. In addition, natural vegetation covers, such as the forests in Laos PDR and Cambodia, can decrease soil erosion at rates greater than those of agricultural areas in Thailand.

The mean annual nitrate flux of the Mekong River before entering the floodplain and delta (at Kratie, 361.8±83.5×10^3 t/year, from 1985-2016 could be comparable to other major Asian main rivers flowing into the coastal waters of China such as the Yangtze River, Yellow, Red River and Pearl. The average annual nitrate yield in the upper 80% of the total Mekong River Basin was an estimated 202 kg/km^2/year from 1985-2016. The major source of this high yield resulted from fertilization. However, other factors such as spatial variability in slope and surface runoff also affect nitrate yields.

8.1.2. Hydrology, Sediment and Nutrient Flux of the Mekong River-Tonle Sap System

The reverse system started to change direction from Tonle Sap Lake towards the Mekong River in October. Generally, water flow from Mekong River into Tonle Sap Lake counted from 70 to 157 days per year and, on average, 118 days per year between late May to end of September, whereas the opposite direction from Tonle Sap Lake towards Mekong River varies annually from 209 days to 295 days on average 247 days per year in between October and April/May.

From 1995 to 2000, the Tonle Sap contributed more sediment load to the Mekong River than was deposited in the lake, on an average of 0.65 Mt annually. However, the rate decreased, and then since 2001, an average net 1.35±0.7 Mt of sediment has been deposited in the lake annually. An assessment of water discharge and sediment loads variability of Mekong River and Tonle Sap system presented the Tonle Sap Lake has become a sediment sink for about 1.35±0.7 Mt annually. The study also highlighted that the fact that Tonle Sap is the sediment sink in the Mekong basin lead to a reduction in sediment supply, which compounds the threat to the delta from accelerated subsidence and sea-level rise. The study has emphasized the interaction role of Tonle Sap Lake and Mekong in nutrient supply for the Mekong delta

For the nutrient exchanging between Tonle Sap Lake and Mekong River, the amount of annual nitrate and TP flux from Tonle Sap Lake to the Mekong on average was approximately 34±13.8 kt/yr and 6.6±1.4 kt/yr. Furthermore, the amount of inflow nutrients to the lake from the Mekong amounted to 35.8±12.5 kt/yr of nitrate and 8.7±3.3 kt/yr of total phosphorus, respectively. The study also pointed out that Tonle Sap Lake was the nitrate sinks during 2000-2012 and 2007-2015 for total phosphorus. The amount of the nutrient input and output mentioned would lead to

conclude that Tonle Sap Lake gains in the amount of nutrients from the Mekong; in other words, the Mekong River plays the role of the source to Tonle Sap Lake and its floodplain.

8.1.3. Role of Tonle Sap in the Mekong River

The role of Tonle Sap in the Mekong River can be in a different context. The main themes for the hydrological roles of the Cambodian floodplain are Mekong River flood reduction and dry season flow augmentation. The great water inflow can be attributed to runoff from the Mekong to the Tonle Sap Lake basin across the Tonle Sap River channel, and floodplain lying to the west of the Mekong River (~10% of the annual Mekong River flow) significantly reduce the peak flow magnitude of Mekong. The outflow of the lake to the Mekong plays a great important contribution to the base flow (~18% of the Mekong River flow) in the Mekong Delta, downstream of Chaktumuk confluence from June to May of the year. Hydrologically, the lake plays a key role in the lower Mekong as the Mekong flood regulator and maintains the low flow to the Delta.

The sediment loads variability of the Mekong River and Tonle Sap system presented that Tonle Sap Lake has become a sediment sink (1.35±0.7 Mt annually), thereby reducing the annual sediment transport to the Mekong delta. The fact that Tonle Sap is the sediment sink in the Mekong basin lead to a reduction in sediment supply, which compounds the threat to the delta from accelerated subsidence and sea-level rise. The study has emphasized the interaction role of Tonle Sap Lake in nutrient supply for the Mekong delta that 34 kt/year of nitrate and 6.6 kt/year of total phosphorus were outflow from Tonle Sap.

8.2. Perspectives

For improving and cope with the uncertainty of the sediment and nutrient flux assessment through the monitoring data, sediment and water quality monitoring data from more stations along the main river and major tributaries, and more extended and high-frequency dataset (in depth-integrated sampling), longer time-series data will be helpful.

The management of sediment in large watershed such Mekong river facing a series of water impoundment requires the integration of various effective sediment management approaches and tools. There is a need to better understand integrated sediment management on reservoir sustainability for a large basin. The use of integrated or coupling sediment and water quality modelling frameworks can introduce model error due to the different theoretical assumptions and

how the model is integrated or coupling. Therefore, there is a need to develop a single tool under the SWAT modelling framework for sediment, water quality, reservoir management, and other output, which can evaluate both catchment-level and reservoir-level sediment management options watershed development scenarios.

Future studies of hydrology together with sediment and nutrients can be carried on based on this model. Also, scenarios of global changes, such as climate changes, land-use changes, new dam implementations in the future, can be done by this model. Furthermore, this model can be coupled with a delta model and then with a sea model to investigate the impacts of global changes on the biochemical function in the coast.

In the SWAT model, the sediment routing parameters (peak ratio factor, linear factor for channel sediment routing and Exponential factor for channel sediment routing) can only be applied to the entire watershed scale (one value for entire reaches). However, each tributary might have different sediment routing conditions depending geography and characteristic of each tributary. These sensitive parameters should be applied at a sub-basin or reach scale or stream order to improve the model performance. In this study, land use during this decade was not taken into account.

The input of sediment to the Tonle Sap Lake (TSL) is one of the key factors, together with the flood pulse, that contributes to the high productivity of the lake. Understanding the sources, load, and balance of sediment in the TSL is another important to address this concern. Thus, the further study shall focus on the sediment and nutrient input to Tonle Sap Lake system and partly supporting the study of interconnect and sediment/nutrient balance of the Lower Mekong River.

CONCLUSION GENERALE ET PERSPECTIVES

CONCLUSION GENERALE ET PERSPECTIVES

Conclusion

L'étude vise à comprendre le transport dynamique des sédiments et des nutriments dans le bassin du Mékong et le rôle du Tonlé Sap à travers des évaluations couplant données et modélisation. Ce travail améliore et fournit une meilleure compréhension des sédiments et des nutriments dans le fleuve Mékong et le rôle des lacs connectés tel que le lac Tonlé Sap.

Régime hydrologique, dynamique des sédiments et des nitrates du Mékong

Dans le bassin du Mékong en amont de la zone inondable et du delta, les précipitations annuelles moyennes de 1985 à 2016 étaient de 1 540 mm ; 67 % (1032 mm) des précipitations annuelles moyennes ont été éliminés par l'évapotranspiration et 33 % (508 mm) par l'écoulement fluvial. L'apport en eau annuel moyen de 404 km^3 an^{-1} (avec une profondeur d'eau annuelle moyenne de 508 mm an-1 et un débit annuel moyen de 12 684 m^3 s^{-1}). L'apport en eau de 508 mm provient du ruissellement de surface (proportion de 34 %), de l'écoulement latéral (proportion de 21 %) et des eaux souterraines (proportion de 45 %). Les eaux souterraines sont la principale composante du débit fluvial dans le bassin du Mékong, en particulier pendant la saison sèche. Par rapport aux grands fleuves du plateau tibétain, bien que le débit et le rendement annuel de l'eau du bassin du Mékong soient inférieurs à ceux du Yangtze et du fleuve Jaune Yellow, sa profondeur d'eau annuelle est la plus élevée mais inférieure à celle de l'Irrawaddy de Myanmar.

Le Mékong fait partie des fleuves qui transportent une très grande charge sédimentaire et qui ont un débit d'eau très fort, comme les fleuves Yangtze et Pearl, le Gange, le Brahmapoutre et l'Indus provenant du plateau Qinghai-Tibet. La charge sédimentaire actuelle du fleuve Mékong en amont de la plaine inondable et du delta (75 ± 21 Mt de 1993 à 2017 à Kratie) est plus faible que la charge sédimentaire sur des échelles de temps plus longues (144 ± 34 Mt/an de sédiments moyens à long terme se déversant dans la mer) ce qui est cohérent avec l'estimation pré-barrage. Les charges sédimentaires et le débit du Mékong, comme le reste des fleuves asiatiques, sont principalement contrôlés par le climat, l'hydrologie, la végétation, le sol et la géomorphologie. En outre, la dynamique des sédiments dans le Mékong est principalement influencée par la couverture et l'utilisation des terres, ce qui modifie les processus d'érosion. En outre, les couvertures végétales naturelles, telles que les forêts du Laos et du Cambodge, peuvent réduire l'érosion des sols à des taux supérieurs à ceux des zones agricoles dans Thaïlande.

Le flux annuel moyen de nitrate du Mékong avant d'entrer dans la plaine inondable et le delta (à Kratie, 361,8 ± 83,5 × 103 t/an, de 1985 à 2015) peut être comparer à ceux d'autres grands fleuves asiatiques se jetant dans les eaux de la mer de Chine, tels que le fleuve Yangtze, le fleuve Jaune, le fleuve Rouge et le fleuve du Perle. Le rendement annuel moyen en nitrate du bassin du Mékong en amont du delta est estimé à 202 kg/km^2/an, la principale source de ce rendement élevé étant la fertilisation. Cependant, d'autres facteurs tels que la variabilité spatiale de la pente et du ruissellement de surface affectent également les rendements en nitrate.

Hydrologie, flux de sédiments et de nutriments du système Mékong-Tonlé Sap

Le système inverse typique entre le lac Tonlé Sap et le fleuve Mékong change de sens en octobre. Généralement, le débit d'eau allant du Mékong vers le lac Tonlé Sap dure de 70 à 157 jours par an et, en moyenne, dont 118 jours par an entre fin mai et fin septembre, alors que le flux inverse allant du lac Tonlé Sap au fleuve Mékong varie annuellement de 209 jours à 295 jours en moyenne, dont 247 jours par an entre octobre et avril/mai.

De 1995 à 2000, le Tonlé Sap a apporté plus de charge sédimentaire au fleuve Mékong qu'il n'en a déposé dans le lac, ie. en moyenne 0,65 Mt par an. Cependant, ce taux a diminué au fil des années, puis depuis 2001, la moyenne annuelle nette en sédiments est de 1,35 ± 0,7 Mt déposée dans le lac. Une évaluation de la variabilité des débits d'eau et des charges sédimentaires du fleuve Mékong et du système Tonlé Sap a montré que le lac Tonlé Sap est devenu un puits de sédiments avec un stockage de 1,35 ± 0,7 Mt par an. L'étude a également souligné que le fait que Tonlé Sap soit un puits de sédiments dans le bassin du Mékong entraîne une réduction de l'apport en sédiments, ce qui menace delta d'un affaissement accéléré et d'une élévation du niveau de la mer. L'étude a également souligné le rôle des interactions du lac Tonlé Sap et du Mékong dans l'approvisionnement en nutriments du delta du Mékong.

Concernant les échanges de nutriments entre le lac Tonlé Sap et le fleuve Mékong, la quantité de flux annuel en nitrate et de phosphore total du lac Tonlé Sap au Mékong est respectivement en moyenne d'environ 34 ± 13,8 kt/an et 6,6 ± 1,4 kt/an. De plus, la quantité de nutriments entrants dans le lac en provenance du Mékong s'éleve à 35,8 ± 12,5 kt/an en nitrate et à 8,7 ± 3,3 kt/an en phosphore total, respectivement. L'étude a également souligné que le lac Tonlé Sap a été un puit de nitrate entre 2000-2012 et un puit en phosphore total 2007-2015. La quantification des apports et exports en éléments nutritifs évaluée dans cette étude a permis de conclure que le lac Tonlé Sap

reçoit des éléments nutritifs du Mékong ; en d'autres termes, le fleuve Mékong joue le rôle de source pour le lac Tonlé Sap et sa plaine inondable.

Rôle du Tonlé Sap dans le Mékong

Le rôle du Tonlé Sap dans le fleuve Mékong peut varier. La réduction des crues du Mékong et l'augmentation du débit en période d'étiage sont les principaux facteurs du comportement hydrologique de la plaine inondable cambodgienne. L'important afflux d'eau peut être attribué au ruissellement du Mékong vers le lac Tonlé Sap à travers le canal de la rivière Tonlé Sap, et la plaine inondable située à l'ouest du fleuve Mékong (~ 10% du débit annuel du fleuve Mékong) réduit considérablement l'impact du pic de crue du fleuve Mékong. L'écoulement du lac vers le fleuve Mékong contribue de façon importante au débit de base (~18% du débit du fleuve Mékong) dans le delta du Mékong, en aval du confluent Chaktumuk de juin à mai de l'année. Sur le plan hydrologique, le lac joue un rôle clé dans le bas Mékong en tant que régulateur des crues du Mékong et maintien d'un débit minimum durant l'étiage vers le delta.

La variabilité des charges sédimentaires du fleuve Mékong et du système Tonlé Sap a montré que le lac Tonlé Sap est un puits en sédiments (1,35 ± 0,7 Mt par an), réduisant ainsi le transport annuel en sédiments vers le delta du Mékong. Le fait que Tonlé Sap soit un puits en sédiments dans le bassin du Mékong a entraîné une réduction de l'apport de sédiments, ce qui menace le delta d'un affaissement accéléré et d'une élévation du niveau de la mer. L'étude a souligné le rôle du lac Tonlé Sap dans l'approvisionnement en éléments nutritifs du delta du Mékong, à savoir que 34 kt/an de nitrate et 6,6 kt/an de phosphore total quitte le lac Tonlé Sap.

Perspectives

Finalement, cette étude ouvre plusieurs perspectives. Des futures études en hydrologie ainsi que sur les sédiments et les nutriments peuvent être menées sur la base du modèle développé durant cette thèse. En outre, des scénarios de changements globaux, tels que les changements climatiques, les changements d'utilisation des sols, et la mise en place de nouveaux barrages, peuvent être testés par ce modèle. De plus, ce modèle peut être couplé à un modèle delta puis à un modèle marin pour étudier les impacts des changements globaux sur la fonction biochimique de la côte maritime. L'apport en sédiments au lac Tonlé Sap est l'un des facteurs clés, grâce à l'impulsion de crue, qui contribue à la productivité élevée du lac. Comprendre la dynamique des sédiments en terme d'apport, d'export et de stockage dans le bassin de lac Tonlé Sap est un autre élément important

pour répondre à cette préoccupation. Ainsi, la suite de cette étude pourra se concentrer sur l'apport de sédiments et de nutriments au système du lac Tonlé Sap et approfondir l'étude des interconnexions et du bilan sédiments/nutriments du cours d'eau aval du Mékong.

REFERENCES

References

Abbaspour, K.C., 2013. Swat-cup 2012. SWAT Calibration and uncertainty program—a user manual.

Adamson, P.T., Rutherfurd, I.D., Peel, M.C., Conlan, I.A., 2009. The hydrology of the Mekong River, The Mekong. Elsevier, pp. 53-76.

Arnold, J.G., Srinivasan, R., Muttiah, R.S., Williams, J.R.J.J.J.o.t.A.W.R.A., 1998. Large area hydrologic modeling and assessment part I: model development 1. 34, 73-89.

Arthurton, R.K. et al., Dynamics of the Coastal Zone.

Bannwarth, M. et al., 2015. Simulation of stream flow components in a mountainous catchment in northern Thailand with SWAT, using the ANSELM calibration approach. 29, 1340-1352.

Benaman, J., Shoemaker, C.A., Haith, D.A., 2005. Calibration and validation of soil and water assessment tool on an agricultural watershed in upstate New York. Journal of Hydrologic Engineering, 10, 363-374.

Bonnet, M.-P. et al., 2008. Floodplain hydrology in an Amazon floodplain lake (Lago Grande de Curuaí). 349, 18-30.

Bouraoui, F., Benabdallah, S., Jrad, A., Bidoglio, G.J.P., Chemistry of the Earth, P.A.B.C., 2005. Application of the SWAT model on the Medjerda river basin (Tunisia). 30, 497-507.

Cakir, R., Sauvage, S., Gerino, M., Volk, M., Sánchez-Pérez, J.M., 2020. Assessment of ecological function indicators related to nitrate under multiple human stressors in a large watershed. Ecological Indicators, 111, 106016.

Campbell, I.C., Say, S., Beardall, J., 2009. Tonle Sap Lake, the heart of the lower Mekong, The Mekong. Elsevier, pp. 251-272.

Carriquiry, J., Sánchez, A.J.M.G., 1999. Sedimentation in the Colorado River delta and Upper Gulf of California after nearly a century of discharge loss. 158, 125-145.

Chang, C.C., Kendall, C., Silva, S.R., Battaglin, W.A., Campbell, D.H., 2002a. Nitrate stable isotopes: tools for determining nitrate sources among different land uses in the Mississippi River Basin. Canadian Journal of Fisheries and Aquatic Sciences, 59, 1874-1885.

Chang, C.C. et al., 2002b. Nitrate stable isotopes: tools for determining nitrate sources among different land uses in the Mississippi River Basin. 59, 1874-1885.

Chebud, Y.A., Melesse, A.M.J.H.P.A.I.J., 2009. Modelling lake stage and water balance of Lake Tana, Ethiopia. 23, 3534-3544.

Chuenchum, P., Xu, M., Tang, W., 2020. Estimation of soil erosion and sediment yield in the Lancang–Mekong river using the modified revised universal soil loss equation and GIS techniques. Water, 12, 135.

Cohen, S., Kettner, A.J., Syvitski, J.P., Fekete, B.M.J.C., Geosciences, 2013. WBMsed, a distributed global-scale riverine sediment flux model: Model description and validation. 53, 80-93.

Commission, M.R., 2003. State of the Basin report. Mekong River Commission.

Conley, D.J. et al., 2009. Controlling eutrophication: nitrogen and phosphorus. 123, 1014-1015.

David, M.B., Gentry, L.E.J.J.o.E.Q., 2000. Anthropogenic inputs of nitrogen and phosphorus and riverine export for Illinois, USA. 29, 494-508.

David, S.E., Chattopadhyay, M., Chattopadhyay, S., Jennerjahn, T.C.J.S.o.t.T.E., 2016. Impact of human interventions on nutrient biogeochemistry in the Pamba River, Kerala, India. 541, 1420-1430.

Dawidek, J., Ferencz, B.J.H., Sciences, E.S., 2014. Water balance of selected floodplain lake basins in the Middle Bug River valley. 18, 1457-1465.

De Vente, J. et al., 2013. Predicting soil erosion and sediment yield at regional scales: where do we stand? , 127, 16-29.

Depetris, P.J., Pasquini, A.I., Lecomte, K.L., 2014. Weathering and the riverine denudation of continents. Springer.

Dessie, M. et al., 2015. Water balance of a lake with floodplain buffering: Lake Tana, Blue Nile Basin, Ethiopia. 522, 174-186.

Dionne, J.-C., 1998. Trenhaile, AS, 1997. Coastal Dynamics and Landforms. Clarendon Press, Oxford University Press, Oxford et New York, 366 p., 156 fig., 24 tabl., 19 x 25, 5 cm, cartonné, 195$ can. ISBN 0-19-823353-1. Géographie physique et Quaternaire, 52, 395-395.

Douglas-Mankin, K., Srinivasan, R., Arnold, J.J.T.o.t.A., 2010. Soil and Water Assessment Tool (SWAT) model: Current developments and applications. 53, 1423-1431.

Duan, S. et al., 2008. Seasonal changes in nitrogen and phosphorus transport in the lower Changjiang River before the construction of the Three Gorges Dam. 79, 239-250.

Duan, S., Xu, F., Wang, L.-J.J.B., 2007. Long-term changes in nutrient concentrations of the Changjiang River and principal tributaries. 85, 215-234.

Dudgeon, D. et al., 2006. Freshwater biodiversity: importance, threats, status and conservation challenges. 81, 163-182.

Dumont, E., Harrison, J., Kroeze, C., Bakker, E., Seitzinger, S.J.G.B.C., 2005. Global distribution and sources of dissolved inorganic nitrogen export to the coastal zone: Results from a spatially explicit, global model. 19.

Entwistle, N., Heritage, G., Schofield, L.A., Williamson, R.J.C., 2019. Recent changes to floodplain character and functionality in England. 174, 490-498.

Evans, A.E., Hanjra, M.A., Jiang, Y., Qadir, M., Drechsel, P.J.I.J.o.W.R.D., 2012. Water quality: assessment of the current situation in Asia. 28, 195-216.

Fanos, A.M.J.J.o.C.R., 1995. The impact of human activities on the erosion and accretion of the Nile Delta coast. 821-833.

FAO, 2003. Review of World Water Resources by Country. No. 23, FAO: Rome, Italy.

Faramarzi, M. et al., 2013. Modeling impacts of climate change on freshwater availability in Africa. 480, 85-101.

Fen-Li, Z., 2005. Effects of accelerated soil erosion on soil nutrient loss after deforestation on the Loess Plateau. 707-715.

Fierer, N.G., Gabet, E.J.J.J.o.E.Q., 2002. Carbon and nitrogen losses by surface runoff following changes in vegetation. 31, 1207-1213.

Funk, A. et al., 2019. Identification of conservation and restoration priority areas in the Danube River based on the multi-functionality of river-floodplain systems. 654, 763-777.

Galipeau, B.A., Ingman, M., Tilt, B.J.H.E., 2013. Dam-induced displacement and agricultural livelihoods in China's Mekong Basin. 41, 437-446.

Galloway, J.N. et al., 2004. Nitrogen cycles: past, present, and future. 70, 153-226.

Gordeev, V.J.G., 2006. Fluvial sediment flux to the Arctic Ocean. 80, 94-104.

Graham, D.N., Butts, M.B.J.W.m., 2005. Flexible, integrated watershed modelling with MIKE SHE. 849336090, 245-272.

Grigg, B., Southwick, L., Fouss, J., Kornecki, T.J.T.o.t.A., 2004. Climate impacts on nitrate loss in drainage waters from a southern alluvial soil. 47, 445.

Gupta, H.V., Kling, H., Yilmaz, K.K., Martinez, G.F., 2009. Decomposition of the mean squared error and NSE performance criteria: Implications for improving hydrological modelling. Journal of hydrology, 377, 80-91.

Herdendorf, C.E.J.J.o.G.L.R., 1982. Large lakes of the world. 8, 379-412.

Howden, N., Burt, T., 2009. Statistical analysis of nitrate concentrations from the Rivers Frome and Piddle (Dorset, UK) for the period 1965–2007. Ecohydrology, 2, 55-65.

Hu, J., Li, S., 2009. Modeling the mass fluxes and transformations of nutrients in the Pearl River Delta, China. Journal of Marine Systems, 78, 146-167.

Hua-rong, Y., Zhi-feng, Y., Bao-shan, C., 2006. Spatial analysis on soil erosion of Lancang River Watershed in Yunnan Province under the support of GIS. 地理研究, 25, 421-429.

Hua, W. et al., 2019. Dynamics of nutrient export from the Yangtze River to the East China sea. Estuarine, Coastal and Shelf Science, 229, 106415.

Jarvie, H., Whitton, B., Neal, C., 1998. Nitrogen and phosphorus in east coast British rivers: speciation, sources and biological significance. Science of the Total environment, 210, 79-109.

Jennerjahn, T. et al., 2004. Biogeochemistry of a tropical river affected by human activities in its catchment: Brantas River estuary and coastal waters of Madura Strait, Java, Indonesia. 60, 503-514.

Karim, F. et al., 2015. Assessing the impacts of climate change and dams on floodplain inundation and wetland connectivity in the wet–dry tropics of northern Australia. 522, 80-94.

Khafagy, A., Naffaa, M., Fanos, A., Dean, R., 1993. Nearshore coastal changes along the Nile Delta shores, Coastal Engineering 1992, pp. 3260-3272.

Khaki, M., Awange, J.J.S.o.T.T.E., 2019. Improved remotely sensed satellite products for studying Lake Victoria's water storage changes. 652, 915-926.

Kleinman, P.J. et al., 2006. Role of rainfall intensity and hydrology in nutrient transport via surface runoff. 35, 1248-1259.

Kondolf, G.M. et al., 2018a. Changing sediment budget of the Mekong: Cumulative threats and management strategies for a large river basin. Science of the total environment, 625, 114-134.

Kondolf, G.M. et al., 2018b. Changing sediment budget of the Mekong: Cumulative threats and management strategies for a large river basin. 625, 114-134.

Krause, S., Bronstert, A., Zehe, E.J.J.o.h., 2007. Groundwater–surface water interactions in a North German lowland floodplain–implications for the river discharge dynamics and riparian water balance. 347, 404-417.

Krysanova, V., White, M.J.H.S.J., 2015. Advances in water resources assessment with SWAT—an overview. 60, 771-783.

Kummu, M., Lu, X., Wang, J., Varis, O.J.G., 2010. Basin-wide sediment trapping efficiency of emerging reservoirs along the Mekong. 119, 181-197.

Kummu, M., Penny, D., Sarkkula, J., Koponen, J., 2008a. Sediment: curse or blessing for Tonle Sap Lake? AMBIO: A Journal of the Human Environment, 37, 158-163.

Kummu, M., Penny, D., Sarkkula, J., Koponen, J.J.A.A.J.o.t.H.E., 2008b. Sediment: curse or blessing for Tonle Sap Lake? , 37, 158-163.

Kummu, M. et al., 2014. Water balance analysis for the Tonle Sap Lake–floodplain system. 28, 1722-1733.

Kummu, M., Varis, O., 2007. Sediment-related impacts due to upstream reservoir trapping, the Lower Mekong River. Geomorphology, 85, 275-293.

Kuzin, V., Platov, G., Golubeva, E.J.I., Atmospheric, Physics, O., 2010. Influence that interannual variations in Siberian river discharge have on redistribution of freshwater fluxes in Arctic Ocean and North Atlantic. 46, 770-783.

Lane, L.J., Nichols, M.H., Levick, L.R., Kidwell, M.R., 2001. A simulation model for erosion and sediment yield at the hillslope scale, Landscape erosion and evolution modeling. Springer, pp. 201-237.

Lane, R.R. et al., 2004. Changes in stoichiometric Si, N and P ratios of Mississippi River water diverted through coastal wetlands to the Gulf of Mexico. 60, 1-10.

Lauri, H. et al., 2012. Future changes in Mekong River hydrology: impact of climate change and reservoir operation on discharge. Hydrology and Earth System Sciences, 16, 4603-4619.

Le, T.P.Q., Billen, G., Garnier, J., 2015. Long-term biogeochemical functioning of the Red River (Vietnam): past and present situations. Regional Environmental Change, 15, 329-339.

Li, J., Li, T., Liu, S., Shi, H., 2018. An efficient method for mapping high-resolution global river discharge based on the algorithms of drainage network extraction. Water, 10, 533.

Li, S., Bush, R.T., 2015a. Rising flux of nutrients (C, N, P and Si) in the lower Mekong River. Journal of Hydrology, 530, 447-461.

Li, S., Bush, R.T.J.J.o.H., 2015b. Rising flux of nutrients (C, N, P and Si) in the lower Mekong River. 530, 447-461.

Li, Y., Chen, B.-M., Wang, Z.-G., Peng, S.-L.J.H.S.J., 2011. Effects of temperature change on water discharge, and sediment and nutrient loading in the lower Pearl River basin based on SWAT modelling. 56, 68-83.

Li, Y., Wang, C., Tang, H.J.A.E.H., Management, 2006. Research advances in nutrient runoff on sloping land in watersheds. 9, 27-32.

Li, Y. et al., 2019a. Hydrodynamic investigation of surface hydrological connectivity and its effects on the water quality of seasonal lakes: insights from a complex floodplain setting (Poyang Lake, China). 660, 245-259.

Li, Y., Zhang, Q., Liu, X., Tan, Z., Yao, J.J.J.o.H., 2019b. The role of a seasonal lake groups in the complex Poyang Lake-floodplain system (China): Insights into hydrological behaviors. 578, 124055.

Li, Y., Zhang, Q., Liu, X., Yao, J.J.S.o.T.T.E., 2020. Water balance and flashiness for a large floodplain system: A case study of Poyang Lake, China. 710, 135499.

Liljeström, I., Kummu, M., Varis, O.J.I.j.o.w.r.d., 2012. Nutrient balance assessment in the Mekong Basin: nitrogen and phosphorus dynamics in a catchment scale. 28, 373-391.

Liu, S. et al., 2001. Regional variation of sediment load of Asian rivers flowing into the ocean. Science in China Series B: Chemistry, 44, 23-32.

Liu, S.M. et al., 2003. Nutrients in the Changjiang and its tributaries. 62, 1-18.

Lu, X., Kummu, M., Oeurng, C.J.E.S.P., Landforms, 2014. Reappraisal of sediment dynamics in the Lower Mekong River, Cambodia. 39, 1855-1865.

Ludwig, W., Bouwman, A., Dumont, E., Lespinas, F.J.G.b.c., 2010. Water and nutrient fluxes from major Mediterranean and Black Sea rivers: Past and future trends and their implications for the basin-scale budgets. 24.

Ludwig, W., Dumont, E., Meybeck, M., Heussner, S.J.P.i.o., 2009. River discharges of water and nutrients to the Mediterranean and Black Sea: major drivers for ecosystem changes during past and future decades? , 80, 199-217.

Ludwig, W., Probst, J.-L.J.A.J.o.S., 1998. River sediment discharge to the oceans; present-day controls and global budgets. 298, 265-295.

Lweendo, M.K., Lu, B., Wang, M., Zhang, H., Xu, W., 2017. Characterization of Droughts in Humid Subtropical Region, Upper Kafue River Basin (Southern Africa). 9, 242.

Martínková, M., Hesse, C., Krysanova, V., Vetter, T., Hanel, M., 2011. Potential impact of climate change on nitrate load from the Jizera catchment (Czech Republic). Physics and Chemistry of the Earth, Parts A/B/C, 36, 673-683.

Mekonnen, M.M., Hoekstra, A.Y., 2018a. Global anthropogenic phosphorus loads to freshwater and associated grey water footprints and water pollution levels: A high-resolution global study. Water resources research, 54, 345-358.

Mekonnen, M.M., Hoekstra, A.Y.J.W.r.r., 2018b. Global anthropogenic phosphorus loads to freshwater and associated grey water footprints and water pollution levels: A high-resolution global study. 54, 345-358.

Meybeck, M.J.A.J.S., 1982. Carbon, nitrogen, and phosphorus transport by world rivers. 282, 401-450.

Mikhailova, M.J.W.R., 2003. Transformation of the Ebro River Delta under the impact of intense human-induced reduction of sediment runoff. 30, 370-378.

Milliman, J., Farnsworth, K.J.R.d.t.t.c.o.a.g.s., Cambridge University Press, Cambridge, UK, 2011. Runoff, erosion, and delivery to the coastal ocean. 13-69.

Milliman, J.D., Syvitski, J.P.J.T.j.o.G., 1992. Geomorphic/tectonic control of sediment discharge to the ocean: the importance of small mountainous rivers. 100, 525-544.

Moran, E.F., Lopez, M.C., Moore, N., Müller, N., Hyndman, D.W.J.P.o.t.N.A.o.S., 2018. Sustainable hydropower in the 21st century. 115, 11891-11898.

Moriasi, D.N. et al., 2007. Model evaluation guidelines for systematic quantification of accuracy in watershed simulations. Transactions of the ASABE, 50, 885-900.

Moriasi, D.N., Gitau, M.W., Pai, N., Daggupati, P., 2015. Hydrologic and water quality models: Performance measures and evaluation criteria. Transactions of the ASABE, 58, 1763-1785.

MRC, 2003. State of the basin report. Mekong River Commission.

Müller, B., Berg, M., Pernet-Coudrier, B., Qi, W., Liu, H.J.G.b.c., 2012. The geochemistry of the Yangtze River: Seasonality of concentrations and temporal trends of chemical loads. 26.

Nash, J.E., Sutcliffe, J.V., 1970. River flow forecasting through conceptual models part I—A discussion of principles. Journal of hydrology, 10, 282-290.

Oeurng, C., Cochrane, T.A., Arias, M.E., Shrestha, B., Piman, T., 2016. Assessment of changes in riverine nitrate in the Sesan, Srepok and Sekong tributaries of the Lower Mekong River Basin. Journal of Hydrology: Regional Studies, 8, 95-111.

Olivera, F. et al., 2006. ARCGIS-SWAT: A GEODATA MODEL AND GIS INTERFACE FOR SWAT 1. 42, 295-309.

Ollesch, G., Kistner, I., Meissner, R., Lindenschmidt, K.-E.J.C., 2006. Modelling of snowmelt erosion and sediment yield in a small low-mountain catchment in Germany. 68, 161-176.

Ovando, A. et al., 2018. Multi-temporal flood mapping and satellite altimetry used to evaluate the flood dynamics of the Bolivian Amazon wetlands. 69, 27-40.

Pandey, A., Himanshu, S.K., Mishra, S., Singh, V.P.J.C., 2016. Physically based soil erosion and sediment yield models revisited. 147, 595-620.

Peng, J., Chen, S., Dong, P.J.C., 2010. Temporal variation of sediment load in the Yellow River basin, China, and its impacts on the lower reaches and the river delta. 83, 135-147.

Peng, J., Li, D., Zhang, Y., 2007. Analysis of spatial characteristics of soil erosion in mountain areas of northwestern Yunnan based on GIS and RUSLE. Journal of Mountain Science, 25, 548-556.

Qu, H.J., Kroeze, C.J.R.E.C., 2012. Nutrient export by rivers to the coastal waters of China: management strategies and future trends. 12, 153-167.

Raymond, P.A., Oh, N.-H., Turner, R.E., Broussard, W.J.N., 2008. Anthropogenically enhanced fluxes of water and carbon from the Mississippi River. 451, 449-452.

Reid, D.F., Beeton, A.M.J.G., 1992. Large lakes of the world: A global science opportunity. 28, 67-72.

Rex, W., Foster, V., Lyon, K., Bucknall, J., Liden, R., 2014. Supporting hydropower: An overview of the World Bank Group's engagement.

Robinson, S.J. et al., 2015. Statistical description of wetland hydrological connectivity to the River Murray in South Australia under both natural and regulated conditions. 531, 929-939.

Rudorff, C.M., Melack, J.M., Bates, P.D.J.W.R.R., 2014. Flooding dynamics on the lower Amazon floodplain: 2. Seasonal and interannual hydrological variability. 50, 635-649.

Runkel, R.L., Crawford, C.G., Cohn, T.A., 2004. Load Estimator (LOADEST): A FORTRAN program for estimating constituent loads in streams and rivers. 2328-7055.

Santhi, C. et al., 2001. Validation of the swat model on a large rwer basin with point and nonpoint sources 1. 37, 1169-1188.

Schuol, J., Abbaspour, K.C., Srinivasan, R., Yang, H.J.J.o.h., 2008. Estimation of freshwater availability in the West African sub-continent using the SWAT hydrologic model. 352, 30-49.

Seitzinger, S., Harrison, J., Dumont, E., Beusen, A.H., Bouwman, A., 2005a. Sources and delivery of carbon, nitrogen, and phosphorus to the coastal zone: An overview of Global Nutrient Export from Watersheds (NEWS) models and their application. Wiley Online Library.

Seitzinger, S. et al., 2010a. Global river nutrient export: A scenario analysis of past and future trends. Global Biogeochemical Cycles, 24.

Seitzinger, S.P., Harrison, J.A., Dumont, E., Beusen, A.H., Bouwman, A., 2005b. Sources and delivery of carbon, nitrogen, and phosphorus to the coastal zone: An overview of Global Nutrient Export from Watersheds (NEWS) models and their application. Global Biogeochemical Cycles, 19.

Seitzinger, S.P. et al., 2010b. Global river nutrient export: A scenario analysis of past and future trends. 24.

Shen, Z.-L., Liu, Q., 2009. Nutrients in the changjiang river. Environmental monitoring and assessment, 153, 27-44.

Shrestha, B., Cochrane, T.A., Caruso, B.S., Arias, M.E., 2018. Land use change uncertainty impacts on streamflow and sediment projections in areas undergoing rapid development: A case study in the Mekong Basin. 29, 835-848.

Sok, T., Oeurng, C., Ich, I., Sauvage, S., Miguel Sánchez-Pérez, J.J.W., 2020. Assessment of Hydrology and Sediment Yield in the Mekong River Basin Using SWAT Model. 12, 3503.

Stevens, C.J., Dise, N.B., Mountford, J.O., Gowing, D.J.J.S., 2004. Impact of nitrogen deposition on the species richness of grasslands. 303, 1876-1879.

Supit, C., Ohgushi, K., 2012. Dam construction impacts on stream flow and nutrient transport in Kase River Basin. International Journal of Civil & Environmental Engineering, 12, 1-5.

Syvitski, J.P. et al., 2005a. Dynamics of the coastal zone, Coastal Fluxes in the anthropocene. Springer, pp. 39-94.

Syvitski, J.P. et al., 2009. Sinking deltas due to human activities. 2, 681-686.

Syvitski, J.P., Kettner, A.J.P.T.o.t.R.S.A.M., Physical, Sciences, E., 2011. Sediment flux and the Anthropocene. 369, 957-975.

Syvitski, J.P., Vörösmarty, C.J., Kettner, A.J., Green, P.J.s., 2005b. Impact of humans on the flux of terrestrial sediment to the global coastal ocean. 308, 376-380.

Takamatsu, M., Kawasaki, A., Rogers, P.P., Malakie, J.L., 2014. Development of a land-use forecast tool for future water resources assessment: case study for the Mekong River 3S Sub-basins. Sustainability science, 9, 157-172.

Tan, M.L., Gassman, P.W., Srinivasan, R., Arnold, J.G., Yang, X., 2019. A Review of SWAT Studies in Southeast Asia: Applications, Challenges and Future Directions. 11, 914.

Thomas, R.F. et al., 2015. Mapping inundation in the heterogeneous floodplain wetlands of the Macquarie Marshes, using Landsat Thematic Mapper. 524, 194-213.

Tong, Y. et al., 2017. Estimation of nutrient discharge from the Yangtze River to the East China Sea and the identification of nutrient sources. 321, 728-736.

Turner, B.L., Chudek, J.A., Whitton, B.A., Baxter, R.J.B., 2003. Phosphorus composition of upland soils polluted by long-term atmospheric nitrogen deposition. 65, 259-274.

Turner, R.E., Rabalais, N.N.J.N., 1994. Coastal eutrophication near the Mississippi river delta. 368, 619-621.

Ty, S., Oeurng, C., Sauvage, S., KONDOL, G.M., SÁNCHEZ-PÉREZ, J.M.J.A.P., 2020. Temporal Variability of Sediment Load in the Tonle Sap and Lower Mekong Rivers, Cambodia.

van der Most, M., Hudson, P.F.J.G., 2018. The influence of floodplain geomorphology and hydrologic connectivity on alligator gar (Atractosteus spatula) habitat along the embanked floodplain of the Lower Mississippi River. 302, 62-75.

Vörösmarty, C.J. et al., 2003. Anthropogenic sediment retention: major global impact from registered river impoundments. 39, 169-190.

Wainwright, J., Parsons, A.J., Schlesinger, W.H., Abrahams, A.D.J.J.o.A.E., 2002. Hydrology–vegetation interactions in areas of discontinuous flow on a semi-arid bajada, southern New Mexico. 51, 319-338.

Walling, D., Fang, D.J.G., change, p., 2003. Recent trends in the suspended sediment loads of the world's rivers. 39, 111-126.

Walling, D.J.G., 2006. Human impact on land–ocean sediment transfer by the world's rivers. 79, 192-216.

Wang, H. et al., 2007. Stepwise decreases of the Huanghe (Yellow River) sediment load (1950–2005): Impacts of climate change and human activities. 57, 331-354.

Wang, J.J., Lu, X., Kummu, M., 2011. Sediment load estimates and variations in the Lower Mekong River. River Research and Applications, 27, 33-46.

Wang, X. et al., 2009. Simulation of nitrogen contaminant transportation by a compact difference scheme in the downstream Yellow River, China. 14, 935-945.

Wassen, M.J., Venterink, H.O., Lapshina, E.D., Tanneberger, F.J.N., 2005. Endangered plants persist under phosphorus limitation. 437, 547-550.

Wei, X. et al., 2019. A modeling approach to diagnose the impacts of global changes on discharge and suspended sediment concentration within the Red River Basin. Water, 11, 958.

Wu, G. et al., 2019. Riverine nutrient fluxes and environmental effects on China's estuaries. Science of The Total Environment, 661, 130-137.

Wu, Y., Chen, J.J.F.o.E.S.i.C., 2009. Simulation of nitrogen and phosphorus loads in the Dongjiang River basin in South China using SWAT. 3, 273-278.

Yang, S. et al., 2006. Drastic decrease in sediment supply from the Yangtze River and its challenge to coastal wetland management. 33.

Yao, H., Yang, Z., Cui, B., 2005. Soil erosion and its environmental background at Lancang Basin of Yunnan Province. Bulletin of Soil and Water Conservation, 25, 5-14.

Yoshimura, C. et al., 2009. 2020s scenario analysis of nutrient load in the Mekong River Basin using a distributed hydrological model. Science of the total Environment, 407, 5356-5366.

Yu, D., Pan, Y., Long, Z., Wang, Y., Liu, X., 2006. Value evaluation of conserving water and soil for ecosystem supported by remote sensed technique in Yunan province. J. Soil Water Conserv, 20, 174-178.

Abstract

The Asian river basins are great contributors to sediments and nutrient to the seas. These rivers are subject to the influence of climate variability and human activities, which alter the nutrient transport and fate of water quality. The Mekong River is a transboundary river in Southeast Asia and plays an important role in economy, agriculture and also by contributing fluxes into the Mekong delta and into the sea. Within the Mekong basin, the Tonle Sap area is a complex system with a unique reverse flow between Tonle Sap Lake and the Mekong River. Sediment and nutrient in the Mekong River are important to sustain the geomorphology of the floodplains and particularly the Tonle Sap Lake. At the same time, Tonle Sap Lake are contributing the sediment and nutrient for the Mekong delta. Therefore, the sediment and nutrient assessment in the Mekong River and its linkage between the Mekong mainstream and the Tonle Sap Lake would be necessary to evaluate.

The study was to assess the dynamic transport of sediment and nutrient in the Mekong River Basin and evaluate the role of the Tonle Sap to the Mekong River through the coupling data and modelling approaches. The physical-based SWAT model was used upstream of the Mekong delta to simulate the water regime and suspended sediment and nutrient flux of the Mekong River. The SWAT model was calibrated based on observed discharge at eight gauge stations, suspended sediment load at six stations and nutrient data at five stations from 1995 to 2016 at a monthly time step. To understand the role of Tonle Sap Lake in sediment and nutrient to Mekong River, the study considered the balanced of the Tonle Sap reverse system at seasonal and annual scales.

Before entering the confluence of Mekong and Tonle Sap Lake and delta, the sediment load is found 72±26 Mt/year with a decreasing annual trend from 1995 to 2018. The annual sediment yield of the upper 80% Mekong River basin (310 t/km^2/year) is comparable with sediment yields reported for other world major rivers. The Mekong annual average riverine nitrate yield was 202 kg/km^2/year with 361.8±83.5 kt/year from 1985-2016 of annual nitrate flux before entering the Mekong delta. The sediment loads variability of the Mekong River and Tonle Sap system presented in this study helps clarify the exchange annual discharge and sediment load toward the Mekong delta. The study also highlighted that the fact that Tonle Sap is the sediment sink (1.35±0.7 Mt annually) in the Mekong basin lead to a reduction in sediment supply, which compounds the threat to the delta from accelerated subsidence and sea-level rise. The study has emphasized the interaction role of Tonle Sap Lake and Mekong in nutrient supply for the Mekong delta. On the annual scale, it is worth discussing these interesting results revealed Tonle Sap Lake contributed 34 kt/year of nitrate and 6.6 kt/year of total phosphorus to the Mekong system or Mekong Delta. In contrast, the Mekong River shared nitrate flux 35.8 kt/year and 8.7 kt/year of total phosphorus to Tonle Sap Lake and its floodplain during the high flow season. Future studies of hydrology together with sediment and nutrients can be carried on based on this model with scenarios of global changes, such as climate changes and land-use changes and include the sediment and nutrient input to Tonle Sap Lake system from the lake tributaries and interconnect with the Mekong River basin model.

Résumé

Les bassins versants asiatiques contribuent grandement aux sédiments et aux éléments nutritifs des mers. Ces bassins sont soumis à l'influence de la variabilité climatique et des activités humaines, qui modifient le transport des nutriments et le devenir de la qualité de l'eau. Le Mékong est un fleuve transfrontalier situé en Asie du Sud-Est, qui joue un rôle important dans l'économie et l'agriculture, d'autant plus que ce fleuve contribue aux flux du delta du Mékong et de la mer associée. Dans le bassin du Mékong, la région du Tonlé Sap est un système complexe caractérisé par un flux unique inversé entre le lac Tonlé Sap et le fleuve Mékong. Les sédiments et les éléments nutritifs du Mékong sont importants pour maintenir la géomorphologie des plaines inondables et en particulier celle du lac Tonlé Sap. De même, le lac Tonlé Sap contribue aux sédiments et aux nutriments du delta du Mékong.

L'étude consiste à évaluer la dynamique du transport des sédiments et des nutriments dans le bassin du Mékong, et, à évaluer la contribution du lac Tonlé Sap vers le fleuve Mékong à partir d'un couplage entre données et approches de modélisation. Le modèle à base physique SWAT a été appliqué en amont du delta du Mékong pour simuler le régime hydrologique et les flux de matières en suspension et de nutriments du Mékong. Le modèle SWAT a été calibré pour l'hydrologie à partir des débits observés au niveau de huit stations, pour les sédiments au niveau de six stations et pour les nutriments au niveau de cinq stations de 1995 à 2016 au pas de temps mensuel. Pour comprendre la contribution du lac Tonlé Sap dans les flux de sédiments et de nutriment du fleuve Mékong, l'étude a considéré le système inverse du lac Tonlé Sap aux échelles saisonnières et annuelles.

En amont de la confluence du fleuve Mékong, du lac Tonlé Sap et du delta du Mékong, le flux de sédiment évalué est de 72±26 Mt/an avec une tendance annuelle à la baisse entre 1995 et 2018. La moyenne annuelle en sédiments en amont de la confluence du lac Tonlé Sap et du Mékong (310 t/km^2/an) est comparable aux sédiments évalués dans d'autres grands fleuves du monde. Le rendement moyen annuel en nitrate dans le fleuve du Mékong est de 202 kg/km^2/an avec 361,8 ± 83,5 kt/an de 1985 à 2016 de flux annuel de nitrate avant d'entrer dans le delta du Mékong. La variabilité des charges sédimentaires du Mékong et du système Tonlé Sap présentée dans cette étude permet de clarifier les échanges de débit annuel et de flux de sédiment au sein du delta du Mékong. Cette étude souligne aussi la capacité du lac Tonlé Sap à être un puits de sédiments (1,35 ± 0,7 Mt par an) du bassin Mékong, réduisant ainsi la charge annuelle en sédiments s'écoulant vers le delta du Mékong. Cette faculté du lac Tonlé Sak a être un puit entraîne une réduction de l'apport en sédiments, ce qui menace le delta d'un affaissement accéléré et d'une augmentation du niveau des mers. L'étude a souligné le rôle du lac Tonlé Sap et du fleuve Mékong dans l'approvisionnement en nutriments du delta du Mékong. À l'échelle annuelle, il convient de discuter de ces résultats intéressants qui montre que le lac Tonlé Sap contribue de 34 kt/an en nitrate et de 6,6 kt/an de phosphore total au delta du Mékong. En parallèle, le fleuve Mékong envoie 35,8 kt/an en nitrates et 8,7 kt/an en phosphore total vers le lac Tonlé Sap et sa plaine d'inondation pendant la saison des crues. Les études à venir en l'hydrologie et en biogéochimie pourront être menées sur la base du modèle développé dans cette thèse en appliquant des scénarios de changements globaux, tels que les changements climatiques, ou encore, les changements d'occupation des sols, et pourront inclure dans le modèle les flux de sédiments et de nutriments allant au lac Tonlé Sap en provenance des affluents du lac et des interconnexions avec le bassin du Mékong.